JOURNAL OF
ATMOSPHERIC AND TERRESTRIAL
PHYSICS

EDITORIAL ADVISORY BOARD

H. O. G. ALFVÉN–STOCKHOLM · **J. BARTELS**–GÖTTINGEN · **P. M. S. BLACKETT**–LONDON · **E. G. BOWEN**–SYDNEY · **SIR DAVID BRUNT**–LONDON · **R. BUREAU**–BAGNEUX · **S. CHAPMAN**–ALASKA · **J. EGEDAL**–COPENHAGEN · **H. FICKER**–VIENNA **V. F. HESS**–NEW YORK · **E. O. HULBURT**–WASHINGTON, D. C. · **H. ISRAEL**–AACHEN **D. K. MENZEL**–CAMBRIDGE, MASS · **S. K. MITRA**–CALCUTTA · **M. NICOLET**–UCCLE **E. H. NORINDER**–UPSALA · **B. van der POL**–GENEVA · **N. V. PUSHKOV**–MOSCOW **J. A. RATCLIFFE**–CAMBRIDGE · **O. E. H. RYDBECK**–GOTHENBURG · **SIR GEORGE SIMPSON**–LONDON · **H. SOLBERG**–OSLO · **J. VELDKAMP**–DE BILT · **M. WALDMEIER**–ZÜRICH · **J. ZENNECK**–ALTHEGNENBERG

EDITOR IN CHIEF

SIR EDWARD APPLETON, F.R.S.
EDINBURGH

A SPECIAL SUPPLEMENT
1957

PROCEEDINGS OF THE POLAR ATMOSPHERE SYMPOSIUM

PART II

Ionospheric Section

Held at Oslo, 2–8 July 1956

PERGAMON PRESS

NEW YORK · LONDON · PARIS · LOS ANGELES

Suppl.
Part.II
1956

CONTENTS

PAGE

OPENING SPEECH ix
F. L. Wattendorf

INTRODUCTORY SPEECH xi
H. U. Sverdrup

SECTION I

1. THEORETICAL VIEWS ON DRIFT MEASUREMENTS - - - 3
I. L. Jones,
Cavendish Laboratory, Cambridge

2. THE DRIFT OF AN IONIZED LAYER IN THE PRESENCE OF THE GEOMAGNETIC FIELD - - - - - - - - 12
K. Weekes,
Cavendish Laboratory, Cambridge

3. THE HEIGHT-VARIATION OF HORIZONTAL DRIFT VELOCITIES IN THE *E*-REGION - - - - - - - - - 20
I. L. Jones,
Cavendish Laboratory, Cambridge

4. RESULTS OF IONOSPHERIC DRIFT MEASUREMENTS IN THE UNITED STATES - - - - - - - - - 23
Vaughn Agy,
National Bureau of Standards, Boulder, Colorado

5. RESULTS OF IONOSPHERIC DRIFT MEASUREMENTS IN NORWAY 26
Leiv Harang
Norwegian Defence Research Establishment

6. LARGE-SCALE MOVEMENTS OF THE LAYERS - - - 33
H. W. Wells,
Carnegie Institution of Washington, Department of Terrestrial Magnetism, Washington 15, D.C.

7. MOVEMENTS OF IONOSPHERIC IRREGULARITIES OBSERVED SIMULTANEOUSLY BY DIFFERENT METHODS - - - 41
I. L. Jones, B. Landmark and C. S. G. K. Setty,
Cavendish Laboratory, Cambridge

8. MEASUREMENTS OF IRREGULARITIES AND DRIFTS IN THE ARCTIC IONOSPHERE USING AIRBORNE TECHNIQUES - - - 44
George J. Gassmann,
Air Force Cambridge Research Center

CONTENTS

PAGE

9. Turbulence in the Ionosphere with Applications to Meteor Trails, Radio Star Scintillation, Auroral Radar Echoes, and other Phenomena - - - 52
H. G. Booker,
School of Electrical Engineering, Cornell University, Ithaca, New York

10. Electron Distribution in a New Model of the Ionosphere 82
H. K. Kallmann,
Institute of Geophysics, University of California at Los Angeles, Los Angeles, California, U.S.A.

Discussion - - - - - - - - - - - - 88

SECTION II

1. Prediction Techniques at High Latitudes - - - 101
J. H. Meek,
Radio Physics Laboratory, Ottawa

2. Geographic Distribution of Geophysical Stations on the Polar Cap - - - - - - - - - - - 108
A. H. Shapley,
National Bureau of Standards, Boulder, Colorado

3. Statistical Results and their Shortcomings concerning the Ionosphere within the Auroral Zone - - 109
R. W. Knecht,
National Bureau of Standards, Boulder, Colorado

4. Polar Disturbances - - - - - - - - - 120
J. H. Meek,
Radio Physics Laboratory, Ottawa

5. Polar Blackout Occurrence Patterns - - - - 129
Vaughn Agy,
National Bureau of Standards, Boulder, Colorado

6. Quantitative Measurements of Absorption in the Auroral Zone - - - - - - - - - - 135
F. Lied,
Norwegian Defence Research Establishment

7. Forecasting of Disturbed HF Communication Conditions 147
R. C. Moore,
Chief Forecaster, North Atlantic Radio Warning Service, National Bureau of Standards, Fort Belvoir, Virginia

Discussion - - - - - - - - - - - 157

Supp
Part.
195

CONTENTS

PAGE

SECTION III

1. The Spectrum of the Electron Density Fluctuations in the Ionosphere - - - - - - - - - 165
Roger M. Gallet,
National Bureau of Standards, Boulder, Colorado

2. A Theory of Long-Duration Meteor-Echoes based on Atmospheric Turbulence with Experimental Confirmation - - - - - - - - - 171
H. G. Booker and Robert Cohen,
School of Electrical Engineering, Cornell University, Ithaca, New York

3. Some Implications of Slant-E_s - - - - - - 195
E. K. Smith and R. W. Knecht,
Boulder Laboratories, National Bureau of Standards, Boulder, Colorado

4. Results of Scatter Measurements at 36 Mc/s over a 1200 km Path - - - - - - - - - 205
Tor Hagfors,
Norwegian Defence Research Establishment

Discussion - - - - - - - - - - 210

uppl.
rt.II
1956

Sup
Part
19

Suppl.
art.II
1956

OPENING SPEECH

by

FRANK L. WATTENDORF

Director

ADVISORY GROUP FOR AERONAUTICAL RESEARCH AND DEVELOPMENT

of the

North Atlantic Treaty Organization

ON behalf of AGARD, it is a great pleasure to welcome the participants in this Symposium on the Polar Atmosphere and to extend a special greeting in the name of our distinguished chairman, Dr. Theodore von Kármán, who is presently in California.

Many of you may not be too well acquainted with AGARD since this is the first symposium we have held in this particular field. I think therefore it might be appropriate to review some background information on our organization, the Advisory Group for Aeronautical Research and Development (AGARD).

AGARD is really the brainchild of Dr. von Kármán. From his earliest years he was influenced by the thinking of his father, Professor Maurice von Kármán, a prominent philosopher with constructive international views. This gentleman, a professor of philosophy in the University of Budapest, Hungary, as early as 1900 expressed the opinion that in about fifty years there would arise organizations for active international co-operation; that the chief hope of lasting peace was for all nations to work together for the common good.

It is interesting to note that it was just about fifty years later that NATO came into being, and that his son, Dr. Theodore von Kármán, used that as a framework to establish an international organization of scientific co-operation.

The more recent history of AGARD dates from 1945 when Dr. von Kármán was called upon by General H. H. Arnold, Chief of the United States Army Air Forces, to advise him on the shape of things to come.

As an initial step, Dr. von Kármán gathered together a small group of scientific and technical experts, and with them visited Europe in April 1945. After this visit he was more than ever convinced that the most important thing for the future was that all nations should work together in scientific and technical fields. To further this ideal, he recommended the formation of an international Scientific Advisory Board. Several years were to pass before there was a mechanism to form such an organization.

Finally, when NATO came into being, it provided a potential framework. Dr. von Kármán, with the support of the United States Air Force, called a preliminary meeting in 1951 in Washington of Research Directors of the NATO countries. This meeting unanimously recommended the formation of

an Advisory Group for Aeronautical Research and Development to the North Atlantic Treaty Organization. This was approved in February 1952 as an organization reporting directly to the Standing Group; in other words on the same organization level as SHAPE.

The objectives of AGARD are to recommend ways and means of increasing the NATO research and development potential. The approach is by taking limited constructive steps. Instead of trying to cover the whole field, AGARD acts as a catalyst and stimulates work in certain fields where there are known deficiencies. In particular, several technical panels were formed in fields where tangible accomplishments could be expected in relatively short time. Then there was established an exchange program, whereby young scientists and engineers of different nations were given an opportunity for training and experience in laboratories of other nations. From time to time, special committees are set up to advise on specific problems referred to AGARD by SHAPE and NATO Agencies. Finally, there are certain fields where it has been found more expedient to hold exploratory symposia devoted to topics not wholly covered by other organizations.

The present symposium comes under the latter category.

At the Second AGARD General Assembly in Rome in December 1952, the delegates of the different NATO nations were asked to make recommendations as to fields of activities which would be of particular importance to their own nation. The representative of Norway, Dr. Harang, who is with us today, stressed the importance of the polar atmosphere, and recommended AGARD activities along this line. It was decided that the way to approach the project was to hold an exploratory symposium assembling the appropriate experts of different NATO nations to examine the more pressing problems of the polar atmosphere; then conclude from their findings the best way of proceeding in the future. Out of the above considerations came the recommendations for this particular symposium.

Since Norway had made the original suggestion, it was appropriate that Norway be invited to plan the program. The Executive Committee for this symposium is under the chairmanship of Prof. Harald Sverdrup* and the Arrangement Committee is headed by Dr. Harang.

It is interesting to note that the polar atmosphere is of prime importance to both commercial and military aviation, and to advancing knowledge in the geophysical sciences, including weather prediction and control. For this reason, this symposium is quite in spirit with the new look in NATO; in other words, the placing of greater emphasis on Article 2 of the North Atlantic Treaty, which concerns activities contributing toward the further development of peaceful and friendly international relations. A committee of three foreign ministers was appointed to provide proper recommendations. It is notable that among the "three wise men" chosen to make this study, the Foreign Minister of Norway is one. It is also significant that this Polar Symposium was already in preparation well in advance of the Council Meeting, which is a tribute to the vision and forward thinking of the scientists of Norway in this regard.

In conclusion, I wish to extend the personal best wishes of our chairman and the AGARD organization for a successful meeting.

* Deceased August, 1957.

INTRODUCTION SPEECH

H. U. SVERDRUP*
Norsk Polarinstitutt, Oslo, Norway

Dr. Wattendorf, Delegates and Guests,

IT is a great pleasure to me, on behalf of the Executive Committee from Norway, to welcome all the delegates and guests to this meeting.

I dare say, when it was first suggested that such a meeting should be held here in Oslo, we who were asked to take steps towards arranging it, hesitated quite a great deal for two reasons. On the one hand, Norway lies in a corner of Europe, somewhat out of the way, although, thanks to the air communications, distances have been reduced so much that after all the location is not all-important.

Of greater concern was that we might not be able from here to contribute so much to the meeting as we would like to do. But when we still went ahead, the reason was that we felt that a meeting of this sort would be a tremendous stimulus to the work going on in this country.

The particular reason why I am standing here as chairman of the Executive Committee of Norway is perhaps that I am a sort of exhibit A, because it so happens that I am the oldest living meteorologist who has worked actively in the Arctic. I cannot claim the same position when it comes to the Antarctic, where Sir George Simpson, who is still going strong, took part in the British Antarctic Expedition 1910–13, quite a number of years before I went into Arctic. There is also another reason why I may be exhibited here, namely that I think that of all present I have spent more time in the Arctic than anybody else, and I also believe that you had to get together several of those present here, who worked in the Arctic, in order that their combined time of services would equal to the one that I have behind me. Therefore, to me this meeting here is a historical event, because it will indeed throw light over the tremendous development which has taken place during the 38 years now which have passed since in 1918 I left northern Norway on board Roald Amundsen's ship the *Maud*. The changes which have taken place cover not only the means of transportation and communications, but also the instrumental equipment and the possibilities of undertaking systematic research in the very high latitude. As far as communications are concerned I may mention that, when we left in 1918, we were prepared upon being absent for four years and carried no radio. Nothing would be heard about the expedition until it returned, if it returned. Actually, however, it so happened that the expedition fell in two parts, and it took seven and a half years before it was back again in the country.

But it is not only the communications, it is particularly the types of observa-

* Professor Sverdrup died suddenly in Oslo on 21st August, 1957.

tions which have been subject to enormous changes. Going back again, the only work pertaining to the ionosphere, which was done at that time, was the study of the aurora. The technique of measuring the height of the aurora had been developed, and the analysis of the spectrum of the aurora had been started, but the entire knowledge of the ionosphere was based upon the indeed difficult interpretation of the results of the aurora observations. Turning to the atmosphere, the examination of the free atmosphere had to be undertaken exclusively by means of pilot-balloons and kites. By means of the latter one could not reach appreciable altitudes in spite of the often back-breaking work of hauling down the kite against a strong wind. But the expedition to which I refer was actually the last of the long-lasting pioneering expeditions to the Arctic. I have always looked upon the period of these expeditions as a period in which two things were accomplished. In the first place the geographical exploration was carried through, not completed, but to a considerable degree brought to an end. In the second place these expeditions demonstrated fully the possibilities of survival in the Arctic, and that under the rigorous conditions of the Arctic one could use the same types of instrumental equipment, which we employ in lower latitudes. From these points of view the pioneering attacks have been amply rewarded, because now we find permanent stations established at the most remote localities, and we find them equipped with the most complete instrumentations.

The changes which have taken place are particularly reflected in the titles of the papers to be presented here now at this symposium. Within meteorology, for instance, most of the papers deal not only with surface conditions, but partly or exclusively with conditions of the free atmosphere. Within the ionospheric section, about which I know very, very much less, practically nothing, the situation is indeed that there is not a single paper dealing with the aurora, but, instead, there are papers there which are of direct interest to the meteorologists, dealing with the drifts and turbulence in the ionosphere. This overlapping of interests now between the meteorologists and the group working with the ionospheric problems is paid a certain attention to in arranging this programme, because on Thursday there will be no session of the meteorological section, but the ionospheric section will then deal with papers which are of interest also to the meteorologists.

A symposium on the polar atmosphere seems indeed justified from the point of view that it is desirable to review the recently gathered knowledge and to exchange views as to the interpretation of the results. However, when this symposium was first discussed, an objection was raised: why a special symposium on the polar atmosphere? Can we deal with the polar atmosphere without considering that it is not isolated, without considering that the atmosphere of the northern region plays a role in the general circulation similar to that of the atmosphere above any other part of the world? I am now referring particularly to the meteorological part of the programme. Obviously we cannot neglect the importance of the characteristics of the polar atmosphere to the general circulation, and this topic will therefore also be dealt with here, but still I believe that it is quite justified to talk about polar meteorology as a special subdivision within meteorology. We speak of tropical meteorology, and it seems justified to talk about the meteorology of the middle latitudes where conditions both from the tropical and from the polar parts of the at-

mosphere will have to be taken into account. However, it is not only because of certain climatic contrast that one conveniently introduces the subdivisions "tropical" and "polar" meteorology. There are certain essential differences. When dealing with the dynamics of the systems, there are differences because of the latitude change of the Coriolis-acceleration, but fundamentally the differences within the dynamics are not especially important. The fundamental difference is found when one considers the energy transformations within the atmosphere in these two regions. In the tropics the most important energy transformations are represented by the addition of latent heat to the atmosphere through the condensation of water vapour. That, besides the phenomena associated with radiation, leads to instabilities which play a tremendous part in all problems pertaining to the meteorology of the tropics. In the polar regions, on the other hand, the most important energy transformations are related to processes of radiation, and a characteristic of the polar atmosphere is that processes of instability are there of very much smaller importance. This also is reflected in the titles of papers to be presented here, because there is not a single paper which deals with questions pertaining to precipitation or to cloud-formations in the polar atmosphere, whereas there are several papers dealing with processes of radiation and dealing with the types of inversions which are typical under stable conditions. Because of the character of the energy transformations I considered that it is fully justified to speak about polar meteorology in contrast to tropical meteorology.

In concluding this very brief introduction I would like to return to the character of this symposium. I believe that it will serve particularly two purposes. It will help to clarify a number of the problems of the polar regions and, in the second place, it will stress the importance of developments in the polar regions to the problems in our latitudes. In that respect it will of course deal not only with the strictly polar conditions, but also with those which concern the regions around the Arctic with their very dense population and with their increasingly important problems in meteorology.

We who have had to deal with the arrangement of the meeting are pleasantly surprised by the attendance which the meeting has obtained and by the fact that so many contributions will be presented here. We are also, I would add, extremely grateful to the different speakers because they have conscientiously sent in abstracts of their talks at such an early date that the abstracts are available now. We feel that what little effort we have been able to put into the arrangement has indeed been amply rewarded by the attendance, and by the interest shown in the meeting which starts here now. In view of that background I feel confident that some of the goals of the meeting here, which were also mentioned by Dr. Wattendorf, will be attained.

Supp
Part.
195

SECTION I

uppl.
rt.II
1956

Supp
Part.
195

THEORETICAL VIEWS ON DRIFT MEASUREMENTS

I. L. Jones
Cavendish Laboratory, Cambridge, U.K.

Measurements of ionospheric drifts by observing the fading of a singly reflected wave at three closely spaced points on the ground are discussed.

The magnitudes and directions of drift velocities observed from time delays between maxima and minima of the fading records are subject to large variations. These can be explained partly in terms of the variable orientation of a line of maximum amplitude and partly by changes in the amplitude pattern as it moves.

The drift observed when the pattern on the ground is anisometric may be markedly different from the true drift, and tends to lie in a direction perpendicular to the direction of stretching. The effect on the average drift due to random orientation of the stretching and due to stretching in a preferred direction is discussed.

When the amplitude variations at three stations are available, the auto-correlation and cross-correlation functions can be determined. From these, it is possible to determine the true magnitude and direction of the drift, the size and shape of the amplitude pattern on the ground and also a quantity related to the random changes of the pattern.

uppl.
rt.II
1956

1. Determination of Drift Velocities from Time Delays

Observations of the amplitude variations of radio waves singly reflected from the ionosphere, at three points on the ground separated by about one wavelength have been used by numerous workers to determine horizontal drifts in the ionosphere. The amplitude at one point varies in a random manner, but the fading records at the three points separated by this distance are found to be similar. The individual time delays between maxima or minima of the records, however, are subject to large variations. These large variations in the time delays seem to indicate equally large variations in the magnitude and direction of drift in the ionosphere. It is very difficult to think of a physical reason why large variations in the true drift should occur. Also whether the mean value of the time delays gives a velocity of drift which is significant.

1.1. *The reasons for variable time delays*

To investigate this problem further, we must look at the amplitude pattern produced on the ground. The radiation at the ground from a rough ionosphere arrives within a cone of angles, and the varying amplitude over the ground is due to interference between different components in this cone of rays. If the ionosphere is perfectly smooth, the amplitude at the ground will be constant, and the method of determining drifts described above cannot be

used. The shape of the contours of constant amplitude on the ground depends on the shape of the irregularities in the ionosphere, but the size on the ground can be different from the size of the irregularity in the ionosphere. Contours of constant amplitude produced by the interference between the rays are shown in *Fig. 1*. By observing the time delays between fading re-

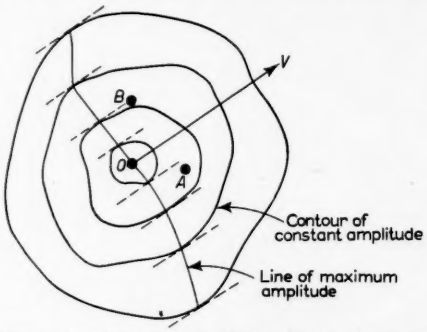

Fig. 1. Contours of constant amplitude showing the line of maximum amplitude

cords, we are observing the motion of these amplitude patterns on the ground, so that here we may find the origin of the large variability in the time delays. If it is assumed that a true steady drift V is present, then it is possible to construct a line of maximum amplitude for each irregularity, such that when this line passes over the receivers at O, A and B, an amplitude peak is observed. The line of maximum amplitude passes through the points of contact between a line parallel to the direction of drift and the amplitude contours. Thus, the orientation of this line depends on both the direction of drift, and on the shape and orientation of the amplitude contours. Because the separation of the aerials is about a wavelength, and there can be no "structure" in the diffraction pattern with size less than a wavelength, the lines of maximum amplitude must be approximately straight over the distances considered.

The question of variable time delays will now be considered further. Suppose that the drift in the ionosphere is constant, and in an E–W direction, then if the lines of maximum amplitude remained perpendicular to the

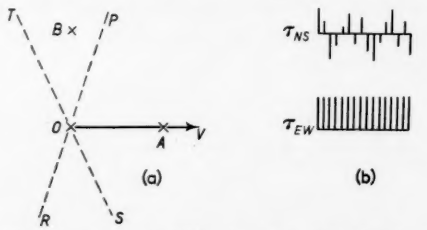

Fig. 2. The time delays observed for variable orientation of the line of maximum amplitude

direction of drift, there would be zero time delay between the N–S pair of fading records, and a constant time delay between the E–W pair. If the line of maximum amplitude can have any orientation, then the observed time delays between the N–S pair will be variable, while those between the E–W pair will be constant as shown in *Fig. 2* (*b*). The N–S component of velocity

appears to be very variable. If the lines of maximum amplitude have random orientation, this is exactly the type of time delays to be expected because if we look at *Fig. 2 (a)* when the line of maximum *POR* passes the site, the maximum crosses *B* before *O* whereas *TOS* gives the opposite time delay. Similarly if the true drift is in the N–S direction the E–W time delays would be variable. When the true drift is in some other direction, the time delays on both the E–W and N–S pair will be subject to variations.

It can be shown, RATCLIFFE[1] that if the line of maximum amplitude can have any orientation, then the mean value of the drift velocity deduced from the time delays will have the same magnitude and direction as the constant true drift.

1.2. *The effect of random changes of the pattern*

We have assumed that while the pattern drifts over the receiving site, it retains its shape. This need not necessarily be the case, as random changes of the pattern may occur while it passes over the receiving site. This effect will produce additional variability into the time delays, and averaging over many samples will not give the true velocity, but a value greater than the true velocity. Thus, if the pattern on the ground is on the average circular and subject to random changes, the velocity deduced from time delays will always give an upper limit to the true velocity. When the random component is smaller than the steady drift, and when the random changes are of the same magnitude in all directions, then the observed average direction of drift will be the same as the true direction of drift, but the magnitude of the velocity will be different. The supposition that the random movement is the same in all directions may be incorrect, as the movement of electrons depends on the earth's magnetic field, and the random movements may be different along, and perpendicular to, the earth's magnetic field. In this case the mean direction of drift will be incorrect.

A more detailed analysis of the probability distributions of the time delays has been given by BRIGGS and SPENCER,[2] who showed how it is possible to deduce the true velocity of drift, and also a quantity V_c, which is a measure of the random changes taking place in the pattern.

Thus the large variability in the magnitude and direction of the drift velocity can be explained in terms of the variable orientation of the lines of maximum amplitude, and of random changes in the pattern as it drifts.

1.3. *Errors introduced by the method of time delays when the pattern is anisometric*

The case when the shape of the amplitude pattern on the ground was on the average isometric, has been discussed. We now consider the effect of an anisometric pattern on the observed velocity. Here it will be assumed that to a first approximation the average shape of the amplitude contour is elliptical.

For an infinitely extended pattern, only motion perpendicular to the direction of stretching will be detectable. When the stretching is not infinite, the observed velocity will lie in a direction near to the direction of the minor axis of the ellipse.

Thus when velocities are deduced from time delays when the pattern is elongated, both the magnitude and direction will be different from the true

Suppl.
art.II
1956

value. Let us now see what effect this anisometry has on the time delays, and on the line of maximum amplitude.

The elongation of the pattern will restrict the variability of orientation of the line of maximum amplitude, in that it will always lie approximately in the direction of stretching. Thus if the direction of stretching from one irregularity to the next is the same, then the time delays observed will only have small variations. If it were not known that the amplitude pattern was stretched, we would probably think that as the mean velocity had a small scatter, that this observed velocity was in fact the true velocity.

Now let the direction of the elongation vary, so that the magnitude and direction of the velocity determined changes. From the time delays between the fading records an apparent velocity V_a will be determined, which is the component of the true velocity V perpendicular to the line of maximum amplitude, which in turn is approximately parallel to the major axis of the

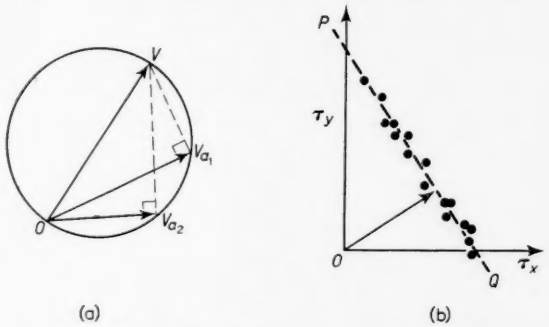

Fig. 3. The relation between the apparent and true velocities

elliptical contour. If V is the true velocity, then the end points of the vectors V_{a1}, V_{a2}, etc. will lie on a circle of diameter V as shown in *Fig. 3(a)*[3 4] also

$$\frac{1}{V_a} = \frac{1}{V \cos \theta},$$

or

$$\tau = T \sec \theta,$$

where $\tau \propto \frac{1}{V_a}$, $T \propto \frac{1}{V}$ and

$$\tau = \sqrt{(\tau_x^2 + \tau_y^2)}$$

where τ_x and τ_y are the time delays observed in the E–W and N–S directions, respectively.

The construction shown in *Fig. 3 (b)* fits the above requirements, as $\tau = T \sec \theta$ defines the line PQ. Thus a plot of τ_x against τ_y will give a straight line and the normal to it from the origin gives the velocity and direction of the true drift V.

When the direction of the line of maximum can have all values, the direction of drift deduced from a τ_x, τ_y plot will be the same as that deduced from the mean time delays. When the amplitude pattern is elongated so that the direction of the line of maximum is restricted, the drift measured from the

τ_x, τ_y plot will be the true drift while that from the mean time delays will be incorrect.

If, however, the amplitude pattern is elongated in a preferred direction, the lines of maxima for successive amplitude maxima will be parallel, and so the points on the τ_x, τ_y diagram would lie very close together and it would be impossible to construct a straight line. This is found to occur with observations of drift obtained from the scintillation of a radio star, where the amplitude contours on the ground are elongated in a N–S direction with axial ratio of about 5 : 1.

Another restriction on this method is that when random changes occur, the scatter of the points is large and a straight line cannot be constructed.

The danger of obtaining spurious results when the pattern is elongated can be illustrated in the following manner. Let the true drift be towards the north, and the direction of elongation of the ellipse also in a northerly direction, then a small change in the direction of orientation of the ellipse from the NE to the NW quadrant will reverse the apparent direction of drift, without any change in the true drift.

Thus when no random changes are present, the mean from simple time delay measurements will give a true value for the velocity and direction of drift, if the direction of stretching can have all values. When the direction of stretching is restricted, the τ_x, τ_y plot will give the true velocity provided that the elongation of the pattern is not too great. When random changes are present, the methods are unreliable.

Suppl.
art.II
1956

2.1. *The full method of calculation with correlation functions*

When the pattern on the ground is anisometric and changing as it moves, information from simple time delays is unreliable, and a more detailed statistical approach has been developed to deal with this case by BRIGGS, PHILLIPS and SHINN,[5] and extended by PHILLIPS and SPENCER.[6] In this method the three fading records have to be observed, and from these the auto-correlation and cross-correlation functions can be determined. The analysis is rather complicated, and only the results will be quoted.

The time delays for maximum cross-correlation can be used to determine a

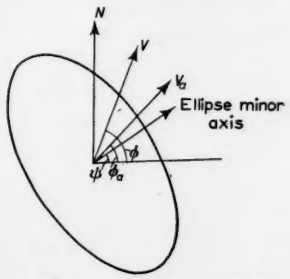

Fig. 4. The velocities and directions involved in the theory

velocity of drift. This would be the velocity of drift in the ionosphere assuming that the amplitude pattern was isometric and did not change as it moved. This velocity is called the apparent velocity. The results of the correlation

analysis have been given in the form of a correction to this apparent velocity, so that the true drift can be determined. If the time delays alone are observed, the apparent velocity can be calculated, while the full correlation analysis gives the true velocity of drift.

The average shape of the amplitude contour on the ground can be determined and hence the relationship between the apparent velocity, and the true velocity can be determined. Let V be the true velocity at an angle ϕ from north, V_a and ϕ_a the apparent velocity and direction, ψ the direction of the minor axis of the ellipse and r its axial ratio as shown in *Fig. 4*.

Then the following relationship holds:

$$\tan(\phi - \phi_a) = \frac{(r^2 - 1)\tan(\phi_a - \psi)}{1 + r^2 \tan^2(\phi_a - \psi)}.$$

The graphical representation is as shown in *Fig. 5*. When the true direction of drift is along either the major or minor axis, then the apparent direction

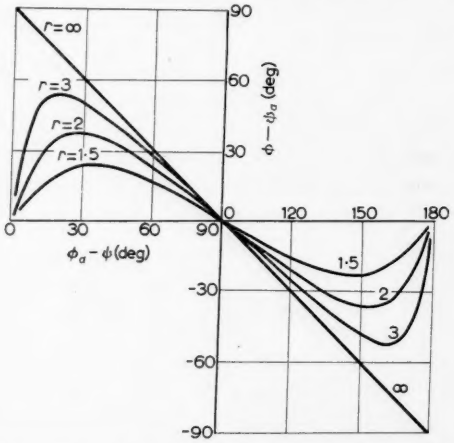

Fig. 5. The required correction $\phi - \phi_a$ plotted as a function of the angle $\phi_a - \psi$ between the apparent direction and the minor axis of the ellipse, for various axial ratios of the ellipse

will be the same as the true direction. For some other direction of drift, the difference $(\phi - \phi_a)$ depends on the axial ratio of the ellipse, and for $r = 3$, can be as large as 55°.

The magnitude of the apparent velocity V_a, is not equal to the true velocity, and the following relationship holds between them.

$$\frac{V_a}{V'} = \cos(\phi - \phi_a)$$

where V' is the velocity in the true direction before removing the effect due to random changes. This ratio depends on the axial ratio as shown in *Fig. 6*. Again $V_a = V'$ when the true drift is along the major or minor axis.

If a systematic departure from the isometric pattern exists, and all values of true drift direction are equally probable, then the apparent directions will tend to lie in a group about a most likely value of $\phi_a = \psi$, i.e. there will be high probability of the drift being in a direction perpendicular to the preferred direction of elongation. The probability distribution of $(\phi_a - \psi)$ for

different values of r is shown in *Fig. 7.* Thus, if the auto-correlation and cross-correlation functions of the fading records observed at three points on the ground are determined, it is possible to obtain the following information:

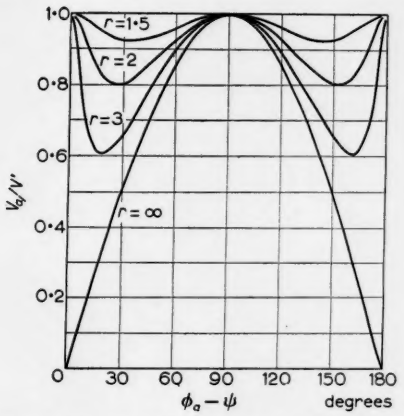

Fig. 6. The ratio of V_a, the apparent velocity, to V', the velocity which would be deduced from a correct analysis, plotted in the same way as Fig. 5

(*a*) The size, shape and orientation of the average amplitude contour on the ground.
(*b*) The true magnitude and direction of drift.
(*c*) A quantity V_c related to the random changes of the pattern.

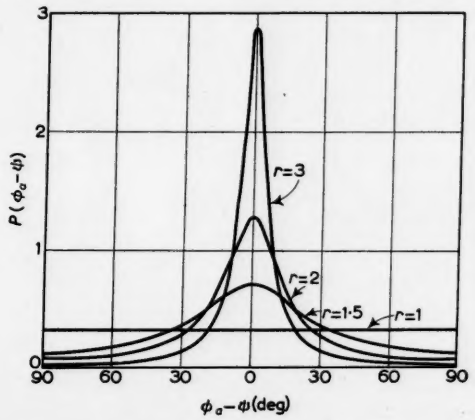

Fig. 7. The grouping of apparent directions for various departures from isometric properties, assuming a uniform distribution of true directions

2.2. *Experimental results*

The determination of auto-correlation and cross-correlation functions is very laborious, but at Cambridge some of this analysis has been carried out on an electronic digital computer. Up to the present, ten *E*-region daytime records have been analysed and a typical result is shown in *Fig. 8.*

From these ten records, the mean value for the axial ratio of the ellipse is 1·4, and all the values lie in the range 1·1–2. The few results so far obtained indicate that there does not appear to be a preferred direction of orientation.

In contrast with these results an example of the shape of the amplitude

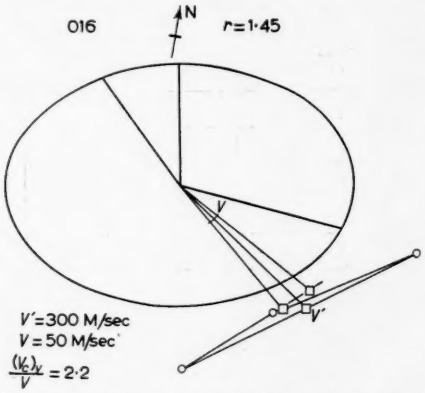

Fig. 8. Contours of constant amplitude for waves of frequency 2 Mc/s reflected from the E-region. The velocities are those of the amplitude pattern on the ground, and the ratio of $(V_e)_x/V$ of 2.2 shows that the random changes are more important than the drift of the pattern in producing the fading

pattern on the ground produced when radio waves from the radio source in Cassiopeia pass through the *F*-region is shown in *Fig. 9.* These amplitude

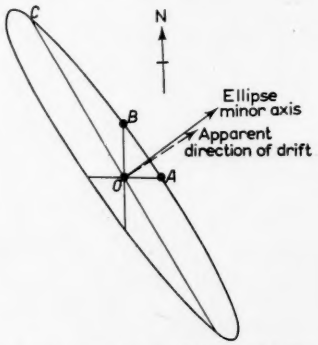

Fig. 9. Contours of constant amplitude for radio stellar scintillation

contours are highly elongated in a N–S direction, so that measurements of the drift velocity from time delays is very misleading, as the apparent drift will always lie in an E–W direction.

The drift velocities that have been determined apply only to the movement of the amplitude pattern on the ground. The relation between this movement, and the physical processes occurring in the ionosphere give rise to the following problems:

(1) Is the movement a real movement of the electron density irregularities, or is it a horizontal wave motion in the ionosphere, where the electron density irregularities are not moved bodily in the direction of drift?

(2) If the observed movements are real, are they the same as the movement of the surrounding neutral air?

These problems will not be discussed in this paper, but they show that when the movement on the ground has been determined, further complications arise in interpreting these movements in the ionosphere.

The author is very much indebted to Mr. J. A. Ratcliffe and Dr. B. H. Briggs of the Cavendish Laboratory for much helpful advice and discussion.

References

[1] Ratcliffe, J. A. *J. atmos. terr. Phys.* Vol. 5, p. 173, 1954

[2] Briggs, B. H. and Spencer, M. *The Physics of the Ionosphere;* Physical Society, London, 1955

[3] Court, G. W. G. *J. atmos. terr. Phys.* Vol. 7, p. 333, 1955

[4] Putter, P. St. *The Physics of the Ionosphere;* Physical Society, London, 1955

[5] Briggs, B. H., Phillips, G. J. and Shinn, D. H. *Proc. phys. Soc.* B Vol. 63, p. 106, 1950

[6] Phillips, G. J. and Spencer, M. *Proc. phys. Soc.* B Vol. 68, p. 481, 1955

uppl.
rt.II
1956

THE DRIFT OF AN IONIZED LAYER IN THE PRESENCE OF THE GEOMAGNETIC FIELD

K. WEEKES
Cavendish Laboratory Cambridge, U.K.

1. INTRODUCTION

DURING the past 10 years many data have been obtained on the movement of ionization in the ionosphere. If there were no geomagnetic field these data would be simply interpreted in terms of movements of the mass of neutral air molecules caused by conventional hydrodynamic forces. However, the geomagnetic field complicates the motion of the charged particles and makes the interpretation of the data much less certain.

The most general method of attack on the problem of the movement of ionization in a plasma in the presence of a steady magnetic field is that of magnetic hydrodynamics in which Maxwell's equations and the equations of hydrodynamics are set up with boundary conditions appropriate to the particular problem. Unless some simplifying assumptions can be made it is often impossible to obtain the solution to these equations and consequently the method is perhaps most satisfactory for the case of a strongly ionized plasma.

An alternative approach, which will be used in this note, may be made by considering the motion of the individual ions and by using the mobilities of the ions and the boundary conditions to deduce the movements of the ionization. In general, this method is only appropriate when the plasma is weakly ionized, which is the case throughout most of the ionosphere.

The application of these methods to a homogeneous unbounded plasma (Sec. 2) shows that if there is a movement of the neutral air there will be both a current flow and a drift of the ionization in the plasma which is superposed on the original air movement. The drift of an irregularity in the plasma (Sec. 6), on which many of the movement data are based, is not necessarily the same as either the neutral air or the ionization as a whole.

The case of an unbounded inhomogeneous plasma presents further complications which are discussed in Sec. 4.

2. HOMOGENEOUS, UNBOUNDED PLASMA

In the absence of a steady applied magnetic field the drift velocity of an ion is related to the applied force by a scalar mobility k. The presence of a magnetic field transforms the scalar, k, into a tensor so that generally the drift velocity is no longer parallel to the applied force. The principal values of the mobility may conveniently be called the longitudinal mobility, k, parallel to the steady magnetic field $\mathbf{B}$, the transverse mobility, t, in the plane

of **B** and the applied force **F** perpendicular to **B**, and the Hall mobility, h, perpendicular to both **F** and **B**.

Simple kinetic theory (see, for example, CHAPMAN and BARTELS[1]) gives the values of these mobilities in terms of the mass, m, collision frequency ν and gyrofrequency $\omega(=eB/m)$ as:

$$k=\frac{1}{m\nu}$$

$$t=\frac{\nu}{m(\nu^2+\omega^2)} \qquad \ldots.(1)$$

$$h=\frac{\omega}{m(\nu^2+\omega^2)}$$

If, for simplicity and because it is the case which concerns us most, we suppose that the force **F** arises from an electric field **E**, we may write the drift velocities in the principal directions using (1) as

$$v_o=\frac{1}{m\nu}eE_{\parallel}=\frac{\omega}{\nu}\frac{E_{\parallel}}{B}$$

$$v_t=\frac{\nu}{m(\nu^2+\omega^2)}eE_{\perp}=\frac{\nu\omega}{\nu^2+\omega^2}\frac{E_{\perp}}{B} \qquad \ldots.(2)$$

$$v_h=\frac{\omega_e E_{\perp}}{m(\nu^2+\omega^2)}=\frac{\omega^2}{\nu^2+\omega^2}\frac{E_{\perp}}{B}$$

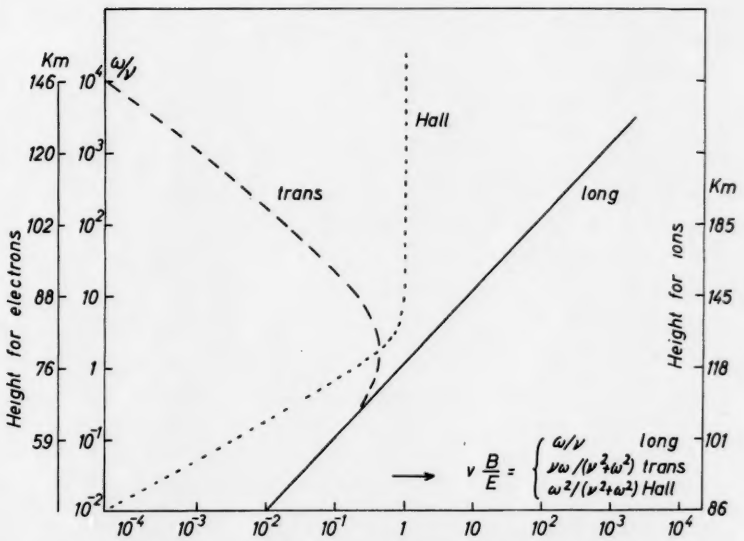

Fig. 1. Drift velocities of ions in the presence of a magnetic field as a function of ω/ν
Drift along the magnetic field B ———
Drift parallel to E and perpendicular to B - - - - - -
Drift perpendicular to E and B . . . . . .

In *Fig. 1* $|v|B/E$ is plotted as a function of ω/ν for the different components of v. Although the ionosphere is not a homogeneous plasma it is useful to know

what values of ω/ν are found at different levels in the ionosphere. To give a rough indication of this scales of height for electrons and ions are shown in the figure, these scales have been derived using NICOLET's[2] values of collision frequency for electrons and with the additional assumptions $\nu_i/\nu_e = 1/50$,* $m_i/m_e = 4{\cdot}5 \times 10^4$, $\mathbf{B} = 0{\cdot}45$ gauss.

We may note that when $\omega/\nu < 10^{-1}$, $t = k$ and $h \ll t$ whereas at low pressures where $\omega/\nu > 10$, v_0 is large, v_t is nearly zero and $v_h = E/B$ independent of the type of ion involved.

The set of Eqs. (2) shows that generally the velocity $\mathbf{v}$ of the ion is not parallel to the applied field $\mathbf{E}$. In the simple case of $\mathbf{E}$ perpendicular to $\mathbf{B}$ the angle between $\mathbf{E}$ and $\mathbf{v}$ is $\tan^{-1}(\omega/\nu)$; thus the velocities of ions and electrons will also not be parallel to one another. An example of the arrangement of the velocities is shown in *Fig. 2*. The current density in the plasma is given by

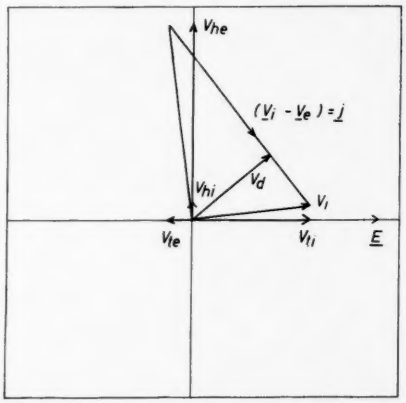

Fig. 2. Drift velocities for ions and electrons in an electric field E, perpendicular to the magnetic field, at a pressure such that $\omega_e/\nu_e \sim 10$

$ne(\mathbf{v}_i - \mathbf{v}_e)$ and perpendicular to this direction the velocities of ions and electrons are equal. Simple calculations from Eqs. (2) (MARTYN[3]) show that this drift velocity perpendicular to the current j is given by:

$$v_d = \frac{\omega_e \omega_i}{\sqrt{\{(\nu_e^2 + \omega_e^2)(\nu_i^2 + \omega_i^2)\}}} \frac{E}{B} \qquad \ldots.(3)$$

This drift velocity is exactly the value which would be deduced by assuming that the ions and electrons were acted on by a force $\mathbf{j} \wedge \mathbf{B}$ due to the interaction of the current and the steady magnetic field.

We see easily from Eqs. (2) that the direction of current flow departs appreciably from the direction of $\mathbf{E}$ in the pressure range where $(\omega/\nu)_e > 1$ and $(\omega/\nu)_i < 1$. At high and low pressures the current is parallel to $\mathbf{E}$ and the drift of the ionization perpendicular to $\mathbf{E}$.

If there is a wind (velocity $\mathbf{C}_0$) in the plasma the movements may be derived either by using Eqs. (1) and an effective force $F = m\nu\mathbf{C}_0$ applied to each

* This assumption is probably reasonable up to a height of about 140 km in the ionosphere, but above that height ν_i/ν_e is likely to decrease due to collisions between ions and electrons.

particle or by using Eqs. (2) with the induced field $\mathbf{E}=\mathbf{C}_0 \wedge \mathbf{B}$ which is equivalent to transforming to axes moving with the velocity C_0. From Eq. (3) it is clear that if $\omega_{i,e} \gg \nu_{i,e}$, $\nu_d = -C_0$ and the ionization remains stationary, whereas when $\omega_{e,i} \ll \nu_{e,i}$ $\nu_d = 0$ and the ionization moves with $\mathbf{C}_0$, i.e. with the neutral gas.

Thus at high pressures the ionization may be moved by the air wind much more efficiently than by an applied electric field, and at low pressures air movement is ineffective in moving the ionization, but an applied electric field moves the ionization with velocity E/B (which is the velocity which would be necessary to produce E by electromagnetic induction).

3. The Bounded Homogeneous Plasma

In the case just considered there was no limitation on the current flow which could take place at any angle to the applied electric field. In the case of a bounded plasma there will generally be some limit on the directions of current flow, there must be no flow of current across the boundaries. If Eqs. (2) lead to a current flow across the boundaries, then a space charge will be set up which will produce a field just adequate to stop the flow of current across the boundary; this does not imply that there will be no drift of the boundary and unless an additional mechanical force is provided the boundary of the plasma will move.

The total electric field to be used in Eqs. (2) or (3) is now the sum of the applied field and the polarization field to prevent current flow across the boundaries; in some cases this polarization field may be much greater than the applied field and the drift velocity, v_d, will be correspondingly enhanced.

4. The Inhomogeneous Plasma

The ionosphere presents a still more complicated problem as the decrease of collision frequency with height makes the plasma inhomogeneous and the nature of the ionosphere limits to some extent the possible directions of current flow.

If the ionosphere were considered as a series of concentric spherical shells the currents and polarization fields would be different in each shell. But it is shown in *Fig. 1* that at most heights the mobility, k, along the magnetic field is much larger than either t or h. Thus a solution which implies differences of electrostatic potential at different points of a line of B must be unsatisfactory. The high value of k will make the lines of B very nearly equipotentials. The polarization fields set up at one level may be partly short-circuited by the ionization at other levels and the problem of the electric fields throughout the ionosphere must be considered as a whole. In particular a polarization field set up in E-region, where the conductivity per ion pair is a maximum, will be carried by the lines of B to the F-region as originally pointed out by Martyn.

5. Applications to the Ionosphere

To apply these ideas to the movements of the ionospheric layers it is necessary to know the currents and electric fields at the different levels. An estimate of the currents may be obtained from magnetograms observed at a suitable

Suppl.
art.II
1956

network of observatories. While it is possible from the magnetic records to show that the source of the variations is external to the earth, it is not generally possible to determine the height of the current system. However, if it is assumed that the currents flow in the ionosphere, then by using a model of the electron density distribution and the variation of collision frequency with height it is possible to estimate the total electric field necessary to drive the "observed" currents.

This electric field may be either an electromagnetic field resulting from movements of the charges in the geomagnetic field or an electrostatic field due to space charges set up in some way.

There are three current systems, inferred from the magnetic effects, which may be of importance in the ionosphere; they are the solar and lunar quiet day variation currents and the current system associated with the magnetic disturbance field.

The quiet day current systems are supposed to be due to the air movements associated with the barometric tides carrying the ionization across the geomagnetic field. It seems fairly certain from rocket studies (SINGER[4]) and from the fact that the conductivity per ion pair is highest near 100 km that these currents flow mainly in the neighbourhood of 100 km. The movement of the ionization in *E*-region would be expected to be derivable from the interaction of the currents and the geomagnetic field. The effects in *F*-region would be due to the electric field in *F* due to the currents in *E*-region. If the air movement were the same at all heights the electric field in *F*-region would be the same as in *E* but this is unlikely and the most probable situation would be that the electric field in *F* was simply the polarization field in *E* modified by the fact that the lines of *B* are equipotentials.

To deduce the movements in *F* it is then necessary to estimate how much of the total electric field in *E*-region is due to polarization charges and how much to induced electric field. This problem has been discussed by BAKER and MARTYN and by FEJER in studies of the dynamo theory. These workers used different models of the ionosphere with different approximations and their results for the ratio of polarization to induced electric field are entirely different.

BAKER and MARTYN[5] assumed that the ionospheric conductivity was independent of longitude and of latitude except for a zone of increased conductivity near the equator, they concluded that in general the polarization field was about 4 times the induced field. FEJER[6] assumed that the ionospheric conductivity varied with latitude in a definite way and deduced that the polarization field was approximately equal to the induced field. It is clearly impossible to deduce accurately the movements of *F*-region from the quiet day magnetic variations until the dynamo problem has been solved for a more realistic ionospheric model.

The currents in a magnetic disturbance are much greater than in the quiet day variations and it is doubtful whether they can be due to air movements. As a first approximation it is probably safe to assume that they are due to electric fields set up by the incoming particles. Two problems remain in deducing the *F*-region movements.

(1) It is now known how much of the current system is in the ionosphere; this is not very serious at high latitudes since the S_D variation which is cer-

tainly due to currents in the ionosphere, predominates at high latitudes. But at middle and low latitudes the problem is serious.

(2) At high latitudes the ionospheric model is uncertain in the presence of incoming particles.

It would be possible if the current system were determined for a particular disturbance, to estimate the fields and use them to determine the expected movements of the *F*-region. This comparison might be useful in checking the various theories involved.

6. The Movement of an Irregularity in the Ionosphere

All the discussion so far has been concerned with the movement of the ionization in a uniform layer; this drift would not be detectable in general although

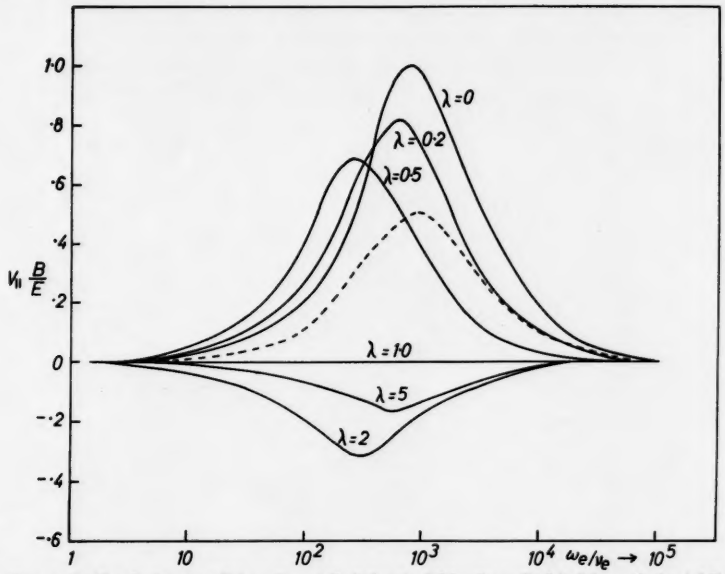

Fig. 3. Drift velocity, parallel to the applied electric field, of a cylindrical irregularity (full line) as a function of the ratio of electron density in the cylinder to that in the surrounding plasma. Drift of the surrounding plasma (dotted line)

it may have important implications for the worldwide distribution of the ionization. The majority of methods of measuring ionospheric drifts take advantage of the existence of irregularities in the regions. It is not at all obvious that such irregularities will move in the same way as the background ionization or with the neutral air if there is a wind.

Martyn[3] attempted to study the behaviour of a cylindrical irregularity, with the axis of the cylinder along the geomagnetic field, in a uniform homogeneous plasma, he was unable to find a satisfactory solution to his problem and concluded that such an irregularity would be unstable. Clemmow, Johnson and Weekes[7] studied the same problem and concluded that there is a steady state solution in which the cylinder moves with a velocity dependent on the ratio λ of the ionization in the cylinder to that in the plasma and on the value of ω/ν.

In *Figs. 3* and *4* the values of vB/E for movement parallel to **E** and perpendicular to **E** are plotted together with the drift velocities for the background ionization. A similar solution was found for the case of an infinite slab with the magnetic field in the plane of the slab and in this case a time varying solution of the equations for small departures from the plasma density was possible; this solution showed that the slab did in fact move with the steady state velocity, changing its form only slowly.

No steady state solution was found for any three-dimensional irregularity where the high mobility parallel to **B** seems to imply that the irregularity will change its form rapidly with time. No solution has yet been obtained for the case of an inhomogeneous plasma.

7. Summary

An ionized layer or an irregularity in such a layer may be moved either by a wind in the neutral gas or by an applied electric field. In comparing the relative efficiencies of these two cases we may compare the velocities of drift resulting from a wind of velocity C_0 and from an electric field $\mathbf{E} = \mathbf{C}_0 \wedge \mathbf{B}$. It

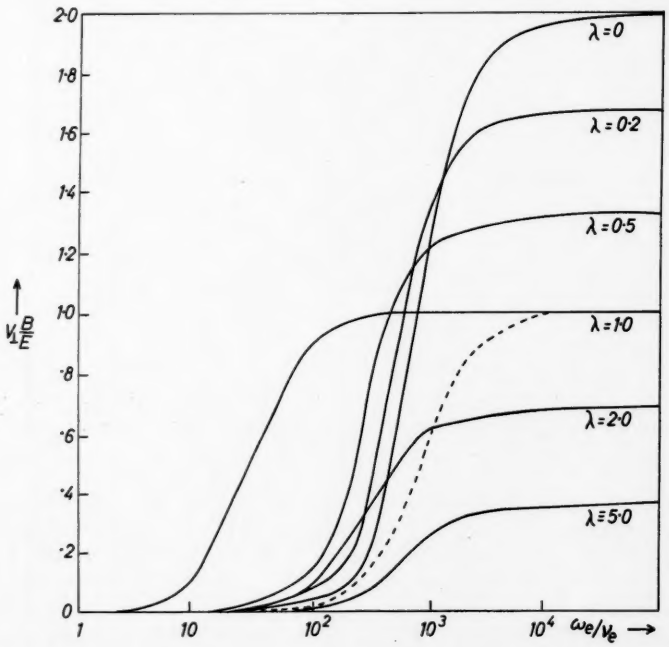

Fig. 4. Drift, perpendicular to the applied electric field, of a cylindrical irregularity (full line). Compared with the drift of the surrounding plasma (dotted line)

should be noted that for the drift of an irregularity shown in *Figs. 3* and *4* the velocity components are relative to the air. If there is a wind C_0, contributing $E_\perp = C_0 B$ to **E** the velocity relative to the fixed observer is $(V - C_0)$.

The discussion presented in this paper leads to the conclusions:

(1) *In F-region* ($\omega_e/\nu_e > 10^4$)

(*a*) A wind is very inefficient in causing drift of a layer, the induced field $\mathbf{C}_0 \wedge \mathbf{B}$ produces a drift $-C_0$ and the ionization does not move.

(*b*) An electric field, due to polarization changes, causes a drift E/B.

(*c*) A cylindrical irregularity, with its axis along B, moves perpendicular to E with a velocity proportional to E/B and dependent on λ. If λ is equally distributed above and below unity the average drift would be nearly E/B; scatter of the estimated drifts could be due to different values of λ.

Fig. 4 shows that a wind could cause movement of an irregularity of the order of C_0 provided the ionization in the irregularity were appreciably different from that in the plasma, drifts for $\lambda \gtrless 1$ would be in opposite directions.

(2) *In E-region* ($10 < \omega_e/\nu_e < 10^4$)

(*a*) C_0 and E are roughly equally efficient in producing drift of a layer. It must be remembered that E is not necessarily equal to $\mathbf{C}_0 \wedge \mathbf{B}$ and may be much larger due to polarization charges.

(*b*) A cylindrical irregularity has now components of velocity parallel and perpendicular to **E**; both components depend rather markedly on λ and the resulting drift velocity for different values of λ is difficult to estimate. Much scatter in apparent drifts would arise from different values of λ.

(3) *In D-region* ($\omega_e/\nu_e < 10$)

The electromagnetic effects are now of little importance and the efficient method of moving the layer or an irregularity would be by a wind.

References

[1] Chapman and Bartels. *Geomagnetism*. Chap. XV; O.U.P., 1940

[2] Nicolet. *J. atmos. terr. Phys.* Vol. 3, p. 200, 1953

[3] Martyn. *Phil. Trans.* A Vol. 246, p. 306, 1953

[4] Singer. *J. geophys. Res.* Vol. 56, p. 265, 1951

[5] Baker and Martyn. *Phil. Trans.* A Vol. 246, p. 281, 1953

[6] Fejer. *J. atmos. terr. Phys.* Vol. 4, p. 184, 1953

[7] Clemmow, Johnson and Weekes. *The Physics of the Ionosphere*, p. 136; Physical Society, London, 1955

THE HEIGHT-VARIATION OF HORIZONTAL DRIFT VELOCITIES IN THE *E*-REGION

I. L. Jones

Cavendish Laboratory, Cambridge, U.K.

Observations of ionospheric drift velocities have been made simultaneously on two neighbouring frequencies. The frequencies used were 2 Mc/s and about 2·5 Mc/s, so that during the daytime, reflections were obtained from the E-region. The heights of reflection on the two frequencies differed by about 5 km, thus information about the drifts at heights separated by this amount could be obtained.

During the winter months it was found that the phase of the semi-diurnal component of velocity, varied with height, the phase being advanced with height.

The fact that the results from the neighbouring reflection heights are different, suggests that they are representative of the conditions near those heights.

The phase change with height is consistent with the observations made on drifting meteor trails.

Introduction

The amplitude of a radio wave singly reflected from the ionosphere is found to vary in a random manner. By observing this fading at the three corners of a right-angled triangle of sides about 1 wavelength, it is possible to determine the drift velocity of electron density irregularities in the ionosphere.

Briggs and Spencer[1] surveyed the results available in 1954, and showed that the observed velocities could be analysed into components which changed with:

(*a*) The season.
(*b*) A period of one day.
(*c*) A period of half a day.

Comparison with the results of other workers using the same method showed good agreement. The results obtained by observing the drifting of meteor trails showed similar behaviour to those obtained by the method of closely-spaced receivers, but the phase of the semi-diurnal component did not agree.

The work described in this paper endeavours to investigate the finer details of these movements, and especially to find how they vary with height in the *E*-region.

Experimental Arrangement

To observe the variation of drift with height, observations were made simultaneously on neighbouring frequencies. The frequencies employed were 2 Mc/s and about 2·5 Mc/s.

Two pairs of receivers were available, and switching between the North-Local, and Local-East pair of aerials was done every 7½ min, so that the mean drift for 15 min periods was obtained on the two frequencies. The recording of the time delays was done on a "Phillips" recorder.

An estimate of the true height separation for reflection of the frequencies used was made assuming a parabolic *E*-layer, and a given critical frequency. This height separation was of the order of 5 km.

Results

Observations of about one week's duration have been made during several months since March 1955. The mean curve was taken on each frequency for

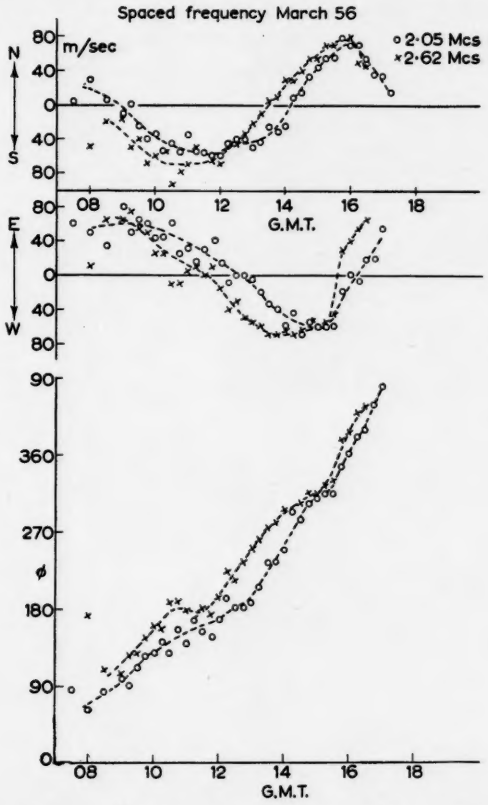

Fig. 1. Measurements of drift on two frequencies, 2·05 and 2·62 Mc/s

a week's observation. This averaging process eliminates the effects that may be present due to turbulent eddies, which could give rise to short term differences at the two levels of reflection.

The results show that during the winter months, the phase of the semi-diurnal component was advanced at the greater heights (*Fig. 1*). The height gradient of the phase was about 5 deg. km^{-1}. During the summer months, the phase of the semi-diurnal component did not vary in any consistent way.

Discussion of Results

One of the great difficulties in the interpretation of drift observations by the method of closely-spaced receivers has been to decide on the height in the ionosphere to which the measurements apply. Any irregularities below the level of reflection could affect the wave as it passed through these irregularities.

These observations of different behaviour of the drift velocity at heights separated by about 5 km show that for the *E*-region, the fading is imposed on the wave within about 5 km of the level of reflection.

Booker[2] has given reasons which suggest that the fading is imposed on the wave near the level of reflection, where the wavelength in the medium is large.

The phase of the semi-diurnal component observed by the meteor workers, Greenhow and Neufeld,[3] in the height range 80–100 km is different from that observed by the diffraction method in the height range 100–120 km.

However, when the phase change with height of the semi-diurnal component is included, the results by these two completely different methods are consistent.

References

[1] Briggs, B. H. and Spencer, M. *Rep. Progr. Phys.* Vol. 17, p. 254, 1954
[2] Booker, H. G. *J. atmos. terr. Phys.* Vol. 7, p. 343, 1955
[3] Greenhow, J. S. and Neufeld, E.L. *Phil. Mag.* Vol. 1, p. 1157, 1955

Suppl.
art.II
1956

RESULTS OF IONOSPHERIC DRIFT MEASUREMENTS IN THE UNITED STATES

VAUGHN AGY

National Bureau of Standards, Boulder, Colorado

No work has been carried out on drift measurements at the Bureau of Standards for the past couple of years. They had about 3 years' data and about 2 years of that was taken with the "Phillips" type of equipment to give time delays and the results are summarized in *Figs. 1* and *2*. These results agree well with those of similar studies made in Ottawa, Canada and at Cambridge, England.

These diagrams represent, averaged over 3 years, 2 months at a time throughout the year, the wind vector (blowing away from the origin) and its general swing throughout the day, determined from data taken near Washington, D.C.; the general character is evident. During the winter months, January and February, there is a pronounced clockwise rotation in phase of the wind, and this diagram might be thought of as representing a constant wind towards the SW of about 50 m/sec with a superimposed semi-diurnal component of about 30 m/sec. As we move on through the year the March and April equinox months show a less pronounced clockwise rotation, but the diagrams for the summer months show that the clockwise rotation still seems to be present. The direction of the average wind changes through the year from SW in January and February to perhaps south in March and April, east during the summer months, May, June, July and August, around to perhaps N in September and October and in November and December back to about SW. Now this can be represented in somewhat different fashion, giving overall averages for the 3 years. If the N–S component and E–W component be plotted against time, both show pronounced semi-diurnal variation and the two will be found to be about 90° out of phase. During the night-time when sporadic-*E* is relatively unimportant, reflections were taken at this same frequency of 2·3 Mc/s off the *F*-layer. The results of these measurements show again a tendency for a clockwise rotation of the wind vector except during the summer months when the rotation seems to be counter-clockwise. Things are not as simple as they seem to be for *E*-region reflections.

Some of the most recent work is that done at Puerto Rico by D. Yerg. He worked at two frequencies, 2·33 Mc/s and 4·57 Mc/s. He finds that, contrary to the results that have been presented in the past, as you move up in frequency, which suggests also that you are moving up in the height at which these drifts occur, that the velocity, at least as measured at Puerto Rico, gets lower instead of higher. He has also made a detailed study of comparing the effect of what he calls the correlation method, a rather detailed and laborious

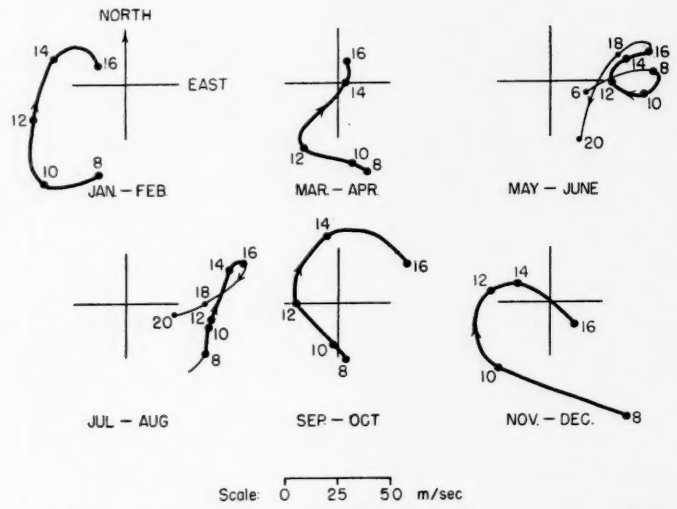

Fig. 1. Polar plot of daytime E-region winds. Bi-monthly averages over a three-year period July 1950–June 1953. Wind blows away from origin

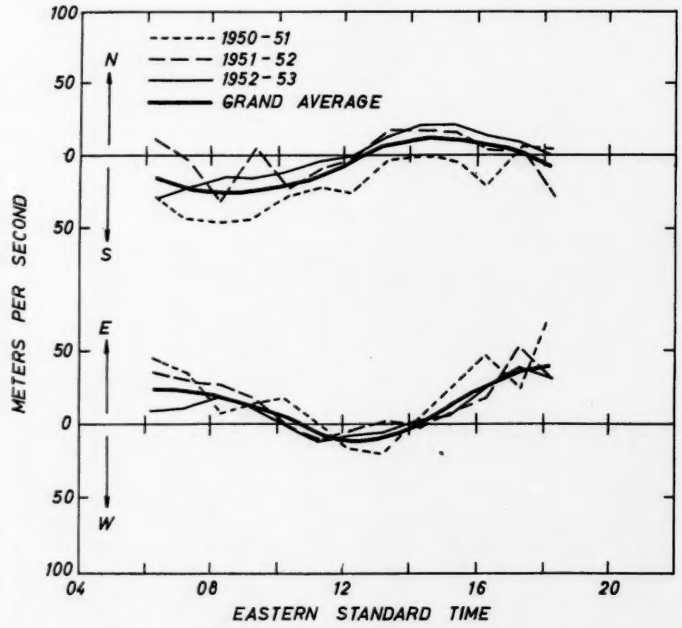

Fig. 2. Annual means of E-region winds

procedure (although he has modified the original methods somewhat), with the method of comparison of similar fades which is Yerg's terminology to describe the Phillips method, and he finds that in general and quite usually the Phillips method gives you more scatter in your observations and quite often much higher values of the drift speeds. In the extreme case an order of magnitude difference may be found between the results you get with the Phillips method and with the correlation method, and he is suggesting quite strongly that even for cases where the fades are similar and the time delays are well-defined, it is probably far better to go to the extensive correlation method than to use the Phillips method in order to get results which have more meaning.

Suppl.
art.II
1956

RESULTS OF IONOSPHERIC DRIFT MEASUREMENTS IN NORWAY

LEIV HARANG
Norwegian Defence Research Establishment

IN the following a survey of the results of *E*-layer drift measurements during a 2-year period 1953–1955 will be given. In the first part the mean seasonal and diurnal values of drift will be given based on the assumption of an isotropic diffraction pattern, in the second part effects indicating anisotropy in the diffraction pattern will be demonstrated.

The drift measurements were made according to the Mitra method, with three receiving points spaced somewhat less than one wavelength apart, the

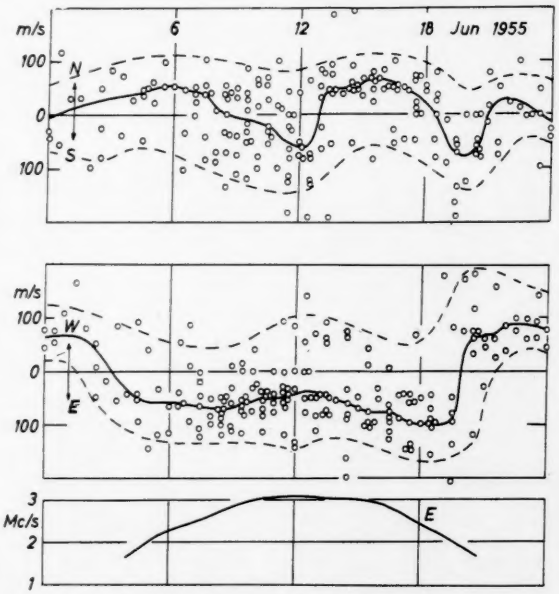

Fig. 3. Values observed during one month

frequency used was 2 Mc/s. During the first year the three complete fading curves were recorded on a three-beam oscillograph. During the last year the time shifts were recorded using a Phillips recorder.

In *Figs. 1* and *2* examples of records are illustrated. In *Fig. 3* the observations during one month are shewn.

Graphs have been prepared showing the diurnal variation during the four

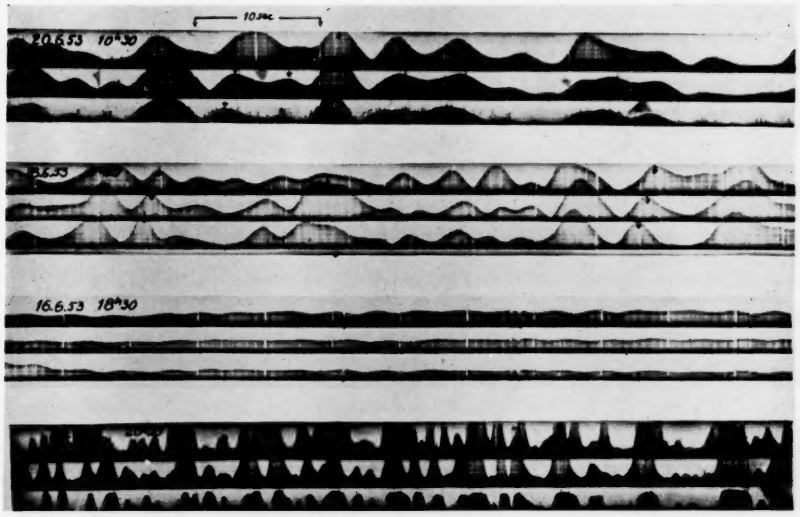

Fig. 1. Different types of fading curves

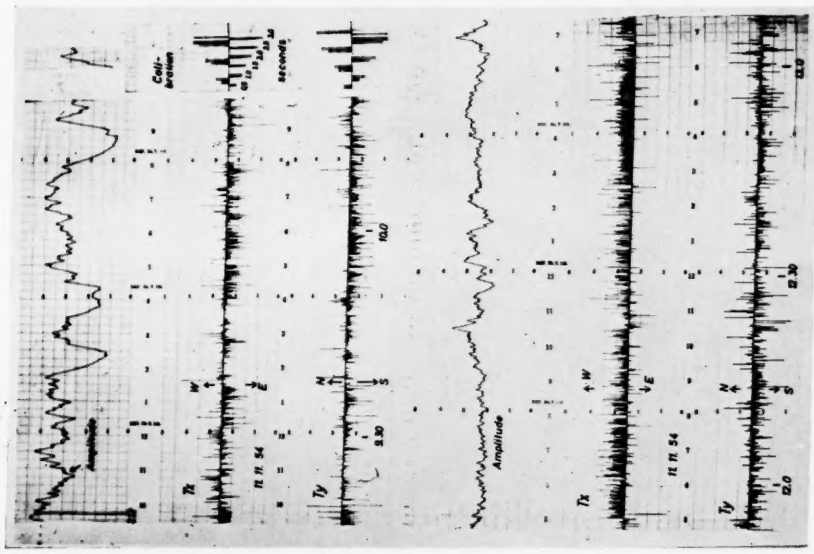

Fig. 2. Drift-records using the Phillips method. The upper curve shows a record with considerable variations in the mean fading amplitude

Supp
Part.
195

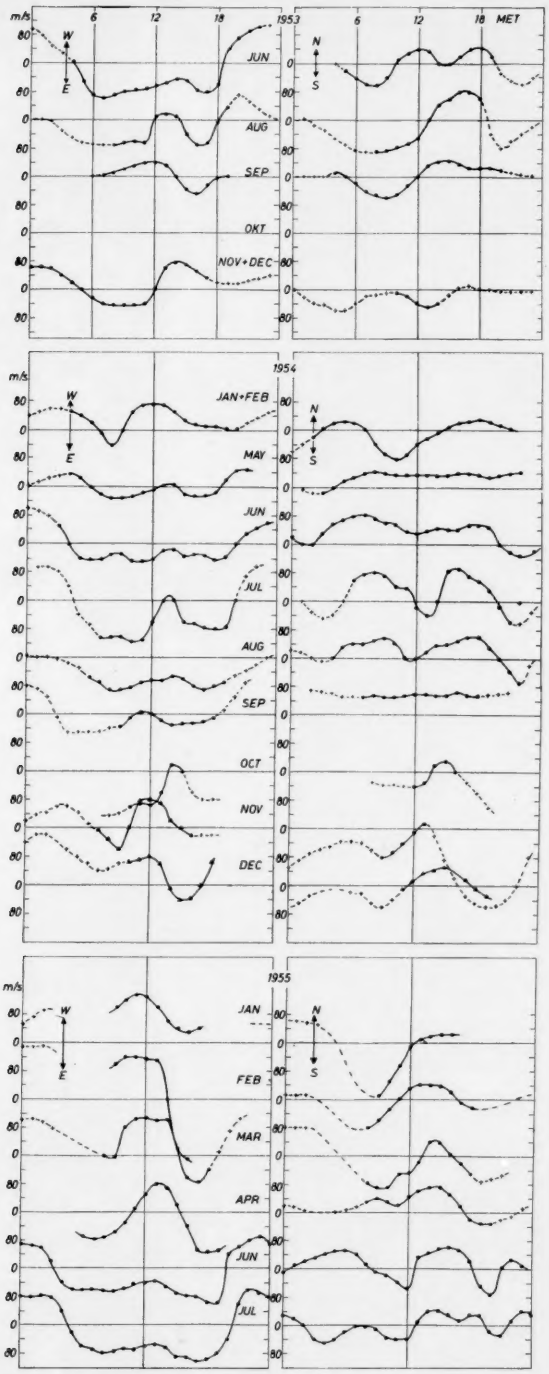

Fig. 4. Monthly mean values of diurnal variation, smoothed. The crosses indicate part of the curve where only few and scattered observations have been available

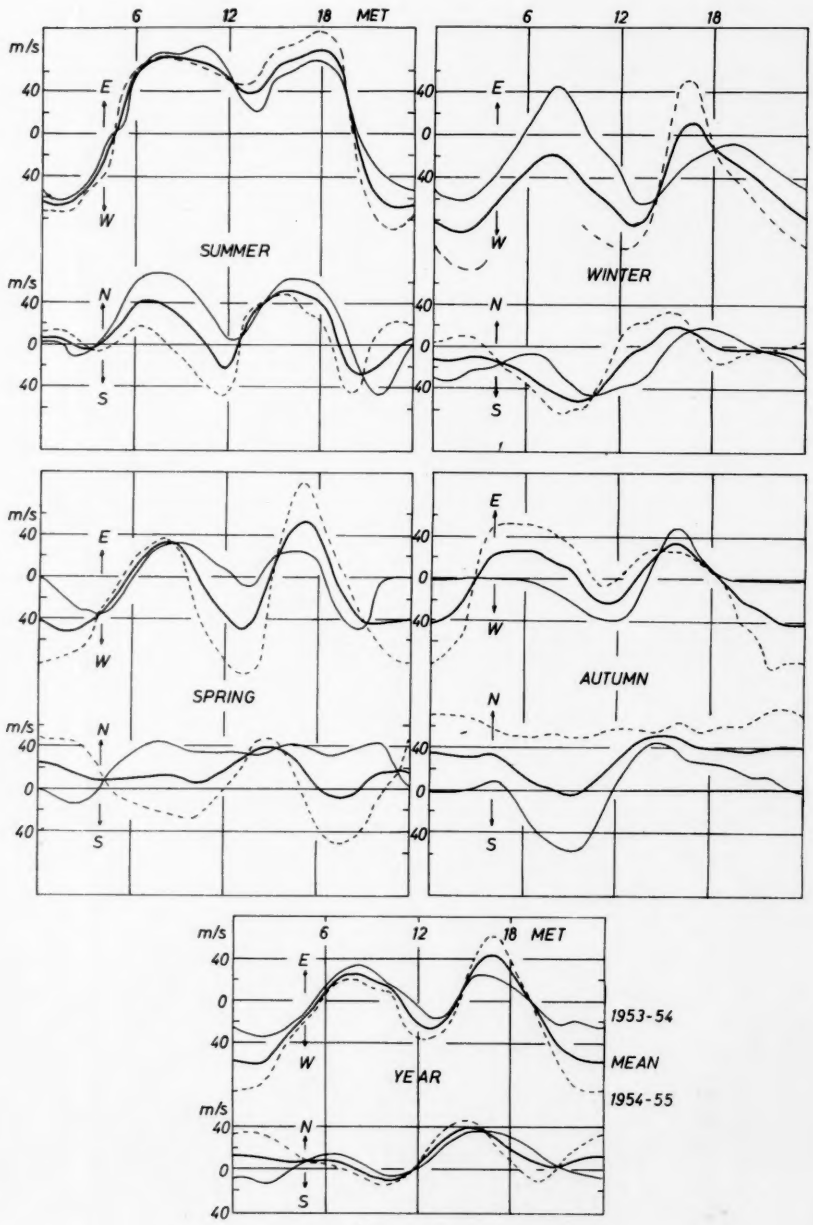

Fig. 5. Seasonal mean values

seasons: winter, spring, summer and autumn, together with annual means for the 2 years. In *Fig. 5* these diurnal variations during the four seasons are demonstrated.

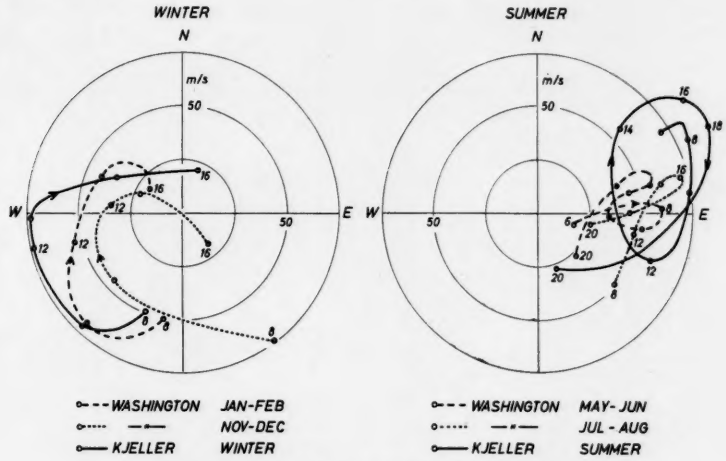

Fig. 6. Wind vector diagrams for Kjeller and Washington

The summer values are the far more reliable ones, and we notice the close resemblance between the two summers 1954 and 1955.

We will now compare the values of drift for Kjeller with similar recordings from Washington and Cambridge. *Fig. 6* shows the change of the wind

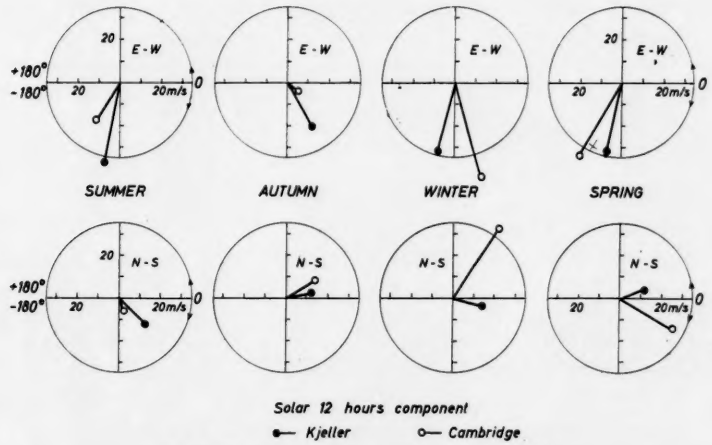

Fig. 7. The 12 hourly term at Kjeller and Cambridge

vector during the day at Washington and Kjeller during winter and summer seasons.

There is an astonishing resemblance in the diurnal trend of the wind vector at these two distant places. The *winter-values* show a very close re-

semblance: there is a constant term corresponding to a prevailing wind towards SW, and with a parallel rotation during daytime. In *summer* we have in both cases a constant term corresponding to a prevailing NE wind, but whereas Washington exhibits a complex structure in the rotation of the wind vector during the day, the Kjeller values show a clear 12-hour period of rotation.

BRIGGS and SPENCER[1] have made a detailed analysis of the 12 hourly

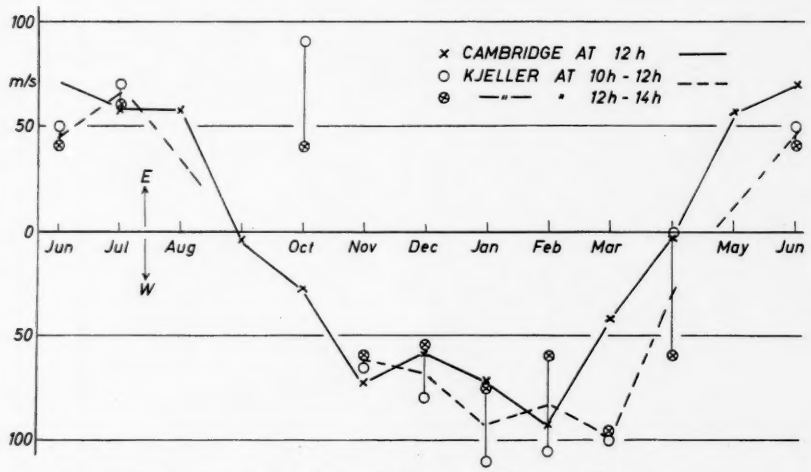

Fig. 8. Noon values of the E–W component at Kjeller and Cambridge

term at Cambridge. A comparison between Cambridge and Kjeller shows a parallel trend in phases and amplitudes for all four seasons.

If we take the annual mean we obtain the following close resemblance:

Cambridge	Kjeller	
$\Delta N = 14 \sin(2t - 12°)$	$\Delta N = 12 \sin(2t - 14°)$	m/sec
$\Delta E = 21 \sin(2t - 93°)$	$\Delta E = 31 \sin(2t - 97°)$	m/sec

Also the annual variation of the noon values show a close resemblance, which is evident from *Fig. 8*.

A closer inspection of the wind vector curves for Kjeller demonstrates the effects of E_s. On *Fig. 9* the values which have been determined from normal E-echoes have been drawn with heavy lines; the night values which have been determined from E_s-echoes have been drawn up with broken lines.

For all four seasons there is a tendency to close the wind vector diagrams in about 12 hours shown by the heavy lines, whereas as soon as the E_s appears in the night there is a strong tendency to show a strong *westerly* wind component. Schematically we may say that the wind vector diagrams consist of (*a*) a circular or elliptic part which makes one rotation in about 12 hours, and (*b*) a strong westerly component appearing during night which is due to E_s.

In the presentation of the values of drift we have up to now assumed an isotropic diffraction pattern from which the true values of drift could be

Suppl.
art.II
1956

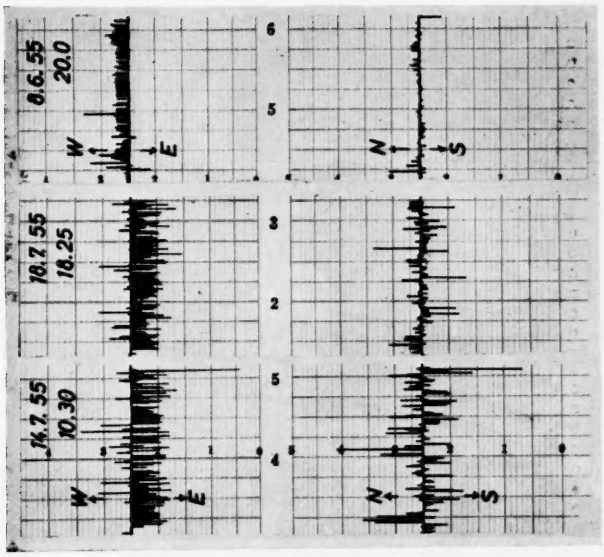

Fig. 11. Records of E–W drifts showing different "widths" of distribution

Sup
Part
19

determined. The effect of E_s, demonstrated through *Fig. 9* indicates, however, that the assumption of isotropy is not fulfilled. The strong westerly wind component during E_s is, however, explained if we assume that the diffraction pattern has "ridges" in N–S direction.

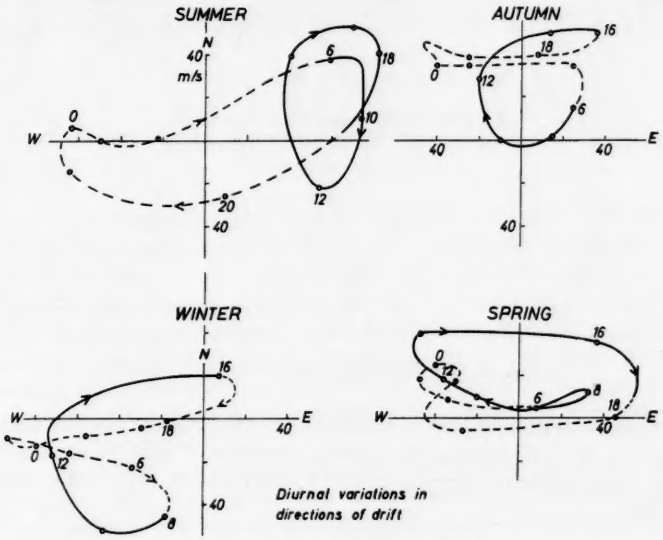

Fig. 9. Wind vector diagrams for Kjeller

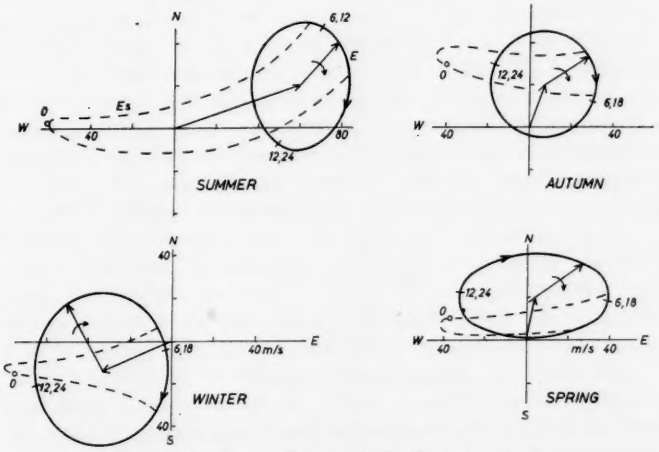

Fig. 10. Wind vector diagrams for Kjeller, schematically

This assumption is confirmed through a study of the probability distribution of the time shifts. An example of this is shown in *Figs. 11* and *12*.

In all three cases we have approximately $T_y = 0$ (no mean time shift along the N–S base). During the day we have a broad distribution curve in T_y

(which is to be expected for an isotropic pattern), during night, however, the T_y-distribution may be very narrow, indicating that the maxima in the

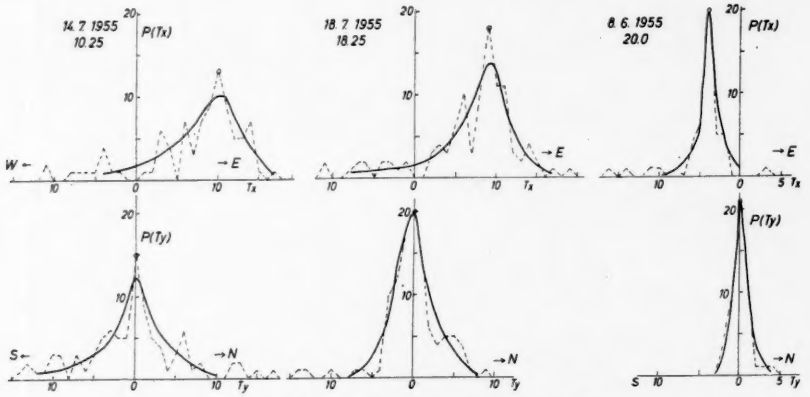

Fig. 12. Distribution curves with decreasing "widths"

field-strength landscape have a tendency to orientate themselves as uniform "ridges" in N–S direction. We have a number of such examples demonstrating the extreme narrowness of the T_y-distribution (N–S direction) of the time shifts.

Reference

Briggs, B. H. and Spencer, M. *Rep. Progr. Phys.* Vol. 42, p. 245, 1954

LARGE-SCALE MOVEMENTS OF THE LAYERS

H. W. WELLS

Carnegie Institution of Washington,
Department of Terrestrial Magnetism,
Washington 15, D.C.

uppl.
rt.II
1956

INITIALLY I would like to make an acknowledgment of the source material which, although based largely on results of investigations conducted by the Carnegie Institution of Washington, also includes some results of back-scatter observations from the National Bureau of Standards principally from Messrs. Silverstein and Tveeton. I will confine my remarks to large-scale irregularities in the *F*-region of the ionosphere, and, I will spend some time in describing the technique since we are now talking in terms of phenomena which are many times greater in dimensions than those which were discussed earlier in these meetings.

I would again like to emphasize that the results to be presented here are largely samples; the observations are not continuous. They may be considered as representative only of the times and conditions under which these particular observations were made.

With any indirect method of obtaining information concerning the ionosphere or upper atmosphere, there is a problem of first identifying or observing some form of irregularity; secondly, it must be identified at several spaced stations and any question of ambiguity should be eliminated; and thirdly, the observational information, which is essentially in terms of a time differential between the different observing stations, must be converted (after making certain basic assumptions) in terms of apparent drift motion with a specified velocity and direction. In making such observations, several techniques may be used. In one method, several fixed-frequency stations may be used to probe the ionosphere overhead and from that obtain a sample of the conditions characteristic over each particular place at a particular time. This gives information principally concerning one level of the ionosphere. In another method, one may use sweep-frequency techniques which become more elaborate and complicated. These have the added advantage of providing information throughout the entire height range of the ionosphere, establishing a dynamic cross-section of ionospheric events. Thirdly, there is another technique which has not been very fully exploited as yet, but which offers a great deal of promise in studies of the large-scale irregularities of the ionosphere. That is the back-scatter technique which gives information concerning events at different heights in the ionosphere (particularly the *F*-layer) and also characteristics of a disturbance with distance. Now there are basic limitations to all of these techniques, since the results are far from continuous. In particular, we found that the difficulties

of operating three sweep-frequency stations simultaneously were so great that the limited amount of useful data hardly justified the level of effort required for the operation. Hence our organization, in the past year or two, has

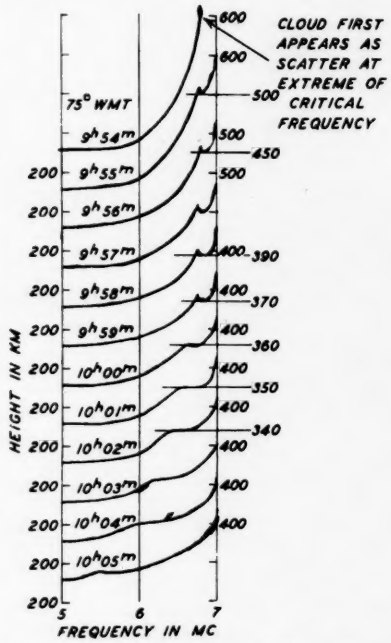

Fig. 1 Typical cloud-like surge in f°F2 taken from Charlottesville record, 20 Sept., 1950

been investigating other simpler means of studying drift movements in the upper atmosphere.

Fig. 1 is a sketch of a typical disturbance. The figure shows a succession of sweep-frequency records taken at intervals of 1 min. There is a "kink" progressing gradually downward and passing through the *F*-region in a period of about 10 min.

Fig. 2 is a back-scatter record from the Bureau of Standards' results, called a synthetic range-time record, for an azimuth of 150°. The definite

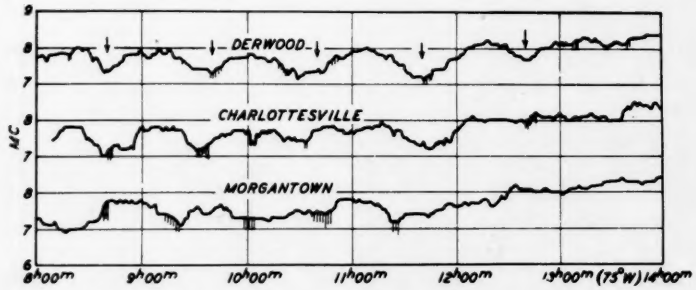

Fig. 3. Variation of f°F2, 29 Sept., 1950 (offset frequency scale)

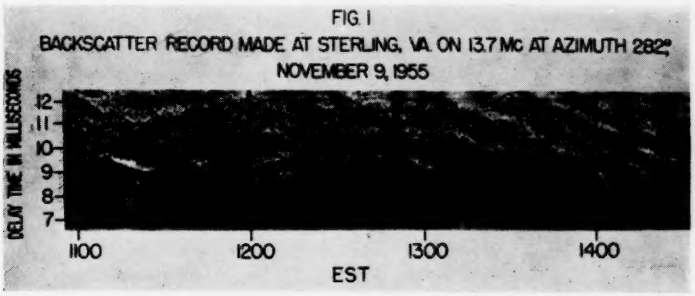

Fig. 2. Back-scatter record made at Sterling, Va., on 13·7 Mc/s at azimuth 282°, 9 November, 1955

uppl.
rt.II
1956

Fig. 4

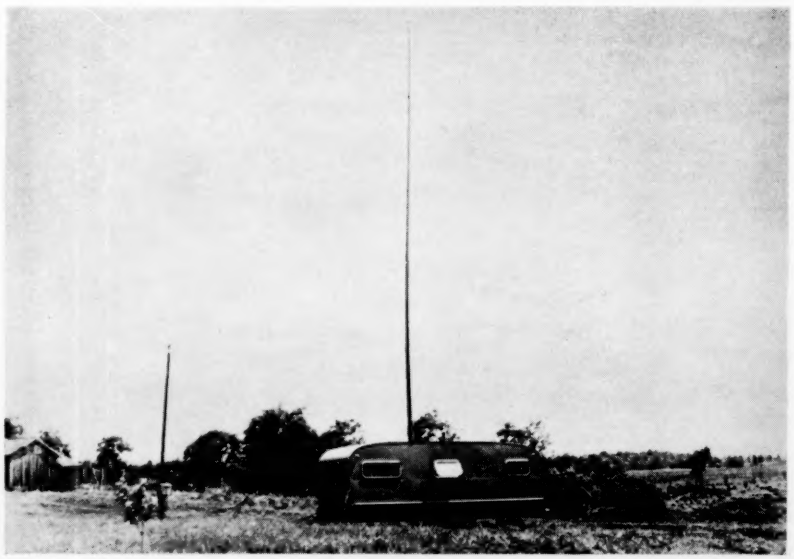

Fig. 5

Supp
Part.
19

ridges in the figure are evidence of large-scale disturbances which are quite similar in nature to those which we have observed using the sweep-frequency techniques.

In *Fig. 3* are given graphs of critical frequencies for stations spaced 150–200 km or more apart on the legs of a triangle. Features of the wavelike variations may be identified and applied to establish essential features of a large-scale traveling disturbance. The graphs refer to (1) Derwood, the base station in

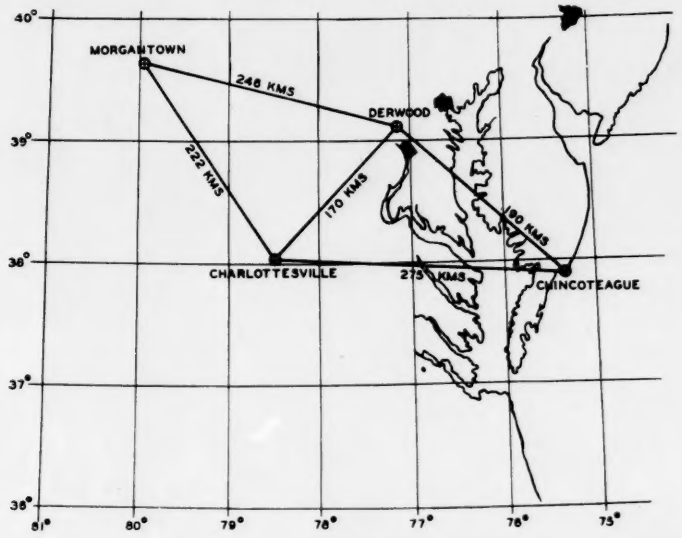

Fig. 6

Maryland near Washington, D.C., (2) Charlottesville, Virginia, which is the site of the University of Virginia, and (3) Morgantown, West Virginia, at the location of West Virginia University.

Fig. 4 shows the mobile laboratory which was used in our investigations. A sweep-frequency instrument of the panoramic type was housed in the trailer. This could be moved around fairly readily, even over some of the mountainous regions in the eastern United States.

In *Fig. 5* we see one of the instruments in operation at a location not too far from Washington, D.C. Adjacent to the trailer, a portable mast has been erected. The antenna system is not shown, but it is a scaled-down version of the inverted delta antenna which I think evolved from a suggestion by Cox. The observing networks which we used are shown in *Fig. 6*. One triangulation system was between Derwood, Maryland; Morgantown, West Virginia, a distance of nearly 250 km; and Charlottesville, Virginia, which is southwest of Washington, approximately 170 km. Later, for some special eclipse observations, we used another network based on Derwood, Charlottesville and Chincoteague, Virginia. Analyses of the eclipse data showed some interesting results concerning the characteristics of the large-scale traveling disturbances in the ionosphere.

After operating with the above triangulation networks we established another network using much shorter base-lines for the principal objective of

uppl.
rt.II
1956

minimizing the confusion or identification problem. *Fig. 7* shows the station separation to be 30 and 20 km, respectively. A fourth station indicated at Glenwood was used as a shock point on our calculations. In other words, the apparent drift or movement of an irregularity identified at the three stations was converted into a vector of velocity and direction. We then compared the observed and computed arrival times at the fourth station as a check on the accuracy of our system.

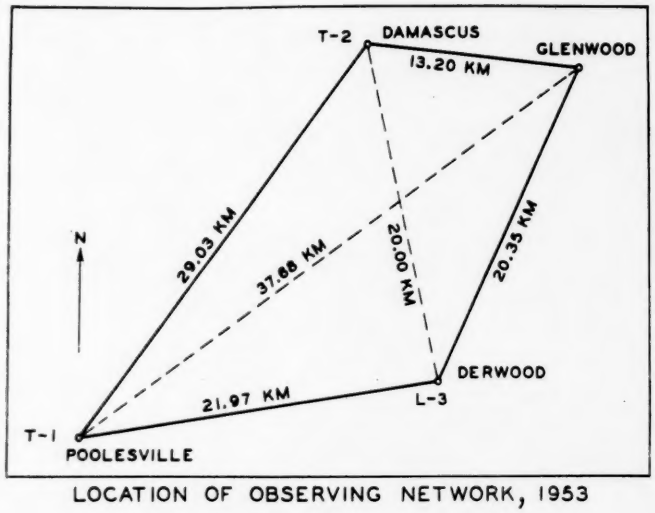

Fig. 7. Location of observing network, 1953

Some of these results are shown in *Fig. 8 (a)*. I will point out briefly that there is a range of apparent velocity from 60 to about 150 m/sec which agrees with the results of other investigators. In particular there seems to be a predominance of velocities in this particular range. Results of drift measurements are plotted as vectors on *Fig. 8 (b)*. Velocity is determined from the concentric circles at 50, 100, 150, and 200 m/sec and directions east, south, west, and north as indicated. There is a notable lack in these particular observations of apparent movement in the third quarter. I do not know that this has any particular significance. There is a predominance of movements *into* the east, often with a southerly component.

Velocity components obtained from back-scatter observations of the National Bureau of Standards are shown in *Fig. 9*. We must convert the scales, since this is a velocity component in kilometres per hour (100 m/sec corresponds to 360 km/hr). There appears to be a fair degree of consistency in morning and mid-day results, somewhat greater than 100 m/sec, followed by a greater range of velocity component in the evening.

In the following I wish to emphasize the opportunity of adding another dimension to knowledge of traveling disturbances in the *F*-region of the ionosphere, a dimension which is achieved through the use of sweep-frequency techniques.

It is recalled that *Fig. 1* showed the downward progress of a disturbance

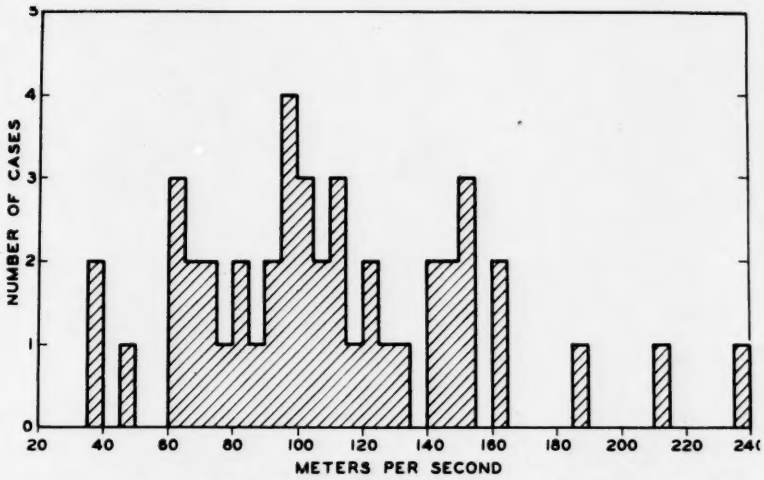

VELOCITY DISTRIBUTION, SEPTEMBER 8-24, AND OCTOBER 10-19, 1953

Fig. 8 (a). Velocity distribution, 8–24 Sept., and 10–19 Oct., 1953

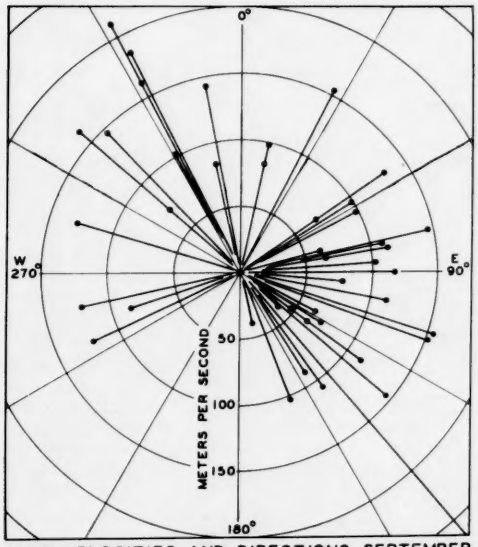

WIND VELOCITIES AND DIRECTIONS, SEPTEMBER 8-25, AND OCTOBER 10-19, 1953

Fig. 8 (b). Wind velocities and directions, 8–25 Sept., and 10–29 Oct., 1953

through the *F*-layer. The apparent *vertical* component of *velocity* is determined from the time interval required for transit through the *F*-layer after converting to true heights. A horizontal component of velocity and direction may be

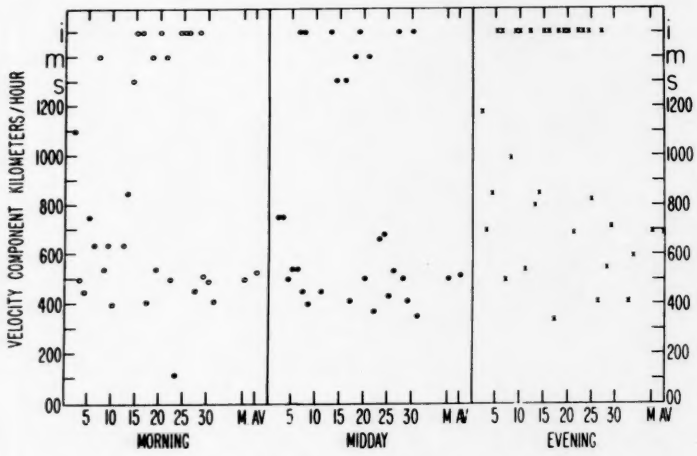

Fig. 9. Variation of average velocity component, December 1952

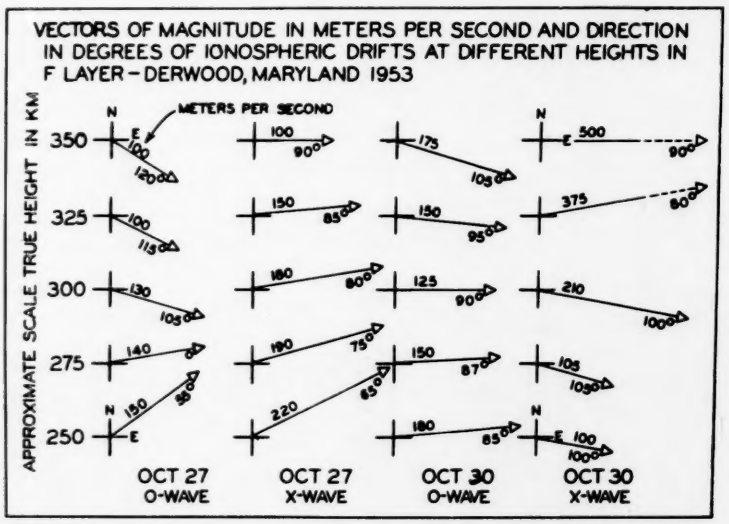
VECTORS OF MAGNITUDE IN METERS PER SECOND AND DIRECTION IN DEGREES OF IONOSPHERIC DRIFTS AT DIFFERENT HEIGHTS IN F LAYER – DERWOOD, MARYLAND 1953
APPROXIMATE SCALE TRUE HEIGHT IN KM
METERS PER SECOND
OCT 27 O-WAVE
OCT 27 X-WAVE
OCT 30 O-WAVE
OCT 30 X-WAVE

Fig. 10. Vectors of magnitude in metres per second, and direction in degrees of ionospheric drifts at different heights in F-layer—Derwood, Maryland, 1953

obtained at a number of different true heights in the *F*-layer by analysis of sweep-frequency observations at three stations, preferably with short baselines as indicated earlier.

Some results based on analysis of both ordinary and extraordinary wave components are shown in *Fig. 10*. On the left is a scale of approximate true

Suppl.
art.II
1956

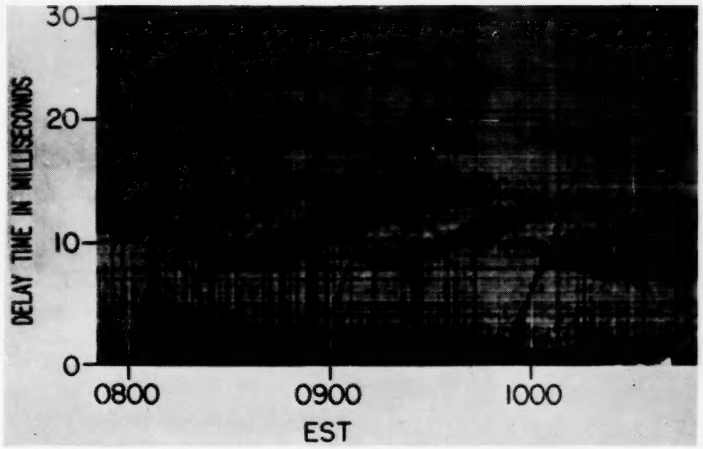

Fig. 11. Synthetic range-time back-scatter record at azimuth 150°, 3 Dec., 1952

Supp
Part.
195

height across the *F*-layer. The arrows are vectors showing magnitude and direction of drift motions at each significant height. For example, the Oct. 27 "*O*"-wave analysis shows a drift of 100 m/sec moving slightly south of east (120°) at a level of 350 km corresponding to the height of maximum ionization. As this disturbance progresses downward through the *F*-layer the apparent velocity increases to 150 m/sec and the direction swings counterclockwise to nearly northeast (55°). The events of Oct. 30 may be described in similar fashion. In each case the "*O*"- and "*X*"-wave analyses are for the same disturbance. The extent of agreement between "*O*"- and "*X*"-wave results is influenced by dispersion of the wave components and by any other factor affecting the precise timing or identification of a disturbance at the separate stations.

In *Fig. 11* we have another back-scatter record from Sterling, Virginia, at 13·7 Mc/s looking into the west. Your attention is invited to the pronounced

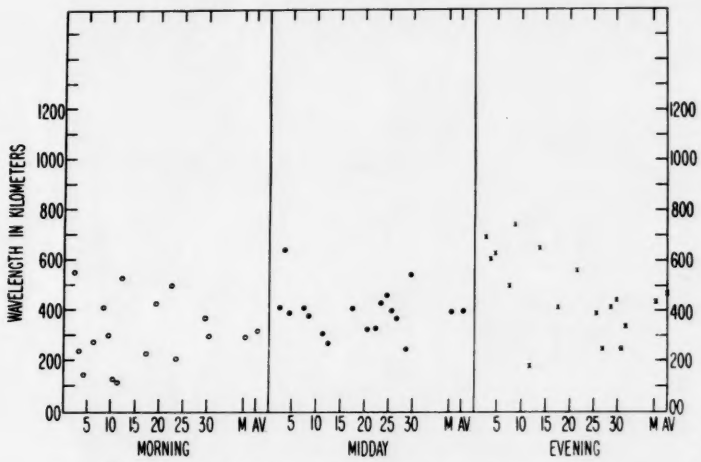

Fig. 12. Variation of average wavelength component, Dec. 1952

ridges or strata which are superimposed on the other conditions of turbulence. Inspection of a particular ridge shows that it is sloped so that it appears to get closer as time progresses. In other words, the disturbance is moving *toward* the observing station. If we now re-examine *Fig. 2* which was made looking into the southeast (150°) we will observe that the slope of the ridges has changed and the disturbances are moving *away* from the observing station. Although these records of the National Bureau of Standards were made in different years, but the same month, their results independently verify the predominant characteristics of movement into the east during the hours of daylight.

Since the interval between successive ridges in the back-scatter records may be considered to be a measure of wavelength for a series of disturbances, it is interesting to examine analyses as shown in *Fig. 12*. Nearly all of the events are included between 200 and 400 km in wavelength. There is no significant difference between morning, midday, or evening. Stations observing at vertical incidence along the direction of movement (perpendicular

to the wave front) would note a maximum differential at a spacing of one half-wavelength. Similarly, stations spaced along the wave-front would be expected to vary more or less in phase. The variations of critical frequencies at three stations within a few hundred km of each other, as shown earlier in *Fig. 3*, may also be interpreted in a similar fashion after velocity and direction have been established.

In summarizing our knowledge of these events, I draw your attention to the evidence of both vertical and horizontal components of apparent movement. The magnitudes of the vertical and horizontal velocity components often appear to be similar so we may now visualize these disturbances as having inclined wave-fronts. The basic assumptions necessary to our analyses regarding size of the irregularities (large compared with spacing of stations in the triangulation net) have been verified. The persistence or lasting qualities of these large-scale *F*-region disturbances continues to be an interesting problem and their basic nature or cause has yet to be resolved. One investigator (Munro in Australia) is attempting to track such disturbances across continents with considerable promise of success.

The effects described here are definitely independent of magnetic activity. In fact, some of our most useful observations were obtained during conditions of extremely quiet magnetic conditions. In addition to the apparent inclined wave-front, these events appear to have more characteristics of wave-like motions rather than winds involving physical transport in the *F*-region. In this respect I am in complete accord with the remarks of Dr. Weekes at an earlier session. However, it may be in order to suggest another possible mechanism for the propagation of this type of disturbance; that is, a form of compressional wave which could be propagated without the added complications of electric fields.

The Carnegie Institution of Washington expects to continue its work on traveling disturbances or "winds" in the upper atmosphere through the use of radio star scintillation techniques. Very preliminary results from interferometers at 27 Mc/s operating over a base line of about 20 km indicate that all correlation is *not* lost, especially for the slow type of scintillation. The program is just getting under way and I can do no more than mention this as a very preliminary observation.

MOVEMENTS OF IONOSPHERIC IRREGULARITIES OBSERVED SIMULTANEOUSLY BY DIFFERENT METHODS

I. L. Jones, B. Landmark* and C. S. G. K. Setty
Cavendish Laboratory, Cambridge, U.K.

The horizontal drift of ionospheric irregularities have been measured simultaneously by means of:

(*a*) *Closely-spaced receivers, a common transmitter being used.*
(*b*) *More widely-spaced transmitters, received at a single receiving station.*

The results obtained by the two methods have been compared.

The large-scale irregularities and those irregularities which produce rapid variations of amplitude at the ground are found to move together.

uppl.
rt.II
1956

1. Introduction

Movements of large-scale irregularities in the *F*-region of the ionosphere have been studied by various workers: Beynon,[1] Munro,[2] Price[3] and others. All investigations have shown that the large-scale irregularities move with a horizontal drift velocity of about 100 m/sec^{-1} in a direction showing seasonal and diurnal variations. The results are in fair agreement with those found by observing the rapid variation of amplitude at closely-spaced receivers.

The purpose of the investigation to be described in this note was to make a detailed comparison of the results of the two kinds of measurements. Observations were made in Cambridge in the period 1 March to 15 May, 1956 on waves reflected from both the *E*- and the *F*-layers. The results from these observations are described in more detail elsewhere (Jones, Landmark and Setty[4]) and in this note therefore only a brief account of the results obtained for waves reflected from the *F*-layer will be given

2. Results

In order to determine the movements of large-scale irregularities in the *F*-layer, the waves from three spaced transmitters were received at a single receiving station, and the three group heights and amplitudes were recorded together as functions of time. The transmitters, at Cambridge, Hinxton and Swaffham Prior, were located as shown in *Fig. 1*. The common receiver was at Cambridge. A constant frequency of 4·1 Mc/s was used.

A typical example of observed variations of group height during conditions when a large-scale distortion in the *F*-layer was passing overhead is shown in *Fig. 2* (*a*) and the observed variations of amplitude are shown in *Fig. 2* (*b*).

* On leave from the Norwegian Defence Research Establishment.

Previous workers have deduced the drifts from observations of group height only. We found that observations of the amplitude bursts (isolated increases of the mean amplitude) was at least as useful. The obvious advantage of this method is that amplitude bursts occur more often than well-defined distortions in the group height traces.

The magnitudes V_b and directions ϕ_b of the velocities of the large-scale irregularities determined by method (*b*) are compared in *Fig. 3* with the

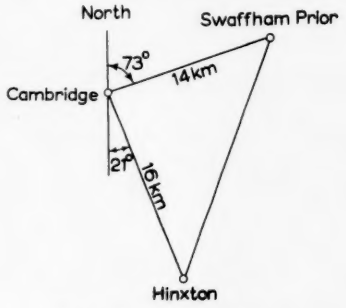

Fig. 1. Location of transmitters

corresponding magnitudes V_a and directions ϕ_a determined simultaneously by method (*a*) for the small-scale irregularities. In those cases when both amplitude bursts and distortions in the group height traces were observed the mean values of the velocities deduced by these two methods were plotted. We see that the directions found by methods (*a*) and (*b*) agree very well.

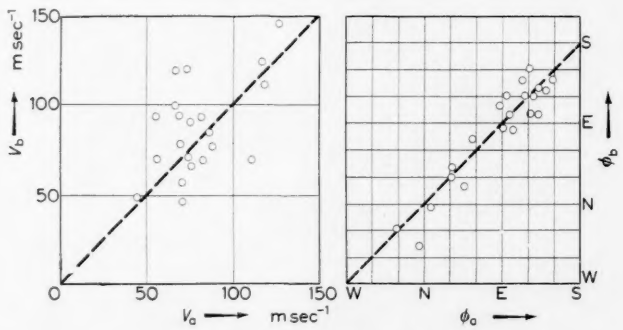

Fig. 3. Comparison of results

The observed magnitudes do not show very good agreement, but the observed correlation is just significant.

The main conclusion from these results is that the irregularities which produce the rapid fading during the bursts, and the large-scale distortions which produce the bursts move together. There is, of course, still the possibility that the fading in between the bursts is produced by irregularities whose movements are different from those of the large-scale distortions. To find out whether or not this was so, the velocity before and after each burst

Suppl.
art.II
1956

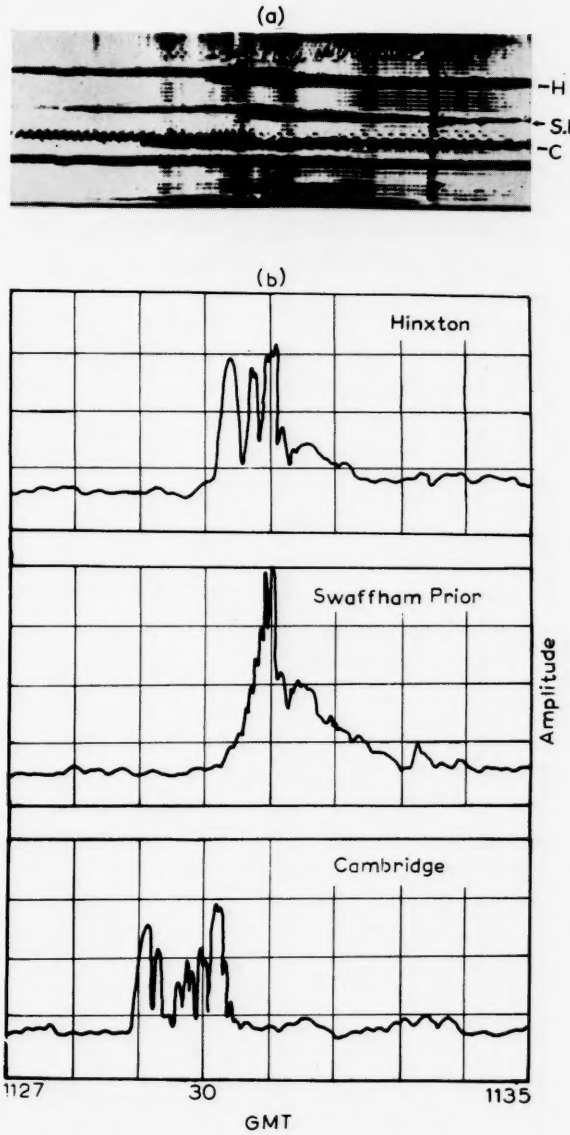

Fig. 2. (a) Typical z-traces, (b) Typical bursts of amplitude

Sup
Part
19

has been determined when possible. The difficulty here was that between the bursts the fading was often so quiet that it was difficult to determine a reliable velocity. Although a good agreement was not found between the values deduced during the bursts and the means of those deduced before and after the bursts, it was found that when good agreement was found between the values deduced before and after the bursts, the values deduced during the bursts also gave the same answer. It was therefore concluded that the large scale irregularities and those irregularities which produce rapid variations of amplitude at the ground move together.

One of us (B.L.) is indebted to the Royal Norwegian Council for Scientific and Industrial Research for a grant enabling him to work at the Cavendish Laboratory.

We have benefited much from discussions with Mr. J. A. Ratcliffe, Dr. B. H. Briggs and Mr. D. M. Schlapp.

References

[1] Beynon, J. G. *Nature, Lond.* Vol. 162, p. 887, 1948

[2] Munro, G. H. *Nature, Lond.* Vol. 162, p. 886, 1948; *Proc. Roy. Soc.* A Vol. 202, p. 208, 1950

[3] Price, R. E. *The Physics of the Ionosphere;* Physical Society, London, 1955

[4] Jones, I. L., Landmark, B. and Setty, C. S. G. K. *J. atmos. terr. Phys.* Vol. 10, p. 296, 1957

Suppl.
art.II
1956

MEASUREMENTS OF IRREGULARITIES AND DRIFTS IN THE ARCTIC IONOSPHERE USING AIRBORNE TECHNIQUES

GEORGE J. GASSMANN
Air Force Cambridge Research Center, Cambridge, Mass.

1. INTRODUCTION

THE advantage of using airborne measuring devices in ionospheric research is obvious. First, one is able to conduct measurements in regions of the globe otherwise inaccessible. More important is the fact that the aircraft is traveling faster than most of the ionospheric irregularities. The basic arrangement used here is an Ionospheric Recorder installed in an airplane, with special antennas and with devices for recording the normal $h'f$ representation, the time and the course of the aircraft and the amplitude of the ionospheric reflection. The type aircraft used is a C97 Boeing Stratocruiser. Of course, it has not been intended to add just another ionospheric station to the number already existing on ground. Accumulation of data for statistical evaluation is impossible anyway. But the idea is to use the airborne equipment in logical connection with the movement of the aircraft for the purpose of studying the dynamic behavior of the ionosphere. The airborne operations have to follow certain techniques which have to include both equipment and aircraft. The first phase in the development of such techniques with respect to the arctic is described here.

2. INTERPRETATION OF $h'f$ RECORDS

The airborne $h'f$ records obtained in 1954 and 1955 in the area between Fairbanks, Alaska and Thule, Greenland and the North Pole with a total of about 70 flying hours show the same common features as already known from many years of records at Arctic ionospheric stations. Since the airborne technique deals with individual phenomena on the records changing from frame to frame, it has been found necessary to attempt the interpretation of characteristic arctic $h'f$ records. The most important feature to be investigated was the "spread", which appears very often as the tail of the vertical trace toward greater virtual heights and greater frequencies. One can explain this sort of spread by assuming a scattering layer below the reflecting ionospheric layer. Then a great variety of triangular round-trip ray paths will return to the recorder. Frequencies much higher than the critical frequency of the layer according to the secant law come back only in very oblique rays and consequently with long travel times so causing the ascending tail on the $h'f$ record. This explanation, however, after examining the airborne records has been considered unsatisfactory for several reasons. The

phenomena observed suggested mirror-like reflections on steep surfaces and indicated that the oblique round trip ray paths prefer the magnetic N–S plane.

In recent years work on radar reflections from aurora indicated that large areas of the arctic ionosphere often seem to be interspersed with laminae, the plane of which includes the geomagnetic vector. Since this assumption often has to be made even when no aurora is present, it suggests itself for the explanation of the spread, too.

Fig. 1 schematically depicts all possible ray paths in the N–S plane under the schematic assumption of interspersed partial reflecting laminae everywhere in the ionosphere. Each ray path is passing through a multitude of

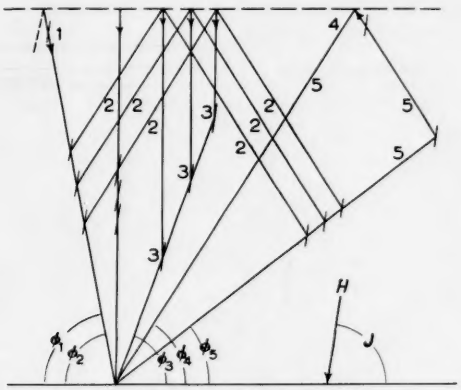

Fig. 1. Schematic of round-trip ray paths

laminae and is losing intensity because each lamina subtracts a certain amount of energy by partial reflection. According to the optical laws this effect must be greatest for ray directions nearly parallel to the plane of the laminae. One can see that in high magnetic latitudes this effect, if present at all, must be detectable for vertical ray paths. The vertical ray path which is the only one normally returning to the recorder would appear attenuated when such conditions take place associated with "spread". On the other hand, all rays leaving the transmitter in other than the vertical direction now have several chances (in the N–S plane) of returning to their origin. In *Fig. 1* five possible round-trip ray paths are indicated. Holding the operating frequency constant and varying the angle of departure, one obtains for each kind of ray path a certain variety. The ray paths 2 and 3 are possible in a twofold (three rays for one are drawn in) or two dimensional variety; the ray paths 1, 4 and 5 occur with a one-dimensional variety. The later ones need *one* partial reflection during their round trip. The ray paths 2 and 3 need *two* partial reflections. Each variety is possible only within certain limits of departure angles. The ray paths 1 and 4 are considered as most important in the Arctic for reasons mentioned later. These round-trip ray paths are possible with departure angles $90° > \phi > (90° - \mathcal{I})$ where $\mathcal{I}$ is the geomagnetic inclination. This permits a wide range of angles in the Arctic which is necessary to explain the observed spread.

Fig. 2 depicts the same ray paths as *Fig. 1* but in an actual ionosphere. The drawing is made with help of the results of the work of POEVERLEIN[1] and that of RYDBECK[2] on ray path construction. Details are discussed below. If we confine ourselves to the ray paths 1 and 4, corresponding *h'f* traces can be constructed. This has been done using the SMITH method[3] of the National Bureau of Standards. *Fig. 3* shows the result. For simplicity of construction 90° has been taken for the geomagnetic inclination. But almost identical curves result from other angles of the earth's magnetic field occurring in the Arctic.

Depending on whether one keeps the departure angle ϕ or the distance B constant one obtains one or the other variety of oblique traces. The envelope of the curves turns out to be what is actually observed as the spread or tail of

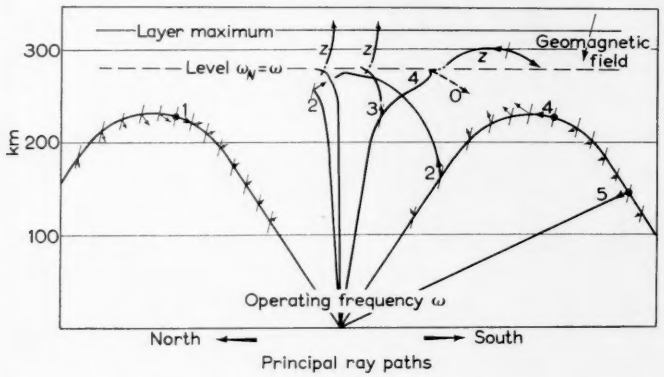

Fig. 2. Principal ray paths

the vertical trace. It can be mentioned here that the construction of corresponding traces resulting from ray path 2 gives a very similar tail as on this figure. Ray path 5 results in an envelope ascending to the right more steeply. In a uniformly smooth ionosphere, where no values of ϕ or B are particularly preferred by casual inhomogeneities, the space above the envelope on *Fig. 3* should not show individual traces but a gradual change in shadowing. The experimental traces, however, show individual curves similar to the ones constructed for constant ϕ. If the interpretation proposed (oblique ray path traveling up and down the same way) be accepted, this observation can easily be explained by inhomogeneities in the space between the ground and the reflection point. This is one point to support the preference of the ray paths 1 and 4.

One important feature of these oblique traces follows from *Fig. 2*. The ray paths are drawn for one particular operating frequency. Now one may consider a slightly higher frequency and the same departure angle. The turning back point of ray path 1, 4 or 5 will shift toward greater distances from the recorder. Now take the case in which the ionosphere overhead is not interspersed with laminae but an area southward is. If this area approaches or if the airborne recorder travels toward this area, such parts of the traces must appear first which correspond to higher frequencies.

Figs. 4 and *5* show such phenomenon observed while the airplane was

traveling toward the geographical North Pole coming from the geomagnetic Pole. The frames have been taken 3½ min apart. One can see one of the oblique traces (actually a bundle of traces) appearing first *in part only* and extending later to lower frequencies. We have observed this phenomenon several times under similar circumstances.

These *h'f* records show also an effect which may be expected according to the foregoing, namely that the vertical trace is weakened. In these frames no vertical traces can be seen at all (a fact which cannot be deduced from the single records but by examining the whole sequence on 16 mm motion picture film). This phenomenon of missing or weak vertical traces seems to be a common feature of Arctic records; during a magnetic storm it occurred during 50 per cent of the time.

If the condition of the ionosphere described as interspersed with laminae

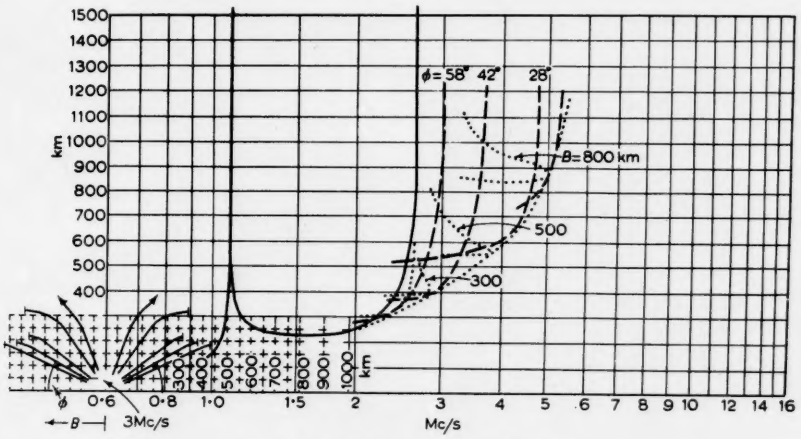

Fig. 3. Partial reflections from vertical laminae

develops at higher levels first, then the spread must appear first associated with the trace of the higher layer. This phenomenon appears in *Figs. 6* and *7*. Although, unfortunately, the gain of the receiver apparently was changed at a time between *Figs. 5* and *6*, it can be seen in *Fig. 6* that the spread of the *F*2-trace already is as strong as 16 min later. No spread of the *F*1-trace can be seen in *Fig. 7*. Before and after this period, high activity in the appearance of the *F*2-trace had been observed.

High activity means often the appearance of traces corresponding to ray path 3 (vertical reflection of the *o*- (or *z*-) and *x*-component in a bent ray path). This ray path causes the original vertical trace unchanged in shape to be shifted to greater heights. *Fig. 8* shows two of these traces. Traces like those have been observed many times at ground stations. They seem to come down from greater heights but very seldom go up again. In the geometry of *Fig. 2* this can occur only if the laminae responsible for ray path 3 are traveling with a component toward magnetic north. The airborne equipment is able to prove or disprove this proposal but until now there has been no opportunity to do it.

The spread in this interpretation refers to the ionosphere in the N–S plane. If parts of the ionosphere in the N–S plane are considerably different or disturbed, then parts of the complete spread must be missing or disturbed, too, if compared with the complete spread constructed in *Fig. 3*. *Figs. 9* and *10* show how the spread develops during a magnetic storm.

The fully developed spread changes within 3 min into a shape which follows from the construction (*Fig. 3*) if one omits ray paths with departing angles between 20° and 30°. If the spread were created by an omnidirectional process a phenomenon like this seems to be hardly explicable.

The interpretation of the "spread" as given here is supported by an observation of ELLIS and REBER[4] in Australia. They observed that the shielding effect of the ionosphere for reception of cosmic noise (normally active up to the critical frequency, for a source overhead) in cases of spread stops at the

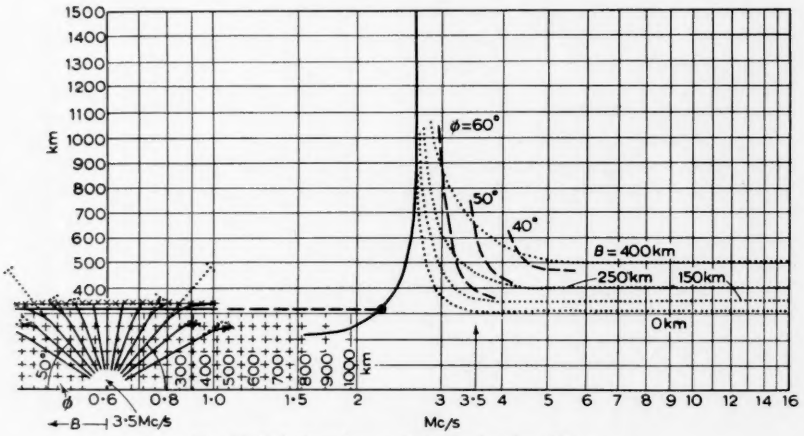

Fig. 11. Reflections from scattering region above F-layer

minimum frequency. The well-defined minimum penetration frequency indicates that the spread observed by the ionospheric recorder is an effect created below the maximum of the layer. In other words the layer maximum is relatively better defined than as it appears from the spread.

It is, of course, natural to assume that the condition responsible for the "spread" also can occur above the *F*-layer. In this case returning oblique ray paths are scarce and can form only a weak tail. If one assumes scattering centers instead of mirrorlike laminae the corresponding traces appear as in *Fig. 11*. Actually observed *h'f* records are on the *Figs. 12*, *13* and *14*. Following this interpretation one must assume strong single scattering clouds above the *F*-region in case of *Figs. 11* and *12* and in case of *Fig. 13* several scattering points.

Here it might be allowed to make some remarks about what we think the laminae might be. The laminae might be created in connection with the electrical currents in the ionosphere. Let us, for example, consider the strong tidal day current which has for a particular meridian between 0800 and 1400 hours in arctic regions a component toward the west. This current has to flow almost entirely across the magnetic field. Regardless of whether we take

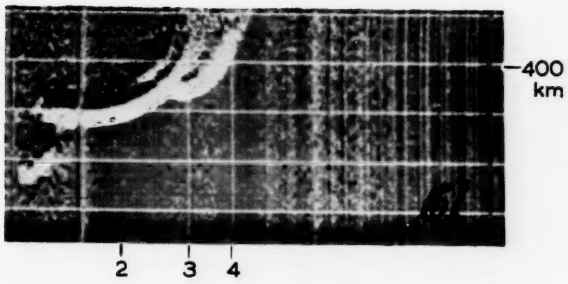

Fig. 4. 14 March, 1954, near North Pole

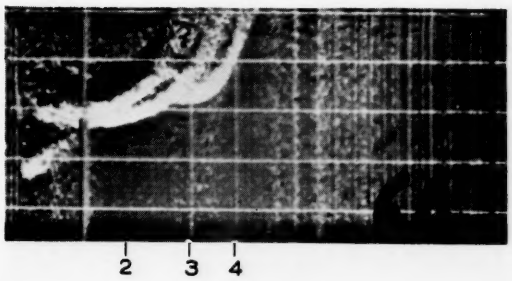

Fig. 5. 0227 EST

Fig. 6. 1 June, 1954, 0041 UT, between North Pole and Thule

uppl.
rt.II
1956

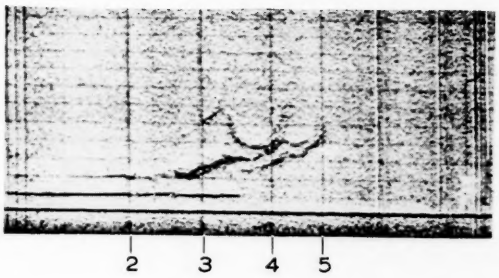

Fig. 7. 0057 UT

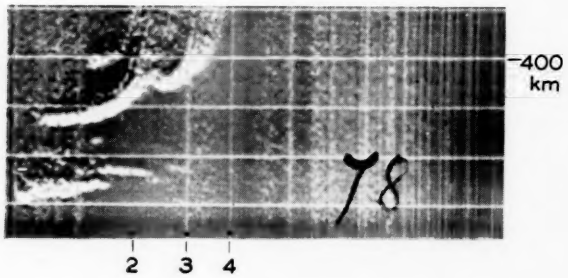

Fig. 8. 14 March, 1954, 0355 EST

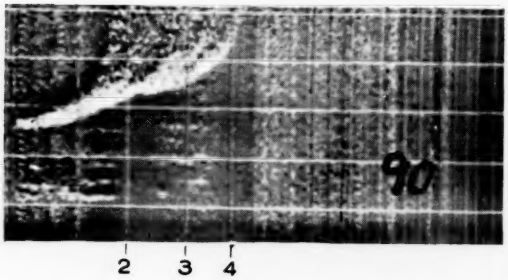

Fig. 9. 14 March, 1954, 0554 EST

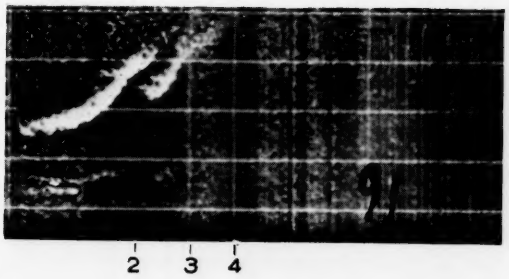

Fig. 10. 0557 EST

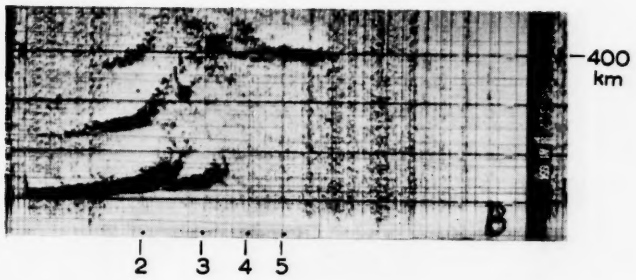

Fig. 12. 13 March, 1954, 0220 UT, near North Pole

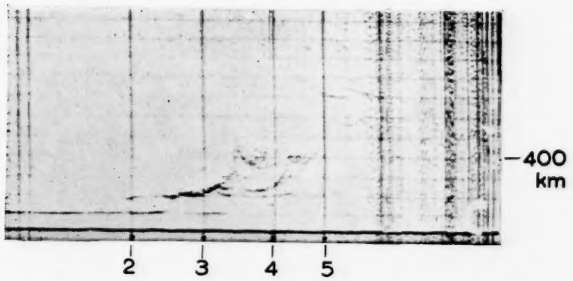

Fig. 13. 31 May, 1954, 2312 UT, near Thule

Suppl.
art.II
1956

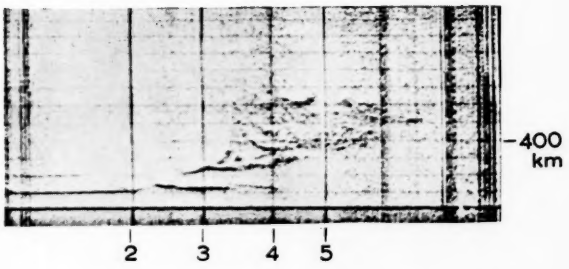

Fig. 14. 2 June, 1954, 1848 UT, near Gotnhavn, Greenland

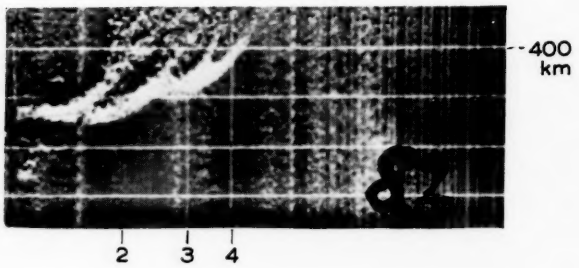

Fig. 15. 14 March, 1954, 0445 EST, near North Pole

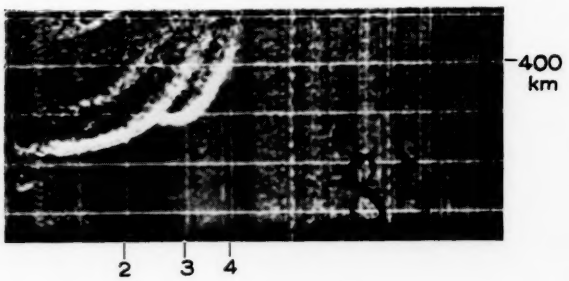

Fig. 16. 0505 EST

the current itself or the corresponding electric field, the theory requires that there is an ionic drift toward the south. But such movement seems to have unstable motion conditions. MARTYN[6] found that a column of a plasma of ionized matter in a conducting medium, when forced to move across a magnetic field, moves unstablely, because the movement constantly disturbs the original uniformity of the ionization in the column. This is also true if the force is created by an electrical field and a current is allowed in the column. Because of the different motion of electrons and positive ions the electrons accumulate at the front of the column during the motion; the positive ions at the back. Original small inhomogeneities within such a layer will be enhanced and might form the laminae. The separation of charges within the column creates an additional electrical field, which prevents the Hall current from flowing. This means that the effective conductivity in the column is considerably increased. This process is nothing other than what the workers on tidal motions already assume for middle latitudes and especially for the equator; namely that strong (vertical) polarization fields built up and improve the conductivity along the current ring. In the Arctic the current might split and run through millions of oblique laminae each providing better conductivity.

This is only a speculation and needs further investigation, but it serves the purpose of experimental planning.

Suppl.
art.II
1956

The ability of the laminae—provided its existence is accepted to cause partial reflections is larger at greater heights. This follows from the fact that on one hand the geometry of ray path 4 allows the same occurency of spread in both Arctic and middle latitudes (down to ca. 30° magnetic latitude), but on the other hand the spread actually observed at moderate latitudes is less frequent than in the Arctic. The only difference of the geometry in the Arctic is that the point of partial reflection on one of the laminae is much nearer to the zenith point of the ray path (see *Fig. 2*), which is the nearest point to the level $\omega_N = \omega$. At that level a small disturbance $\Delta\omega_N$ of electron density (what the laminae may consist of) will have the most effect $\Delta\mu/\mu$ on the refraction index μ. This follows easily from the simple formula for the refractive index, from which one obtains:

$$\frac{\Delta\mu^2}{\mu^2} = \frac{\Delta\omega_N^2/\omega^2}{1-(\omega_N^2/\omega^2)},$$

the value of which approaches infinity at the said level. This explains partly why the spread is more frequent in the Arctic. The higher grade of disturbance, of course, is another factor.

Inhomogeneities in the horizontal stratification of the ionosphere at or near the level $\omega_N = \omega$ invalidate ray optics already in trouble at that level. This is especially true with respect to the third magnetoionic split component, the z-mode. According to the theory the z-mode emerges from the ordinary mode at the level $\omega_N = \omega$ and penetrates to greater heights of the layer. For a particular departure angle toward the equator (depending on the magnetic inclination and the collisional frequency at the said level) there is *only* the z-mode (see *Fig. 2*), the "z-hole" in the ionosphere. At other departure angles the z-mode is more or less decreased in favour of the o-mode. The z-mode which emerges from the *vertical* o-mode is normally the only one returning to

the transmitter, but it is too weak to be observed. In fact, recent observations of ELLIS[7] have proved that the observable z-mode in Australia arrives from an angle corresponding to the z-hole of the theory. The geometry involved is easily explained by assuming reflecting laminae. In *Fig. 2* one ray path of the z-mode is indicated.

Our airborne observations may be summarized as follows. During quiet ionospheric conditions the z-trace has been seen occasionally and no dependency on magnetic latitude could be established. During high ionospheric activity the z-mode has been on the records almost all the time of an arctic flight. But the trace shows that it is not a truly "vertical" trace but created by a bundle of oblique ray paths. It looks like the one on *Fig. 16* while the z-trace on *Fig. 15* is a vertical one and is seldom seen.

3. First Ionospheric Drift Measurements at the North Pole

A new method of measuring ionospheric drifts has been applied to the Arctic. The measurements made until now are rare and the method needs improvements, but a short description shows the advantages.

If the airplane flies along a 4 min circle and the amplitude of the ionospheric reflection of a particular frequency is being recorded one obtains a characteristic fading curve. This curve appears compressed at one side of the circle and expanded at the opposite side. In order to have a measure for this phenomenon we divided the fading curve into 10 sec sections. For each section we took the sum of all changes in amplitude, measured from maxima to minima, divided by the time and also by the average amplitude:

$$A = \frac{\text{normalized average}}{\text{speed of fading}} \approx \frac{\Sigma \left| \partial\,(\text{amplitude}) \right|}{\partial\,(\text{time})} \cdot \frac{1}{\text{amplitude}}$$

The obtained "normalized average speed of fading" A runs through a minimum and a maximum during one circle of the airplane. Under simplifying assumptions it is easy to show that the quantity A is proportional to the speed of the aircraft relative to the moving ionospheric field strength pattern. Then the drift speed is obtained by the formula:

$$\frac{\text{Speed of airplane} + \text{speed of drift}}{\text{Speed of airplane} - \text{speed of drift}} = \frac{\text{Maximum value of } A}{\text{Minimum value of } A}$$

Fig. 17 shows the experimental values of a measurement in June 1954 at the North Pole with an E_s-layer reflection. The minimum of the curve is near 270° which is the direction of the drift. The drift speed obtained from the simple formula was 33 m/sec. Another measurement at the North Pole was made in January 1955 at 0130 UT, using an F-layer reflection and it resulted in 41 m/sec toward 290°.

The evaluation used here assumes a field strength pattern independent of time, omnidirectional and drifting as a whole. In other words, it disregards turbulence and the fact that the inhomogeneities are not circular. We therefore consider these measurements only as a beginning. For future improvements we may vary the speed of the aircraft, we may employ two or three receiving antenna devices and we may make use of autocorrelation methods for the evaluation. For the moment the results are good enough to show that

even in the Arctic the inhomogeneities are sufficiently constant throughout several minutes to apply this method.

4. Concluding Remarks

After having investigated some experimental phenomena with respect to the theory now we have enough ideas for a more effective experimental setup.

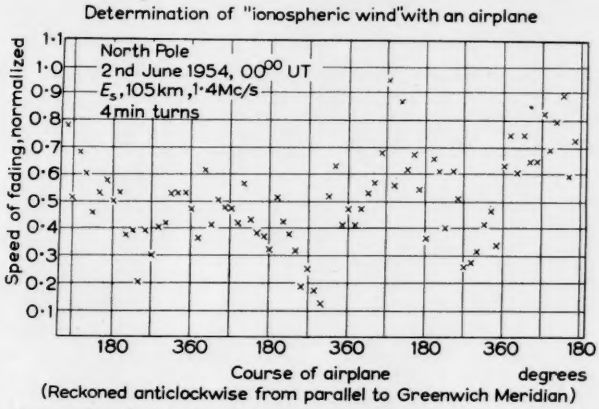

Fig. 17. Course of airplane (reckoned counterclockwise from parallel to Greenwich meridian)

The advantage of the airborne equipment for the investigation of the small- and large-scale structure of the ionosphere is beyond question, but the technique is still not completely developed.

The experimental information used in this presentation has been obtained with help of a well-trained airplane crew—over 20 officers and airmen of the 6520th Air Force Test Group—and under unusually hard physical conditions. The equipment has been operated by J. Butler and R. Whidden. The drift measurements have been analyzed by R. Winkelman. This work has been initiated by N. Gerson and W. Pfister who contributed in many ways.

Records of the American Ionospheric Arctic Stations have been made available by courtesy of the National Bureau of Standards and the Canadian Defence Research Board.

References

[1] Poeverlein, H. *Bayer. Akad. Wiss.* 1948; *Z. angew. Phys.* Vol. 1, p. 517, 1949: *ibid*; Vol. 5, p. 15, 1953

[2] Rydbeck, O. E. H. *Chalmers tek. Högsk. Handl.* Vol. 101, p. 1, 1951

[3] Smith, N. *Proc. Inst. Radio. Engrs., N.Y.* Vol. 27, p. 332, 1939

[4] Ellis, G. R. and Reber, G. R. *J. geophys. Res.* Vol. 61, p. 1, 1956

[5] Ellis, G. R. *J. atmos. terr. Phys.* Vol. 3, p. 263, 1953

[6] Martyn, D. F. *Phil. Trans.* A Vol. 263, p. 306, 1953

[7] Ellis, G. R. *J. atmos. terr. Phys.* Vol. 8, p. 43, 1956

uppl.
rt.II
1956

TURBULENCE IN THE IONOSPHERE WITH APPLICATIONS TO METEOR TRAILS, RADIO STAR SCINTILLATION, AURORAL RADAR ECHOES, AND OTHER PHENOMENA

H. G. Booker

School of Electrical Engineering, Cornell University,
Ithaca, New York

The irregularities in electron density responsible for incoherent scattering of radio waves in the ionosphere are discussed on the assumption of isotropic turbulence in the neutral molecules, with allowance made for the effect of the earth's magnetic field on the associated irregularities in the density of the charged particles. The atmospheric model used is based on rocket observations, extrapolated upwards in height where necessary. Tentative formulas are deduced for the large eddies based on a nonstandard application of the Richardson number. For the small eddies the standard formulas of turbulence theory are used.

These formulas all depend on a quantity w, which is the rate of supply of turbulence energy to the large eddies and also the rate of removal of turbulence energy from the small eddies, measured per unit mass of atmosphere. The value of w at the meteoric level (90 km) is found to be around 25 W/kg by comparison between the theory and meteoric observations (both visual and radio). By the same technique a more tentative value of 1000 W/kg is deduced for the level responsible for scintillation of radio stars although a lower value is probably appropriate when scintillation is weak. These values of w in the ionosphere are high compared with Brunt's value of 5×10^{-4} W/kg for the troposphere. It is shown, however, that these high values of w in the ionosphere are quite possible and even reasonable.

It is deduced that the time of onset of irregular fading of meteoric echoes in the VHF band is more likely to be due to roughness of the trail caused by the small eddies than to gross distortion of the trail caused by the large eddies. It follows that, after about a second, VHF radar echoes from a meteor trail must be calculated using a theory based on incoherent scattering, thereby ruling out the theory of Kaiser *and* Closs[37] *as an explanation of long-duration meteor echoes. It is also shown that radio star scintillation cannot be explained in terms of turbulence at a level of 400 km, but that reasonable results can be obtained if the level is reduced to 200–300 km.*

Among other applications considered is the possibility of radio communication via incoherent scattering in the F-region of the atmosphere. The conditions under which such communication should be sought are described in Sec. 11.

1. Introduction

It is the object of this paper to examine certain features of the theory of atmospheric turbulence in relation to phenomena involving irregular scattering of radio waves in the ionosphere. There are many such phenomena,

Supp
Part.
195

and in no case is there a generally accepted quantitative explanation at the present time. In some cases there is no agreement even on qualitative cause. These phenomena are listed below:

(*a*) Even for a quiet ionosphere, the simplest radio echo at normal incidence has a fading range comparable with the mean signal, indicating that, in the formation of the echo, some kind of irregular scattering is nearly as important as classical internal reflection.[1]

(*b*) Under certain ionospheric conditions, including magnetically disturbed conditions, echoes from the *F*-region of the ionosphere become extremely spread in range. The fading of the parts of the echo at different ranges is largely uncorrelated, and the fading range is comparable with the mean signal. This phenomenon of "spread-*F*" has been known for more than 20 years but is still without satisfactory explanation.[2]

(*c*) Radar echoes are obtained in the HF band above the penetration frequency of the ionosphere in such directions and at such ranges as to suggest back-scattering from irregularities of electron density aligned along the earth's magnetic field.[3] There is also a similar phenomenon associated with the *E*-region.[3]

(*d*) Noise from radio stars received in the VHF band shows twinkling similar to that produced in the troposphere with visual stars.[4, 5] Radio star twinkling frequently shows correlation with spread-*F* and is believed to be associated with irregularities in the *F*-region that are elongated along the earth's magnetic field.[6] Correlation with sporadic ionization in the *E*-region also occurs however.[7]

(*e*) Radar echoes from meteor trails, after about $\frac{1}{2}$ sec, develop irregular fading that cannot be explained in terms of a trail that remains straight. Visual observations of meteor trails likewise indicate twisting of the trail in a manner suggesting atmospheric turbulence at heights between 80 and 100 km.[9] It is usually assumed that the irregular fading of radar echoes from meteor trails is due to the effect of turbulence on the ionized trail and that this turbulence is not produced by passage of the meteor.

(*f*) At frequencies of the order of 2 Mc/s weak echoes can be obtained almost continuously at normal incidence from levels somewhat below the level of reflection for the regular *E*-region.[10, 11] The echoes are spread in range, have uncorrelated fading at different heights, and a fading range comparable with the mean signal. It is presumed they are due to scattering by irregularities of electron density in the *D*- and lower *E*-regions.

(*g*) Above the maximum usable frequency for regular ionospheric transmission, signals can be received at distances from a few hundred up to 2000 km at frequencies up to about 100 Mc/s.[12, 13] Signals have fading that is characteristic of scattering from a large number of irregularities. The height at which the scattering occurs is about 90 km at night, and perhaps a little lower during the daytime. Somewhat similar observations have been made at ranges of the order of 2500 and 2900 km, possibly due to scattering in the *F*-region.[14]

(*h*) At times of auroral activity, radar echoes are obtained in the VHF band from regions of the sky that bear some relation to the regions of visual activity.[15, 16, 17] There is sometimes a close correspondence between the regions

of visual activity and those from which radio echoes are obtained. However, radio echoes do not usually occur overhead or at short ranges and are mainly confined to the quadrant centered on magnetic north. Fading is of the type associated with random scattering and is at least a power of ten faster than would be expected for a quiet ionosphere. There is a Doppler shift in the frequency of auroral echoes comparable in magnitude to the fading rate. The Doppler shift does not correlate with the rate of change in the slant range of echoes. The height from which echoes come is almost certainly that of the *E*-region.

All of the above phenomena could be explained qualitatively in terms of atmospheric turbulence at ionospheric levels. That such turbulence does exist up to and within the *E*-region is not in serious doubt. Whether turbulence can exist in the *F*-region is, however, debatable, although the radio data seem to suggest turbulence at this level, especially at times of magnetic disturbance. At present, however, there is no comprehensive theory of ionospheric turbulence capable of presenting all of the above observations as different aspects of a single atmospheric phenomenon. It is the object of this paper to take some steps in this direction.

Turbulence in the upper atmosphere arises in a way that theory does not at present describe in any detail. It is assumed that large eddies of scale L_1 are produced, and that in so doing energy is used at a rate per unit mass of atmosphere that we shall denote by w. This important quantity w cannot usually be determined numerically by theoretical argument, but its value can sometimes be assessed by comparison of theoretical deductions with experimental observations. BRUNT[18] has estimated that the value of w in the troposphere is:

$$5 \times 10^{-4} \text{ W/kg} \qquad \ldots.(1)$$

At levels in the atmosphere where turbulence is important, the Reynolds number associated with the large eddies is large, indicating that the direct effect of viscosity in damping the large eddies is small. On the other hand, there is a scale L_2 for eddies, less than L_1, for which the Reynolds number is unity, indicating that viscosity would quickly damp out eddies of scale L_2. It is supposed that the large eddies of size L_1 break up into successively smaller eddies until the size L_2 is reached, when viscosity converts the energy of turbulence into energy of thermic motion. Thus there is a spectrum of eddy sizes from L_1 down to L_2. Energy is transferred to the large eddies at a rate w per unit mass; it is removed from the small eddies and converted into heat at practically the same rate w per unit mass.[19]

The distribution of turbulent energy with eddy scale L has been studied by KOLMOGOROFF[20] for the range $L_1 > L > L_2$ and by HEISENBERG[21] for $L < L_2$. Methods for converting the spectrum of turbulence into a function giving the dependence on radio wavelength λ of the cross-sectional scattering area per unit volume of atmosphere have been studied by BOOKER and GORDON,[22] MEGAW,[23] VILLARS and WEISSKOPF,[24, 25] GALLET,[26] BATCHELOR,[27] SILVERMAN,[28] and BOOKER.[29] The precise form of the scattering function will not be required in this paper. The following points should, however, be noted:

(*a*) For forward scattering involving angles of deviation less than $\lambda/(2\pi L_1)$,

the phenomenon is controlled primarily by the large irregularities (those whose scale is of the order of L_1).

(*b*) For back-scattering, the phenomenon is controlled either (i) by the small irregularities (those whose scale is the order of L_2) if $L_2 > \lambda/4\pi$, or (ii) by the eddies whose scale is of the order of $\lambda/4\pi$ if $L_2 < \lambda/4\pi$.

In discussing turbulence in the ionosphere we shall assume that the turbulence in the neutral molecules is isotropic. While this may not be true, it is considered a useful approximation at the present stage in the development of the subject. The possible effect of non-isotropic turbulence in the neutral molecules is, however, mentioned in discussion. On the other hand we shall not in general assume isotropy in the irregularities of ions and electrons. Owing to the influence of the earth's magnetic field, the irregularities in the charged particles are constricted perpendicular to the field. This constriction is calculated in Sec. 5 on the basis of certain somewhat over-simplified assumptions.

In Sec. 2 of the paper, formulas are developed appropriate to the large eddies in the upper atmosphere. These formulas are based on a use of the Richardson number, whose properties are discussed in books on dynamical meteorology.[18] In Sec. 3, formulas are given appropriate to the small eddies. These formulas are taken from BATCHELOR.[19]

A number of the quantities involved in the formulas for the large and small eddies can be calculated as a function of height in the ionosphere from the atmospheric data presented by the ROCKET PANEL.[30] The rocket data as interpreted by WEEKES[31] have been used up to a height of 160 km. Above this height some extrapolation is necessary, though results may be considered fairly reliable up to a height of, say, 300 km. Above 120 km it has been assumed that temperature increases with height at a rate of 5° K per km up to any height used. Complete dissociation of oxygen has been assumed above 120 km, and dissociation of nitrogen has been neglected. Above 120 km complete mixing of molecular nitrogen and atomic oxygen has been assumed up to any level under discussion. The reason for this is that it is a basic hypothesis of this paper that turbulence exists in the atmosphere up to any level under discussion. The atmospheric model just described will be briefly designated "the rocket atmosphere".

After introducing the data from the rocket atmosphere into the formulas of Secs. 2 and 3 for the large and small eddies, we are still left with the important unknown parameter w. This is the turbulence power per unit mass. It is the rate at which turbulent energy is supplied to the large eddies and removed from the small eddies, measured per unit mass or atmosphere. In the troposphere the order of magnitude of w is known roughly to have the value (1) from the work of BRUNT.[18] At the meteoric level, which will be taken as 90 km, a value will be deduced for w by fitting the formulas of Secs. 2 and 3 to visual observations of meteor trails made by LILLER and WHIPPLE,[9] and to radio observations of meteor trails made by GREENHOW.[8, 34] This comparison between turbulence theory and meteoric observations is made in Sec. 4.

In Sec. 5 a similar procedure is followed at the level where scintillation of radio stars occurs, making use particularly of the observations of SPENCER.[6]

It will, however, be necessary to abandon the estimate of HEWISH[5] that the level at which scintillation of radio stars occurs is 400 km. Not only is it difficult to explain the existence of turbulence at 400 km, but even in the presence of turbulence at this level it would be difficult to explain why the irregularities of electron density have the size and shape observed. A lower height is therefore deduced for the level of star scintillation, which is at first estimated as 170 km but is subsequently modified in Sec. 9 to a value between 200 and 300 km.

An important feature of the application of the formulas of Secs. 2 and 3 to turbulence at the meteoric and star scintillation levels is the high values of turbulence power deduced for ionospheric heights. At the meteoric level the estimate of turbulence power is 25 W/kg and at the star scintillation level it is 1000 W/kg. These values are to be compared with Brunt's value (1) for the troposphere. In Sec. 6 an investigation is undertaken in order to see whether these remarkably high values of turbulence power deduced for the ionosphere are unreasonable. Both lower and upper bounds are deduced for the tur bulence power at any level. From the lower bound it is found that turbulence in the ionosphere is only possible if the turbulence power per unit mass is considerably greater than in the troposphere. It transpires in fact that the values of turbulence power required to explain observations at both the meteoric and the star-scintillation levels lie comfortably within the permitted range of values.

With only three values for the turbulence power per unit mass (one in the troposphere, one at the meteoric level, and one at the star-scintillation level) it is difficult to draw a curve of w vs. height. Nevertheless such a curve is tentatively drawn in Sec. 6 and the variations with height of the other turbulence parameters are deduced from it. In converting these parameters into values for the scale of electronic irregularities measured along and perpendicular to the earth's magnetic field some consideration has to be given to the minimum possible values of these scales, and this is done in Sec. 7. The remaining sections consider applications of the theory to auroral echoes (Sec. 8), to radar echoes from irregularities in the F-region at frequencies above the penetration frequency (Sec. 9), to scattering phenomena at the 90 km level (Sec. 10), to the possibility of F-region scatter communication (Sec. 11), and finally to spread-F and other reflection phenomena (Sec. 12).

2. THE LARGE EDDIES

In applying the theory of turbulence to the upper atmosphere, difficulty has been experienced due to the lack of suitable formulas to describe the properties of the large eddies. Some formulas appropriate to the large eddies will be derived in this section using the Richardson number. The Richardson number depends on temperature T, on the rate of increase of T with height z, on the adiabatic lapse rate of temperature Γ, on the acceleration g due to gravity, and on the rate of change with height z of the horizontal velocity v of the atmosphere. The expression for the Richardson number is:[18]

$$\frac{(g/\mathrm{T})\ \{(\mathrm{dT}/\mathrm{d}z)+\Gamma\}}{(\mathrm{d}v/\mathrm{d}z)^2} \qquad \ldots . (2)$$

According to the simplest derivation of the Richardson number, turbulence

in the atmosphere increases if the Richardson number is less than unity and decreases if the Richardson number is greater than unity.

Application of the Richardson number is not without its difficulties. It is not clear that unity is necessarily quite the proper critical value of the Richardson number for separating the domain of increasing turbulence from that of decreasing turbulence. In the ionosphere, however, where orders of magnitude are still uncertain, this is not an important point at the present time, and we shall use unity as the critical value. Another point of difficulty in using the Richardson number concerns the interpretation of the denominator in (2). This denominator might be interpreted as either (*a*) the square of the mean value of the shear, or (*b*) the mean value of the square of the shear. The observations of LILLER and WHIPPLE[9] (see *Fig. 3*) at the meteoric level seem to indicate that (*a*) is less than (*b*), sometimes by more than a power of 10. Since increasing and decreasing shears are equally associated with turbulence we shall assume that the denominator of the Richardson number is to be interpreted as the mean value of the square of the shear.

There is little doubt that turbulence in the ionosphere sometimes increases and sometimes decreases. We shall confine ourselves to discussion of a steady state in which turbulence is neither increasing nor decreasing. In these circumstances we assume that the Richardson number is unity, and derive from (2) the equation:

$$\left(\frac{\mathrm{d}v}{\mathrm{d}z}\right)^2 = \frac{g}{\mathrm{T}}\left(\frac{\mathrm{dT}}{\mathrm{d}z} + \Gamma\right) \qquad \ldots.(3)$$

The right-hand side of this equation may be plotted as a function of height in the ionosphere from the rocket atmosphere. We thereby deduce, as a function of height, an order of magnitude for the mean square shear involved in a steady state of turbulence.

We do not interpret the square root of (3) as giving the mean wind shear. Instead we interpret $|\,\mathrm{d}v/\mathrm{d}z\,|$ as follows. The dimensions of $|\,\mathrm{d}v/\mathrm{d}z\,|$ are those of angular velocity, and the angular velocity concerned is the angular velocity of a vertical line drawn in the fluid. We interpret this angular velocity as the angular velocity of the large eddies, and its reciprocal as the time constant t_1 of the large eddies. The formula that we shall use therefore for the time constant of the large eddies is:

$$t_1 = \left\{\frac{g}{\mathrm{T}}\left(\frac{\mathrm{dT}}{\mathrm{d}z} + \Gamma\right)\right\}^{-\frac{1}{2}} \qquad \ldots.(4)$$

On the basis of the rocket atmosphere described in Sec. 1, the quantity t_1 is plotted as a function of height in *Fig. 1*. Values of the time constant of the large eddies range between 40 and 100 sec.

The time constant t_1 of the large eddies, besides being the time taken by a large eddy to rotate 1 radian, is also interpreted as the lifetime of a large eddy. It is at this point that we introduce the turbulence power w per unit mass. Energy is supplied to the large eddies at a rate w for an average time t_1. Hence the turbulence energy per unit mass associated with the large eddies is wt_1 per unit mass. But if v_1 is the turbulence velocity associated with the large eddies, this turbulence energy is of the order of v_1^2 per unit mass. Hence:

$$v_1^2 = wt_1 \qquad \ldots.(5)$$

or

$$v_1 = (wt_1)^{\frac{1}{2}} \qquad \ldots.(6)$$

This equation gives the turbulence velocity of the large eddies in terms of the parameter w and the time constant (4) of the large eddies.

The scale of L_1 of the large eddies is given by:

$$L_1 = v_1 t_1 \qquad \ldots.(7)$$

This equation may be interpreted as a relation between radius L_1, linear velocity v_1, and angular velocity $1/t_1$. Alternatively it may be interpreted as

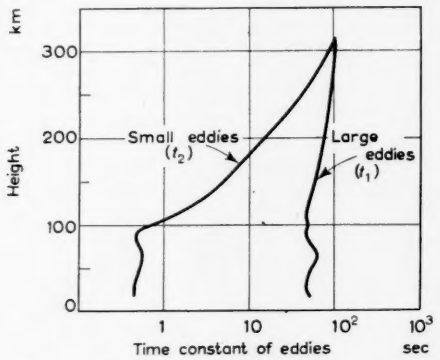

Fig. 1. The time constants for large and small eddies

giving the distance L_1 that an eddy moves during its lifetime t_1. By substituting for v_1 from (6) into (7) we obtain:

$$L_1 = (wt_1^3)^{\frac{1}{2}} \qquad \ldots.(8)$$

This equation gives the scale of the large eddies in terms of the parameter w and the time constant (4) of the large eddies.

Since we have determined t_1 as a function of height from equation (4)

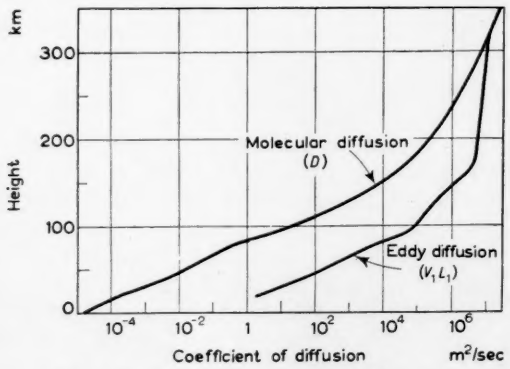

Fig. 2. The coefficients of molecular and eddy viscosity

and the rocket atmosphere, we are prevented from determining v_1 and L_1 as a function of height from (6) and (8) only by our ignorance of the turbulence power w per unit mass as a function of height.

3. The Small Eddies

The formulas for the small eddies depend on the same parameter w involved in the large eddies and also upon the kinematic viscosity of the atmosphere. The kinematic viscosity may be taken to be identical with the coefficient of molecular diffusion D, for which there is a simple formula in the kinetic theory of gases.[32] This formula, used in conjunction with the rocket atmosphere, gives D as a function of height. In *Fig. 2* is shown the coefficient of molecular diffusion D as a function of height deduced in this way. The value of D has been checked experimentally at the meteoric level by Greenhow[33] from the decay time of short-duration meteor echoes.

In terms of D and w, the formulas for the turbulence velocity and scale of the small eddies are:

$$v_2 = (wD)^{\frac{1}{4}} \quad \ldots.(9)$$

$$L_2 = \left(\frac{D^3}{w}\right)^{\frac{1}{4}} \quad \ldots.(10)$$

These formulas may be found in Batchelor[19] and are based on simple dimensional considerations. It is easily verified that the Reynolds number for the small eddies, namely $v_2 L_2/D$, is unity. Formulas such as (5) and (7) apply to eddies of all sizes and therefore, in particular, to the small eddies. Hence:

$$v_2^2 = wt_2 \quad \ldots.(11)$$

$$L_2 = v_2 t_2 \quad \ldots.(12)$$

By substituting from (9) and (10) into either (11) or (12), we obtain:

$$t_2 = \left(\frac{D}{w}\right)^{\frac{1}{2}} \quad \ldots.(13)$$

Eqs. (9), (10), and (13) would give the turbulence velocity, scale, and time constant of the small eddies as a function of height if we know the variation with height of the turbulence power w per unit mass.

4. Meteor Trails

In discussing meteor trails we shall take 90 km as a convenient standard height at which to make calculations. From the rocket atmosphere we have at 90 km;

$$\mathrm{T} = 212^\circ \mathrm{K} \quad \ldots.(14)$$

$$\frac{\mathrm{dT}}{\mathrm{d}z} = 1{\cdot}1^\circ \mathrm{K/km} \quad \ldots.(15)$$

$$\Gamma = 9{\cdot}5^\circ \mathrm{K/km} \quad \ldots.(16)$$

$$\frac{\mathrm{dT}}{\mathrm{d}z} + \Gamma = 10{\cdot}6^\circ \mathrm{K/km} \quad \ldots.(17)$$

From (3) we deduce that the root mean square shear is:

$$20\ (\mathrm{m/sec})/\mathrm{km} \quad \ldots.(18)$$

While this might at first sight seem a high value, it is nevertheless of the order of magnitude observed by Liller and Whipple.[9] *Fig. 3* illustrates one of Liller and Whipple's curves for meteoric trail velocity vs. height, and the large cross drawn on the diagram corresponds to shears of ± 20(m/sec)/km.

By taking the reciprocal of (18) we deduce that the time constant of the large eddies at 90 km is of the order of:

$$t_1 = 50 \text{ sec} \qquad \ldots.(19)$$

Let us turn now to formula (6) for the turbulence velocity v_1 of the large

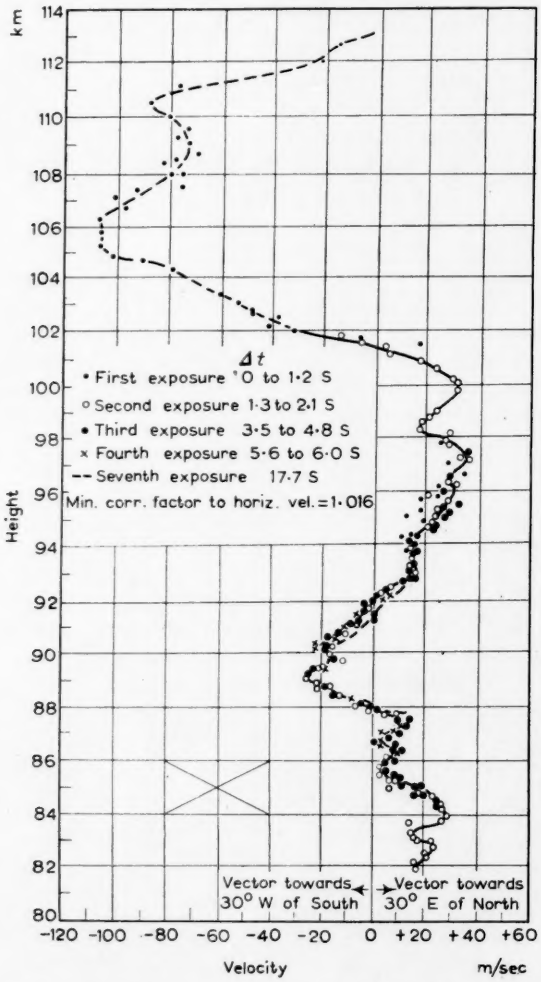
km
Height
Δ t
• First exposure 0 to 1·2 S
○ Second exposure 1·3 to 2·1 S
• Third exposure 3·5 to 4·8 S
× Fourth exposure 5·6 to 6·0 S
-- Seventh exposure 17·7 S
Min. corr. factor to horiz. vel. = 1·016
Vector towards 30° W of South
Vector towards 30° E of North
Velocity
m/sec

Fig. 3. Observations by LILLER *and* WHIPPLE[9] *of the velocity of a meteoric trail as a function of height*

eddies. There are three sources of experimental information concerning the turbulence velocity of the large eddies:

(*a*) The photographic observations of LILLER and WHIPPLE,[9] which clearly reveal the motions due to the large eddies.

(*b*) The radar measurements of "wind", particularly those of GREENHOW.[34]

Wind as measured by GREENHOW includes the turbulence velocity, which shows up as variability in the wind.

(*c*) Measurements of the fading rate of long-duration meteor echoes.[35] These fading rates are proportional to the radio frequency used, showing that the phenomenon can be explained as Doppler broadening of the transmitted frequency due to turbulent motion.

All three methods lead to turbulence velocities of the order of 30–40 m/sec. We therefore adopt for the turbulence velocity of the large eddies the value:

$$v_1 = 35 \text{ m/sec} \quad \ldots.(20)$$

We now substitute the value (19) for t_1 and the value (20) for v_1 into formula (6) and deduce that the turbulence power per unit mass at 90 km is of the order of:

$$w = 25 \text{ W/kg} \quad \ldots.(21)$$

This value seems remarkably high in comparison with the value (1) for the troposphere. By multiplying w by the atmospheric density, we deduce that the turbulence power per unity volume in the troposphere is about 5×10^{-4} W/m^3 while that at 90 km is about 10^{-4} W/m^3. Thus turbulence energy is being supplied to the atmosphere at the meteoric level at a rate per unit volume not much less than that prevailing in the troposphere in spite of the drastically lower atmospheric density. The high value (21) deduced for the turbulence power per unit mass at 90 km will be subjected to further study in Sec. 6. It may be stated immediately, however, that the value (21) for w implies a turbulence energy wt_1 per unit mass which is only a fraction 3×10^{-4} of the thermic energy per unit mass at 90 km.

With the value (21) for w and the value (19) for t_1, we can now substitute into (8) and deduce for the scale of the large eddies at the 90 km level:

$$L_1 = 1{\cdot}6 \text{ km} \quad \ldots.(22)$$

This value is in tolerable agreement with the observations of LILLER and WHIPPLE.[9]

Having now put numerical values on the principal quantities associated with the large eddies at 90 km, let us now turn our attention to the small eddies. For this purpose we need a value for the coefficient of molecular diffusion at 90 km. We shall use the value:

$$D = 4 \text{ m}^2/\text{sec} \quad \ldots.(23)$$

which may be derived either from the rocket atmosphere or from the decay time of short-duration meteor echoes.[33]

Substituting the value (21) for w and the value (23) for D into Eqs. (9), (10), and (13), we deduce for the turbulence velocity of the small eddies:

$$v_2 = 3 \text{ m/sec} \quad \ldots.(24)$$

for the scale of the small eddies:

$$L_2 = 1{\cdot}3 \text{ m} \quad \ldots.(25)$$

and for the time constant of the small eddies:

$$t_2 = 0{\cdot}4 \text{ sec} \quad \ldots.(26)$$

The turbulence velocity v_2 of the small eddies cannot be conveniently observed in practice by any method at present available since its effect is over-

shadowed by the turbulence velocity (20) of the large eddies, which is ten times bigger.

The value (25) for the scale of the small eddies is susceptible to experimental verification. The value of L_2 vitally affects the frequency dependence in the strength of long-duration meteor echoes. The value of L_2 also vitally affects the frequency dependence of long distance VHF scatter communication. The value of L_2 required to explain these phenomenon is in fact quite close to the value (25). This matter is taken up in greater detail in a companion paper by BOOKER and COHEN.[36]

In discussing radar reflection from long-duration meteor trails some importance attached to the wavelength:

$$4\pi L_2 = 16 \text{ m} \qquad \ldots.(27)$$

using the numerical value (25) for L_2. For a wavelength λ longer than (27), incoherent back-scattering is controlled by irregularities whose scale is of the order of $\lambda/(4\pi)$. But for wavelengths shorter than (27) incoherent back-scattering is controlled by the small eddies, whose scale is given by (25).

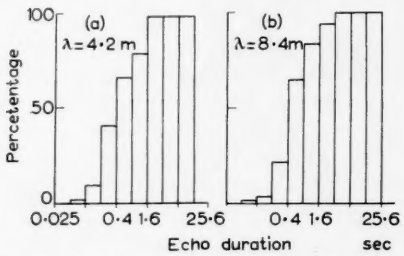

Fig. 4. Observations by GREENHOW[8] *of the time taken for meteoric echoes to develop irregular fading*

Since most radar observations of meteor trails are made in the VHF band, it follows that the strength of incoherent back-scattering from meteor-trails is controlled almost entirely by the small eddies.

We now come to discussion of the value (26) for the time constant of the small eddies. This value for t_2 appears to cut across much of the current thinking concerning radar reflections from long-duration meteor trails. What (26) shows is that the trail is mixed on the scale L_2 of the small eddies after a time of the order of 0·4 sec from formation of the trail. Since the value (27) for $4\pi L_2$ exceeds the wavelengths normally used for radar investigation of meteor trails, it follows that, after about 0·4 sec, the trail is rough instead of smooth. Thus, when the time since the formation of the trail exceeds the time constant of the small eddies, the echo from the trail should be calculated by an incoherent scattering theory and not by a smooth reflection theory. This rules out the theory of KAISER and CLOSS[37] as a theory of long-duration echoes from meteor trails. The theory of KAISER and CLOSS is a correct modification of the theory of LOVELL and CLEGG[38] to allow for overdense ionization, but it applies only before the eddies have rendered the trail rough, that is, for a few tenths of a second. There is a possibility that some extension of this time arises from the modification in local wavelength as the wave enters the trail. But there seems no likelihood of the theory of KAISER and CLOSS

being applicable in the VHF band at times large compared with a second after formation of the trail. An alternative theory of long-duration meteor echoes based on incoherent scattering is presented in the companion paper by BOOKER and COHEN.[36]

After the eddies have made the trail rough, a radar echo should have a probability distribution of amplitude that is of Rayleigh type. GREENHOW[8] has demonstrated experimentally that the long-duration meteor echoes develop a Rayleigh distribution of amplitude. Moreover he has ascertained experimentally the time taken by an echo to develop irregular fading. His results are reproduced in *Fig. 4* for a wavelength of 4 m and a wavelength of 8 m. It is seen that the time taken to develop irregular fading varies between 0·1 and 1·6 sec, with a median value of 0·4 sec. In other words GREENHOW has demonstrated experimentally that the time taken by a radar echo from a meteor trail to develop irregular fading is approximately equal to the expected value at 90 km for the time constant of the small eddies. It is concluded, therefore, that the time measured in this experiment of GREENHOW is the time constant of the small eddies.

That the development of irregular fading in echoes from long-duration meteor trails is controlled primarily by the small eddies is a concept that does not seem to have been considered anywhere in the literature on radio-meteoric echoes. The conventional viewpoint is that the development of irregular fading is due to distortion of the trail produced by the large eddies. The most elementary argument in favor of the large eddy theory is supposed to be the following: The large eddies cause random motion in the different portions of the trail with velocity v_1 given by (20). Randomly fading echoes will develop when the corresponding displacements have reached $\lambda/(4\pi)$. Hence the time required for development of fading is:

$$\frac{\lambda}{4\pi v_1} \qquad \ldots\ldots(28)$$

That this argument is wrong may be seen in two ways. Firstly, the time (28) is proportional to wavelength, whereas the time observed by GREENHOW[8] was virtually identical at 4 and 8 m (see *Fig. 4*). Secondly the time (28) is around 9×10^{-3} sec for a wavelength of 4 m and $1{\cdot}8 \times 10^{-2}$ sec for a wavelength of 8 m, whereas the time observed by GREENHOW was about 0·4 sec.

The next stage in the large eddy argument is that Rayleigh fading does not develop in the time (28) because it takes a longer time for the production of multiple perpendiculars from the radar onto the distorted trail. Let us calculate this effect on the assumption of a linear profile of mean wind. Consider an initial trail for which the perpendicular from the radar falls within the length of the trail, and let the length of the perpendicular be r. Consider the effect on the trail of the large eddies only, and suppose that these render the trail sinuous with a wavelength $2\pi L_1$ and with an amplitude $v_1 t$ at time t after formation of the trail. The maximum deviations in slope of the trail at time t are therefore of the order:

$$\frac{v_1 t}{L_1} = \frac{t}{t_1} \qquad \ldots\ldots(29)$$

from (7). Now, when two perpendiculars onto the trail develop, their feet will have a separation of the order of either about $\frac{1}{4}\ 2\pi L_1$ or about $\frac{3}{4}\ 2\pi L_1$.

The angle between the two perpendiculars may therefore be taken to be roughly:

$$\frac{\pi L_1}{r} \qquad \ldots.(30)$$

Multiple perpendiculars will not develop until the deviation (29) in slope has reached the angle (30). Equating (29) and (30), we see that the time taken to develop multiple perpendiculars is of the order:

$$t = \pi \frac{L_1 t_1}{r} \qquad \ldots.(31)$$

The question at issue is whether the time t_2 taken by the small eddies to render the trail rough is less or greater than (31). The condition that the development of irregular fading should be controlled by the large eddies is:

$$t < t_2$$

or

$$r > \pi L_1 \frac{t_1}{t_2} \qquad \ldots.(32)$$

$$= 600 \text{ km}$$

using the values of L_1, t_1, and t_2 given by (22), (19), and (26). Thus, for a linear profile of mean wind, it is possible for the time taken to develop irregular fading to be controlled by the large eddies, but only for meteors at extremely long range. Of course, it is also possible to devise nonlinear profiles of mean wind that would either increase or decrease the time taken by the large eddies to make multiple perpendiculars possible. For a linear profile of mean wind, however, and for a reasonable mean meteoric range of 150 km, the small eddies render the trail rough for a VHF radar in about a quarter of the time that the large eddies take to make multiple perpendiculars possible. Of course, after the small eddies have made the trail rough, perpendiculars from the radar onto the trail are no longer of interest.

It is concluded, therefore, that, while it is possible in some cases for the time of development of irregular fading to be controlled by the large eddies, this time will usually be controlled by the small eddies and will be equal to their time constant t_2. Since this time constant is of the order of 0·4 sec at 90 km, it is not surprising that, in averaging results for some hundreds of meteor trails, GREENHOW obtained the results reproduced in *Fig. 4*.

The above arguments confirm the view that, after about 0·4 sec have elapsed since formation of the trail, echoes obtained by radars in the VHF band are to be calculated from an incoherent scattering theory applied to the irregularities associated with the small eddies. It should be noted, however, that these small eddies partake of the turbulence velocity of the larger eddies. Thus the fading rate of long-duration meteor echoes is to be calculated mainly from the turbulence velocity v_1 of the large eddies even though the strength of the echoes is to be calculated mainly from irregularities of scale L_2 associated with the small eddies.

Before leaving the subject of meteor trails, let us give some consideration to the coefficient of eddy diffusion at the 90 km level. The usual expression for the coefficient of eddy diffusion is the product of the turbulence velocity

v_1 and the scale L_1 of the large eddies. At 90 km therefore, the coefficient of eddy diffusion has, from (20) and (22), the value:

$$v_1 L_1 = 6 \times 10^4 \text{ m}^2/\text{sec} \quad \ldots.(33)$$

The ratio of the coefficient of eddy diffusion to that for molecular diffusion (which ratio is the Reynolds number of the large eddies) is therefore about 10,000. An experimental value for the coefficient of eddy diffusion at the meteoric levels has been estimated by DOBROVOL'SKII[39] from observations of the rate of spread of those occasional visual meteors which, for some unknown reason, can be seen for periods of many minutes. DOBROVOL'SKII estimates from the observations of various Russian workers that the coefficient of eddy diffusion is large compared with the coefficient of molecular diffusion. The value derived is, however, about a power of 10 less than in (33), probably because the height involved is less than 90 km.

Since there is such a drastic difference between the values of the coefficients of molecular and eddy diffusion, it is necessary to be clear about the signi-

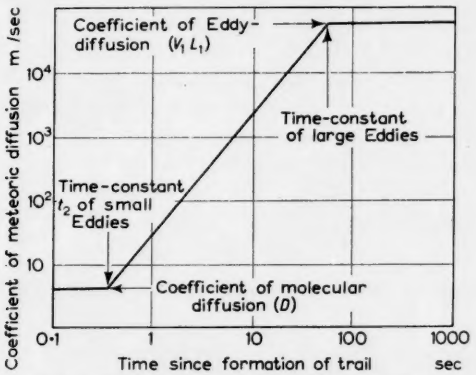

Fig. 5. Variation of the coefficient of meteoric diffusion with time measured from formation of the trail

ficance of each coefficient, about when each should be applied, and about how, for a meteor trail, a transition takes place from the one to the other. Diffusion of a meteor trail should be calculated as follows:

(*a*) At a time t after formation of the trail less than the time constant t_2 of the small eddies, the appropriate coefficient of diffusion is the coefficient of molecular diffusion D.

(*b*) At a time t greater than the time constant t_1 of the large eddies, the appropriate coefficient of diffusion is the coefficient of eddy diffusion $v_1 L_1$.

(*c*) As the time t after formation of the trail increases from t_2 to t_1, there is a continuous increase in the appropriate coefficient of diffusion from the value D to the value $v_1 L_1$.

This state of affairs is illustrated in *Fig. 5* using the numerical values for t_1, t_2, D and $v_1 L_1$ previously derived.

The reasons that the coefficient of meteoric diffusion behaves in the above way are the following. For $t \ll t_2$, rotation even of the smallest eddies is small compared with one radian. In this interval of time the trail, besides suffering molecular diffusion, becomes distorted, but not drastically. For

$t<t_2$ the distortion of the trail is still sufficiently simple so that its geometry can be imagined. Now consider the situation for $t \gg t_1$. By this time the rotation of all eddies, including the largest, has become large compared with one radian, and the trail is hopelessly tangled. In principle, we could still take the trouble to describe this complicated geometry, and think of the tangled trail as subject merely to molecular diffusion. In practice, however, this is inconvenient and indeed virtually impossible. For $t>t_1$ we make no attempt to describe the detailed contortions of the trail and content ourselves by merely stating the rate of expansion of a cylinder enveloping the tangled trail. It is the rate of expansion of this enveloping cylinder that is described by the coefficient of eddy diffusion v_1L_1. Now consider the situation at a time t intermediate between the time constant t_2 of the small eddies and the time constant t_1 of the large eddies. For the smaller eddies, whose time constant is less than t, distortion of the trail is drastic and it is convenient to use the concept of eddy diffusion. For the larger eddies, however, whose time constants exceed t, distortion of the trail is still moderate and capable of being imagined. At a time t between t_1 and t_2, therefore, it is convenient to think of an enveloping cylinder that is expanding at the rate corresponding to eddies of time constant t; this expanding cylinder is being distorted, however, by the eddies whose time constants exceed t. The appropriate coefficient of diffusion required at time t is therefore calculated as follows. The turbulence velocity v and scale L of eddies of time constant t are given by (cf. Eqs. 6 and 8)

$$v=(wt)^{\frac{1}{2}} \qquad \ldots.(34)$$

$$L=(wt^3)^{\frac{1}{2}} \qquad \ldots.(35)$$

Hence the coefficient of eddy diffusion applicable to a meteor trail at time t is:

$$vL=wt^2 \qquad \ldots.(36)$$

This obviously increases to the usual coefficient of eddy diffusion v_1L_1 as t increases to t_1, and from Eqs. 9 and 10 it may be seen that it reduces to the coefficient of molecular diffusion D as t reduces to t_2.

It follows that the coefficient of meteoric diffusion is given approximately by

$$\begin{array}{ll} D, & 0<t<t_2 \\ wt^2, & t_1<t<t_2 \\ v_1L_1, & t>t_2 \end{array} \qquad \ldots.(37)$$

It is this behavior that is plotted in *Fig. 5* using the values of the parameters that we have deduced for the 90 km level.

5. Scintillation of Radio Stars

Let us turn now to the more difficult problem of scintillation of radio stars. Such scintillation can occur in both the *E*-region and the *F*-region. It is the *F*-region phenomenon that has been studied more intensively, however, and it is to this that we shall confine our attention.

Maxwell[40] has already made an attempt to explain scintillation of radio stars in terms of turbulence in the *F*-region, after offering criticisms of certain alternative suggestions. It is our objective to reconsider the approach of Maxwell with certain important changes. Since the scintillation phenomenon is one of forward scattering, it depends on the irregularities associated

with the large eddies. While MAXWELL had available the formulas for small eddies given in Sec. 3 of this paper, he did not have available the formulas for large eddies given in Sec. 2. Thus he did not have available formulas for eddies of the size directly involved in the scintillation phenomenon. Furthermore, at the time of MAXWELL's work, it had not been demonstrated that the electronic irregularities responsible for scintillation are constricted perpendicular to the earth's magnetic field, so that he omitted the major allowance that has to be made for this important phenomenon. Thus while our objective in this section is broadly the same as that of MAXWELL, the development will follow different lines in certain major respects.

Owing to the influence of the earth's magnetic field, care is necessary in

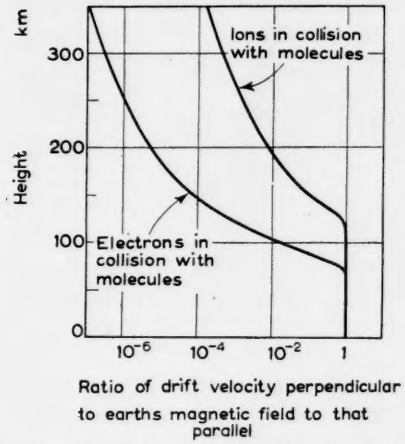

Fig. 6. The reduction ratio for the velocity of charged particles in motion perpendicular to the earth's magnetic field

the *F*-region to distinguish between the eddies in the neutral molecules and the irregularities of ion density and electron density to which they give rise. Even in the *E*-region this effect is of some importance for the electrons. Let ν be the collisional frequency of collisions between charged particles and neutral molecules and ω_M be the radian gyromagnetic frequency for the charged particles in the presence of the earth's magnetic field. Values of ν and ω_M are different for the ions from what they are for the electrons. Appropriate numerical values can be derived from the rocket atmosphere interpreted in the manner described in Sec. 1. If the neutral molecules move parallel to the earth's magnetic field with a certain velocity, then (after a collision interval) both the ions and electrons will move parallel to the earth's magnetic field with the same velocity. The same is not in general true in a direction perpendicular to the earth's magnetic field, however. Motion of the charged particles is not in general in the same direction as that of the neutral molecules, and the velocity of the charged particles is reduced[32] in the ratio*

$$\frac{\nu}{(\omega_M^2+\nu^2)^{\frac{1}{2}}} \qquad \ldots.(38)$$

* SPENCER[6] uses an expression which is the square of (38) due to neglect of one component in the motion of the charged particles.

This expression is plotted in *Fig. 6* as a function of height for both the ions and the electrons, on the basis of the rocket atmosphere. Now consider isotropic turbulence in the neutral molecules. This involves equal turbulence velocities along and perpendicular to the earth's magnetic field. It follows that the ratio of the drift velocity for the charged particles perpendicular to the field to that parallel to the field is (38). We shall assume that this velocity ratio for the charged particles is also the ratio of the scale of the irregularities in the density of the charged particles measured perpendicular to the field to that measured parallel to the field. On this basis the scale of irregularities in the density of the ions or electrons measured parallel to the earth's magnetic field is the same as the scale of the corresponding eddies in the neutral molecules, and the scale of the irregularities measured perpendicular to the earth's magnetic field is obtained by multiplying the scale measured parallel to the field by the appropriate ratio read from *Fig. 6*.

An important correction is required in the above statement arising from the tendency of irregularities in ion density to create irregularities in electron density of the same size and shape as a result of electrostatic forces.[43] In fact, eddies of scale L in the neutral molecules are likely to create irregularities in electron density by two mechanisms; namely:

(*a*) Collisions between electrons and neutral molecules.

(*b*) Collisions between ions and neutral molecules, with allowance made for electrostatic forces between ions and electrons. In both mechanisms the scale of electronic irregularities measured along the earth's magnetic field is L. In case (*a*) the scale of electronic irregularities transverse to the earth's magnetic field is T_e, where the ratio T_e/L is given by the electronic curve in *Fig. 6*. In case (*b*) the scale of electronic irregularities transverse to the earth's magnetic field is T_i, where the ratio T_i/L is given to only a rough approximation by the ionic curve in *Fig. 6*. For an isolated irregularity the tendency of electrons to follow the ions would reduce the ratio T_i/L to unity. Since, however, we are dealing with a continuum of irregularities of small intensity, this effect is greatly reduced but not completely destroyed. The appropriate value of T_i/L is therefore almost certainly less than that given by the ionic curve in *Fig. 6*, but we shall tentatively assume that it is not drastically less. The relative importance of the above two mechanisms for creation of electron irregularities is not known theoretically. However, reasons will be given, based on observations, for thinking that both mechanisms are important in the ionosphere.

It may also be mentioned that it is in connection with the interpretation of the ratios shown in *Fig. 6* that the assumption of isotropic turbulence in the neutral molecules is particularly important. These ratios would have to be modified by the ratio of the turbulence velocity of the neutral molecules perpendicular to the earth's magnetic field to that parallel to the earth's magnetic field. There is more than one respect therefore in which the ratios shown in *Fig. 6* may require correction. Nevertheless, we shall use the ratios shown in *Fig. 6* without modification to indicate the shape of electronic irregularities controlled by collision between electrons and neutral molecules (electronic curve) and by electrostatic coupling with the ions (ionic curve).

Scintillation of radio stars, being a phenomenon of forward scattering,

depends on the largest irregularities of electron density present. These irregularities will arise from the large eddies, of scale L_1, in the neutral molecules, operating via mechanism (*b*) to form electronic irregularities of scale L_1 measured along the earth's magnetic field and scale T_{i1} measured transverse to the earth's magnetic field, the ratio T_{i1}/L_1 being somewhat less than that given by the ionic curve in *Fig. 6*. The measurements of SPENCER[6] show that $2\pi T_{i1}$ is of the order of 3 km. We shall, therefore, take it as an observed fact that, at the level where scintillation of radio star occurs, we have:

$$T_{i1} = 0{\cdot}5 \text{ km} \qquad \ldots.(39)$$

SPENCER has also attempted to measure the ratio of T_{i1} to L_1, but the results are somewhat vague. Ratios of the order 1 : 10 are explicitly mentioned, but ratios as big as 1 : 100 are not explicitly mentioned. For the purpose of discussion we shall assume that the value of the ratio at the scintillation level is:

$$\frac{T_{i1}}{L_1} = \frac{1}{30} \qquad \ldots.(40)$$

The value of this ratio is important to the discussion, so that it is unfortunate that its value is not better determined. Combining (40) with (39) we see that SPENCER's results indicate a scale of turbulence at the scintillation level of:

$$L_1 = 15 \text{ km} \qquad \ldots.(41)$$

It should be realized that, of the three quantities (39), (40), and (41), only (39) may be considered a firm value.

It has been estimated by HEWISH[5] that the height at which the scintillation of radio stars occurs is about 400 km. This was never a highly accurate measurement of height, however, and its reliability is further reduced now that it is known that the electronic irregularities concerned are constricted round the lines of the earth's magnetic field. We shall assume that the HEWISH argument merely indicates that the scintillation level must be somewhere in the *F*-region.

There seems little doubt that 400 km is an impossibly great height at which to explain the scintillation phenomenon by means of turbulence. In the first place there is difficulty in having turbulence at 400 km. In the second place, even if turbulence could exist at 400 km, it would not lead to electronic irregularities of the size and shape required to explain the scintillation observations. The ratio (38) for the transverse scale to the longitudinal scale is so small at 400 km that the largest conceivable transverse scale would be much less than the observed value (39). If, therefore, the scintillation phenomenon is to be explained in terms of atmospheric turbulence, it will clearly have to be at a level below 400 km.

Let us tentatively accept the statement (40) and use it in conjunction with the ionic curve in *Fig. 6*. We then read off 170 km as the scintillation height. Although this estimate is probably too low, let us use it as a basis of further discussion. It follows from this and from (41) that the scale of the large eddies at 170 km is 15 km. From the rocket atmosphere we also derive for 170 km:

$$\mathrm{T} = 518^\circ \text{ K} \qquad \ldots.(42)$$

$$\frac{\mathrm{dT}}{\mathrm{d}z} = 5^\circ \text{ K/km} \qquad \ldots.(43)$$

$$\Gamma = 8{\cdot}5^\circ \text{ K/km} \qquad \ldots.(44)$$

$$\frac{dT}{dz} + \Gamma = 13{\cdot}5^\circ \text{ K/km} \qquad \ldots.(45)$$

From (4) we therefore obtain for the time constant of the large eddies

$$t_1 = 60 \text{ sec} \qquad \ldots.(46)$$

Now substituting from (41) and (46) into (8), we obtain for the turbulence power per unit mass at the scintillation level:

$$w = 1000 \text{ W/kg} \qquad \ldots.(47)$$

This value is even higher than that found at the meteoric level. The value (47) for w implies a Reynolds number for the large eddies of about a hundred, while keeping the turbulence energy to somewhat less than one per cent of the thermic energy. High though the estimated value for the turbulence power per unit mass at the scintillation level may seem to be at first sight, it does not violate the obvious criterion that the turbulence energy should be small compared with the thermic energy.

From the value (47) for w and the formulas of Secs. 2 and 3, we may deduce the following numerical values for the scintillation level, none of which seem capable of verification at the present time:

$$v_1 = 250 \text{ m/sec} \qquad \ldots.(48)$$

$$v_2 = 80 \text{ m/sec} \qquad \ldots.(49)$$

$$t_2 = 7 \text{ sec} \qquad \ldots.(50)$$

$$L_2 = 0{\cdot}5 \text{ km} \qquad \ldots.(51)$$

The fading rate involved in scintillation cannot be checked with the above value of v_1 because the fading rate is controlled by the rate of horizontal drift of irregularities, due presumably to the influence of an electric field.

We conclude that it is feasible to explain the phenomenon of scintillation of radio stars in terms of turbulence in the *F*-region. The height, however, must be less than 400 km although it no doubt exceeds somewhat the value of 170 km used above. To explain star scintillation by means of turbulence, the rate of supply of turbulence energy to the large eddies, and its rate of conversion into thermic energy by the small eddies, must have the high value of about a 1000 W/km.

6. Discussion of the Magnitude of the Turbulence Power

At present we only have three approximate values for the turbulence power w per unit mass, namely:

(*a*) 5×10^{-4} W/kg in the troposphere.
(*b*) 25 W/kg at the meteoric level.
(*c*) 1000 W/kg at the scintillation level.

Moreover, the last of these values refers to condition of strong scattering in the *F*-region, and a value for w of perhaps 100 W/kg might be more appropriate to a quiet ionosphere. While it is impossible to construct a reliable curve of w as a function of height from this information, there are nevertheless some useful statements that can be made.

At each level in the rocket atmosphere it is possible to specify a range of

values within which w must lie, and to plot the upper and lower bounds as a function of height. This is done in *Fig. 7*, where the shaded area denotes the portion of the diagram within which w cannot lie. The curve specifying the left-hand edge of the permitted area expresses the condition that the Reynolds number for the large eddies is unity. Since the Reynolds number for the small eddies is always unity, the equation of this curve is given by:

$$L_1 = L_2 \qquad \ldots.(52)$$

Using formulas (8) and (10) for L_1 and L_2, Eq. (52) reduces to:

$$w = \frac{D}{t_1^2} \qquad \ldots.(53)$$

Hence a lower bound for the value of the turbulence power per unit mass at any height is:

$$\frac{D}{t_1^2} \qquad \ldots.(54)$$

For the rocket atmosphere we have already calculated D as a function of height (see *Fig. 2*) and also t_1 as a function of height (see Eq. (4) and *Fig. 1*).

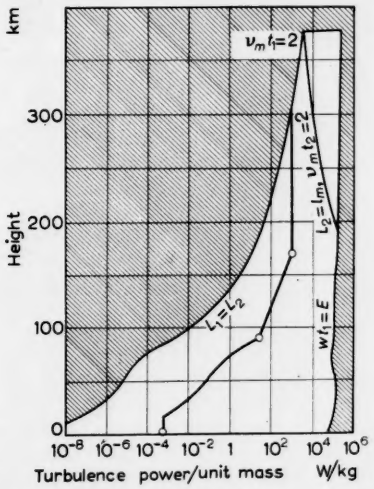

Fig. 7. Restrictions on the value of the turbulence power per unit mass

We can, therefore, calculate (54) as a function of height, and it is this curve that gives the left-hand boundary of the permitted area in *Fig. 7*.

Since the energy of turbulence is associated mainly with the large eddies, the turbulence energy per unit mass is approximately wt_1. This must obviously be less than the thermic energy E per unit mass. Hence an upper bound for the value of w at any level is:

$$\frac{E}{t_1} \qquad \ldots.(55)$$

and the value of this can be calculated for the rocket atmosphere at any height. The right-hand boundary of the permitted area in *Fig. 7* is a plot of (55) as a function height for the rocket atmosphere.

The top of the permitted area in *Fig. 7* is set by the fact that a molecule must make collision within a time equal to the time constant t_1 of a large eddy.

We deduce from *Fig. 7* the important fact that it is impossible to have turbulence in the ionosphere unless the turbulence power per unit mass is much higher than Brunt's value, 5×10^{-4} W/kg for the troposphere. We further notice that the value 25 W/kg that we have deduced for the meteoric level lies in the middle of the permitted range at 90 km. The value 1000 W/kg for the scintillation level is also satisfactory provided that this level is significantly below 400 km.

The permitted area in *Fig. 7* is cut into two parts by a curve marked $L_2 = l_m$. This curve expresses the condition that the scale L_2 of the small

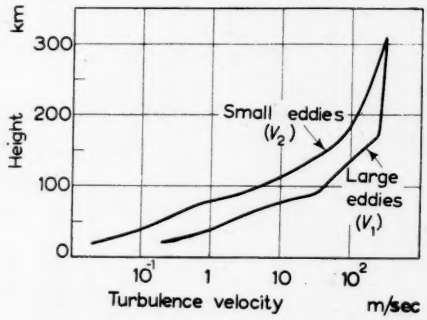

Fig. 8. The turbulence velocity for the large and small eddies

eddies given by (10) is equal to the molecular mean free path l_m. Below this curve the cut-off in the spectrum of turbulence at the small eddy and is controlled by viscosity in the usual way and occurs at the scale L_2. Above this curve the cut-off in the spectrum of turbulence is given by the molecular mean free path l_m as contemplated by DUNGEY and WILLSON.[41] It is seen that, over the majority of the permitted area, and over practically all the area in which we are likely to be interested, the cut-off in the spectrum of turbulence is likely to be determined by viscosity in the usual way. This means that we are unlikely to encounter any revolutionary modification in the principles that form the basis of the Kolmogoroff–Heisenberg theory of turbulence.

For purposes of illustration, a curve of turbulence power per unit mass versus height has been drawn in *Fig. 7* through the three points corresponding to the troposphere, the meteoric level, and the scintillation level. The departure from a linear segment in the interval of height from 18 to 90 km arises from an arbitrary (and unimportant) assumption that the turbulence energy per unit volume does not vary with height in this range. Using this curve of ω vs. height, we may calculate for the rocket atmosphere the variation with height of the various parameters associated with the large and small eddies. On this tentative basis the time constant t_2 of the small eddies has been added to *Fig. 1*, and the coefficient of eddy diffusion has been added to *Fig. 2*. The ratio of the two coefficients of diffusion gives the Reynolds number of the large eddies. On the same basis the turbulence velocities for the large and small eddies are plotted as functions of height in *Fig. 8*, and the scales of the large and small eddies are plotted as functions of height in *Fig. 9*.

It may be noted that the scale of the large eddies indicated in *Fig. 9* becomes comparable with the scale height of the atmosphere at *F*-region levels. This is not thought to be objectionable. If the size of eddies is not small compared with the scale height of the atmosphere, this merely underlines the importance of allowing for adiabatic expansion and contraction in picturing the eddy motion. Furthermore, if under quiet ionospheric conditions the turbulence power per unit mass at 200 km were only 100 W/kg, it follows

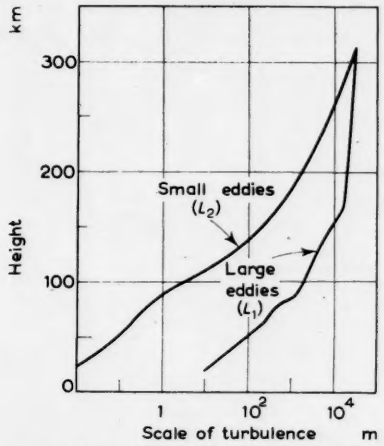

Fig. 9. The scales of the large and small eddies

from *Fig. 7* that there would be little turbulence above 200 km and that the scale of the large eddies would be less than the scale height of the atmosphere at all relevant levels.

7. Discussion of the Scales of Electronic Irregularities

It has been pointed out by Dungey and Willson[41] that eddy scales less than the molecular mean free path are impossible. Some care, however, is necessary in making corresponding statements about electronic irregularities. For electronic irregularities, the scale along the earth's magnetic field cannot be less than the electronic mean free path l_e, and it has to be remembered that:

$$l_e = 4\sqrt{2} \cdot l_m \qquad \ldots.(56)$$

where l_m is the molecular mean free path. In a direction perpendicular to the earth's magnetic field, however, the minimum permissible scale for electronic irregularities, is from (38);

$$\frac{\nu}{(\omega_M^2+\nu^2)^{\frac{1}{2}}} l_e \qquad \ldots.(57)$$

where ν is the electronic collisional frequency and ω_M is the electronic radian gyrofrequency. When $\nu \gg \omega_M$ (heights below about 70 km), (57) simply reduces to the electronic mean free path l_e, and there is no constriction of electronic irregularities perpendicular to the earth's magnetic field. However, when $\nu \ll \omega_M$ however (heights above 90 km), (57) becomes:

$$\frac{\nu l_e}{\omega_M} \qquad \ldots.(58)$$

Now the numerator of (58) is the thermic velocity of the electrons and the denominator is the angular velocity with which electrons spiral round the earth's magnetic field. Hence (58) is the gyroradius of electrons in the earth's magnetic field, which is of the order of a centimeter or two. Thus, above 90 km, the minimum possible scale of electronic irregularities measured transverse to the earth's magnetic field is given by the electronic gyroradius, although the minimum possible scale measured along the earth's magnetic field is given by the electronic mean free path.

For the ions there are similar considerations that are important because

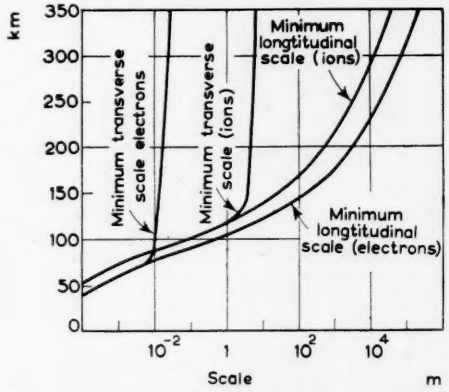

Fig. 10. The minimum scales for irregularities in the density of charged particles

of the control that ionic irregularities are likely to have on electronic irregularities. For the ions, the minimum possible scale of irregularities measured along the earth's magnetic field is the molecular mean free path:

$$l_m \qquad \ldots.(59)$$

and the minimum possible scale measured transverse to the earth's magnetic field is;

$$\frac{\nu}{(\omega_M^2+\nu^2)^{\frac{1}{2}}} l_m \qquad \ldots.(60)$$

where ν must now be interpreted as the molecular collisional frequency and ω_M as the ionic radian gyrofrequency. The various minimum possible scales are plotted in *Fig. 10* as functions of height, using the above formulas in conjunction with the rocket atmosphere.

For ionic irregularities, and consequently also for electronic irregularities controlled by ionic irregularities, the large and small scales measured along the earth's magnetic field are simply the scales of the large and small eddies in the neutral molecules, and may consequently be read from *Fig. 9*. For electronic irregularities controlled directly by collisions with the neutral molecules, the same is true, except that some account has to be taken of the minimum possible scale along the earth's magnetic field plotted in *Fig. 10*. The appropriate curve from *Fig. 10* intersects the curves in *Fig. 9*, thereby removing electronic irregularities at the greater heights. Above about 160 km an electron can pass right through a small eddy without making a collision, and above about 260 km it can do this even for a large eddy. This does

not happen for electronic irregularities controlled by ionic irregularities because of the lower mean free path for ions.

Let us now turn our attention to the scale of electronic irregularities measured transverse to the earth's magnetic field. These are obtained by applying to the scales shown in *Fig. 9*, the fractions plotted in *Fig. 6* and paying attention to the appropriate minimum possible scales shown in *Fig. 10*. We thereby obtain the diagram of *Fig. 11*. It is seen that, for electronic irregularities controlled by collision between electrons and neutral molecules, the curves giving the scale of irregularities are decapitated by the curve

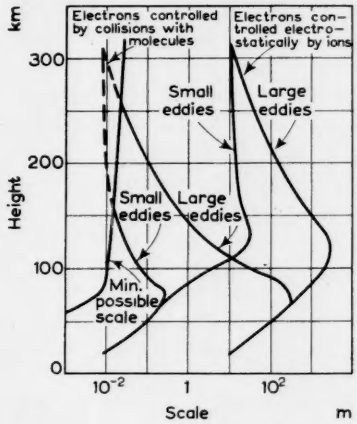

Fig. 11. The scales of irregularities of charged particles measured perpendicular to the earth's magnetic field

giving the minimum possible scale of irregularities in the same way as for scales along the earth's magnetic field and for the same reason. For electronic irregularities controlled by ionic irregularities no such limitation is involved.

It will be noticed that, while we have considered the controlling effect of ionic irregularities on electronic irregularities via electrostatic forces, we have not considered any such control via collisions between ions and electrons even though these collisions are the ones of greatest frequency in the *F*-region. It is not difficult to show that any electronic irregularities occurring in the *F*-region as a result of collisions between ions and electrons would have scales so small that they would be blurred by the spiraling of electrons round the earth's magnetic field.

8. Auroral Echoes

Let us now consider the significance of the curves in *Figs. 9* and *11*, turning our attention first to the phenomenon of auroral echoes.[15] It is well known that ionospheric echoes are obtained by radars operating in the VHF band during auroral activity, and that these echoes occur predominantly at long range in the northern quadrant even when the auroral activity is distributed over practically the whole sky. It has been shown by Booker[29] that this aspect sensitivity is to be explained in terms of irregularities of electron density that are elongated along the earth's magnetic field and have a scale

Suppl.
art.II
1956

along the field of the order of 7 m. The scale *transverse* to the field is small compared with this, and controls *the shortest wavelength down* to which auroral echoes can be observed. Let us assume that these irregularities arise from turbulence in the *E*-region. On this view the only functions of the auroral activity would be:

(*a*) To provide increased electron density and increased gradients of electron density, thereby increasing the intensity of the electronic irregularities.

(*b*) To provide, in association with phenomena of terrestrial magnetism, an unusually large electric field that would cause drift of the electronic irregularities at such a speed as to explain the fading and Doppler phenomena observed with auroral echoes.[17]

If auroral echoes are due to electronic irregularities caused by turbulence, these irregularities would have to be the smallest irregularities present at the level concerned. The 7 m derived by Booker would, therefore, have to be the scale measured along the earth's magnetic field of the smallest electronic irregularities, and this is the same as the scale of the small eddies in the neutral molecules. We accordingly deduce that, at the level where auroral echoes occur, we have:

$$L_2 = 7 \text{ m approximately} \qquad \ldots.(61)$$

From *Fig. 9* we deduce, therefore, that auroral echoes must occur at a height of about 100–110 km. This is in remarkably good agreement with the other features of auroral echoes.

Let us now read from *Fig. 11* the transverse scale for the smallest electronic irregularities at the level where (61) applies. We deduce:

$$T_{2e} = 6 \text{ cm} \qquad \ldots.(62)$$

from which it should follow that the wavelength below which auroral echoes are unimportant is:

$$4\pi T_{2e} = 70 \text{ cm} \qquad \ldots.(63)$$

This fits in with the experimental observation that auroral echoes are obtained in the VHF band but not in the UHF band, though it should be noted that sufficiently careful experiments may not yet have been made in the UHF band. We conclude that the turbulence explanation of auroral echoes is highly likely.

It will be observed that we would not have been able to explain the phenomenon of aspect sensitivity of auroral echoes in terms of turbulence if we had not taken account of the electronic irregularities produced directly from eddies by collision between electrons and neutral molecules without the ions being involved. However, it is equally true that we would have been unable to explain the phenomena of star scintillation in terms of turbulence if we had not taken account of electronic irregularities controlled electrostatically by ionic irregularities. It is for these reasons that we believe in the importance of both of these mechanisms for converting eddies in the neutral molecules into irregularities of electron density.

9. Radar Echoes from Irregularities in the *F*-region at Frequencies Above the Penetration Frequency

Aspect sensitive echoes from *F*-region levels having properties somewhat like auroral echoes, but not associated with auroral activity, have been observed

by workers at Stanford University[3] in the HF band and presumably have the same explanation. Similar echoes have also been obtained by these observers in the HF band from *F*-region levels, and again the explanation is presumably the same. From geometrical considerations it has been deduced that these *F*-region echoes originate at heights between about 200 and 300 km. It seems quite likely that this phenomenon, the phenomenon of spread-*F*, and the phenomenon of star scintillation all arise from the effects of turbulence in the *F*-region at levels between 200 and 300 km. But whereas scintillation of radio stars is produced by the largest electronic irregularities present, the aspect sensitive *F*-region echoes should be produced by the irregularities whose scale transverse to the earth's magnetic field is as near as possible to $\lambda/4\pi$. There is no doubt that the scale of irregularities in the *F*-region along the earth's magnetic field is large compared with any HF wavelength, and the primary cause of the aspect sensitivity of the *F*-region echoes reported from Stanford University is obvious. The variation with frequency of the strength of these echoes is not known, however, with any certainty. From *Fig. 11* we would expect scales measured transverse to the earth's magnetic field at 200 km to range from 200 m down to 10 m and from 10 cm down to 2 cm. At 300 km we would expect scales of the order of 10 m. Whether those scales can explain the observations is not clear at the present time. Neither is it clear whether the two spectra of irregularities transverse to the earth's magnetic field shown in *Fig. 11* at *F*-region heights can be regarded as uncoupled.

Suppl.
art.II
1956

It should be noted that there is a real likelihood of electronic irregularities in the lower part of the *F*-region with scales measured along the earth's magnetic field of the order of 20 km and measured transverse to the earth's magnetic field of the order of a few centimeters. In principle, such irregularities should give echoes for radars in the UHF band if directed so that their beams are normal to the earth's magnetic field in the lower part of the *F*-region. It seems unlikely that such echoes could be strong enough to be observable even with high-power equipment. It would be interesting, however, to take any opportunity that may occur to look for such echoes, especially at times of strong star scintillation and strong spread-*F*.

10. Scattering Phenomena at the 90 Km Level

Another application of the results summarized in *Figs. 9* and *11* is to the phenomenon of long-distance scatter communication in the VHF band.[12] This phenomenon as observed by Bailey, Bateman, and Kirby[13] over distances of the order of 1000–2000 km can be fairly completely explained in terms of scales read from *Figs. 9* and *11* for the 90 km level. This subject will be taken up in the companion paper by Booker and Cohen.[36] The only point that will be made here is that, in accordance with *Fig. 6*, electronic irregularities controlled directly by collision with neutral molecules should show some constriction perpendicular to the earth's magnetic field at the 90 km level. It may be, therefore, that the beams used in this type of communication should be turned somewhat off the great-circle path in a direction away from the equator, especially at the highest frequencies involved. Likewise, for individual long-duration meteor echoes, there may be an aspect sensitivity phenomenon qualitatively similar to that for auroral echoes,

but in an appreciably less striking manner because of the lower height involved.

There seems little doubt that the 90 km echoes of GARDNER and PAWSEY[10] and the similar echoes of DIEMINGER[11] at frequencies around 2 Mc/s are due to radar reflections from the same irregularities that cause VHF scatter communication. Using the scales derived for the 90 km level in Sec. 4 in conjunction with the Kolmogoroff–Heisenberg spectrum of turbulence, it is possible to derive some equations describing the 2 Mc/s phenomenon. It would be nice to check the spectrum of turbulence by comparing the 2 Mc/s observations with the VHF observations. This is unfortunately rendered difficult because we are unable to allow with sufficient accuracy for the effect of absorption on the 2 Mc/s observations.

11. THE POSSIBILITY OF *F*-REGION SCATTER COMMUNICATION

Ever since the discovery of long-distance communication in the VHF band using incoherent scattering in the lower part of the ionosphere, there has been discussion of the possibility of a similar phenomenon using scattering by electronic irregularities in the *F*-region. It was at first argued that eddies in the *F*-region were bound to be larger than in the *E*-region and that this would increase the wavelength down to which communication via scattering in the *F*-region would be possible. It is now clear that this argument was fallacious. It is quite true, as shown in *Fig. 9*, that eddies in the neutral molecules are likely to be bigger in the *F*-region than in the *E*-region. This further implies that the scale of electronic irregularities measured along the earth's magnetic field is likely to be larger in the *F*-region than in the *E*-region. But *Fig. 11* shows that the scales of irregularities measured transverse to the earth's magnetic field are smaller in the *F*-region than in the *E*-region. This is because the effect of the earth's magnetic field in constricting the scale of electronic irregularities measured transverse to the field increases with height above the *E*-region faster than does the scale of the eddies in the neutral molecules. The result is that the smallest scales of electronic irregularities occurring anywhere in the ionosphere are likely to occur in the *F*-region, but only in the direction transverse to the earth's magnetic field. So far as scale is concerned, therefore, there is no reason why there should not be a phenomenon of scatter communication employing irregularities in the *F*-region, and extending down to even shorter wavelength than is involved in scatter communication via the lower ionosphere. It is essential, however, that due allowance be made for the fact that electronic irregularities in the *F*-region are very elongated along the earth's magnetic field.

Our lack of knowledge of the spectrum of electronic irregularities measured transverse to the earth's magnetic field in the *F*-region makes it impossible to predict the frequency dependence of *F*-region scatter communication at the present time. It is, however, possible to list three conditions that should be satisfied in experiments designed to investigate the phenomenon and that arise from the fact that the irregularities are very elongated along the earth's magnetic field. There are:

(*a*) Successful *F*-region scatter communication is more likely for an E–W path than for a N–S path.

(*b*) The E–W path should not be in too high a lattitude, otherwise the "echo-point" will be in the *E*-region instead of the *F*-region; see CHAPMAN.[42] For an experiment in the United States this means that a path should be chosen near the Mexican border rather than near the Canadian border.

(*c*) Both the transmitting and receiving beams must be swung from the great-circle path away from the equator through a substantial angle. Thus, for communication between Miami, Florida, and San Diego, California the beams should be pointed, not at the *F*-region over Texas, but at the *F*-region over Iowa.

Experiments should presumably be initiated in the 20–30 Mc/s band and extended upward in frequency as far as possible. Experiments that may involve scattering in the *F*-region have recently been described by ABEL and PHILLIPS.[14] In these experiments, however, none of the above conditions were well satisfied. It seems desirable, therefore, that these experiments be repeated, bearing in mind the three conditions listed.

12. SPREAD-F AND OTHER REFLECTION PHENOMENA

It seems fairly clear that the cause of spread-*F* must be scattering by the electronic irregularities in the *F*-region of the type that we have been discussing. Consider the following over-simplified picture of the phenomenon. Suppose that an HF wave that is reflected from the *F*-region has to cross and recross the stratum of atmosphere responsible for star scintillation. Suppose furthermore that, in the stratum containing the irregularities, mean refraction is negligible, while at the level of reflection irregularities are unimportant. In the scintillation stratum the HF wave is subjected to predominantly forward scattering by the largest electronic irregularities. The size of these irregularities as given by *Figs. 9 and 11* show that angles of scattering for a wave in the HF band will be small. Consequently the reflected wave will not involve large deviations from the vertical. Now it is known that, even in the VHF band, star scintillation sometimes involves fluctuation indexes of the order of unity, indicating that multiple scattering must be involved. Since forward scattering increases proportionally to the square of wavelength, this would be true *a fortiori* in the HF band. It is easy to see, therefore, that the scintillation stratum could frequently involve multiple scattering at a frequency below the penetration frequency. This leads to a qualitative explanation of spread-*F* that does not involve large departures from the vertical in the direction of arrival of the downcoming wave.

The above picture is obviously over-simplified; it is unlikely that the scattering stratum can be dissociated from the reflecting stratum in the way supposed. As soon as one attempts to integrate the two, however, one is up against a serious theoretical difficulty. There is no theory available at present that is capable of describing the effect of turbulence upon the phenomenon of total internal reflection in an ionized medium. It is for this reason that difficulty is being experienced in relating the theory of turbulence quantitatively to observations of irregularities using waves reflected from the ionosphere, whereas comparative success is being achieved for the various ionospheric scattering phenomena observed in the VHF band.

References

[1] McNichol. *J. Instu. elect. Engrs.* Vol. 96, p. 517, 1949
[2] Meek. *Terr. Mag.* Vol. 54, p. 339, 1949
[3] Peterson, Villard, Leadabrand, and Gallagher, *J. geoph. Res.* Vol. 60, p. 497, 1955
[4] Ryle and Hewish. *Mon. Not. R. astr. Soc.* Vol. 110, p. 381, 1950
[5] Hewish. *Proc. Roy. Soc.* A Vol. 209, p. 81, 1951; *Proc. Roy. Soc.* A Vol. 214, p. 494, 1952
[6] Spencer. *Proc. Phys. Soc.* B Vol. 68, p. 493, 1955
[7] Wild and Roberts. *J. atmos. terr. Phys.* Vol. 8, p. 55, 1956
[8] Greenhow. *Proc. Phys. Soc.* B Vol. 65, p. 169, 1952
[9] Liller and Whipple. *Rocket Exploration of the Upper Atmosphere*, p. 112; Pergamon Press, London, 1954
[10] Gardner and Pawsey. *J. atmos. terr. Phys.* Vol. 3, p. 321, 1953
[11] Dieminger. *Physics of the Ionosphere*, p. 53; Physical Society, London, 1954
[12] Bailey, Bateman, Berkner, Booker, Montgomery, Purcell, Salisbury, and Wiesner. *Phys. Rev.* Vol. 86, p. 141, 1952
[13] Bailey, Bateman, and Kirby. *Proc. Inst. radio Engrs. N.Y.* Vol. 43, p. 1181, 1955
[14] Abel and Phillips. Paper presented at URSI meeting, Washington, D.C., May 1956
[15] Booker, Gartlein, and Nichols. *J. geophys. Res.* Vol. 60, p. 1, 1955
[16] Dyce. *J. geophys. Res.* Vol. 60, p. 317, 1955
[17] Bowles. *J. geophys. Res.* Vol. 59, p. 553, 1954
[18] Brunt. *Physical and Dynamical Meteorology.* Chap. 12; Cambridge University Press, 1941
[19] Batchelor. *The Theory of Homogeneous Turbulence.* Chap. 6; Cambridge University Press, 1953
[20] Kolmogoroff. *C. R. Acad. Sci. U.R.S.S.* Vol. 30, p. 301; Vol. 32, p. 16, 1941
[21] Heisenberg. *Z. Phys.* Vol. 124, p. 628, 1948
[22] Booker and Gordon. *Proc. Inst. radio Engrs. N.Y.* Vol. 38, p. 401, 1950
[23] Megaw. *Nature, Lond.* Vol. 166, p. 1100, 1950
[24] Villars and Weisskopf. *Phys. Rev.* Vol. 94, p. 232, 1954
[25] Villars and Weisskopf. *Proc. Inst. radio Engrs. N.Y.* Vol. 43, p. 1232, 1955
[26] Gallet. *Proc. Inst. radio Engrs. N.Y.* Vol. 43, p. 1421, 1955
[27] Batchelor. *Research Report EE 262*, Cornell University School of Electrical Engineering, 1955; to be published
[28] Silverman. Paper presented at URSI meeting, Washington, D.C., May 1956; to be published
[29] Booker. *J. atmos. terr. Phys*; Vol. 8 p. 204 1956
[30] The Rocket Panel. *Phys. Rev.* Vol. 88, p. 1027, 1952
[31] Weekes. *Quart. J. met. Soc.* Vol. 80, p. 2, 1954
[32] Chapman and Cowling, *The Mathematical Theory of Non-Uniform Gases*; Cambridge University Press, 1939
[33] Greenhow and Neufeld. *J. atmos. terr. Phys.* Vol. 6, p. 133 1955
[34] Greenhow. *Phil. Mag.* Vol. 45, p. 471, 1954
[35] Greenhow. *Phil. Mag.* Vol. 41, p. 682, 1950

Supp
Part.
195

[36] Booker and Cohen. Paper presented at URSI meeting, Washington, D.C., May 1956; page 171 of this volume.
[37] Kaiser and Closs. *Phil. Mag.* Vol. 43, p. 1, 1952
[38] Lovell and Clegg. *Proc. Phys. Soc.* Vol. 60, p. 491, 1948
[39] Dobrovol'skii. *Bull-Stalinabad Ast. Obs.* No. 1, p. 15, 1952 (*Rand Corp. translation* T-39)
[40] Maxwell. *Phil. Mag.* Vol. 45, p. 1247, 1954
[41] Dungey and Willson. *J. geophys. Res.* Vol. 60, p. 521, 1955
[42] Chapman. *J. atmos. terr. Phys.* Vol. 3, p. 1, 1952
[43] Dungey. *J. atmos. terr. Phys.* Vol. 8, p. 39, 1956

uppl.
rt.II
1956

ELECTRON DISTRIBUTION IN A NEW MODEL OF THE IONOSPHERE*

H. K. KALLMANN

Institute of Geophysics, University of California at Los Angeles,
Los Angeles, California, U.S.A.

A theoretical analysis of the formation of the ionosphere has been made which has led to a model of the ionized regions at altitudes between 80 and 300 km above the earth's surface. The study is based primarily on a new model of the pressure, density, and temperature distribution derived from rocket observations, and upon solar radiation measurements, also made by means of rockets, above 90 km. The calculated electron density distribution is then compared with the electron densities measured directly at the pertinent altitudes, again by rockets carrying the measuring devices and telemetering equipment.

THE ionosphere, including the *E*-, *F*1-, and *F*2-regions, is usually pictured to extend from about 100 km to 300 or 400 km. The apparent height of the *F*1-region is above 200 km, and of the *F*2-region around 300 km. Apparent heights of 400 and 500 km have frequently been observed. The true height of reflection is always less than the apparent or virtual height because of the retardation of the velocity in an ionized medium, the difference in height being dependent upon the electron density distribution throughout the region of travel. It is because of this that true heights are difficult to determine; in general, they depend on the assumed model of the atmosphere and of the ionosphere — unless the electron density can be measured directly and continuously up to the altitude of reflection, as has been done more recently by means of rockets. As it will be seen, the difference in true and apparent height in the *F*-region is very great indeed, a fact which can be explained from the new ionospheric model as well as from observations.

The ionospheric models presented before, as well as the new model arrived at here, are fundamentally based on the theory first proposed by Chapman in 1931, namely, that short-wave radiation emitted from the sun penetrates into the earth's atmosphere and ionizes the air particles, thereby producing electrons which are able to reflect radio waves sent up from the ground.

The so-called Chapman theory is generally evaluated under the simplified assumption that monochromatic radiation corresponding to one wavelength only, is absorbed by and able to ionize one air constituent only. Thus in any one region in the ionosphere, one constituent absorbing one wavelength is the only source of electrons. Furthermore, it has been customary to assume that the molecular weight and the temperature are constant for any one region.

* The research reported in this paper has been sponsored in part by the Geophysics Research Directorate of the Air Force Cambridge Research Center, Air Research and Development Command, under Contract No. AF 19(604)-111.

As a result of this, the ionosphere has been pictured to consist of more or less parabolic layers of electron densities.

A detailed analysis of the whole problem is by necessity very complex, since it involves a study of the variation of the physical properties of the earth's atmosphere with height, up to great altitudes — like temperature, pressure, and density — as well as a study of the intensity of radiation as a function of wavelength from the sun and its atmosphere, the chromosphere and the corona.

The determination of pressure and density in the earth's atmosphere up to about 200 km has been based on the data obtained by means of rockets. The density above 200 km has been extrapolated, using the theory of the exosphere — an isothermal region above the ionosphere — described by SPITZER.[1] The temperature has been derived from pressures and densities under the assumption that from the macroscopic point of view molecular oxygen begins to dissociate around 90 km, and that the region of dissociation is larger than has usually been assumed. Above 130 km, about 25 per cent of molecular oxygen is still present. These are facts which have been observed from rockets. An exponential rather than a linear decrease in molecular oxygen, and consequently in molecular weight, has been assumed.

Due to the fact that no ions of atomic nitrogen have been observed below 200 km, it has been assumed that molecular nitrogen begins to dissociate appreciably only above 200 km.

As a result of these assumptions, a continuous temperature distribution throughout the ionosphere has been obtained, the lapse rate of which does not exceed 5 deg/km, and for the most part is much less; a fact which is in agreement with studies made by BATES[2] and others[3] on the basis of the heat conduction theory. Thus, a continuous variation with altitude of individual particle concentrations of molecular and atomic oxygen and nitrogen has been obtained from what may be called an average model atmosphere which is in agreement with present knowledge.

Fig. 1 shows the variation of temperature with altitude for a model atmosphere derived from observations and assumptions stated above. This model atmosphere is the result of a joint effort by KALLMANN, WHITE, and NEWELL,[4] carried out at the request of the working group on the extension of the U.S. standard atmosphere and was submitted to the group at the beginning of this year.

The results obtained and used for the intensity of radiation coming from the solar atmosphere, in particular from the chromosphere, which is able to ionize the air particles, rely heavily on the extensive studies made on this subject by the astrophysicists, in particular by NICOLET[5] and DE JAEGER.[6] It can be shown that if radiation of wavelength less than 1300 Å has an intensity of more than 10^9 photons/cm^2/sec at the top of the atmosphere, this radiation must come from monochromatic line emission originating in the chromosphere and the corona, and cannot come from the continuous black body radiation emitted by the photosphere. A radiation of about 10^{11} photons per centimeter squared per second between wavelength 1050 to 790 Å has been deduced from rocket observations. This radiation corresponds to an equivalent black body temperature of from 6000 to 7000° K. At still shorter wavelengths, corresponding to the ionization potentials of nitrogen

Suppl.
Art. II
1956

and the second and third ionization potentials of atomic oxygen and nitrogen the equivalent black body temperatures are still higher, and may reach 10^5 ° K at the upper regions of the chromosphere.

The number of photons emitted from highly ionized carbon, silicon, magnesium, iron, etc., corresponding to the ionization potentials of the air

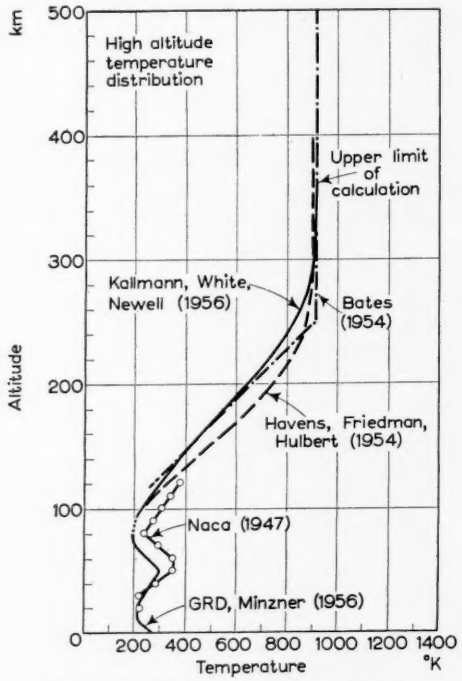

Fig. 1. High altitude temperature distribution

particles, is based on a model chromosphere whose equivalent black body temperature increases considerably from the lower to the upper part of the chromosphere. The wavelength of emission ranges from 1025 Å to about 200 Å. The results are sensitive to the assumed model of the chromosphere.

Mean absorption cross sections of the air constituents at these wavelengths for the molecular species have been taken from the experimental work of WEISSLER[7] and WATANABE,[8] and for the atomic species from BATES'[2] theoretical studies.

The number of ions produced /cm³/sec has been calculated from the following equation:

$$q(h, N, Q, A) = \sum_{\lambda=1}^{e} \sum_{i=1}^{k} N_1 A_1 Q_{\infty\lambda} \exp\left(-H\Sigma N_j A_{j\lambda}\right)$$

The first summation is taken over all wavelengths less than λ, in wavelength intervals between 1025 and 500 Å corresponding to the ionization potential of the air particles. The second summation is taken over all active constituents being ionized, while the summation in the exponential is taken over all constituents which absorb, causing ionization or excitation only.

The predominant processes by which electrons may be lost may differ at different altitudes. An effective recombination coefficient proportional to the square root of the neutral particle density at any one altitude has been assumed, as proposed by ARGENCE, MAYOT, and RAWER.[9] The electron density then has been obtained from the relation

$$N_e = \left[\frac{q}{\alpha_{eff}}\right]^{\frac{1}{2}}$$

Fig. 2 shows the variation of electron density with altitude as calculated by the method outlined here. The calculations were made for the zenith angle

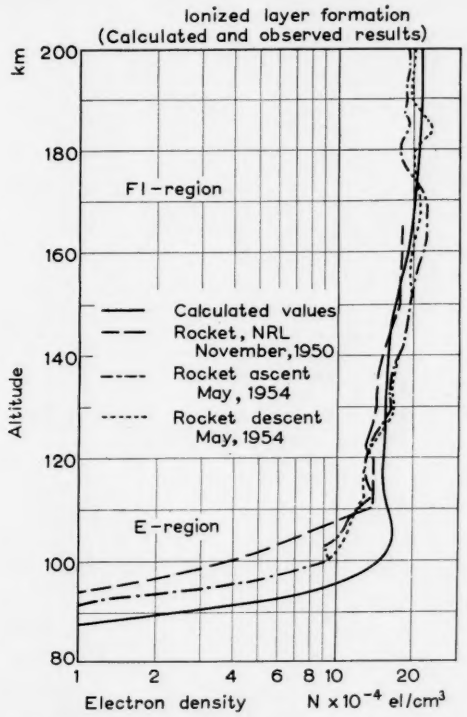

Fig. 2. Ionized layer formation (calculated and observed results)

of the sun at zero. Also shown are electron densities directly observed by and telemetered from rockets by a method developed by SEDDON[10] at the Naval Research Laboratory in Washington. These were the first direct measurements of electron densities in the ionosphere. Observations were made at times when the zenith angle was 40° and 60°, respectively. If calculations had been made for larger zenith angles, the results would have been closer to the observed ones in the *E*-region.

In the *F*2-region, the effective recombination coefficient can no longer be expected to be proportional to the square root of the neutral particle density, since the predominant processes may be ion-electron recombinations. Using effective recombination coefficients studied by MARTYN[11] and by APPLETON,[12]

Suppl.
art.II
1956

for the region above 180 km, the $F2$-region can be explained very well by the theory outlined above. *Fig. 3* shows electron densities calculated between 90 and 300 km, and a comparison with the observed values. Above 200 km the electron densities have been extrapolated[13] from ionospheric recorder records made during rocket flight.

The most important conclusion which can be drawn from this figure (*Fig. 3*) is the absence of any sharply-defined layers. The ionosphere remains heavily ionized throughout the 100–200 km region, with low electron-density gradients at surprisingly low altitudes. The maximum of the $F1$-region occurs around 165 km. It appears that the idea of separate layers must be replaced by the more appropriate concept of adjacent E-, $F1$-, and $F2$-

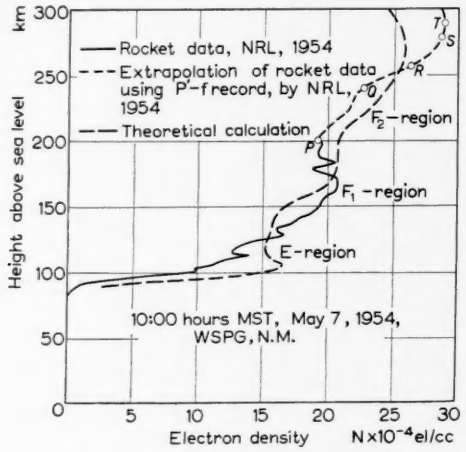

Fig. 3

regions blending gradually into one another. A comparison with the virtual height recordings ($h'f$ records) taken at the time of rocket flight showed an apparent height of

580 km at 4·28 Mc/s — true height 240
470 km at 4·6 Mc/s — true height 260
550 km at 4·8 Mc/s — true height 275
215 km at 4·1 Mc/s — true height 142

The great discrepancy between virtual and true height may be due to only slight gradient variations in such a thick ionosphere.

The whole problem is still very complex since such a great number of uncertainties in the various physical quantities are involved, such as photon emission from the solar atmosphere, air composition of the earth's atmosphere, and true absorption and recombination coefficients. The numerical solution presented here cannot be expected to be perfect or final, but it may not be too early to show that our present picture of the ionosphere will undergo changes, changes which have been indicated by direct observations and which can be explained on the basis of a theoretical analysis of the type presented here.

References

[1] Spitzer, L. *The Atmosphere of the Earth and Planets* (G. P. Kuiper, ed.), pp. 211–247; Univ. of Chicago Press, Chicago, 1951

[2] Bates, D. R. *Proc. roy. Soc.* B Vol. 64, p. 805, 1951; *Rocket Exploration of the Upper Atmosphere* (R. L. F. Boyd and M. J. Seaton, eds.), pp. 347–355; Pergamon Press, London, 1954

[3] Havens, R. J., Friedman, H., and Hulburt, E. O. *Report of 1954 Cambridg Conference*, p. 237; Physical Society, London, 1954

[4] Kallmann, H. K., White, W. B., and Newell, Jr., H. E. "Physical Properties of the Atmosphere from 90 to 300 km", *J. geophys. Res.* Vol. 61, p. 513, 1956

[5] Nicolet, M. *Physics and Medicine of the Upper Atmosphere* (G. S. White and O. O. Benson, eds.), pp. 182–225; Univ. of New Mexico Press, Albuquerque, 1952

[6] De Jaeger, C. *Ann. Geophys.* Vol. 11, p. 330, 1955

[7] Weissler, J. L. and Po Lee. *J. opt. Soc. Amer.* Vol. 42, p. 200, 1952; Weissler, J. L., Po Lee, and Mohr, *J. opt. Soc. Amer.* Vol. 42, p. 84, 1952

[8] Watanabe, K., Marmo, F., and Tun, E. C. *Phys. Rev.* Vol. 90, p. 155, 1953

[9] Argence, E., Mayot, M., and Rawer, K. *Ann. Geophys.* Vol. 6, p. 242, 1950

[10] Seddon, J. C. *J. geophys. Res.* Vol. 58, p. 323, 1953

[11] Martyn, D. F. *Proc. roy. Soc.* A Vol. 189, p. 241, 1947

[12] Appleton, E. V. *Proc. roy. Soc.* A Vol. 162, p. 451, 1937

[13] Seddon, J. C., Pickar, A. D., and Jackson, J. E. *J. geophys. Res.* Vol. 59, p. 513, 1954

Suppl.
art.II
1956

DISCUSSION

Discussion on Wednesday, 4 July and Thursday, 5 July in connection with the papers read on: *Drift of the Ionosphere.*

FINDLAY: We will start with the two important general things that we have heard this afternoon. The first is: how real are drift movements, when you take into account the possibility of irregular movements in the layer itself, and when you take into account the anisotropy possible in the patterns on the ground, roughly along the lines of what Mr. Jones talked about? Secondly, I think along the lines of Dr. Weekes: what you see when you measure a drift, is it a wind or is it something else? In what parts of the atmosphere can it reasonably be described as a wind and where can it not be described this way? Are there any ideas on this? Those will be my suggestions for starting the discussion.

HARANG: I would be interested to hear the opinion of the Cambridge group on using scintillations for drift measurements. When scintillations are recorded at low angles, the drift measurements seem to be completely fictitious as the diffraction pattern will present a pronounced E–W anisotropy, and it is apparent that if you apply scintillation technique with the source coming in at a certain elevation, you cannot come around this difficulty. If you have the scintillation coming in almost at vertical incidence, do you think that we then might get drift measurements which have a physical meaning? The reason why I put this question before you is that we are intending to make scintillation measurements at three points during the Geophysical Year and we have made some preliminary tests at Tromsø.

JONES: In this case when you have irregularities along the earth's magnetic field and you are looking along the line of the magnetic field, then I should think that the shape of the amplitude pattern on the ground should be on the average circular, so that you should not have any difficulties of an asymmetric pattern, so that probably the drift you get will give you the true direction of drift. It may be, however, that you will have difficulties with the magnitude of the drift if random changes are present.

WEEKES: Have you records from three receivers at the moment or are those the only ones?

HARANG: That was only a short series taken in January/February of this year, only to see if the noise level of the base was convenient for the purpose.

WEEKES: Because I should have thought that the important thing was to do a short series, then to do the full analysis and see how the pattern is shaped. Anything on our part I think is speculation at the moment. It might be quite circular and then you are alright. If it did turn out to be eliptical, probably the experiment is not worth doing.

Supp
Part.
195

SCOTT: I do not know if anybody knows whether any results have been obtained yet, but I believe that Dr. Little at Alaska was trying to make measurements of this sort.

HARANG: Then I should like to ask another question also about the discussion of such records: how much can we press out of the records if we plot them in a (T_x, T_y)-plane? This is a much simpler process than a full correlation analysis.

JONES: I should think probably that with this type of (T_x, T_y)-plot, you get quite a good idea of the actual direction of drift, but the magnitude is rather suspect because when you have a spread of the points this seems to indicate that random changes are taking place giving rise to variable time delays, and therefore the magnitude of the velocity may not be quite as reliable as the direction. As you pointed out before, if you take the mean of these points they all lie on a straight line. This straight line will probably, at least I should think, give you the true direction of the drift, but it is the magnitude of the velocity which is still rather suspect.

MAUNDER: Have you worked out statistics of the (T_x, T_y)-plot?

JONES: No, I have not done that. I think that in the United States some work has been done on this where they have tried to extend this (T_x, T_y)-plot to cover the case of random changes taking place. The conclusions arrived at were that it was practically impossible to do this, to get a value for the random changes when you have stretching of the pattern.

MAUNDER: One thing I would like to ask. How do you consider the amount of work in calculating the correlation functions?

JONES: Well, it is rather complicated to work these correlation functions out.

WEEKES: The answer is that the calculation of correlation coefficients is a very, very tedious procedure, and if we had not got a digital computer in Cambridge, we should not be doing it.

MAUNDER: Well, if two quantities are totally, normally distributed (Gaussian) you can get the correlation coefficient exactly by taking a signal frequency count.

WEEKES: It might be worth checking that. Of course the correlograms are by no means Gaussian, certainly the tails are widely different from Gaussian. Whether this means that a method based on a Gaussian distribution will give you the wrong answer can only be told, I think, by trying both and see whether one can in fact use the short procedure.

JONES: The 6-point correlation method, where all you need are six values of the correlation gives a picture like the one you get from the Briggs, Phillips and Shinn analysis. Yerg has done this quite extensively I think, finding values of the true drift, the effect of random changes and also the shape of the amplitude pattern.

BOOKER: Dr. Weekes said that drifts in the *E*-region might be due either to winds or to the effect of an electric field. It would appear that, under auroral conditions, drifts in the *E*-region are due entirely to the electrical field effect. The rate of change of radar range for auroral echoes is quite high and may reach values of the order of 1000 meters per second. Moreover, velocities of

the same order of magnitude are obtained if one measures the Doppler shift of auroral echoes. The velocities obtained by these two methods if measured simultaneously are not, however, the same and even the sign of the velocity may be different at any particular instant. This could be explained in the following way: The rate of change of radar range could be simply a shift in the position of the highly ionized cloud in which back scattering from irregularities is enhanced. On the other hand the Doppler shift could be associated with the drifts of the irregularities through the cloud on account of the electric field effect described by Weekes.

There is one statement that Weekes seemed to make which does not fit in with the picture in my mind. It seems to me that under quiet ionospheric conditions the drifts in the *E*-region might well be due to winds, but that under auroral conditions the electric field effect becomes much bigger and takes over. Weekes seemed to imply that the relative importance of genuine winds and of electric field drifts is controlled purely by the ratio of the collisional frequency to the gyrofrequency for electrons. If this were so, one could not have a change from one effect to the other at a fixed level as is required in order to explain observations. Have I understood Weekes correctly?

WEEKES: No. I think that I probably did not make myself quite clear. If the electric fields which you are concerned with are due to a wind primarily, then what I said is true. It is simply the ratio of collision frequency to gyrofrequency which decides which has the biggest effect in moving things. Now the difference between quiet conditions and auroral conditions may well be that in quiet conditions it is a wind which is basically responsible for everything that happens, but that in auroral conditions it is not a wind but an electric field, and that there is no associated air movement at all. In this case, of course, an electric field is always in the *E*-region and it will always be capable of causing motion. It is only if the electric field is related to a wind and in fact that the air movement is the basic cause of the thing, that you can say whether it is going to move with the air or move mainly as a result of the electric field in some different direction. My idea of what happens under disturbed conditions is that by some mechanism, of which I have not the faintest idea, an electric field is set up, but that this is not associated with a terrific air wind. In other words, I quite agree with what you have been saying.

BOOKER: There is perhaps one other auroral fact which should be kept in mind. Visual auroral rays drift in such a way that they always remain parallel. This would be easy to explain if an electric field is responsible for the movement but impossible to explain on the basis of wind.

WEEKES: Yes, I think that the auroral condition is almost certainly entirely controlled by an electric field which arises somehow in the aurora.

BOOKER: Then under these circumstances, drifts measured at *E*-region levels and at *F*-region levels should be the same. Will someone be able to tell us during this meeting that this is in fact true? It sounds like an easy experiment to perform.

FINDLAY: I am a little lost on the logic there. Because it is drifts caused by the electric field they should be the same in the *E*-region and the *F*-region. Was that your argument?

Supp
Part.
195

WEEKES: I do not think that is necessarily true. An electric field in the *E*-region might cause a motion in a different direction from the same electric field in the *F*-region.

BOOKER: It does not do so for rays, although I admit this is an indirect argument.

WEEKES: No. That is true. It does not do it to rays.

HARANG: As far as I understand, you think that the drift in the *E* and the *F* should be parallel. What would happen if you had a ray going through the *F* from the *E*? Does not this contradict your point of view?

BOOKER: No. I think that this confirms the electric field hypothesis since it would give the same movement in both the *E*- and *F*-regions.

FINDLAY: It rather sounds as though everybody is satisfied. Is everyone satisfied?

COX: There was a suggestion that the Doppler shifts that Dr. Booker was referring to were actually knock-off velocity from the exciting agency, rather than actual drifts. I would just like to ask if he has decided that this is not to be considered, or alternatively, is it possible that they could only be the rate of diffusion of the ionization formed as a blob somewhere along the magnetic field. That is to say, does this particular one have to have the electric field in it at all. Could you explain it?

BOOKER: I do not know what the answer to that question is. In my opinion the electric field mechanism for the Doppler shift in auroral echoes is the simplest one that can be thought of. I favor it on grounds of simplicity.

LIED: In connection with the winds, we have heard a lot about direction and magnitude, but I would just like to ask Mr. Jones, what about the determination of the height at which we determine the wind? That seems to be another weak point, in addition to the weak points pointed out by Dr. Weekes.

JONES: I think I can leave that until tomorrow when I am going to talk about this in the paper I am presenting. I will be talking about the variation with heights.

FINDLAY: I think you must admit that it is a very difficult one to answer. It is very difficult to say precisely what height your wind or your drift measurement refers to. Do you agree with that, or are you going to say it is easy?

JONES: I am going to say that we have some idea.

FINDLAY: The other information of course is from the meteor drift experiments — it is done at Manchester for instance — which do give a much more precise knowledge of the actual height at which the drift has been determined, so perhaps the one way is to use one experiment to validate another one.

HARANG: Is there any direct experimental evidence of an electric field? Does it exist or is it purely hypothetical?

WEEKES: Oh, I think an electric field must exist. You cannot get the current systems without the electric field. Either the quiet day or the disturbance daily variation must be associated with a potential derivable electric field.

uppl.
rt.II
1956

HARANG: Is there a certain gradient, for instance in vertical direction?

WEEKES: The gradient of electric field?

HARANG: Yes.

WEEKES: There will be a small gradient of electric field, but I should think small, very small, above the *E*-region.

BOOKER: There have been indications of discrepancies between observations of star scintillations in Australia and in England. Has this discrepancy been resolved yet, and if not, does it have something to do with the radically different angles to the magnetic field in the two cases?

JONES: Do you mean a discrepancy in the occurrence of the scintillation?

BOOKER: I mean a discrepancy concerning the importance of *E*-region in the star scintillation phenomena.

JONES: Dr. Wild was over in Cambridge some time ago and we compared the type of scintillation observed at Cambridge and in Australia and we seemed to think that they were similar for the *F*-region or for the night-time, but you hardly ever observe any daytime scintillation at Cambridge.

BOOKER: But you do in Australia?

JONES: Yes.

BOOKER: And this is not explained?

JONES: Well, the Australian results apply to measurements at a low angle of elevation of the star.

WEEKES: Is there not a contribution from the lower atmosphere itself in the Australian drifts, ordinary atmospheric irregularities?

BOOKER: That is what I understood from Dr. Wild.

WEEKES: I presume that this is done with very low angles of elevation.

BOOKER: At an elevation of about fifteen degrees.

WEEKES: If nobody else has got anything to say, there is one general point about the reporting of the observations which I should like to make. We hear frequently in this work, particularly for the *F*-region, of a relation between the drift velocity and the *K*-figure. Now it seems to me, if we are thinking in terms of electric fields, and perhaps in any case, that it might be physically more satisfactory if one were to look at the relation between the actual deviations of the magnetic field and the drift velocities, and forget the *K*-figure a little bit. The *K*-figure, after all, in high latitudes means a very great change in the magnetic field and therefore a very much greater current than it does in a lower latitude, and I think it may well be that we ought to be looking at these things in terms of the actual magnetic field changes rather than *K*-figures.

MEEK: Again, if you do it near the aurora you can have relative localized currents.

BOOKER: Yes. And then it is the local variation of the earth's magnetic field which would be important.

HARANG: Do you think it has some sense to study the direction and position of the polar currents causing the geomagnetic bay-disturbances and the drift of the *E*-layer?

WEEKES: I certainly think it has, for the *F*-layer particularly. But also for both of them. It would be very interesting to know where the current is when we make these observations.

BOOKER: I think that drifts in the *F*-region will be easier to interpret. In the *F*-region, drifts can only be due to electric fields and no confusion with genuine winds is likely. Observations for both layers would, of course, be interesting, but it is the drifts in the *F*-region that are likely to give the clearest correlation with the magnetic current system.

HARANG: Of course it is very difficult to get the drift during this small disturbance.

BOOKER: Perhaps, but nevertheless it would be interesting to try.

MEEK: I think this suggestion of plotting the currents from the magnetic field measurements is very nice theoretically, but practically you would need a fairly close network of magnetic stations in order to get anything that is useful at all.

BOOKER: Will we not have such a close network in operation during the IGY?

HARANG: I do not agree with Dr. Meek. I think it should be possible.

MEEK: I think there is a fairly good network in Alaska but certainly it could be improved in other places.

HARANG: I am going to ask about the height effect on the drift measurements of the *E*-layer, and I am again returning to our Geophysical Year programme. We are intending to make *E*-layer drift at Tromsø and this means that we will get a lot of E_s-layer effect. Will these records then be of any value? When we remember the report of Jones, we may ask: how closely should we then have *P'f*-records for control. When taking drift measurements of the *E*-layer with a wide gate we will get mixed up many things in the *E*-region and perhaps we will not get anything sound out of it. I should like to hear Mr. Jones' opinion about this question.

JONES: This variation of drift with height seems to be quite important and the fact that you get the different observations on different frequencies suggests, as I put forward, that the fading is imposed on the wave near the level of reflection. For Dr. Harang's question, it is important to know the heights of reflection of the layers or the frequencies employed, and if possible to get an actual *P'f*-record at the same time so that when analyzing this you can get the actual height. I have not done any *P'f*-records at the same time as I was observing drifts, but this is very desirable and we may do it in the future now that we have a *P'f*-recorder working at these *E*-region heights. I do not think anyone is sure that the drift measurements on E_s are the same as the measurements you get on normal *E*, but it is quite important to know where you are being reflected.

FINDLAY: I shall make a Chairman's remark. It does seem to me a little curious that we in fact are so bad at measuring drifts in the various regions. If I could attempt to summarize, what we really do need to know is what a drift velocity is and to what height that velocity corresponds. Now within the *E*-region itself we are not so badly off. In fact we have got two methods at least at our disposal: meteor streaks observed by radio methods, and what

Suppl.
art.II
1956

we can call the standard three-station drift method. With meteor streak one has got the advantage of making the measurement at a known height. One important thing that can be done and is being done, as Jones suggested, is that the meteor-streak method and the three-station method are being correlated. If that can be done, it will be a valuable validation of the three-station technique. It will still leave that technique, as Professor Harang is saying he is worried about, lacking in height information. We shall never know quite precisely at which height that technique is measuring the drift. *E*-region, however, is not in too bad a state. I should like to see some attempts made to produce any other methods for measuring drifts in region *E*. I wonder, for instance, whether anybody has put down three receivers yet at the end of a VHF forward-scatter link. There at any rate if you put down a three-receiver system you will have information every day and every night throughout the year — there is always a scatter signal and we have got pretty good evidence of the height from which the scatter signal comes. The height of scattering does change, but the change is known. At any rate that might provide you with a 24 hour method.

When we go above region *E* it seems to me that the situation becomes more difficult. The three-station method is still usable, but the difficulties about what height you are measuring the winds at, seems to be much greater. I think we are all doubtful about what results you get when you deal with a kind of thing like a traveling disturbance. I am thinking of the Munroe kind of traveling disturbance. I think Mr. Wells is doubtful about it, and he carefully when he spoke, did not outline too clearly what was the irregularity he was going to deal with. He just said, all you have to do is to observe an irregularity, identify it at the three stations and then measure a drift from it. If you consider such an irregularity in the *F*-region, you have got to ask yourself: am I going to assume that this irregularity, if it appears at different times at different stations, is drifting, or is this an irregularity in the ionization mechanism at the *F*-region. If it is so, then of course you would expect it to move across the *F*-region with a velocity corresponding to the rotation of the earth under the sun, and this will give you a 300 metres per second difficulty which you will not be able to sort out. You will not know if the wind is going one way or whether it is just the atmosphere moving under the sun. So the *F*2-region is a much more difficult one and I thought that Mr. Wells did not pat himself on the back quite hard enough for the possibility of using the back-scatter information which looked as though it might be a very powerful and useful method for studying *F*-region effects.

WEEKES: There are one or two points which I should like to emphasize, in talking about the possible production of these discs of irregularity, referring to Martyn's attempt to solve what happens to an irregularity in the ionosphere. Now I do not think we ought to take too much notice of the theory because although the mathematics were right, as I see it, I think that the physics were quite wrong. What Martyn in fact did was to say: supposing I have an irregularity in an ionized region, is it possible for that irregularity to stay there stably? The answer from his mathematics came out: now Clemmow, Johnson and I looked at the same problem and we would agree with the answer that the irregularity cannot just sit there as a stable thing, but it can, and there is reasonable reason to suppose that it will, just move as

Sup
Part
19

a whole. There is no question of instability in it: the thing will just move. Martyn tried to construct a stable cylinder which stayed. Our answer is that if you put a cylinder of that form in the ionosphere it will not stay, it will move and if it moves it will just move as a cylinder.

The other point that I want to make some comments on is that the impression which may have been given by Mr. Jones that the meteor results on drifts or winds agree more or less with what you would expect on the tidal oscillation theory as we know it at the moment. I do not think that is true. Admittedly if you take the results for the summer season, it looks alright. The phase is difficult to predict on tidal theory because you need to know quite accurately what the distribution of temperature with height is, but the meteor results show a phase reversal in the semi-diurnal component at about September. Now one assumes that the magnetic quiet day variations are the result of the solar wind system and they do not show a reversal at September/October. So we come to the conclusion that this oscillation has changed phase at 80–90 km and has not changed phase at 100 km. From a tidal theory point of view that seems to me to be quite incredible. I do not see how one could persuade the tidal theory to give you any such effect, so at the moment I would be inclined to say that any agreement between the meteor drift results and tidal theory is purely coincidental.

The other quite short point I wanted to ask Mr. Roach about was the following. When he talked of a southerly auroral zone, are there any observations which show that if you go far enough south, this thing is north of you? In other words, is it a zone rather than something stretching right over the equator to perhaps 30° or 40° the other side?

Suppl.
art.II
1956

ROACH: There are observations, Dr. Weekes, that would answer this question specifically. We have some simultaneous data at Sacramento Peak which is 500 miles or about 800 km to our south, and Fritz Peak in Colorado. The evidence for this thing which I called in general "a secondary auroral zone" is rather a broad statistical type of evidence, rather than a specific physical type of evidence.

WEEKES: In fact we want some observatories in the Southern Hemisphere to fix it.

ROACH: We want a chain, which is just what we are planning for the International Geophysical Year, both in the Americas and in the Europe/Africa region, and in the Japanese/Australian region.

WELLS: There are two points which I would like to make. One is concerning the possibility of the back-scatter technique, of which I presented a very brief resume. I think I did point out that it appears to have very attractive possibilities of providing additional and more continuous type of information concerning the nature of the large-scale ionospheric disturbances, especially in the *F*-region. There is a paper in preparation, I think principally by Mr. Tweeton of the staff of the National Bureau of Standards, to whom I am indebted for the use of the material and the slides, which is to appear, I hope, within the next few months.

The other point concerns a question raised by the Chairman on the possibility of using the forward-scatter technique and spaced stations at the

terminus of a forward-scatter link for obtaining additional information concerning, in particular, *E*-region drift motions. My first impression, which may be wrong, is that this would be extremely difficult, if not impossible to achieve. I make this statement on the grounds that our own observations, using for example interferometer techniques similar to those we have used in observing radio stars, have demonstrated that signals over a scatter link arrive in an extremely broad tone of acceptance. This is often so in spite of the fact that the antennas may be quite pencil beams, but they all have side loads and any strong signals or any meteor reflections well out of the main beam, can contribute substantially to the signal that is received at the terminus.

KALLMANN: I would like to ask Dr. Roach about the height of the emission of the 5577 line. He pointed out that it is between 90 and 100 km, and he mentioned that this is primarily due to rocket observation. But he also mentioned that there may be two other reasons. I would like to know the two other reasons and I would also like to know if he would think that the 6300 and 6363 lines are also emitted at approximately the same altitude. Also I would like to ask Dr. Roach if he would think that oxygen is distributed over quite a distance in altitude as may have been indicated from recent Arctic experiments.

ROACH: Now I think I was asked three questions. First, what are the methods for estimating the heights to the air glow? Dr. Tousey and his collaborators at the Naval Research Laboratory have recently done some very exciting work in which the rocket has actually at night gone through the layer and the results are so convincing that there can be no doubt in anyone's mind that the height of 5577, at least on the two rocket flights that they had, is definitely between 90 and 100 km. This is a direct method. The second method is the triangulation one at which I just hinted in my discussion. There have been approximately three attempts at triangulation. The difficulty is that you do not have a very specific patch that you can point at on your records and say: This is something to triangulate on. You have a rather nebulous, large-scale kind of a thing to triangulate on, and so the triangulations which have been fairly successful have had to do with really correlations at various combinations of angles between the two observers, finding the best correlation of the time variation and assuming that that best correlation corresponds to best height. Now the result between two stations in California gave us, rather surprisingly, answers around 100 km, even though at the time we were doing this work we were quite convinced from the third method, which I shall mention, that the height was 200 km, but we published it anyway. From some results which have not been published we again got results just below 100 km between Sacramento Peak in New Mexico and our Colorado station using this correlation method. There can be no doubt from these data of triangulation that 200 km, which is the controversy, is absolutely denied by the data. Now the third method is the classical one suggested by van Rhijn and I think it was in 1920, which takes advantage of this increase in intensity towards the horizon and tries to deduce from that what is the height. This is an indirect method and a very difficult one to apply because nature is against you, as you have to bring in the effect of the lower atmosphere with its extinction and scattering. Unless you know the

coefficients there very accurately, you come out with very wide spread in your height deductions. I have now analyzed a large number of nights by this indirect method and within the knowledge of these coefficients, the heights definitely come out in the 100 km region rather than the 200. You may say: 100 ± 30 or so.

Now you asked the question about 6300 versus 5577. If I speculate now it is very risky because when I was in Washington just about 2 weeks ago they told me they were just about to fire a rocket at night with a 6300 filter to actually measure the height and I do not know what the results are. But if I were to predict, the indirect argument would be as follows. Every attempt to correlate in the air glow of 6300 and 5577 has been unsuccessful in spite of the fact that, as I pointed out, they have a level in common. The mean life of the *S*-level is something of the order of half a second. The mean life of the *D*-level is of the order of 100 sec. Now the negative evidence that there is no correlation with diurnal variation, seasonal variation, is an important negative fact because every time the green line is emitted you leave the oxygen atom in the definite state able to emit the red line, and if there is no correlation it means that something must have happened in this state which prevented the emission of 6300. The obvious thing that may have happened is that during this 100 sec life-time in contrast to the one-half second of 5577 there were so many collisions that this state was destroyed. So, if this is true then you would predict that 6300 should be emitted by some excitation mechanism quite independent of 5577 and should be emitted at some height significantly higher, 5577. The significantly higher might be 10 or 20 km perhaps or it might be more, but the prediction I would make would be that 6300 is higher. If the observers find it at about the same height, I do not know what we are going to do about this lack of correlation.

Suppl.
art.II
1956

Supp
Part.
195

SECTION II

uppl.
rt.II
1956

Supp
Part.
195

uppl.
rt.II
1956

PREDICTION TECHNIQUES AT HIGH LATITUDES

J. H. Meek
Radio Physics Laboratory, Ottawa

This paper will deal only with the method of HF prediction which Mr. J. C. W. Scott has developed in Canada and which is primarily designed for application to high latitude and polar communications circuits.

At present, there are several prediction groups which turn out frequency charts on a routine basis. The communications networks and circuits in which these laboratories are interested are not, for the main part, over high latitude paths. As a result, the emphasis in drawing up prediction charts is obviously on the middle and low latitude regions. Problems peculiar to the high latitudes make it difficult to use the present charts. The main objections are as follows:

(1) The zonal system of making predictions, dividing the world into four sectors on basis of longitude, is not much use in the Polar regions because the apex of these sectors comes within our area. The predictions appear to be produced independently for each zone and we often find considerable discrepancies in the critical frequencies which are predicted for each zone for regions around this apex. For Polar regions it has become necessary to use the method of prediction presentation which gives the critical frequency for one universal time all around the polar regions. This means that we must have one chart for each hour of the day or the equivalent.

(2) The charts which are used in middle latitudes are all based on equatorial projections. This is very inconvenient when dealing with transmission paths over the Polar regions. All these projections require overlays or some similar method of tracing the great circle path (which is exaggerated greatly near the Polar regions). In some cases the type of projection used is such that the North Pole is stretched out into a line. At the high latitudes we must use a projection which is centred on the Pole rather than on the Equator and in order to speed up the process of working out control points (a main requirement of these charts), we wish to draw and measure the great circle path quickly. It is most convenient to use a gnomonic projection centred on the North Pole in which great circles are straight lines. The gnomonic projection has a disadvantage that it cannot be used for paths which approximate 180° around the earth in length. This deficiency has been overcome recently and is described in a short paper due to appear in the September *Journal of Geophysical Research*. Two or three adjoining gnomonic projections are used. A great circle path between any two points on the earth is drawn by segments of straight lines. It is done by very simple construction, with no mathematical calculations required.

(3) The current system depends on working up a number of charts and drawing a complete set of contours for each zone for the month. This procedure is repeated each month. While a certain amount of reference is made to the previous month's charts, it means repeating the work procedure each month of the year and year by year. There are some rather well-known empirical relations and using these we have been able to eliminate the repetitive process of drawing up counter charts each month.

As is the case with other existing methods the Canadian system is based on the linear relationship between the critical frequency and the sunspot number, $f = A + BS$ where f is the critical frequency, S is the sunspot number and A and B are constants. This is an empirical relationship and because we still have no satisfactory explanation for it, it has much to be desired. However, for the moment, it can be used to work out prediction charts. In practice the 12 month running average sunspot number is used because it gives the best relationship. It has the defect that it will always be about 6 months behind the ionospheric conditions when they are changing rapidly. Some correction can be made for this.

Fig. 1 illustrates the relation between the critical frequency and the sunspot number. To describe this relationship we need only to read off the inter-

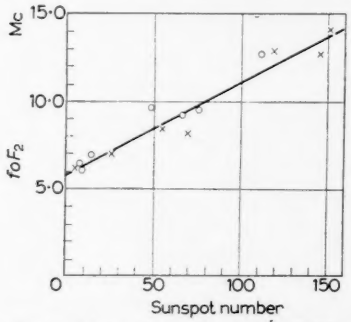

Fig. 1. Ottawa, November, 1100 hr EST.
Monthly meridian f_0F2 vs. 12 months running average sunspot number
⊙ = sunspot number increasing
× = sunspot number decreasing
Intercept = 5·7 Mc/s. Sensitivity = 0·0517

cept at zero sunspot number and measure the slope of the line, A and B respectively in the formula. These constants A and B vary from hour to hour and from month to month and with position on the earth, but their values can be determined once and for all. When this has been done, to find the predicted value of the critical frequency at any time requires only an estimate of the sunspot number. The system of prediction is very dependent on our ability to estimate this sunspot number.

Fig. 2 shows the way in which the zero intercept varies with time of day at one particular station for different seasons of the year. Similar graphs are worked out for all stations which are available. They are plotted on charts. The equivalent values are read off for each 5° of latitude and each 15° of longitude and are put in tables. The calculations are done for parts of the world in which we have a sufficient number of ionospheric stations. For cer-

tain regions where there are no ionospheric stations it is necessary to do some guessing. For the large Russian sector from which data is not received we have to make our best estimates. Apart from these defects and resulting

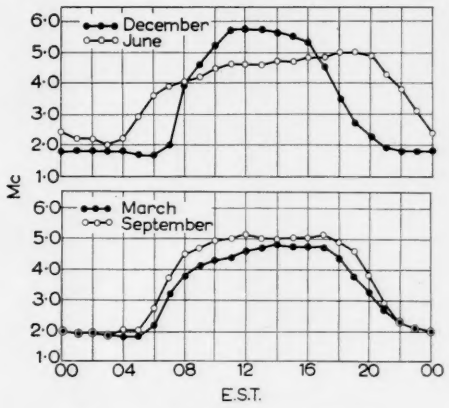

Fig. 2. Ottawa, f_0F2 at zero intercept

Suppl.
art.II
1956

inaccuracies, these calculations are only done once and need not be repeated each month.

Fig. 3 shows a contour plot on a gnomonic chart of the zero intercept across

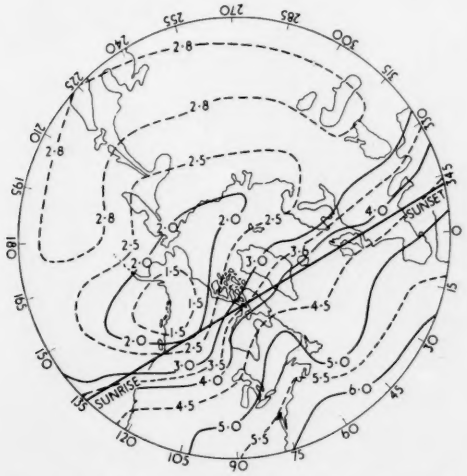

Fig. 3. January 1600 hr GMT. Contours of equal f_0F2
Sunspot number = 0

the polar regions. This type of working chart is used to prepare tabulated values. We only attempt to go down to 35° and so as not to overlap more than necessary with the equatorial system.

Fig. 4 shows a plot of the slope of the frequency-sunspot number relationship. The rather peculiar hump which appears during the four winter months has not been explained.

From the tables for slope and intercept we can make up the tables of critical frequencies which of course, are the transmission frequencies for zero

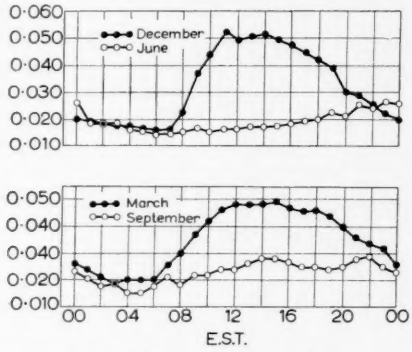

Fig. 4. Ottawa, sensitivity at slope

distance, or vertical propagation. We go through exactly the same process to make up charts and tables for the 3000 km factor for the *F*-region. *Fig. 5*

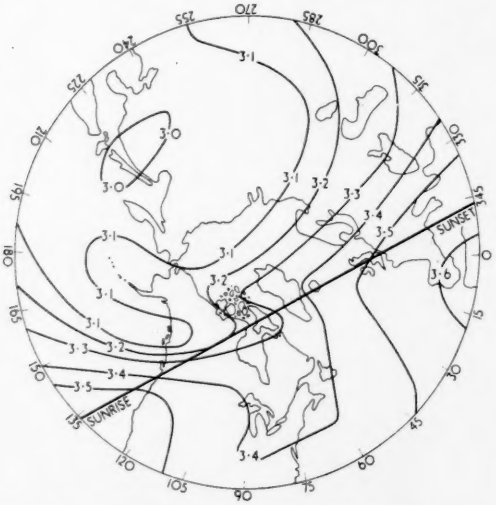

Fig. 5. January 1600 hr GMT. Contours of equal M3000 F2 Sunspot number = 0

shows an example of a plot for the factor at sunspot number zero. *Fig. 6* shows the variation of sunspot number with the factor similar to the one that worked out for the critical frequency. In this case the slope is in the opposite direction, decreasing with increasing sunspot number.

We note that the sensitivity (or slope) of the factor-sunspot number

straight line is essentially constant for any month for all hours of the day and all parts of this region in which we are interested. There is considerable variation in its value but no recognizable slope at any time. *Fig. 7* illustrates variations of the sensitivity for several stations. The lower part of the

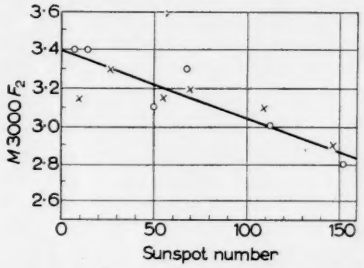

Fig. 6. Ottawa, November, 1100 hr EST
Monthly meridian M3000 F2 vs. 12 months running average sunspot number
⊙ = sunspot number increasing
× = sunspot number decreasing
Intercept = 3·4 Mc/s. Sensitivity = 0·0035

figure shows the means for the points plotted in the upper part. All we can say is that there is no bias that we can observe within the limits of our measurements. We use this relationship for the lack of something better.

In order to make up predictions for a circuit we must get the positions of

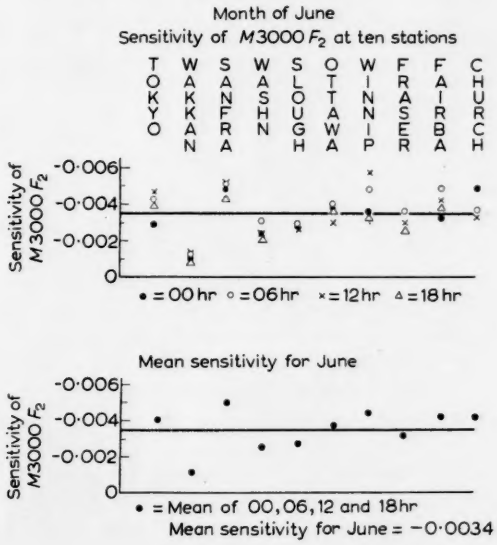

Fig. 7

the control points from a chart. After the sunspot number is estimated then all the rest of the work, calculating the factors and the critical frequencies at the control points can be done without reference to contour charts. The

Suppl.
art.II
1956

next problem is the interpolation for path lengths between 0 and 3000 km since frequencies are determined only for these two distances. This is done now using a nomogram which is very similar to the one produced by CRPL. Its main defect is that a certain height for the layer was assumed when preparing the nomogram. The heights which are used in the CRPL nomogram, of course, will not be valid over the polar regions. The difference is something which we have not yet worked out but must do.

An important limitation of the polar prediction system is that we predict for rather quiet periods whereas the ionosphere is often disturbed.

I have not mentioned the use of the *E*-region predictions. *E*-region predictions are not very much different from those done elsewhere. They are dependent on the solar controlled *E*-region. Also there is some thought of working out suitable predictions for the *E*-sporadic, but we have not found out how to do that yet.

Now that we have a system for making predictions we must test our method to see if it is correct or at least reasonable. For this purpose we have set up several oblique incidence experiments using pulse equipment. The first experiment was done some years ago by J. W. Cox, between Saskatoon and Ottawa (2500 km). A manualiy operated apparatus was used and resulted in some information on the relation of vertical critical frequencies to the oblique frequencies. Since then the experiment has been repeated with better equipment over the same path. More recently an experiment has been set up operating across the auroral zone between Winnipeg and Resolute Bay. Resolute Bay is one of the most northerly islands in the Arctic Archipelago and Winnipeg is about the centre of the continent at 50° N. There are two vertical incidence ionospheric stations between these points with which we can compare the results.

Fig. 8 shows just a single example of an oblique incidence record. The separation between ordinary and extraordinary traces is visible. These traces extend from the MUF back up to the critical frequency. This oblique incidence experiment is still in progress. Some results of the previous oblique experiments are as follows:

(1) The high-angle ray, Pederson-type ray, has considerable signal strength and may constitute quite a considerable part of the signal which is transmitted between two points. Sometimes it may be useful, other times it may cause undesirable fading.

(2) Very often there are considerable spread echoes just around the maximum usable frequency. Sometimes these spread echoes extend beyond this normal maximum usable frequency. They might contribute to the propagation sometimes but they are usually rather variable and it is found that the strongest signals are well below the maximum usable frequency.

(3) For the path from Saskatoon to Ottawa it was found that at some times of the year, particularly in the summer, the *F*1-region is rather important and it must be considered in working out the propagation frequencies.

(4) Using the *F*1-region it was shown that the Lorentz polarization term which turns up in the magneto-ionic theory, probably should be zero.

(5) It appeared that on this path there is no measurable departure from reciprocity. This is that propagation over the path in one direction is the same as over the path in the opposite direction.

Supp
Part.
195

uppl.
rt.II
1956

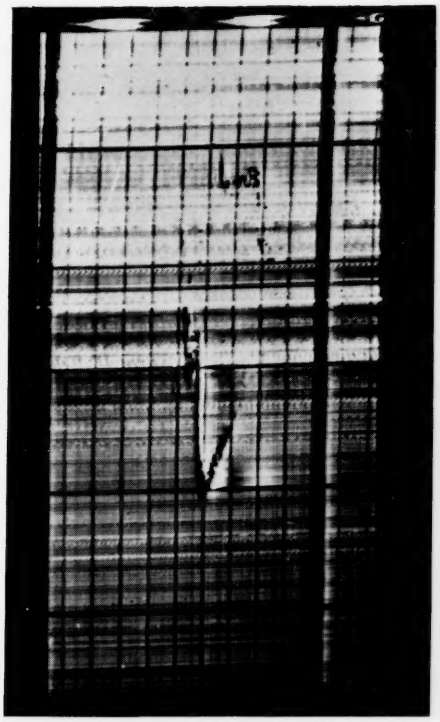

Fig. 8

Supp
Part.
195

In conclusion, I have presented a method of HF predictions which is not very different from other existing methods. It is adapted to polar communications problems and has reduced the work involved in making the prediction charts. Work is still under way with a view to relating these predictions to controlled oblique incidence paths.

uppl.
rt.II
1956

GEOGRAPHIC DISTRIBUTION OF GEOPHYSICAL STATIONS ON THE POLAR CAP

A. H. SHAPLEY
National Bureau of Standards, Boulder, Colorado

Studies of the high atmosphere in polar regions have progressed in recent years not only on account of advances in theory and observational techniques, but to a large degree because the growing network of regular observing stations is making possible more adequate description of the phenomena which we are trying to understand. In the electromagnetic fields of geophysics — ionosphere, aurora, geomagnetism and certain aspects of cosmic rays — the growth of the networks has been considerable in recent years. These fields are approaching the point where actual experience will directly assist considerations of the optimum density and distribution of stations in the networks. Steadily improving arrangements for interchange of basic observations, accelerated by the development of plans for the IGY, will soon put these fields on more nearly the footing of synoptic meteorology.

Regularly observing stations which are north of 60° geomagnetic latitude or north of 60° geographic latitude include:

Ionospheric Vertical Soundings — *Tromsø (Norway), Oslo-Kjeller (Norway), Kiruna (Sweden), Lulea (Sweden), Lycksela (Sweden), Uppsala (Sweden), Thule (Greenland), Godhavn (Greenland), Narsarssuak (Greenland), Reykjavik (Iceland), Inverness (Scotland), Resolute Bay (Canada), Baker Lake (Canada), Churchill (Canada), Barrow (Alaska), College (Alaska), Anchorage (Alaska), Tixie Bay (USSR), Tikhaya Bay (USSR), Providence Bay (USSR).*

Ionospheric Absorption — *College, Churchill, Tromsø, Oslo-Kjeller, Baker Lake, Resolute Bay.*

Auroral Patrol — *visual and photographic — Tromsø, Kiruna, Oslo-Blindern, Uppsala, College, Barrow, Nome, Churchill.*

Geomagnetic Variations — *Thule, Bear Island (Norway), Tromsø, Abiaho (Sweden), Kiruna, Sodankylä (Finland), Dombäs (Norway), Nurmijärvi (Finland), Lovä (Sweden), Barrow, College, Resolute Bay, Baker Lake, Wallen (USSR), Tikhaya Bay (USSR), Cape Chelyushin (USSR), Dixon Island (USSR), Cape Vikhodnoy (USSR), Tixie Bay (USSR), Godhavn, Lovezero (USSR), Sredniken (USSR), Yellowknife (Canada), Dombäs (Norway), Yakutsk (USSR), Lerwick (Scotland).*

Other basic experiments in electromagnetic geophysics, such as ionospheric drifts and cosmic ray geophysical patrols, involve lesser networks up to the present time. Most networks will be significantly strengthened by the time of the IGY.

Suppl.
art.II
1956

STATISTICAL RESULTS AND THEIR SHORTCOMINGS CONCERNING THE IONOSPHERE WITHIN THE AURORAL ZONE

R. W. KNECHT
National Bureau of Standards, Boulder, Colorado

INTRODUCTION

EARLIER papers have discussed problems associated with the *prediction* of certain HF communication parameters such as MUF and LUF. In this paper we shall be concerned with an even more fundamental problem — that of obtaining representative values of ionospheric characteristics such as f_0F2, in and near the auroral zone. Determination of representative values of these characteristics such as medians, is the first, and probably the most vital, step in the prediction process.

Most stations in the Arctic take soundings every 15 min. To be most useful in predictions and in many types of research, these data must then be summarized, or averaged, over a longer time base — generally a month. Usually, hourly medians over the month are calculated. This paper will discuss the problems involved in this summarization of high latitude ionospheric data. Toward this end, it will be divided into two parts. The first will cover a description of the difficulties and the second, some ways by which these difficulties can be reduced or eliminated. The recommendations are essentially the same as those put forward in the report of the Special Committee on High Latitudes that was given to URSI in Brussels in the fall of 1955.[1]

DISCUSSION OF PROBLEMS

Fig. 1 shows the location of the majority of the world's ionosphere stations as of 1955. In this report, we will be primarily concerned with the Canadian chain, the Alaskan chain, the stations in Greenland and Iceland and the Swedish station at Kiruna.

The first step in the determination of monthly characteristics is, of course, the initial reduction or scaling of the individual ionogram. At low latitudes this is generally not difficult using the fairly well established rules that have been laid down. At high latitudes, however, the scaler is often confronted with soundings like that shown in *Fig. 2*. This Godhavn (Greenland) sounding well illustrates two of the major difficulties that confront the high latitude scaler — they are spread echo and sporadic-*E*. Rules formulated for the reduction of low latitude ionograms do not serve well in high latitude cases like this.

The differences between high and low latitude soundings taken at the same time are shown in *Fig. 3*. The ionograms were taken at Barrow, Alaska and Maui, Hawaii at 2000 local time on 30 September, 1955.

Numerical values scaled from the individual ionograms are entered on daily tabulation sheets as shown in *Fig. 4*. The tabulations for 30 September,

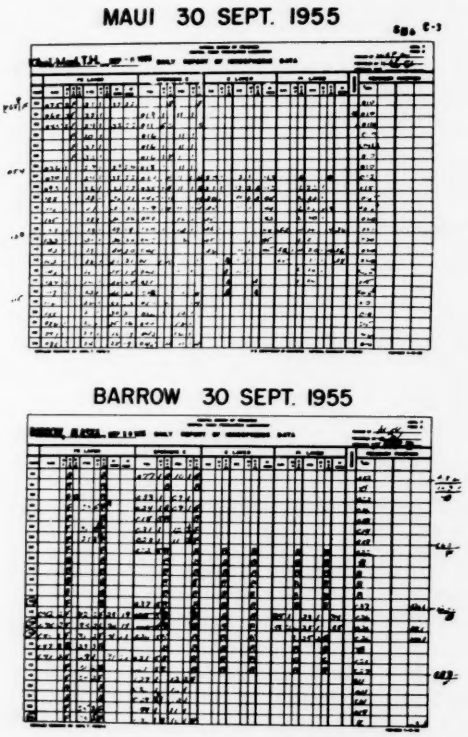

Fig. 4. Daily Tabulation Sheets for Maui and Barrow for 30 September, 1955

1955 for both Barrow and Maui are reproduced here. One immediately notices that Barrow recorded fewer numerical values than Maui. In fact, only one definite (full weight — "WT 1") f_0F2 was observed during the whole day at Barrow (at 1500). There were no measures at all of the regular *E*-region and little on the *F*1-layer.

The data from the daily sheets are summarized, by characteristic, on the monthly day-by-hour tabulation.

Fig. 5 shows this tabulation for f_0F2 during September 1955 at Barrow. It can be seen that the same shortage of numerical values occurs over the entire month. The absence of numerical values is explained in many cases by letter symbols meaning spread echo obscured the critical frequency (*F*), or sporadic-*E* blanketed the layer (*A*), or the echoes were too weak due to absorption (*B*). The attempts of the predictions group to obtain numerical information in place of these symbols can be seen by their addition of a number of "less thans" and "greater thans" in the table. The hourly median values are

Suppl.
art.II
1956

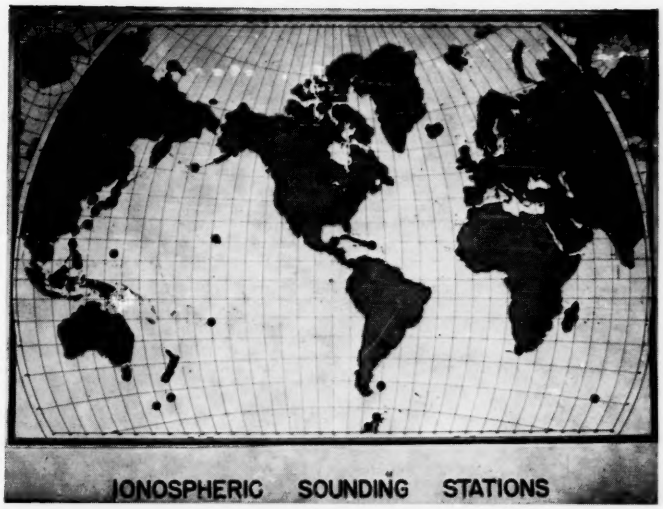

Fig. 1. Ionosphere Stations — 1955

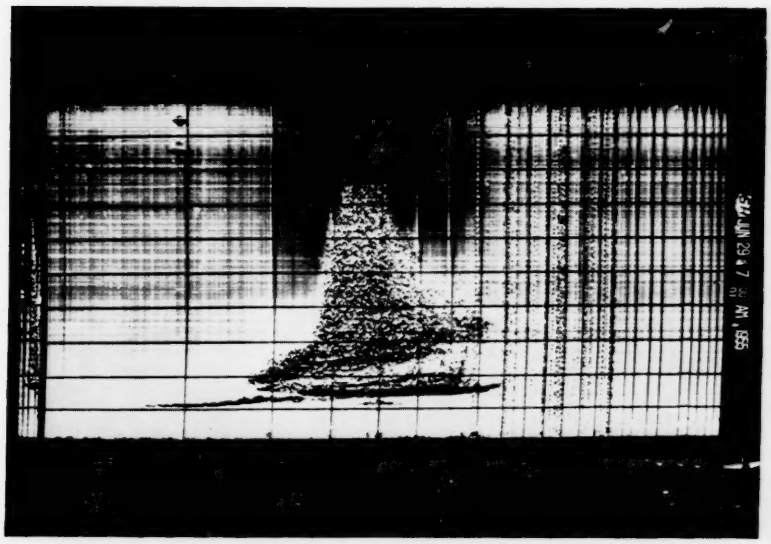

Fig. 2. Ionospheric Sounding — Godhavn, Greenland

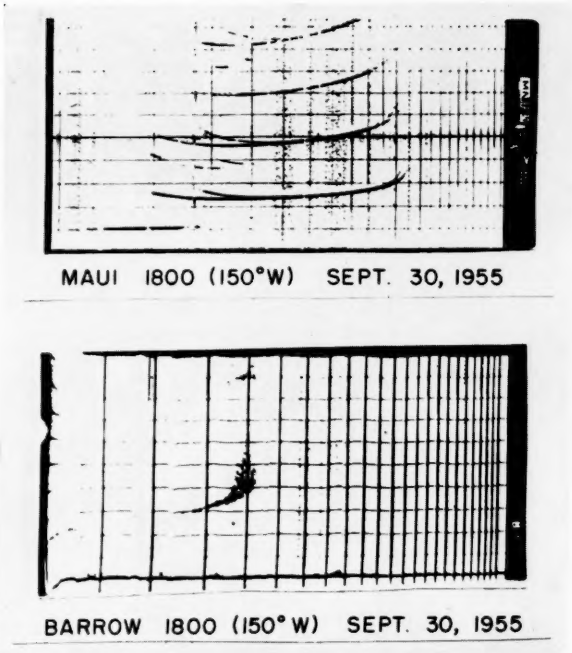

Fig. 3. Ionograms taken at Maui (Hawaii) and Barrow (Alaska) at 1800 (150° W) on 30 September, 1955

shown at the bottom of the table. For many of the hours, there were no values available for computation of the median. For the other hours it can be seen that the number of values entering the median (count) ranges from 5 or 6 up to a maximum of 27 in the late afternoon.

From the monthly summaries, these data then go into publications like the CRPL *F*-Series for the use of those doing research in the field. The sum-

foF2 BARROW SEPT. 1955

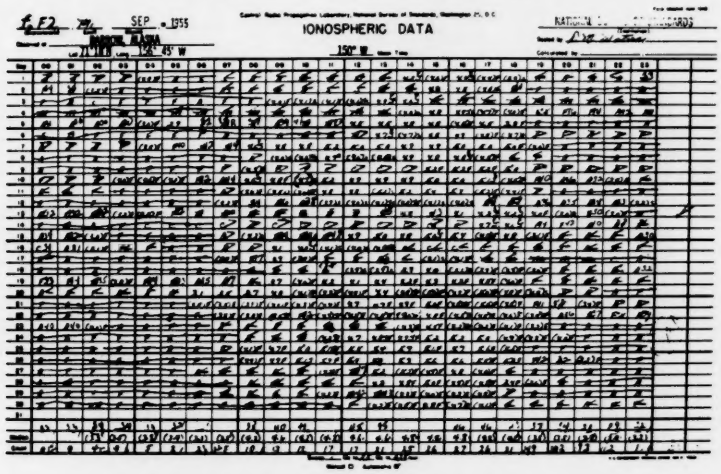

Fig. 5. Monthly Tabulation of f_0F2 — Barrow, September 1955

mary table for Barrow (September 1955) is shown in *Fig. 6*. The sparsity and uncertainty in the numerical data is reflected by the blanks and the parenthesis (indicating doubtful value), however, all too often the data are then used in research work without proper recognition of these shortcomings.

The other equally important use of the monthly data is, of course, in the predictions. In the lower portion of *Fig. 6* is shown the predicted MUF for a path from Narsarssuak to Oslo (September 1955) based on the CRPL *D*-Series charts plus 15 per cent.[2] (The predicted frequencies were increased by 15 per cent to account for an error in predicted sunspot number. The magnitude of the adjustment was derived empirically using a low latitude path.) The solid line indicates the frequencies that are predicted. On this basis, 11 or 12 Mc/s would be taken as a good daytime frequency and 7 Mc during the night. However, on 8 September, a typical day during the month, the dotted curve was actually observed. It was derived from vertical incidence data taken at Reykjavik, Iceland almost precisely at the mid-point of the path. It can be seen that the optimum frequencies, for use on 8 September at least, are considerably above those predicted. It is quite likely that in addition to the daily variations a significant part of this difference is due to the uncertainties in the high latitude numerical data going into prediction charts.

Returning to the *F*-Series monthly summaries for a moment, one might wish, for example, to know the median value of f_0F2 at 1900 at Narsarssuak (Greenland). The appropriate summary table shows it to be a doubtful 7·1

CRPL F-SERIES SUMMARY

Table 43

Point Barrow, Alaska (71.3°N, 156.6°W) September 1955

Time	h'F2	foF2	h'F1	foF1	h'E	foE	f0s	(M3000)F2
00	---	---					6.8	
01	(270)	---					5.1	
02	(280)	---					6.4	---
03	300	---					5.2	---
04	(280)	(3.8)					3.9	---
05	(290)	---					3.4	---
06	---	---	---	---			4.0	---
07	---	(3.5)	---	---	---	---	3.2	---
08	(360)	(4.3)	220	(3.5)	---	---	4.0	(3.0)
09	380	4.1	220	3.6	---	2.2	4.4	2.9
10	(400)	(4.2)	(230)	(3.5)	110	2.5	4.0	(3.2)
11	400	(4.3)	(230)	(3.6)	110	(2.5)	3.1	3.0
12	310	4.6	210	3.7	(100)	(2.5)	3.0	3.2
13	(340)	4.6	220	(3.7)	100	(2.6)	2.7	3.05
14	(340)	4.8	230	(3.8)	110	2.5		3.0
15	310	4.8	230	(3.7)	110	2.4	2.0	3.1
16	300	4.8	240	(3.7)	110	(2.3)	<1.8	3.05
17	270	(4.8)	240	---	120	(2.1)	2.3	(3.15)
18	270	(4.5)	---	---	---	---	2.8	(3.2)
19	(260)	(3.5)			---	---	3.4	(3.1)
20	(280)	---					4.3	---
21	(310)	---					5.4	---
22	---	---					6.0	---
23	(360)	---					6.0	---

Time: 150.0°W.
Sweep: 1.0 Mc to 25.0 Mc in 13.5 seconds.

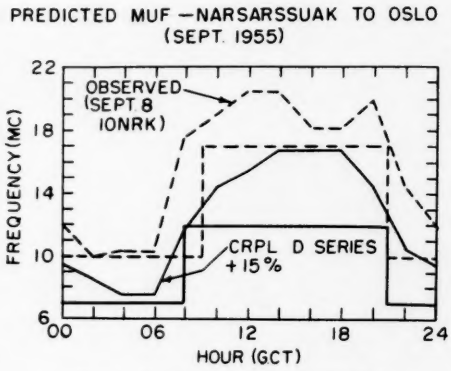

Fig. 6. Uses of Monthly Summary Data

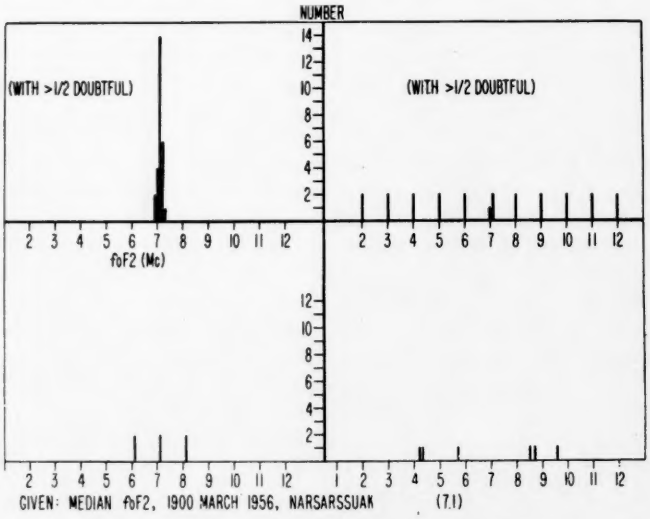

Fig. 7. Several possible distributions given a certain median

Mc. *Fig. 7* shows several of the almost infinite number of distributions of individual numerical values that could have produced this median. One might have a tight distribution around 7·1 with more than half of the values doubtful. Or perhaps a very "loose" distribution of values spread out from 2 to 12 Mc with half doubtful. Another possibility would be 2 values at 6·1, 2 at 7·1, and 2 at 8·1. The median would be doubtful here because of the few values (less than 9). The lower right graph shows what was actually the distribution

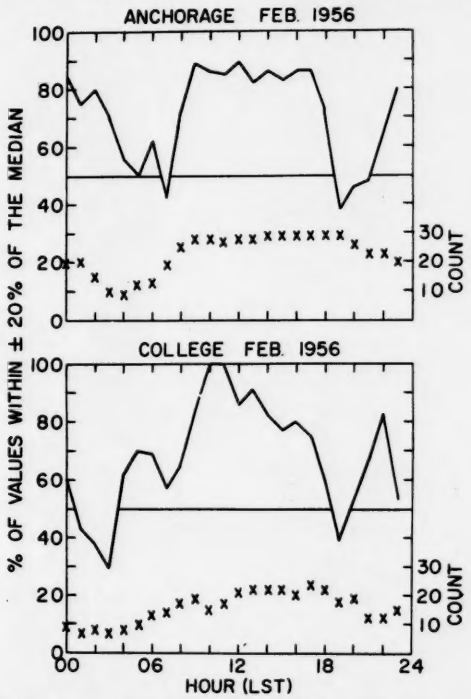

Fig. 8. Measure of dispersion of hourly f_0F2 monthly medians at Anchorage and College, Alaska — February 1956

that gave the doubtful 7·1. Six values, none closer than 1 Mc to 7·1, with a range from 4 to almost 10 Mc. The value of this median is certainly not very great and, more important, the median alone does not well represent the distribution.

The weakness of the median as a representative value can be caused in two ways: (1) little numerical data, and (2) large dispersion in the distribution. Both of these effects are seen in *Fig. 8* where data from Anchorage and College, Alaska for February 1956 are plotted. The ordinate is the percentage of values that are within ± 20 per cent of the median value for that hour or, in other words, a measure of the "tightness" of the distribution. At certain times during the day this index is seen to drop below 50 per cent. That is, more than half of the values are not within ± 20 per cent of the median. During the middle of the day, it tends to reach a maximum of 80 to 90 per cent. The number of values entering into each median (count) is shown along the bottom of the graph.

It was the recommendation of the High Latitude scaling group that the count be included when the medians are published and also that the *quartile range* be included as a measure of dispersion. In *Fig. 9* is shown the median

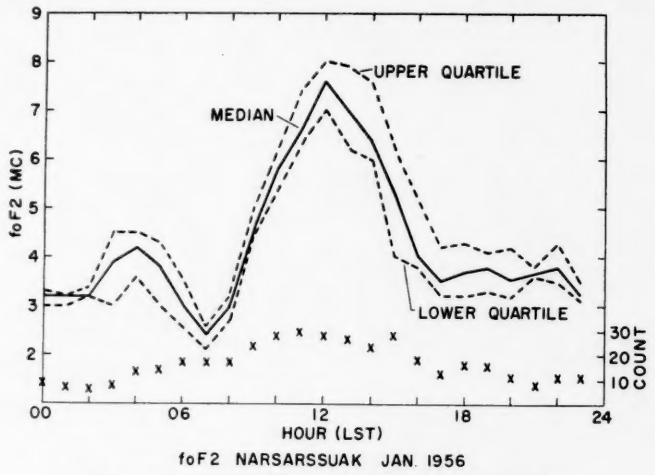

Fig. 9. Median values of f_0F2 — Narsarssuak — January 1956

values of f_0F2 for Narsarssuak for January 1956 with the upper and lower quartiles and the count included. Presented in such a way, the characteristics of the distributions and the representativeness of the median are easily apparent.

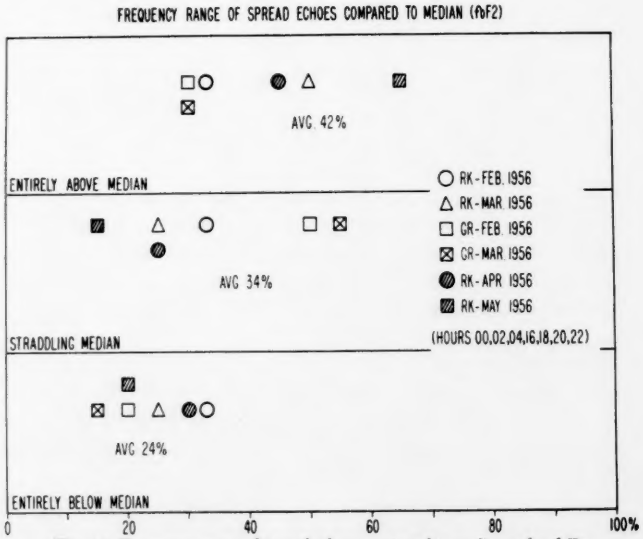

Fig. 10. Frequency range of spread echoes compared to median value f_0F2

At present, critical frequencies of layers that are characterized by hopelessly spread echo are necessarily omitted from the median, at least at CRPL stations. In *Fig. 10* is shown the frequency range of spread echoes that are

omitted from the median and their relation to the median. Each point represents a different station month. It is seen that almost twice as many spreads that were omitted from the median were entirely above it as were entirely below it (42 per cent compared with 24 per cent). Therefore, it may be that the current medians are systematically too low because of the omissions of these spread values.

The different practices in use within the different sounding networks also became apparent in an analysis of this type. *Fig. 11* shows, for instance, a

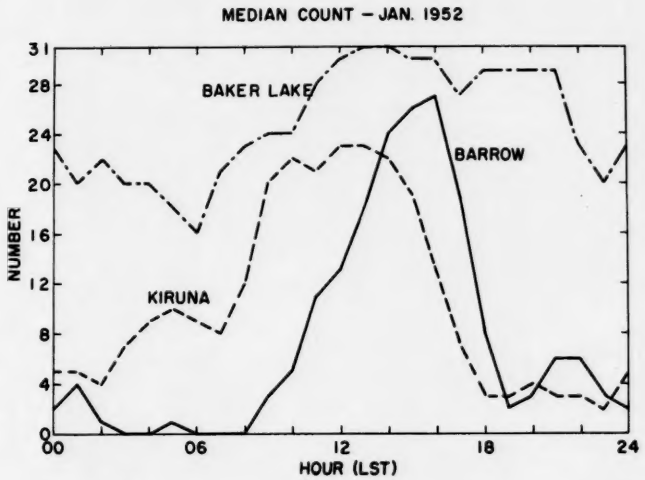

Fig. 11. Comparison of number of values entering median determination at three stations — January 1952

comparison in the number of values entering the median determinations for January 1952 at Barrow (U.S.), Baker Lake (Canadian), and Kiruna (Swedish). These three stations are at roughly similar geomagnetic latitudes and had comparable sounding equipments, Barrow and Baker Lake both having an NBS C-2. One would expect, therefore, similar counts at each station. That this is not the case is plainly seen. Baker Lake had no median determined by less than 16 values whereas Barrow had a number of hours with no numerical values and Kiruna falls somewhere between these two extremes.

Four of the soundings taken during January 1952 from which Baker Lake determined numerical values for f_0F2 are shown in *Fig. 12*. The original ionograms were undoubtedly somewhat clearer than the reproductions shown here but nevertheless CRPL stations would probably not scale definite critical frequencies from the first 3 of these as did the Canadians. This is not a criticism of their practices since as shown earlier it may be more appropriate to include these values in the median but rather an observation of still another problem — that of standardizing scaling practices among the various networks.

Recommendations

As mentioned earlier, the recommendations about to be put forward here are essentially the same as those offered by the URSI High Latitude Committee. This committee consisted of representatives from Canada, the U.S., Norway and Sweden.

It has been found that much of the troublesome spread echo is gain sensitive and therefore one of the important recommendations has to do with the systematic variation of receiver gain. Soundings taken with a series of different gains are shown in *Fig. 13*. *F*2-critical frequencies that would be

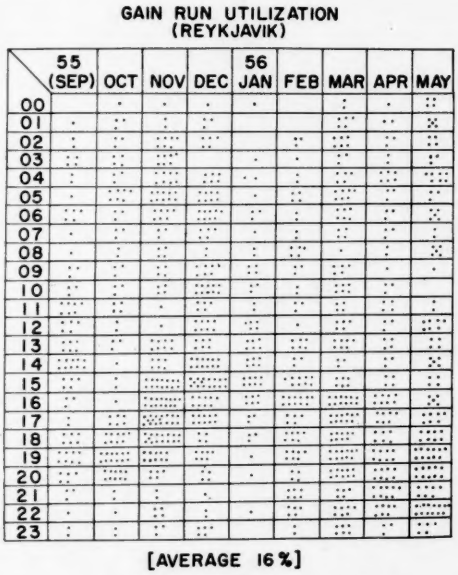

Fig. 15. Gain run utilization — Reykjavik

difficult if not impossible to obtain from the normal or high gain ionograms, are often quite easily discernible on the low gain sounding. *Fig. 14* shows another way in which the gain run is beneficial. Often the medium gain ionogram will, because of absorption, lack measurable *E*-region echoes. However, many times in these cases, the high gain sweep will provide echoes sufficiently strong to allow the determination of *E*-region characteristics.

It has been suggested that the standard *gain run* consists of a low gain sounding one minute before the hour, a normal gain sounding on the hour, and a high gain sweep one minute after the hour.

A number of high latitude stations including those under CRPL supervision have been taking gain runs since late 1955. The question might be raised as to the extent to which the stations are using the gain run in the determination of numerical values. *Fig. 15* shows the use of the gain run at the Reykjavik (Iceland) station since its inception in September 1955. A dot was plotted in the appropriate square every time either the high or low gain

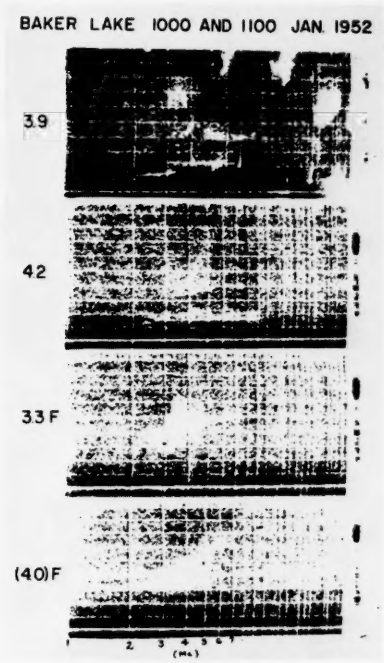

Fig. 12. Four Baker Lake ionograms taken during January 1952

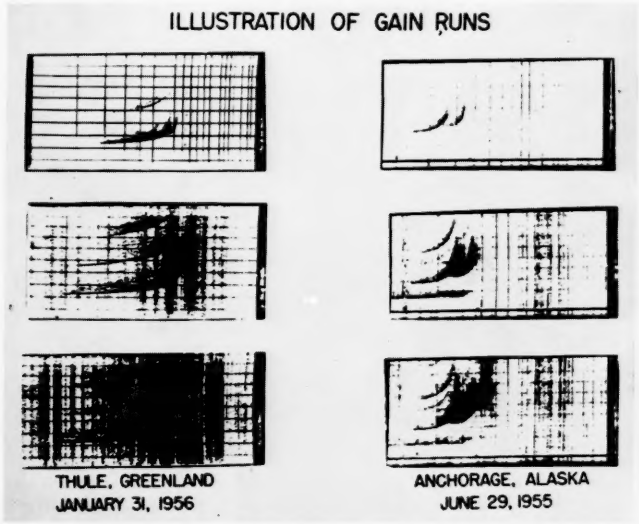

Fig. 13. Soundings taken with different receiver gains

Suppl.
art.II
1956

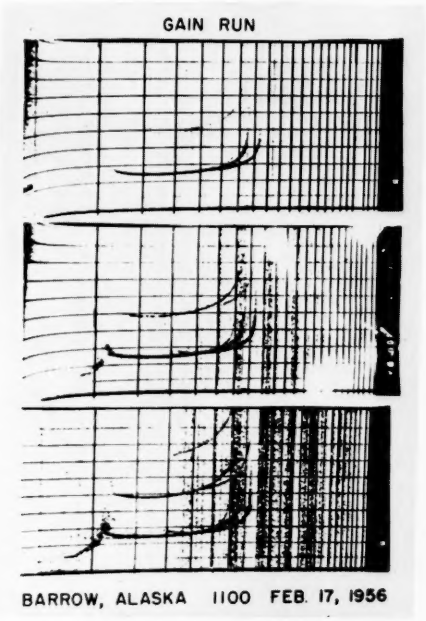

Fig. 14. Gain run at Barrow, Alaska (from top to bottom, low, medium and high gain)

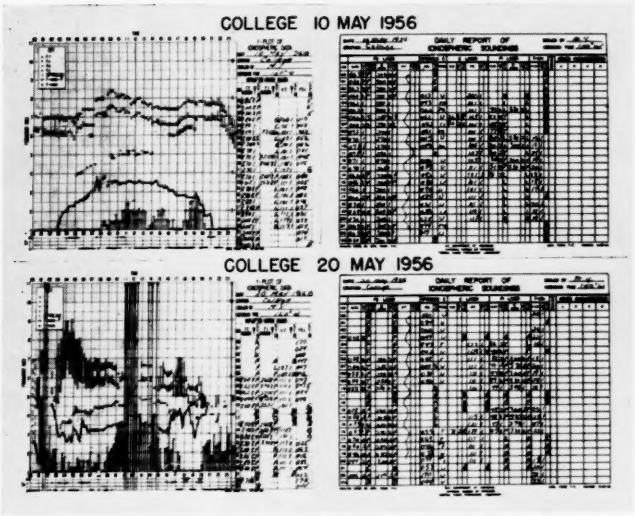

Fig. 17. f-plots and hourly tabulations for 10 and 20 May, 1956, College, Alaska

Suppl.
art.II
1956

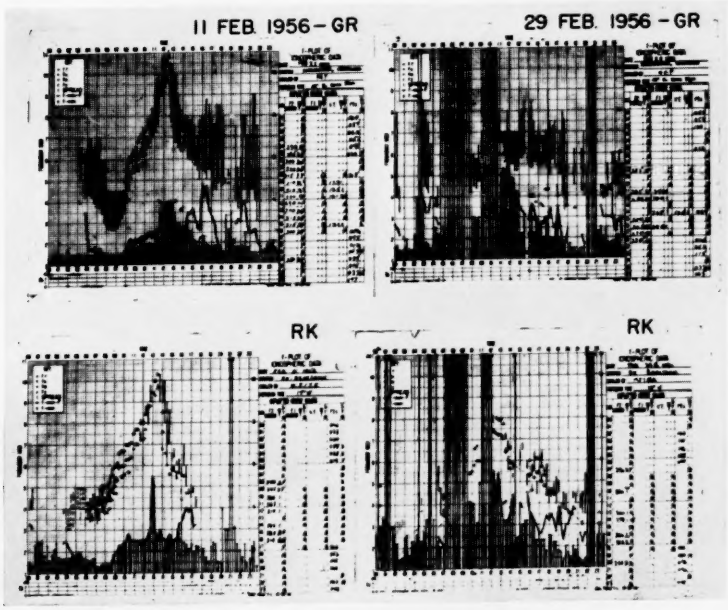

Fig. 18. f-plots for 11 and 29 February, 1956 — Reykjavik and Narsarssuak

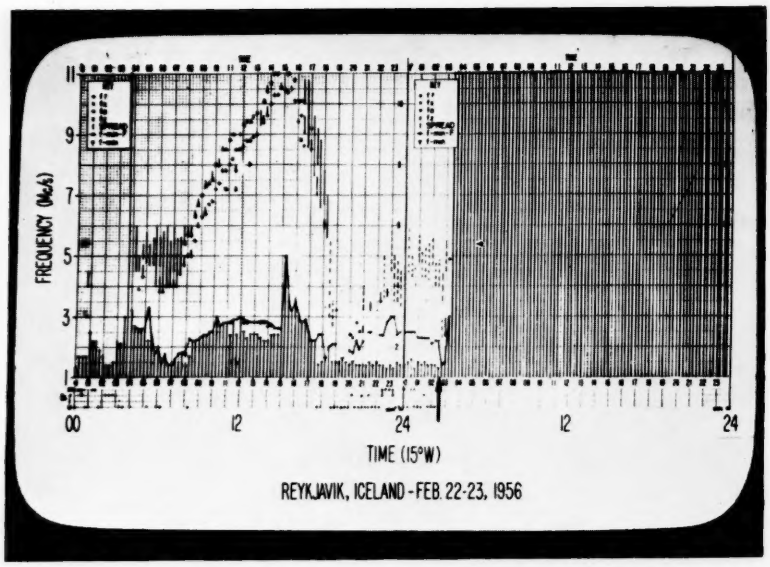

Fig. 19. f-plots for 22–23 February, 1956 — Reykjavik, Iceland

sounding was used in the scaling in preference to the medium gain. On the average, the high or low gain sounding was used 16 per cent of the time, the most frequent time of use being during the 3 or 4 hours about sunset.

If the gain runs are helpful, then an increase in the number of numerical values being obtained should be noted. *Fig. 16* shows the difference in the average number of numerical values obtained January–March 1956 and the same period 1955 when gain runs were not yet being taken (for Narsarssuak). The solid line shows that, on the average, 3 to 4 values were added to each median in the 1956 period, except for the slight decrease during several of the afternoon hours. On a percentage basis (dotted curve), referring to the scale at the right side of the figure, there was an average increase of 32 per cent in the number of values when compared to January 1955. Assuming that the

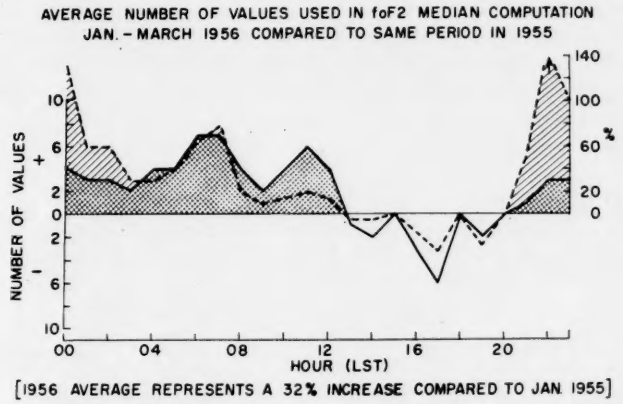

Fig. 16. Comparison between number of values entering into median f_0F2 January–March 1956 and same period in 1955 (Narsarssuak)

two periods were ionospherically similar, it would seem that the use of the gain runs was instrumental in providing a larger number of numerical values.

The major recommendation of the High Latitude group is shown in *Fig. 17*. It is the frequency or *f*-plot. Rather than analyzing isolated hourly soundings and trying to scale them according to low latitude rules, it was discovered that if the frequency data from each 15 min sounding were plotted with a minimum of pre-judgment, then meaningful hourly values could quite easily be obtained from the plot. If spread echo is observed then the *frequency range* of the spread is plotted as a straight line on the plot. Often, when the plot is completed, rather well defined trends in the variation of the critical frequency can be obtained even though many of the soundings were hopelessly spread. In this new concept, the *f*-plot becomes the principal daily data sheet with an auxiliary tabulation sheet used for the notation of the hourly values that are taken from the *f*-plot when it is completed. The data for College (Alaska) for 10 May and 20 May, 1956 are shown in this figure. The *f*-plots illustrate the difference in appearance of a quiet and disturbed day. In the past the daily data from each station consisted of the tabulation sheet alone (shown on the right of the figure). Now, in addition, an *f*-plot for

every day is prepared. The advantages of having the *f*-plot are two-fold — (1) better determination of hourly values, and (2) a valuable daily graphic picture of the ionospheric variations at that location is now available as a research tool.

Fig. 18 shows four more *f*-plots — Narsarssuak and Reykjavik for 11 and 29 February, 1956. (The Reykjavik plots are shifted 2 hours in order to line the plots on the same Greenwich time.) The *f*-plots are useful in facilitating the study of simultaneous ionospheric effects at several stations. These plots are shown to indicate the similarities in the variation of *f*-min (minimum frequency at which echoes are returned), which is a rough measure of absorption, at both stations. *f*-min is plotted as a filled circle connected to the bottom of the frequency scale (1 Mc) by a vertical line. Complete absorption is seen as a vertical line covering the complete frequency scale. Similar short bands of complete absorption are seen to occur at both stations within 15 min of each other. Yet at other times, increases in absorption are seen at only one of the stations. The *f*-plot type of presentation played a very important part in the discovery of the high latitude ionospheric absorption effects associated with the 23 February, 1956 solar-cosmic ray event.[3] *Fig. 19* shows the *f*-plots for 22 and 23 February from Reykjavik which clearly show this unprecedented effect.

Another improvement in high latitude ionospheric data handling might be the presentation of the prediction charts on a polar projection instead of the Mercator projection. *Fig. 20* shows several provisional CRPL prediction charts on a polar projection. Charts of this form should also help reduce some of the uncertainties in the application of vertical incidence data to oblique incidence problems at high latitudes.

Supp
Part.
195

Conclusion

This paper has in reality been a plea for the acceptance of the procedures and recommendations that were outlined in the URSI High Latitude Committee's report. Some networks have been reluctant to accept some of these procedures for fear that prohibitively large amounts of additional time would be necessary for the data reductions. We have not found this to be so. Whereas previously the scaling of one day's ionograms may have taken an hour to an hour and one-half, now the complete job, including *f*-plot, is done commonly in 2 hours. The amount of additional information that becomes available, we feel, certainly justifies this slight increase in work load.

In summary, the recommendations for making statistical summaries of high latitude ionospheric data more meaningful are:

(1) Soundings should be made every 15 min, with extra soundings at 5 min before and 5 min after the hour to help eliminate transient phenomena.

(2) A gain run should be made each hour to assist in the scaling of spread echo and *E*-layer characteristics.

(3) The *f*-plot should be regularly prepared for a clearer view of the variations of high latitude ionosphere and better determination of hourly values.

(4) The number of values entering into the computation and an estimate of the dispersion, such as the quartile range, should be published in addition to the median.

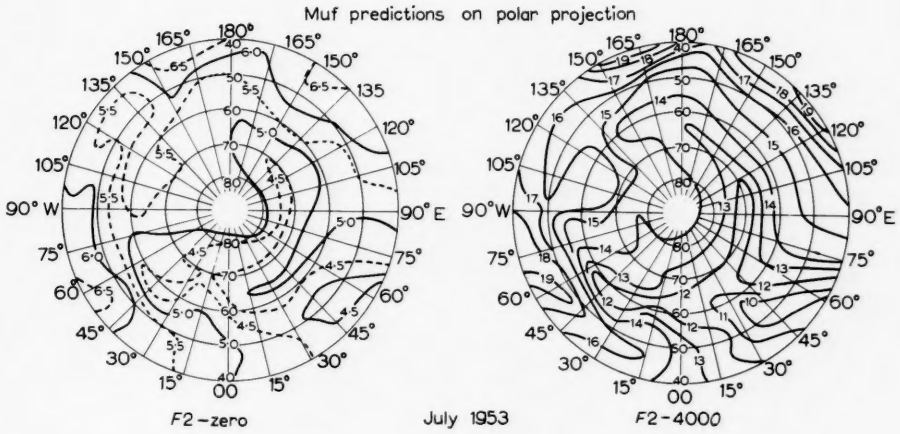

Fig. 20. Provisional CRPL prediction charts on a polar projection

Special experiments such as polarization and angle of arrival at a few selected locations would be valuable in the interpretations of soundings. Also projects such as the Canadian oblique incidence experiments and the airborne measurements Dr. Gassman mentioned yesterday should aid considerably in our understanding of the polar atmosphere.

At the time of the presentation of this paper, the slides were retained and the AGARD had prints prepared from them to use with this edited version of the paper (taken from tape recording) in the publication of the proceedings.

References

[1] *URSI Information Bulletin*, No. 96, 1956
[2] *Nat. Bur. of Stand. Circ.*, No. 465
[3] Paper in preparation

Suppl.
Art.II
1956

POLAR DISTURBANCES

J. H. MEEK
Radio Physics Laboratory, Ottawa

IN spite of, or perhaps as a result of my experience in this field of ionosphere prediction I am rather pessimistic about the future of present methods. The ionosphericist is perhaps in the same state as the meteorologist was about 1900. At that time he was able, for example, to forecast average temperatures for the month and for the year. To forecast the weather he plotted average tracks for cyclones and from these guessed the movement of a particular cyclone. From his chart of the usual cloud systems in various parts of a cyclone, he could estimate the precipitation, etc. He based his predictions on statistics entirely. We are doing the same in the ionospheric work at the moment.

Early this century, Bjerknes worked out a method of forecasting weather from hour to hour, from day to day, based on the air-mass system. The future in ionospheric predictions and forecasting is along the same lines and we are waiting for a Bjerknes of the ionosphere to appear. We must find, rather standard patterns of localized movements in the ionosphere, probably not on the same scale as the weather movements, but similar types of movements. Of course, we have to decide whether we are dealing with ionization movements or not. We must study the ionospheric data by examining successions of records not by merely taking averages for the day or month or year. It is essentially a trial and error method of analysis, or perhaps we should say a "bit of intelligent guessing", but sooner or later we will come up with useful systematic patterns. We may use our existing network of ionospheric stations or design of a network of stations to follow the changes around the world. The significant improvement for communications is to be able to tell what frequency to use three hours from now, or tomorrow morning, or at some other specified time. We can not expect very much additional support from the communications groups until we can do this type of forecasting.

Let us deal first of all with the variations in the critical frequency of the $F2$-layer. This is the most difficult layer to handle but is the one in which we are most interested for communication purposes. By means of the f-plot and the new high-latitude scaling schemes we are able to follow these variations every 15 min and sometimes more frequently. Even now a general pattern is observed during disturbances. The critical frequency of the F-region drops down during the daytime, the minimum coming within an hour or two of local noon. On the other hand at night the critical frequency is liable to be above normal. These remarks are based on critical frequencies as they have been measured in the past. We may have to change our statement in view of the new method of measuring critical frequencies.

Fig. 1 shows a plot for a group of stations along one latitude from Slough in England around to Adak in the Aleutian Islands, on a series of disturbed days from 6 to 13 November. It shows the deviation of the *F*2-critical frequency from its mean for each hour for this series of days. Each day at these stations (all are just a short distance south of the maximum disturbance zone) the critical frequency drops to a minimum in the middle of the day. On the left is a group from Clyde River south through Washington to Falkland Islands, with Christchurch, N.Z. included for comparison. The black horizontal bands indicate the periods during which there were no echoes from

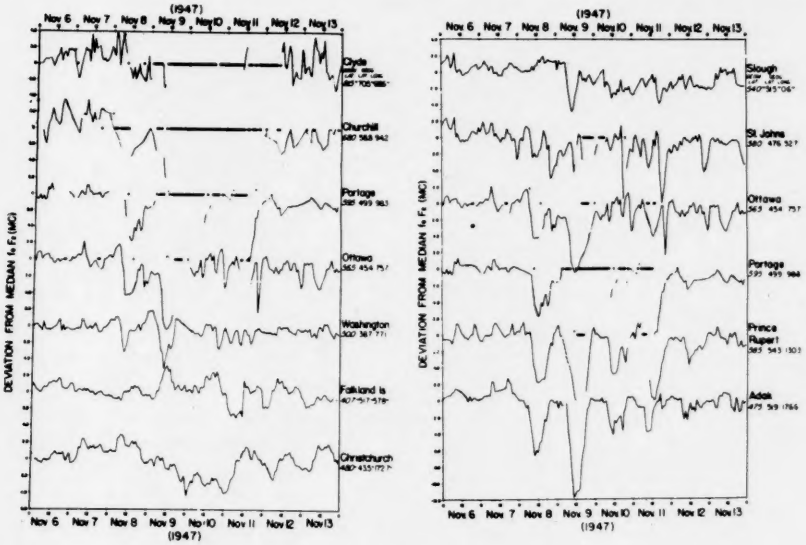

Fig. 1.

the ionosphere on the high-frequency band (total black-out). The sequence of HF absorptions from north to south is quite clear. In this paper I wish to confine my remarks to the less severe disturbances where some *F*-region echoes are observed. The figure shows that while the critical frequency drops in the daytime it goes above normal, not very far, but above normal at night. Analysis is very difficult, of course, and because we have such a strong diurnal effect we must find some other means of describing the phenomenon in terms of an ionospheric disturbance figure. We should like to designate a simple number to represent the amount of disturbance at all times of day, something that is not dependent on the time of day.

The above plots illustrate the great variation in f_0F2 in the polar records. In order to examine the variation more closely an *f*-plot of a number of days is shown on *Fig. 2*. Where there are spread echoes, often as not the spread goes above or below the critical frequencies and very seldom does one or the other edge of the spread stop at the point where you would expect a critical frequency to be at that particular instant. These measurements constitute the data that we use in our prediction schemes and in the northern regions probably the tabulated critical frequencies include many "hidden" doubtful

values. Originally, empirical rules were made for scaling. The rules are now being changed to some extent, and we may still have incorrect ideas on just what we do mean by a critical frequency when we have a record which is spread.

The variation in the *F*2-criticals during disturbances also has a positional variation which is not dependent on the time of day. *Fig. 3* shows the plot of the average of a number of storms normalized so that the depression at each point in this particular area is equivalent to a depression of 2 Mc/s at Ottawa.

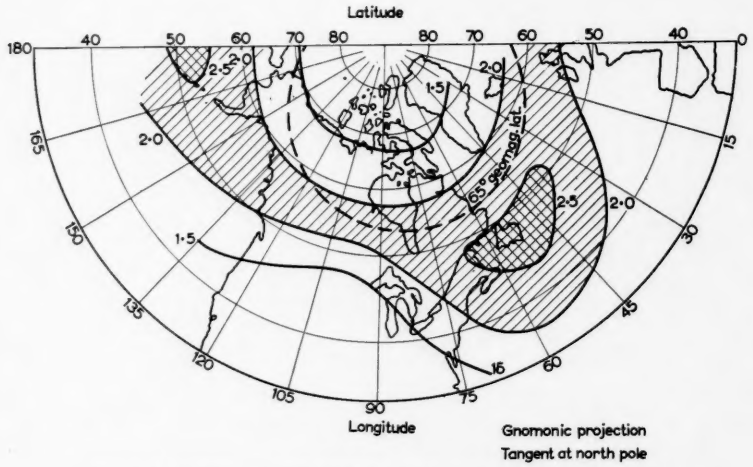

Fig. 3. f_0F2 depression, equivalent to 2 Mc/s at Ottawa, November 1949

We have two areas and possibly another on the other side of the earth, in which the critical frequencies are depressed more than we would expect. These areas are fixed on earth rather than with respect to the solar positions. A number of workers have done similar analyses of deviation of f_0F2 and I would like to mention one done recently by Obayashi in Japan.

Figs. 4, a, b, c, d and *e* is a series of five pictures showing the progress of an ionospheric disturbance. Time is indicated by the position of the sun. Note the deviation area off the east coast of North America remains at the same longitude while the rest of the disturbance moves around with the sun. This corresponds to the onset of a magnetic bay.

Corresponding to the last two pictures, from a magnetic point of view, the peak of the storm has passed, the depression is actually more intense but it is no longer moving around with the sun. In the last picture the disturbance is well on the way to recovery. It is rather interesting that in this example the ionospheric depression moves around with the sun while the storm is on the make, but on the recovery the disturbance is left behind.

There are great difficulties in describing an ionospheric disturbance from ionosonde records alone whereas the measurements of the deviations of the magnetic field of the earth give a rather simple index or indicator of disturbance which is not sensitive to the time of sunrise and sunset. There are differences in disturbance variations from day to night but there is no obvious

Suppl.
art.II
1956

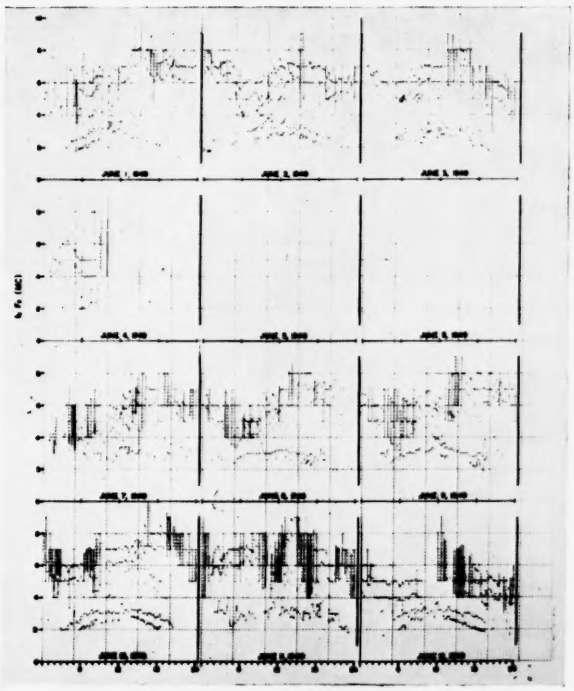

Fig. 2. Baker Lake (optical frequencies)

Supp
Part.
195

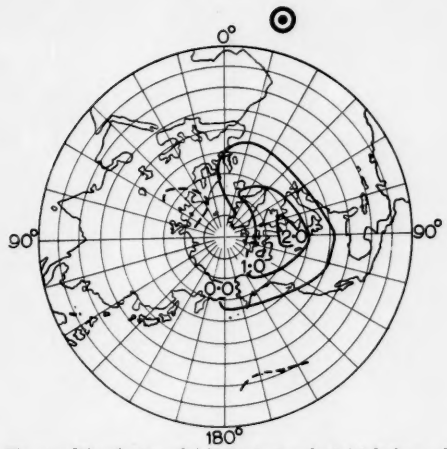

Fig. 4a. Distribution of Δf °F2 during the initial phase of a magnetic storm at 13h UT on 28 October, 1951

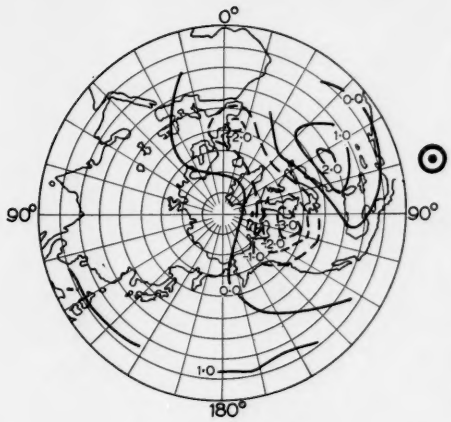

Fig. 4b. Distribution of Δf °F2 during the main phase of magnetic storm at 17h UT on 28 October, 1951

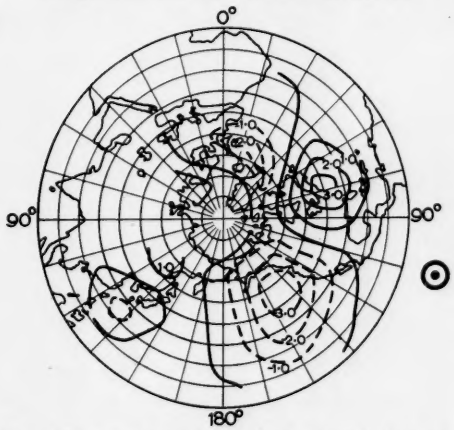

Fig. 4c. Distribution of Δf °F2 during the main phase of magnetic storm at 19h UT on 28 October, 1951

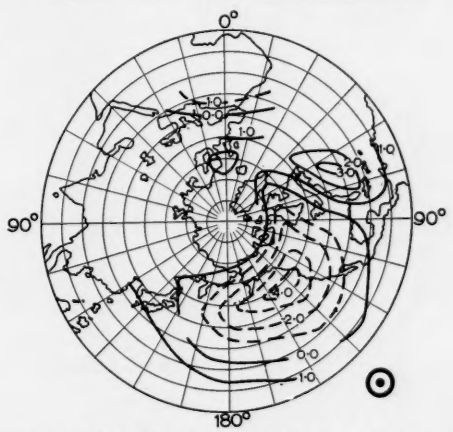

Fig. 4d. Distribution of Δf °F2 during the main phase of magnetic storm at 21h UT on 28 October, 1951

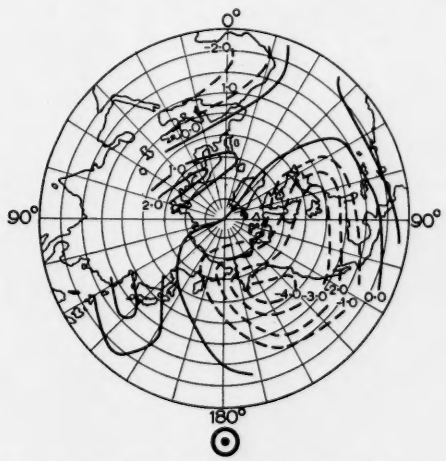

Fig. 4e. Distribution of Δf °F2 during the last phase of magnetic storm at 00h UT on 29 October, 1951

sunrise-sunset effect and no seasonal effect. In the first picture above there was just the positive disturbance at the time, the magnetic field of the north-pointing horizontal component above normal, whereas at the times corresponding to the other pictures the field was well below normal.

The top panel of *Fig. 5* shows a typical magnetic record on a slightly disturbed day. In polar regions, the ordinary quiet day diurnal variation of magnetic field in the horizontal component is negligible in comparison with these variations. The maximum here is more than 600 gammas whereas

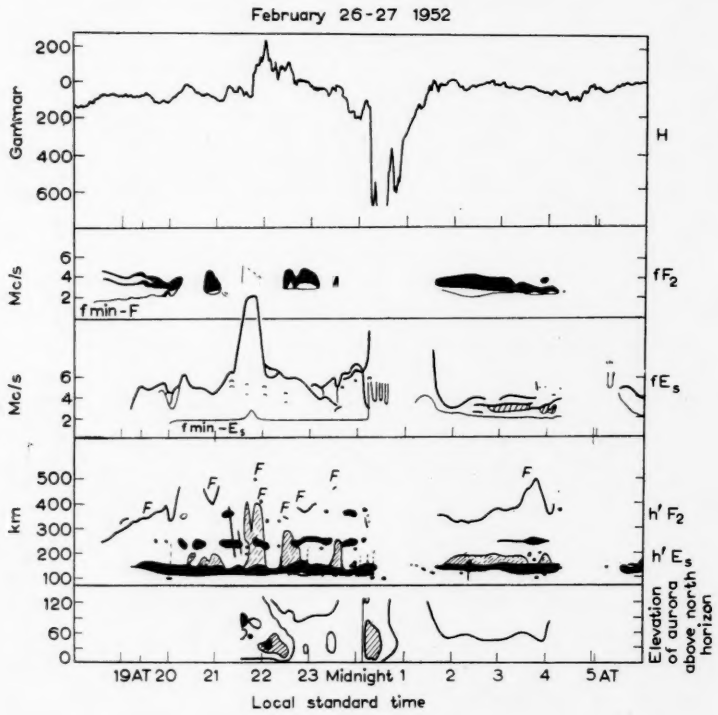

Fig. 5

the quiet day variation is of the order of 10 gammas or less. This is not a very disturbed day, but it is rather typical because we have a single positive magnetic bay and later in the night a single negative magnetic bay. In the lower panels are illustrated some of the variations in the ionosphere at the same time. The second panel shows the critical frequencies of the *F*2-layer, the ordinary and extraordinary rays with spread echoes between them. The lower line is the minimum frequency of the *F*-region trace. It increases rapidly when there is magnetic disturbance. On a quiet day the f_0F2 drops through the night until near sunrise, however, on a disturbed night such as this, the *F*-region patches when visible, are without distinguishable components and are all above the quiet night frequency. We do not know just how widespread these patches are, but they sometimes last for several hours. We do not yet know the connection between these patches of *F*-region ionization and

HF communication difficulties, we hope to find out some of the answers from our oblique incidence experiments.

The next panel shows the maximum frequency of the *E*-sporadic region. Where there are a number of lines and spots, a number of different *E*-sporadic regions exist. You notice one large peak at the positive bay whereas during the negative bay all traces disappear. The next ionospheric phenomenon is illustrated in the bottom panel which gives the intensity and elevation of the aurora above the northern horizon at Saskatoon, which is south of the region of maximum activity. This is a plot of contours of equal brightness with time against elevation above the northern horizon. We notice that there was aurora present corresponding to the positive bay, the brightest parts at fairly low elevations, and as the magnetic field dropped during the negative bay there was a sudden increase in intensity of aurora. The brightest aurora comes at the beginning of the negative magnetic bay the intensity falling off on the recovery. We recall the work of Obayashi illustrated above in which the *F*2 was very active, moving around with the sun, on the wake of the storm, but seemed to stagnate as the magnetic field was recovering afterwards. The auroral light seems to follow the same course. Initially there is a great deal of movement in the aurora and very clear structure bands with very sharp vertical rays, curtains, and so on. Whereas on the recovery of a magnetic bay the aurora is still covering a good bit of the sky but becomes more diffuse. It looks as though the latter is due to residual ionization whereas the aurora on the make of the storm is probably due to the initial excitation.

uppl.
rt.II
1956

While the original purpose of my investigations was to find a disturbance pattern for the ionospheric records, it is obvious now that this can not be done without auroral and magnetic records as well. Magnetic measurements have been taken for many years of course, but in the past, the analysis has been confined almost entirely to statistical work. We are all familiar with the work of Chapman, his model for magnetic disturbance. There is no doubt that this is the good model statistically, but if we are studying the variations of any of the elements of the ionosphere on a particular night, we cannot use this model. Because of the wild variations in the polar ionosphere a single day's records cannot be compared with a statistical model. Since my interest was to find a pattern which could be applied to a particular days data, it was necessary to look back over the past data from my own point of view and to try to pick out things that were happening from day to day rather than on a long-term basis. As a result some of the data which Vestine had worked out and published in Carnegie D.T.M. publication No. 580 was re-examined. The times of maximum magnetic deviation for all stations in the world for 1932–33 polar year were replotted. Positive and negative deviations were considered separately. This is rather important.

Fig. 6 is a polar chart on which are drawn thin lines indicating the approximate hours at which maximum magnetic disturbance occurred. Through these you can draw spirals of maximum positive magnetic deviation and maximum negative deviation. The plots are made on local geomagnetic time merely because it is customary in some magnetic analyses. About the same sort of a picture is obtained using local standard time.

The spirals bring to mind Størmer's original work which showed that the precipitation from outside should reach the auroral zone in the form of a

spiral, and if we have two types of precipitation (oppositely charged) we should expect to have two opposing spirals. It is interesting to note that Størmer's theory definitely shows that one would not expect the light intensity and consequently the amount of precipitation to be equally distributed along the spirals. It appears that we should reconsider Professor Størmer's theory. Although we still cannot tell how the particles acquire the correct energy to get down to the auroral zone from outside, the details of his work do explain the aurora as it is seen. The above provides some evidence that we may have a spiral auroral zone instead of an approximately circular one.

In *Fig. 7* is again a plot of 1932–33 data. Here I attempted to examine the

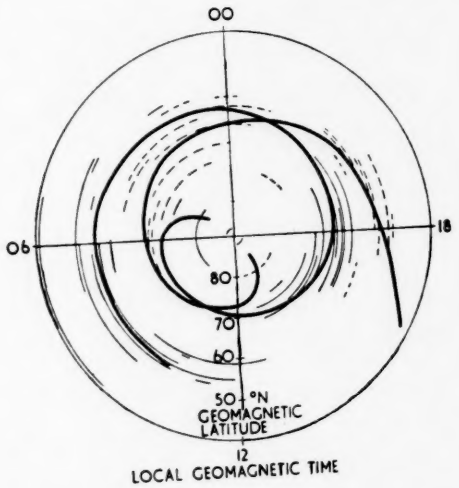

Fig. 6

data for one particular storm in which the magnetic bay lasted about 8 hours. Due to the small amount of data it is understandable why previous workers were content to work with statistics. In order to increase the amount of information it was necessary to use the trick of displacing the information hour by hour to get six points corresponding to each magnetic observatory. Contours of amount of magnetic deviation were then plotted. The shaded parts on the figure are below normal, the unshaded parts are above normal. The intervals between the contours are 200 gammas. With a little imagination you can see the spirals in this plot.

Although I frequently refer to auroral light, I would like to emphasize that this work is all based on magnetic data. Statistically the maximum auroral light appears to coincide with the region of maximum magnetic disturbance. (When Vestine drew up his new auroral frequency chart he used that assumption to help in placing his contours of auroral frequency.) While it is true statistically it is not necessarily true on any particular night and I have tried to see what happens on a particular night. If the maximum deviation line is a spiral it is a rather irregular one and the greatest deviations are confined

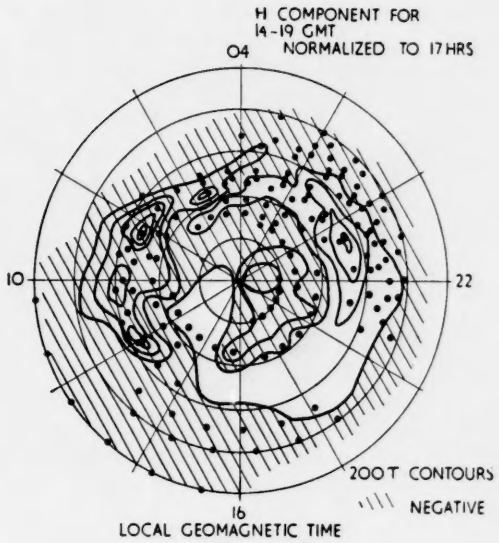

Fig. 7

Suppl.
art.II
1956

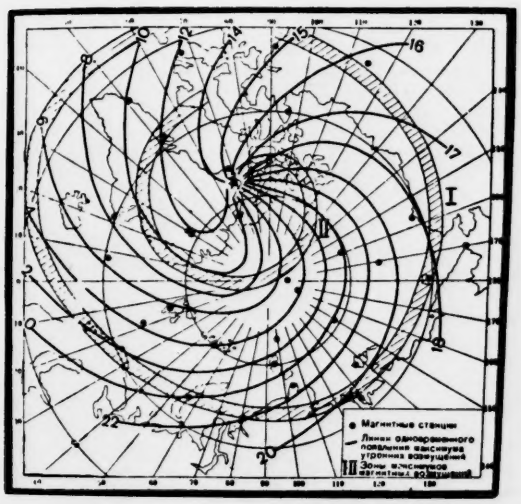

Fig. 8. Isochrons at morning maximum of magnetic disturbance (the figures attached to the isochrons represent world time). •—— *Magnetic stations* —— *isochrons of maximum of morning disturbance. I and II — Maximum zones of magnetic disturbance. The figure, which is taken from ref. 3, is inverted to facilitate comparison with Fig. 2*

to a small part of it. The existence of such a spiral does not mean that there is going to be auroral light right to the Pole. As far as we know this is not so. We still have not shown that the auroral light is coincident in detail with the currents that produce the magnetic field. Some work in Saskatoon on the relation of auroral light recorded in all sky camera photographs to magnetic variations indicates that it is incorrect to suppose that these currents are coincident with the auroral light.

Fig. 8 shows results of recent Russian investigations. (The paper on which this was produced does not give details of data used.) Consider the barred regions indicating the auroral zone. There is a circular zone which looks very much like Vestine's auroral zone. In addition there is the polar spiral which seems to disappear near the circular zone. Apparently these are two regions of maximum magnetic deviation (not auroral) which are fixed with respect to the earth. The circular zone is well known statistically but without further data there remains some doubt as to the existence of the spiral zone. Certainly it does not appear as auroral light.

In conclusion, I have tried to indicate some significant work which has been done in recent years. It is not a complete survey but gives an idea of the type of work that is being done towards solving the problem of the polar geomagnetic disturbances.

Sup
Part
19

POLAR BLACKOUT OCCURRENCE PATTERNS

VAUGHN AGY
National Bureau of Standards, Boulder, Colorado

Suppl.
art.II
1956

THIS paper is related closely to the one given by Dr. Meek and I shall refer to some of the slides he showed. It would give me a great deal of personal satisfaction if I could give you patterns of blackout occurrence which would arouse no dissension. Unfortunately, I cannot do that. I take some slight consolation from the fact that I believe, at least, that no one else can either.

The first work on blackouts at a number of observatories (mentioned by Mr. Knecht as having occurred at Thule in February 1956) consisted of tearing down and rebuilding the equipment when a long-lasting blackout was first observed. I have heard similar reports from Kiruna.

There have been a number of single station blackout studies made and these are important and valuable, I believe, in that they give us an idea of what happens when a magnetic disturbance occurs and we cannot deny that there is a high correlation between magnetic disturbance and blackout occurrence. Now this is a high correlation but there are things that are puzzling about it. For example, at College and at Kiruna it is found that the diurnal variation in the frequency of occurrence of blackouts is almost precisely 12 hours out of phase with the diurnal variation in magnetic activity. This has puzzled me considerably. Lindquist, I think, mentioned it first at Kiruna. Little and Chapman have reported similar variations at College. It is just that there are blackouts that occur when magnetic disturbance is not very marked. Many of you, if you have worked with Arctic ionospheric data must have run into similar problems. One of the first things I did in arctic ionospheric work was to run correlations between auroral brightness and sporadic-*E*, and the number of blackouts corresponding to different brightnesses of the aurora from one winter's data from College, Alaska. Positive correlation coefficients of about 0·7 were obtained. This was fine. The next year we had precisely the same sort of data and some of the correlations came out negative, so this was something we never published.

The appearance of the ionospheric data tabulation sheets, gives an indication that there are time patterns of occurrence of blackout, which appear to be independent of magnetic activity. In order to get at this I used all the available tabulated data for a period of about 4 years. (There are objections to this method I know.) "*B*", indicating absorption occurred on the tabulation sheets in such a way that definite diurnal variations became apparent. A Fourier analysis was then made of each diurnal variation giving the average number of hours during the day when blackout occurred (A_0), the amplitude of the first harmonic diurnal variation (C_1) and the phase, ϕ, i.e. the time at which the first harmonic reaches a maximum. (You might suggest

that this use of Fourier analysis is gilding the lily, but this lily is one that can be gilded with no detriment to the flower itself.) Some of the results are shown in *Fig. 1* and this gives one indication of patterns which occur. The contours are labelled according to the local time at which the first harmonic reaches a maximum, for magnetically quiet periods and for disturbed periods. I am not trying to sell these patterns, although I did a couple of years ago. I was quite excited about them, but I am not happy about them now particularly, except that the contours are so easy to draw. There are 18 stations represented here with about four years of data from each station, with a few exceptions, and in spite of the vast amount of data used (this is a relatively small area of the world, as you can see) the contours almost draw themselves. I have tried to draw contours of Arctic *F*-layer variations and things of that sort and I

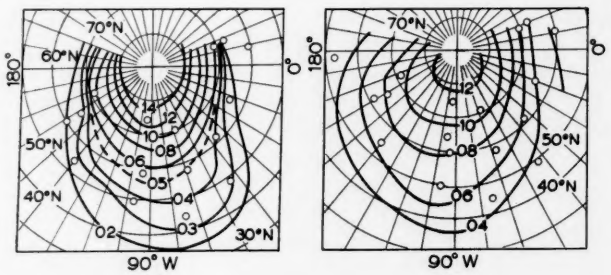

Fig. 1(a). Time of maximum probability of blackout, ϕ_1, L.M.T. (winter omitted), quiet

(b). Time of maximum probability of blackout, ϕ_1, L.M.T. (winter omitted), disturbed

find that I can best leave this to someone who has had experience in it, because it is not easily done. But this is quite simple. The contours came out very nicely. There are a few odd quirks in them, which I will say something about a little later, but you can see the progression in local time of the maximum frequency of occurrence of blackout as you move toward the Pole. This is on a local time basis. Now, one advantage of the Fourier analysis, which may be in some ways an unnecessary refinement, is shown by the fact that you do get 3 parameters, all of which I think are important and in *Fig.* 2 is plotted the average, A_0, as well as the amplitude C_1 of the (first harmonic of the) diurnal variation and these too give us contours which are very easily drawn. The average of the diurnal variation is shown at the top for quiet conditions on the left and disturbed conditions on the right and we see that we get a picture that is nice to look at. I think it was worth some of the excitement that was spent on it. There are also some odd things here. For example, during a quiet period, A_0 increases with latitude to a maximum (of about 15 per cent) and then decreases. The same sort of variation is also found for auroral occurrence and magnetic activity. For blackouts, however, there is minimum somewhere in the neighbourhood of Baker Lake near the 90th meridian. The minimum in this case is shown as a zero contour line. The minimum is quite consistent in all of these plots. Here, for disturbed conditions for A_0 it reaches 5 per cent; and for C_1, 4 per cent after maxima of 50 per cent for A_0 and 25 per cent for C_1.

Another reason for liking these patterns as they developed, is shown in *Fig. 3*, where I took the values along the contours as they crossed the 90th meridian and plotted them against geographic latitude along that meridian showing the variation in the frequency of occurrence of blackouts on the

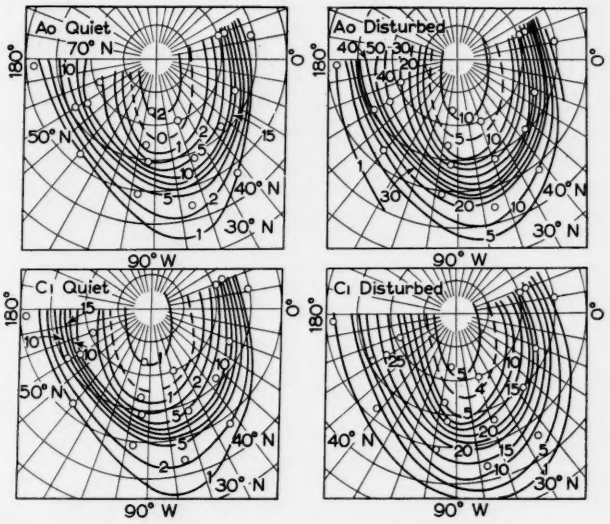

Fig. 2

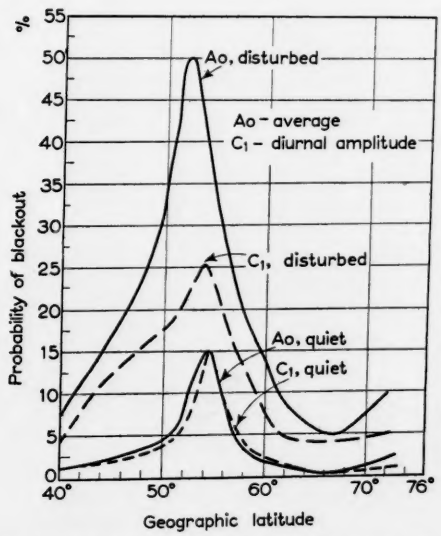

Fig. 3. Variations with latitude (along 90th meridian) of probability of blackout

average (A_0) for the day, quiet and disturbed, and the diurnal amplitude (C_1) for quiet and disturbed days, and we get these plots which are quite nice, the sort of picture you might expect if a similar thing could be done with aurora.

Mr. Piggott, some years ago, had suggested a pattern (I think this was one of the first published attempts to try to derive a pattern), in which he used data from six stations which suggested a 48-hour rotation of a pair of *D*-storm regions about the Pole and this was difficult to accept. A 48-hour motion is, so far as I know, unheard of, in geophysical phenomena but his points fitted the line so exactly that he was led to suggest this motion. The stations he used were at about the maximum of the auroral zone so that he had perhaps more homogeneous data than I did. Another thing which may increase the usefulness of his data is the fact that he sorted, to some extent, the blackouts which occurred during magnetic disturbance and those which did not. Well, I thought the patterns derived at the National Bureau of Standards gave more information than Mr. Piggott's did in that they do give us the latitude variation which I, at least, was not aware of up to that time.

The spiral patterns in magnetic activity which have been suggested, both those derived by Dr. Meek from the Polar Year data and those given by the Russians, may be reliable but I think we should proceed cautiously and with a great deal of effort, not to disprove them necessarily, but to find out what the real picture is. In the case of blackouts we have two problems. We have to do something about those blackouts, I think, which occur with magnetic activity. We also have to find out what the pattern of occurrence is of those which do not.

Fig. 4 shows the plot Mr. Hope referred to (in the paper mentioned by Dr. Meek) in which he suggests that there may be a spiral pattern representing motion of blackout — or to use Piggott's term "Storm-*D* region".

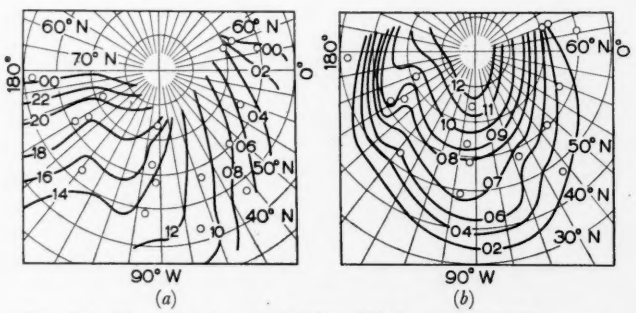

Fig. 4(a). Time of maximum probability of blackout, ϕ_1, G.M.T., summer

(b). Time of maximum probability of blackout, ϕ_1, L.M.T.

For the summer season I found that I could get something which looked like motion around the Pole in 48 hours and so you see I am on both sides of the fence. I did not want to be wrong and in case Mr. Piggott is right, I have the proof of it here. My actual purpose for including this slide is not to suggest that I agreed with Mr. Piggott at all, but to show how we both may have been misled. Now Mr. Hope has used the Greenwich Time plot shown on this slide and found good agreement, between my contours as they crossed the

60th parallel, on this chart, and the Russian spiral contours for the same part of the world and along the same latitude, and he appears to make something of it. I distrust both Mr. Hope and myself in drawing conclusions of that sort.

The business of finding this variation in magnetic activity is a tricky one and statistics may have been over-used in the past, but I do not think we can give it up yet. A recent French thesis by a graduate of the University of Paris, Mayaud, suggests that the spiral patterns may not be real, I think, and he does things in terms of geomagnetic time. My own feeling about geomagnetic time, at least until recently, is that it is a strange and wonderful clock that seems to have a different number of minutes for each hour of the day, and so I have hesitated to use it as being somewhat artificial, but I am not firmly convinced that this is right. As a matter of fact I hope to be able to apply geomagnetic time to the time patterns of blackout occurrence.

Recent work by Little, and more recently by Chapman and Little at College, Alaska, has given a method for measuring the actual amount of absorption during blackouts by recording cosmic noise at relatively high frequencies. Now this is good because the blackouts that are considered here are those producing blank ionospheric records. This is like analyzing the grin of the Cheshire cat but the Little method allows us to swing the cat by the tail a bit, since absorption at, say, 30 Mc is low enough that with adequate sensitivity there will almost always be measurable field strength left to work with. This is a method which should be used.

There are several odd points on these charts. A Canadian work by Davies and Cox, which tends to confirm these results, also shows that there is remarkably little occurrence of polar blackout at Baker Lake. I am inclined to believe that this is real, but I am not sure, and it seems to me that Baker Lake would be an ideal place to put in a cosmic noise recorder to find out just how much absorption they do get there, during blackouts especially.

Another point of difficulty is in the very close spacing of some of the local time contours between Kiruna and Tromsø. Now these stations are separated by no more than a couple of degrees in latitude, and yet the time at which the maximum frequency of occurrence of blackout is given on the charts is different by several hours: now this may be a fault of the data and I admit that my method of analysis of the data has flaws, but valuable information could be gained if a comparison of cosmic noise measurements at the two stations over a period of a year or so could be made.

Dr. Matsushita has been visiting at the Bureau of Standards in the past year and has recently suggested that blackouts may be sorted into two types; "gradual blackouts" and "sudden blackouts". The gradual blackouts are those that occur with magnetic activity: during a magnetic bay if it is strong enough, you will get complete blackout at College. (We are not sure about what happens at points north and south of the auroral zone where presumably the strong currents flow — this is something that should be worked on, of course.) During this period you will see a development of ionospheric conditions into the blackout condition; blanketing by sporadic *E*, perhaps a decrease in the critical frequency of the *F*-layer before that, finally full blackout at the depth of the bay, and then a gradual recovery going through much the same sequence in reverse. The sudden blackouts, on the other hand, may be associated with relatively little change in the upper ionosphere and

little magnetic activity, and he is suggesting that the sudden blackouts are produced by ionization very low in the ionosphere, below 70 km, while those which are associated with magnetic bays are at heights which are more usual for people working with the ionosphere data.

It is interesting that Dr. Matsushita should come up with this at about the same time that Drs. Chapman and Little at the University of Alaska should suggest that there is a mechanism to provide the low level ionization required based on the fact that Van Allen and his co-workers have observed X-rays at heights of about 50 km. These X-rays produced by incoming auroral corpuscles may in turn be the ionizing agent responsible for the "sudden blackouts". The cosmic noise technique, I think, should be used very widely and I hope that the IGY program, for example, will allow for its wide use in order to find out what the patterns of blackout occurrence really are.

Supp
Part.
195

QUANTITATIVE MEASUREMENTS OF ABSORPTION IN THE AURORAL ZONE

F. LIED
Norwegian Defence Research Establishment

uppl.
rt.II
1956

1. INTRODUCTION

IONOSPHERIC recordings at polar stations such as College in Alaska, Baker Lake and Churchill in Canada, and Tromsö in Norway, have generally indicated that the normal level of ionospheric absorption is high, but also frequent occurrence of excessive absorption and of polar radio blackouts even during mild magnetic disturbances. Such disturbances constitute a serious handicap to radio communication which passes near the auroral zone.

Our quantitative knowledge of both the normal ionospheric absorption and of these disturbances is far from complete and we might say that clarity of the physical mechanism involved is partly lacking in spite of the fact that our knowledge of the statistical properties of the disturbances is considerable. Likewise, of course, from a practical point of view we would very much like to be able to predict both the normal and the occurrence of excessive radio absorption.

In this paper, we will first consider the available technique which may be brought to bear on our problem and further summarize briefly the published results of quantitative measurements chiefly from Canada and USA and compare them with some work done here in Norway.

2. OBSERVATIONAL TECHNIQUES

Generally speaking no single observational technique is available which may help us in obtaining a complete picture of the physical mechanism behind the normal or the excessive polar absorption. A short review of the available techniques, their possibilities and limitations, may therefore not be out of place.

2.1. *CW-oblique measurements*

Quite a substantial amount of interesting results have been obtained by CW recordings over oblique paths. Basically the field strengths from a distant transmitter is recorded and gives an integrated picture of ionospheric condition, including absorption, at or near the control point. By combination of a number of transmitters and receivers many paths may be studied simultaneosuly as done by AGY,[1] and by relatively simple means a picture of the geographical location of the absorbing zone may be obtained.

A limitation of the method is that the transmission mode is not known in detail, we don't know if we have 1*E*, 2*E*, 1*F* or combinations of them. It is

therefore, not easy to say what is the real cause of variation in signal strength. Particular attention should be given to the question of E_s which often occurs together with excessive absorption, but which may influence the field strength and obscure the real absorption effects.

The CW-method is nevertheless able to produce interesting results, particularly in the frequency range of 5 to 10 Mc/s.

2.2. *Pulse experiments*

The most common technique for ionospheric absorption measurements is the pulse experiments basically comparing the strength of the first and second echo. The principle is given in *Fig. 1.*

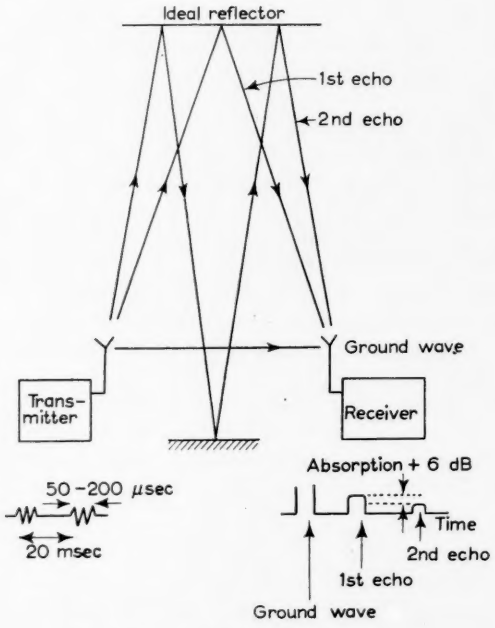

Fig. 1. Principle of pulse-amplitude technique

The radio frequency used is between 1 and 8 Mc/s and the absorption may be determined with an accuracy under ideal conditions of 1 db. With normal available powers and normal noise conditions 60 db is the highest absorption measureable at 2 Mc/s, this is sufficient for measurement of the normal absorption, but not sufficient for following the development of even a reasonably weak radio blackout.

The pulse-amplitude technique gives again the integrated absorption over the path and can not tell where the absorption takes place. Likewise may incomplete reflection from a rough surface be interpreted as being due to dissipative absorption and may give misleading results, at least if careful averaging is not being done.

Suppl.
art.II
1956

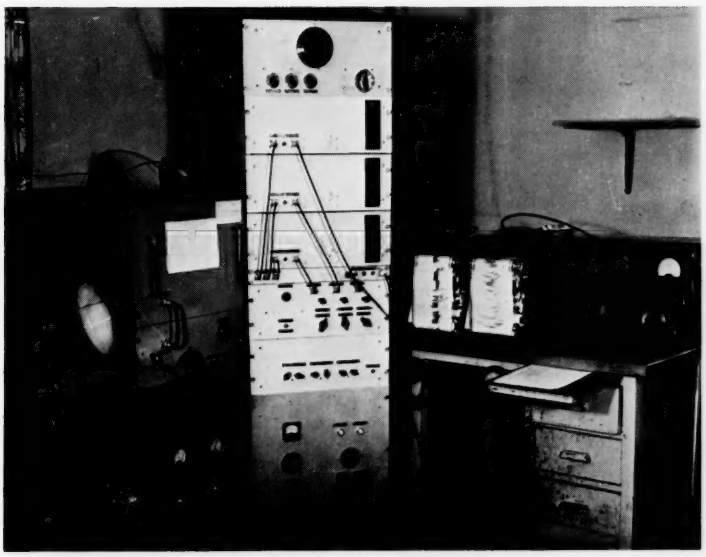

Fig. 2. Pulse-amplitude equipment

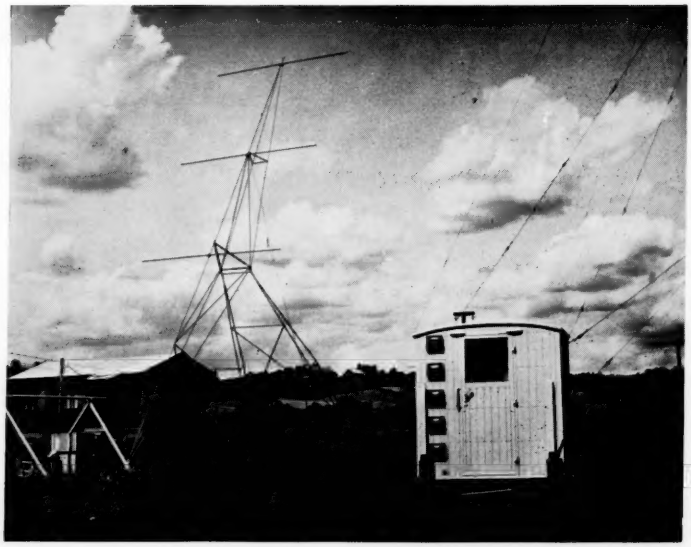

Fig. 4. Galactive absorption equipment

Sup
Part
19

Nevertheless with all its limitations measurements using pulse-amplitude technique have been carried out at a number of places including here in Norway both in Oslo and Tromsö, and *Fig. 2* gives an impression of the equipment involved.

Of course, the most common of all pulse-amplitude equipment is the usual *h'f*-recorder, but this can only provide qualitative measurements of absorption. As we know this has provided us with some very interesting results, but we will not consider it further here.

An interesting development of the pulse-amplitude technique is the pulse phase technique as developed by FINDLAY.[2] The principle of this technique is given in *Fig. 3*. With this technique it is possible to measure phase paths difference of the order of a wavelength and if this is combined with amplitude measurements the techniques may help us to locate in height the extra ionization causing excess absorption.

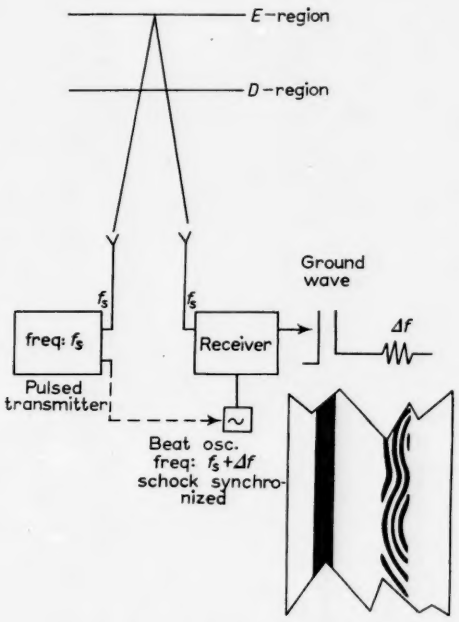

Fig. 3. Pulse-phase technique

2.3. *Galactic technique*

By the galactic technique we measure the strength of the galactic background noise after passage of the whole of an irregular diffracting and absorbing ionosphere. In a sidereal day our receiving aerial will sweep through a greater or smaller part of the sky and the noise recorded will vary in intensity for that reason. But superimposed on this we will have variation in strength due to our normal ionospheric absorption and due to more catastrophal events like the polar radio blackouts and the SID's.

Suppl.
art.II
1956

The frequency we will have to employ is between 15 and 50 Mc/s. Interference will prevent a lower frequency, a higher is prevented by the sensitivity of the apparatus. If we assume that 0·2 db is the lowest variation we may record, the normal daily absorption is just about noticeable when using 30 Mc/s.

The galactic technique is therefore especially useful in connection with stronger disturbances, but it would have been nice if a complete overlap in sensitivity with the pulse-amplitude technique was possible. This point is being worked on here now. In *Fig. 4* the equipment in use at Kjeller is presented.

2.4. *Cross modulation technique*

Recently Canadian workers and FEJER[3] in South Africa have suggested pulsed cross-modulation experiments for studies of the lower ionosphere.

The principle is demonstrated in *Fig. 5*.

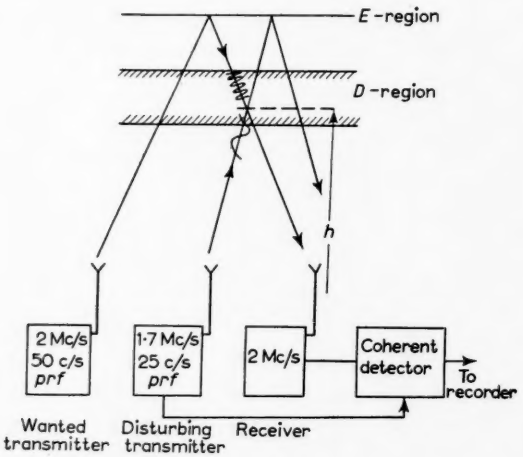

Fig. 5. Cross-madulation principle

The "wanted" transmitter has a pulse frequency of 50 c/s and the disturbing transmitter a pulse frequency of 25 c/s. When the disturbing radio pulse passes through an ionized region, the mean electron temperature increases and with it the absorption of the wanted wave. When this wanted wave on its passage downwards through the ionosphere meets the disturbing wave at a height h, only that part of the ionosphere at and below h is effective in producing cross-modulation. The wanted wave will therefore have a 25 c/s modulation on it due to this cross-modulation, and with certain limitations it should be possible to determine electron density and collision frequency in the lower ionosphere.

This beautiful technique unfortunately suffers from shortcomings. We need a lot of power and a very low noise level at the receiver. At Kjeller we have tried the possibilities with a disturbing transmitter of 500 kW at 1·7 Mc/s and

a wanted transmitter of 35 kW peak power at 2 to 3 Mc/s. In *Fig. 6* a sample of a record obtained is given showing the difficulties due to the noise condition near inhabited areas.

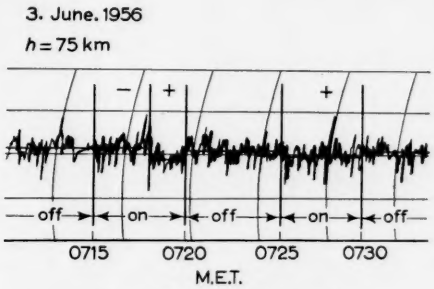

Fig. 6. Cross-modulation record

2.5. *Conclusion on techniques*

In summing up, no single technique available is able to tell us where and how much absorption a radio wave suffers under all conditions. I think that we shall have to apply all the mentioned techniques at the same time and we shall have to force them to overlap. Especially the pulse-amplitude and the galactic techniques should be a good pair, though the pulse-phase and cross-

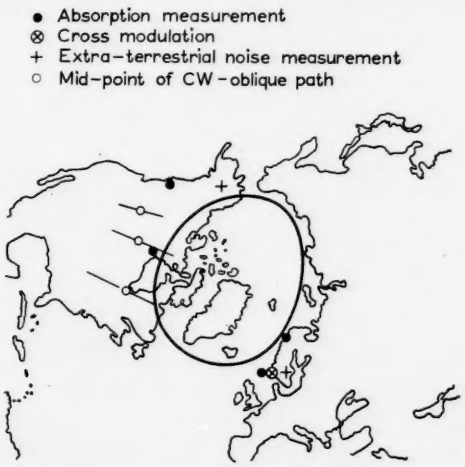

Fig. 7. Location of absorption experiments

modulation techniques ought to provide the skilled hand with some very interesting results.

3. Observed Results

Perhaps a polar map indicating where direct quantitative absorption measurement of different kinds has been carried out, see *Fig. 7*, should be of interest before we discuss the main results of the different workers.

3.1. *General results*

The main difference between the absorption near the auroral zone and elsewhere is the great number of days when the ionosphere generally is disturbed and the great number of periods lasting from hours to days when the absorption is excessively high. These polar blackouts are from an observational point of view of the same nature as an SID (or Dellinger-fade) but they are of longer duration, sometimes lasting even for days, and they may also occur during the night.

3.2. *Canadian and US-results*

Particularly the Canadian and US workers have been active in trying to elucidate the nature of both "*normal*" and *excessive* polar absorption. They have tried to clarify the problem of how the "normal" absorption (if the term may be used) compares with absorption measurements at lower latitudes and they have also studied the frequency of occurrence and the location in its widest sense of the excessive absorption.

(*a*) Quiet days

At Prince Rupert in Canada, approx. 1000 km south of the accepted auroral zone, DAVIES and HAGG[4] have applied the pulse-amplitude method for more than one year. At this location, which perhaps may be classified as semi-polar, they find the *normal* absorption following roughly the same laws as at lower latitudes. The variation with cos χ over the day and year and the frequency law is roughly the same as at Kjeller, also 1000 km from the auroral zone, and as at Slough, nearly 1500 km from the zone.

MEEK *et alia*[5] have carried out some very interesting pulse-amplitude experiments at a number of stations on a line at 100° W between 50° and 59° N ending at Churchill just under the accepted auroral zone. These experiments again show that during "normal" conditions the absorption conditions are more or less as at lower latitudes. There is, however, a slower falling off of absorption with increasing latitude than might be expected from a cos χ-law.

(*b*) Disturbed days

MEEK *et alia*[5] have also by the beforementioned absorption run from 50° N up to Churchill quantitatively studied the excessive absorption and find a maximum at approximately 55° N which is 5° south of the established auroral zone. A maximum further north is also indicated. These results are very interesting, but as pointed out by MEEK, the observations at different locations were carried out at different times and this may make the conclusion less certain.

MEEK[6] has also organized reception on the Loran chain with control points along a longitude of 80° W and 115° W. These tests showed that between 58° and 69° geomagnetic north, the occurrence of blackouts was very great and channels with control points in this region were only open 10 per cent of the time.

This zone of excessive absorption is wider and somewhat further to the south than the absorption zone on ionospherically quiet days. Inside the zone there are some indications that the absorption decreases during disturbances.

AGY[1] applying the CW-technique with 2 transmitters and 4 receivers has analyzed in all 7 HF-channels with control points from 48° N and 61° N, roughly at 95° W. He finds reception most difficult during daytime and the

Supp
Part.
195

zone of excessive absorption he finds nearly at the zone of maximum aurorae and only 6° wide, while MEEK observing at 100° W thinks it may be 10° wide and somewhat further south.

(*c*) Correlation of excessive absorption with magnetic conditions and auroral forms

The correlation studies between measured absorption and magnetic conditions are very important. DAVIES and HAGG[4] in their measurements at Prince Rupert found no significant correlation between measured absorption and *K*-index during day time, but during the night the correlation was very clear. Further the correlation was relatively low for $K<5$ but for greater values of the magnetic index the correlation was very good.

In College, Alaska, LITTLE[7] applying the galactic technique on 65 Mc/s

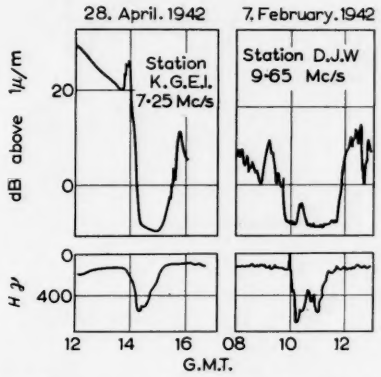

Fig. 8. Signal strength during magnetic bays (after Wells)

observed a very good correlation between *K*-index and excessive absorption. Scintillation was observed together with the increased absorption.

Again at College, Alaska, WELLS[8] has made a very interesting study of the detailed connection between magnetic bays and polar blackouts; the latter was recorded by CW-technique. Examining 69 bays he found a one-to-one connection with blackouts and since bays have a recurrence tendency, WELLS indicates a possibility for prediction. One of WELLS' beautiful examples is given in *Fig. 8*.

Recently MEEK[9,10] has made some very interesting detailed comparisons of magnetic, auroral and ionospheric variations at Saskatoon. He has especially considered the features connected with positive and negative bays. He points out, however, that there is no clear evidence that the same bay repeats at 24 hour intervals as has been suggested and he infers that each bay, positive or negative, is due to a separate group of particles entering the ionosphere in the auroral zone. The general disturbance is made up of a great many bay-type disturbances which collectively may be world-wide, but individually are localized, the individual effects being a band that is probably less than 1000 km in length along the auroral zone.

As to the correlation between excessive absorption and auroral forms, HEPPNER, BYRNE and BELON[11] working at College have made an interesting

study of correlation between different types of aurora and excessive absorption (blackouts). They find little correlation between appearance of non-pulsating forms and blackouts, but in 72 per cent of the case of pulsating aurora they observed complete blackouts. They draw our attention to the suggestion that the pulsating forms on the whole occur at lower heights than non-pulsating forms and this should explain the relationship.

3.3. *Tromsö observations and results*

I would like briefly to indicate some of our observations here in Norway. We have been measuring absorption at Kjeller for a number of years by the

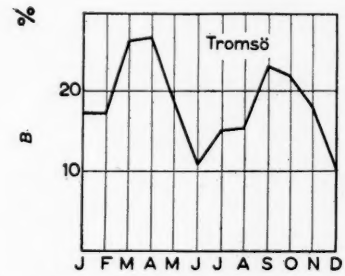

Fig. 9. Average occurrence of blackouts over the year

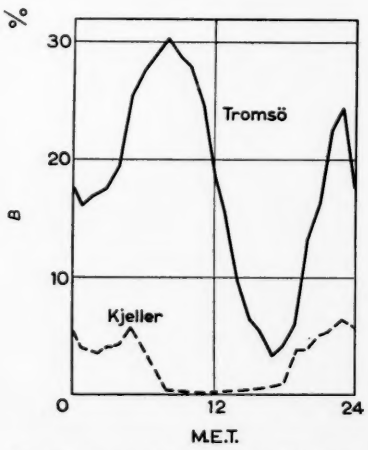

Fig. 10. Average daily occurrence of blackouts

pulse-amplitude method. Recently this has been supplemented by galactic and cross-modulation techniques.

At Tromsö we have been applying the pulse-amplitude method for 16 months. As you will remember, Tromsö is very close to the auroral zone and we have experienced a great number of difficulties due to the extreme variability in ionospheric conditions.

Qualitatively, *h'f*-recordings from 1952–1954 give us the seasonal variations of excessive absorption as given in *Fig. 9*.

We observe the pronounced maximum at the equinoxes in the same way as magnetic and auroral activity.

The daily variation of excessive absorption is demonstrated in *Fig. 10*. We notice the clear maximum in the early morning with the subsidiary maxi-

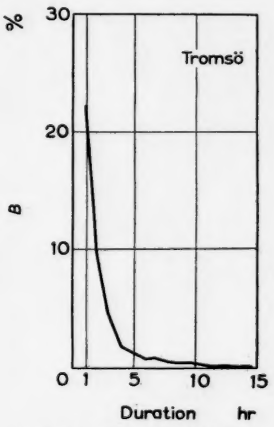

Fig. 11. Duration of blackouts

mum late in the evening. Likewise is shown a comparison between Tromsö and Kjeller results.

In *Fig. 11* the duration of blackouts in Tromsö is demonstrated. We see that normally the blackouts are of short duration.

Turning to more quantitative measurements we will first study the noon

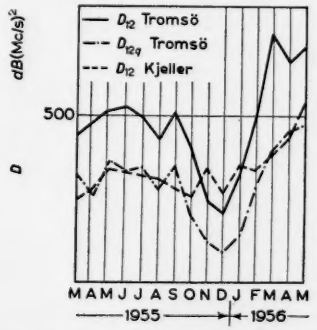

Fig. 12. Seasonal variation of noon absorption index

absorption index which has been deduced on the basis of 2 hours continuous measurement at noon with the pulse-amplitude technique daily for 16 months. The index D is derived from the well known non-deviative formulae

$$Ab = \frac{D}{(f+f_L)^2}$$

In *Fig. 12* the mean absorption index is given from March 1955 to May 1956. Each month the 5 lower noon absorption values are picked out and

averaged and this is given in *Fig. 14* as well. We see that during a quiet period the absorption is approximately as at Kjeller except during midwinter when the sun is below the horizon in Tromsö.

We have also studied the daily variation of absorption by continuous pulse-amplitude technique one day each week. This is not by far sufficient. When magnetic conditions are very quiet, we may obtain absorption values

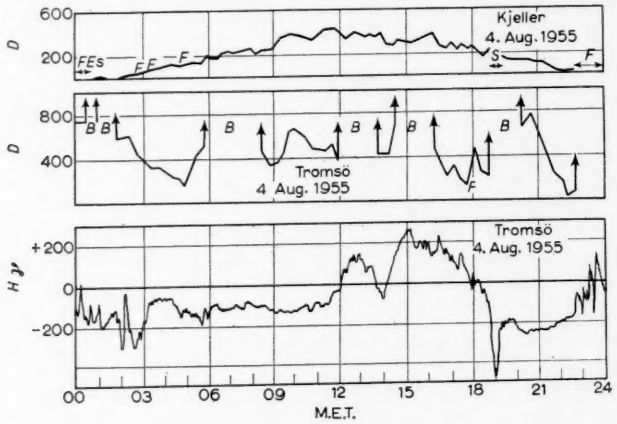

(*a*)

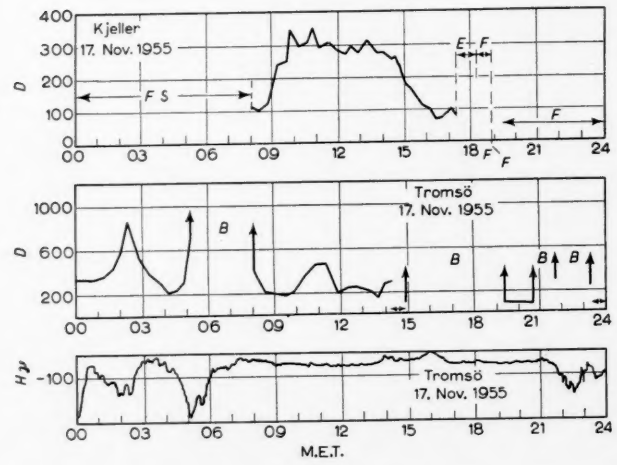

(*b*)

Fig. 13. Absorption on quiet days

as in *Fig. 13*. But conditions like this are very infrequent. We have only a few of this simple type. The more normal behaviour is given in *Fig. 14* showing disturbed days.

Our conclusion from 16 months measurements in Tromsö with identical techniques and interchange of personnel with our Kjeller station is that on the whole we obtain a similar picture as obtained in Canada and in US. During

quiet conditions the absorption follows the same "laws" at Tromsö as at Kjeller, the dependence of cos χ being roughly similar. But the pulse-amplitude technique does not allow us to follow development of any strong disturbances and we really don't know what happens quantitatively.

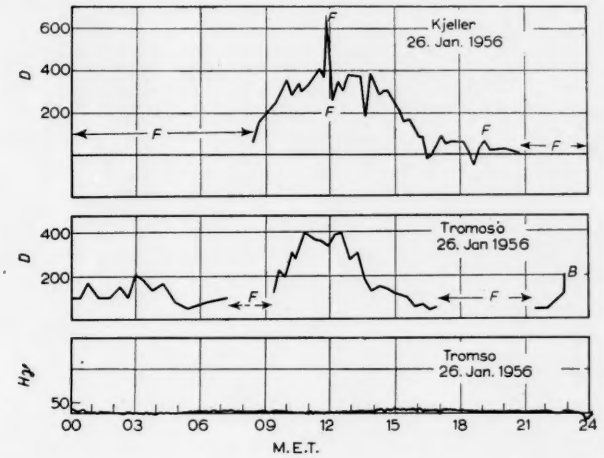

(*a*)

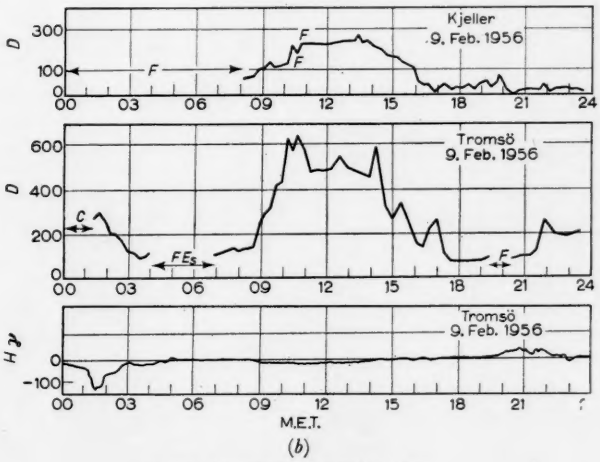

(*b*)

Fig. 14. Absorption on disturbed days

4. Conclusion

In summing up I think it is correct to say that the observational phase in connection with ionospheric absorption is not terminated yet. We especially need application of different techniques with overlapping sensitivity so that we may study both the "normal" auroral absorption as well as the disturbances.

I think we know very much more about the statistical distribution in time and space of the more catastrophic blackouts than we know of the real nature and cause of the general and excessive high absorption near the auroral zone. We all feel that the excessive absorption is due to some ionizing mechanism which sometimes produces aurora, sometimes polar E_s and sometimes excessive absorption. The latter is frequently associated with E_s and specially with pulsating types of aurora, but not always.

We think that it would be worth while to develop a technique which could tell us more precisely where in the ionosphere the excessive absorption takes place and the magnitude of the extra ionization. This might help us in understanding the nature of the particles or radiation responsible. In order to do that we will be forced to concentrate on minor disturbances when conditions are not too complicated. And further, we will have to increase the sensitivity of our equipment, partly by choosing sites for our receivers where the noise level is low.

References

[1] Agy, V. *J. geophys. Res.* Vol. 59, p. 267, 1954
[2] Findlay, J. W. *J. atmos. terr. Phys.* Vol. 1, p. 353, 1951
[3] Fejer, J. A. *J. atmos. terr. Phys.* Vol. 7, p. 322, 1955
[4] Davies, K. and Hagg, F. L. *J. atmos. terr. Phys.* Vol. 6, p. 18, 1955
[5] Meek, J. H. *Defence Res. Board, RPL Rep.* No. 5, 1950
[6] Meek, J. H. *Defence Res. Board, RPL Rep.* No. 9, 1951
[7] Little, C. G. *Proc. Inst. radio Engrs., N.Y.* Vol. 42, p. 1200, 1954
[8] Wells, H. W. *Terr. Mag.* Vol. 52, p. 315, 1947
[9] Meek, J. H. *J. geophys. Res.* Vol. 58, p. 445, 1953
[10] Meek, J. H. *J. geophys. Res.* Vol. 59, p. 87, 1954
[11] Heppner, J. P., Byrne, E. C. and Belon, A. E. *J. geophys. Res.* Vol. 57 p. 121, 1952

Suppl.
art.II
1956

FORECASTING OF DISTURBED HF COMMUNICATION CONDITIONS

R. C. Moore

Chief Forecaster, North Atlantic Radio Warning Service,
National Bureau of Standards, Fort Belvoir, Virginia

The National Bureau of Standards operates radio forecasting centers at Fort Belvoir, Virginia, and Anchorage, Alaska, for the North Atlantic and North Pacific radio paths, respectively. Four types of forecast are issued: long term forecasts, for the periods 1–7 and 8–25 days later; medium term, for the next 24 hours; and short term, for the next 6 hours (Fort Belvoir) or 9 hours (Anchorage). Predictions are based upon the 27-day recurrence tendency in solar-terrestrial effects, ionospheric responses to specific types of solar activity, the normal persistence tendency of ionospheric conditions, and detailed knowledge of current geomagnetic, ionospheric, and radio transmission conditions. Geomagnetic responses to solar phenomena are discussed in some detail

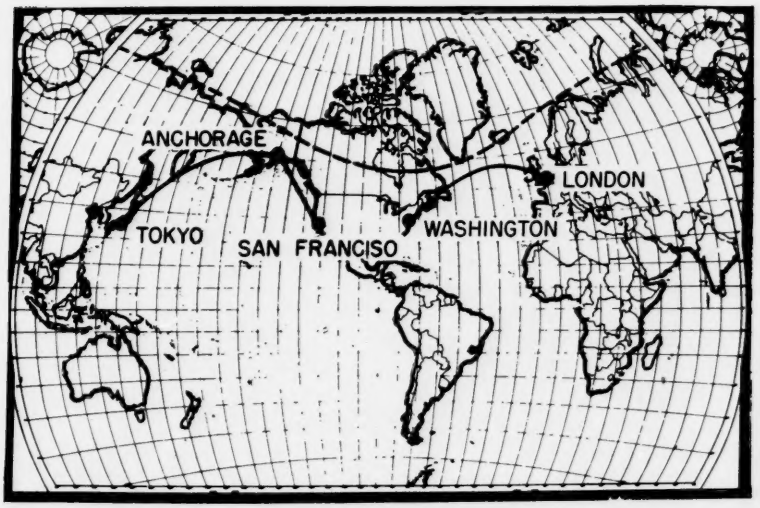

Fig. 1. Transmission paths near the auroral zone

1. Introduction

When conditions in the earth's magnetic field and the ionosphere are normal a radio message originating at a transmitting site is reflected by the ionosphere and detected at a receiving site many miles away with comparative ease, if normal technical precautions are taken. Sometimes, however, the

magnetic field and ionosphere become disturbed. Under these conditions a signal may weaken, fade rapidly, or even be lost altogether, depending upon the severity of the disturbance. It is the responsibility of radio forecasting centers to predict these disturbances and notify message centers as long in advance of each disturbance as possible, so that important traffic may be disposed of before the onset of the disturbance.

2. NBS Radio Prediction Services

The Central Radio Propagation Laboratory of the National Bureau of Standards operates two radio forecasting centers: the North Atlantic Radio Warning Service (NARWS) at Fort Belvoir, Virginia (near Washington, D.C.); and the North Pacific Radio Warning Service (NPRWS) at Anchorage, Alaska. NARWS is situated at one terminus of a typical North Atlantic radio path, that from Washington to Paris. Communication over this path is subject to difficulties, because it passes through the auroral zone. NPRWS, on the other hand, is located approximately at the midpoint of the path between Seattle and Tokyo, and is quite near the auroral zone. The North Pacific path consists of two segments, Seattle to Anchorage and Anchorage to Tokyo.

Path considerations are important, for radio quality forecasting is normally path-dependent. The methods used in making predictions at one center are very similar to those used at another, but familiarity with the peculiarities of a particular path is necessary in order to employ the methods effectively. Radio forecasting is also time-dependent. Techniques used to predict radio quality 25 days in advance will differ from those used to make forecasts for the next 6 hours.

The centers at Anchorage and Fort Belvoir prepare *long-term forecasts* for the periods 1 to 7 and 8 to 25 days in advance. These forecasts are based principally upon specific sun-earth relationships and the 27-day recurrence tendency in geomagnetic and ionospheric conditions; persistence and current conditions are of only minor importance in the long-term forecasts. These centers also prepare daily a *medium-term forecast* for the two 12-hour periods comprising roughly the next night and following day at Fort Belvoir, and the next day and following night at Anchorage. The medium-term forecast is based chiefly on analyses of current ionospheric conditions and on the persistence tendency of the established conditions; here, sun-earth relationships and 27-day recurrence are of minor importance. In fact, the medium-term forecast can be thought of as correcting the 1–7 day forecast, just as the latter corrects the 8–25 day prediction. The last variety of forecast is the *short-term prediction*, for the next 6 hours at Fort Belvoir or the next 9 at Anchorage. These forecasts are broadcast through WWV and WWVH respectively. They also are based on the persistence tendency, allowing for normal diurnal variations, and on current geomagentic, ionospheric, and radio conditions.

The principal forecasts, then, are: the general forecast, 8–25 days in advance; the advance forecast, 1–7 days; the medium-term, 1 day; and the short-term, 6 or 9 hours in advance. The forecasts are based principally on the 27-day recurrence tendency, sun-earth relationships, the persistence tendency, and current conditions.

Supp
Part.
195

Table 1

	General 8–25 days	*Advance 1–7 days*	*Medium one day*	*Short 6–9 hours*
Recurrence	major	major	minor	—
Relationships	—	major	minor	—
Persistence	—	minor	major	major
Conditions	—	minor	major	major

Recurrence — 27-day recurrence

Relationships — sun-earth relationships

Conditions — current magnetic, ionospheric and radio conditions

3. Bases of Forecasting Methods

3.1. *27-day Recurrence*

Perhaps the most reliable aid in long-term forecasting is 27-day recurrence. During a certain portion of the approximately 11-year sun-spot cycle, from about three years before minimum to a few months after, geomagnetic and ionospheric disturbances tend strongly to recur at intervals of about 27 days. This interval corresponds, of course, to the period of one solar rotation as seen from the earth. A recurrent series of storms may last from a few months to several years. The forecaster's main concern is with the time-intensity pattern of the individual storms of a series, especially the profile at the beginning and the duration. Within the pattern, the storms of a series behave in a fairly consistent way. Recurrent disturbances are never of great-storm severity; but they make up in duration for their lack of intensity, the average duration of such storms being about 5 days. Another characteristic of this type of disturbance is the absence of any correlation with localized solar phenomena, particularly those that usually are associated with terrestrial effects. The sources on the sun of the recurrent storms have not been definitely identified; they can perhaps be envisioned as centers of activity just below the visible surface of the sun.

3.2. *Specific solar-terrestrial relationships*

The other aid in long-term forecasting is a group of established relationships between certain transient solar phenomena and their consequent terrestrial effects. Ultraviolet radiation from the sun forms the ionosphere by ionizing the atmospheric gases. Under normal conditions, the ion densities in the various layers of the ionosphere stay within certain limits; these limits vary with the time of day, the seasons, and the phase of the sunspot cycle. From time to time, however, the equilibrium of the ionosphere is disturbed or even destroyed by excessive ultraviolet radiation and charged particles emitted from regions of activity on the sun. The forecaster's task is to make an overall evaluation of the regional activity; he is then able to predict an ionospheric disturbance on the basis of that evaluation and the expected speeds and directions of the particle streams. To do this, he must be aware of the various phenomena involved in solar activity and of their relations to terrestrial events.

Contrary to a common belief, sunspots are not the most directly important of these phenomena. A *sunspot* is a relatively cool area on the sun's apparent

surface, or photosphere. It is a relatively stable object, and can be observed easily in white light. These characteristics are undoubtedly responsible for the popularity of sunspots as indices of solar activity.

It is in the chromosphere, a thin layer of the solar atmosphere directly above the photosphere, that most activity of interest to the forecaster is observed. The *plage*, a region that is abnormally bright in the wavelengths of hydrogen, calcium, and some other elements, is a more basic index of activity than the sunspot. Sunspots always are attended by plages, but plages frequently exist without sunspots. A plage may persist for many solar rotations; it is usually visible before the accompanying sunspot group appears, and it remains long after the spots have disappeared.

In plage areas occur perhaps the most interesting of the short-period solar phenomena, the sudden brightenings called *flares*. A flare is primarily an intense emission of light in the characteristic spectral lines of the solar gases; but it may also involve the ejection of material from the sun. It rises to maximum brightness in a few minutes at most, and declines more slowly; in extreme cases it may take several hours to subside completely. Flares are best observed in the spectral line of H-alpha (6563 A.).

Other phenomena indicative of activity on the sun are:

(*a*) *Surges.*—These are streams of material ejected high into the solar corona and even into space. Of special interest are the surges that are sometimes ejected from flares, moving at speeds of the order of 500 km/sec and appearing dark in projection against the photosphere. Material from these surges is believed to escape into interplanetary space, often reaching the earth.

(*b*) *Prominences.*— This term applies to any of the cloudlike bodies of glowing gas that appear above the chromosphere: they appear as dark filaments in projection against the photosphere. Prominences can be observed only in H-alpha or other monochromatic light.

(*c*) *Emission corona.*— The solar gas above the chromosphere emits line spectra in the wave-lengths of highly-ionized iron, nickel, and other elements. This emission is very faint, and can be observed only with a special coronagraph telescope at high altitude, or during total eclipse. Enhancement of the normal coronal emissions is an indication of an active region.

(*d*) *Radio noise regions.*— The development of radio astronomy has added another and perhaps the most important technique for evaluating the overall activity of a solar region. The intensity of radio emission from a region may prove to be the most reliable basis for discriminating between relatively active and inactive regions, in cases where no visible distinction is present.

Most studies of solar-terrestrial relations have been based on geomagnetic records as the terrestrial parameter. Geomagnetic disturbances are easy to observe, and afford the oldest detailed records of solar-related phenomena. Since they also are closely correlated with ionospheric disturbances, solar-geomagnetic relationships can be used directly in predicting ionospheric conditions. For that reason, it may be well to summarize the characteristics of geomagnetic disturbances and their known relations to solar activity.

The recurrent storms have been discussed; their outstanding characteristic is the absence of direct relation to the active regions on the sun, though they undoubtedly are of solar origin. The magnetic storms initiated by active

regions are typically briefer but often more intense than the recurrent storms. As would be expected, their frequency and severity are correlated with the sunspot cycle. Both kinds of storms are most intense in the auroral zones, and both encircle the earth; whereas a disturbance induced by radiation is necessarily confined to the sunlit hemisphere. Storms attributable to flares occur a day or two later. All of these peculiarities indicate that geomagnetic storms, and the concurrent auroral activity, are caused by streams of charged particles emanating from the sun at speeds of a few thousand km/sec.

Recurrent geomagnetic activity reaches maxima near the dates of the equinoxes; but these are also near the dates on which the heliographic latitude of the earth reaches its maximum of 7·2°, corresponding roughly to the zone of sunspots and related activity late in the cycle.

A number of specific correlations of geomagnetic conditions with solar activity have been discovered. These are necessarily statistical relations, and they are not of uniform reliability. Those listed below, however, are supported by excellent statistical evidence.

(*a*) *Correlations with sunspots.*— Passage of large sunspots across the central meridian of the sun (CMP) tends to be followed by a rise in geomagnetic activity and an increase in the frequency of non-recurrent storms, with a lag of 2 to 4 days; but a similar *negative* correlation is obtained with respect to recurrent storms.

CMP of a pair of similar spot groups, located in opposite hemispheres at about the same longitude and equidistant from the equator, tends to be followed in 1 to 3 days by a decrease in geomagnetic activity.

(*b*) *Correlations with sunspots and 158 Mc radio noise.*— The situations mentioned under (*a*) above are modified by the radio emission characteristics of individual spot groups. The statistical rise in geomagnetic activity following CMP of large spots seems to be attributable to the noisy spot groups alone. CMP of quiet spots is followed by a decrease in geomagnetic activity; and this effect is strengthened when a pair of quiet spots, located north and south of the equator, crosses the meridian. Even if one of such a pair is noisy, its geomagnetic effect is diminished by the presence of the paired quiet spot.

(*c*) *Correlations with flares.*— Crochets (brief minor disturbances) occur only concurrently with flares, and only on the sunlit hemisphere. They evidently are induced by electromagnetic radiation.

Very large flares (class 3+) tend to be followed by geomagnetic storms, often great storms, within 1 to 2 days, particularly if the flare occurs within 45° of the center of the solar disk. The converse relation holds also: i.e., great storms tend to be preceded by large flares near the center of the disk. Flares of classes 2 to 3 similarly precede moderate geomagnetic disturbances. Smaller flares are usually ineffective; but flares that emit 200 Mc radio noise outbursts tend to be followed by geomagnetic disturbances 2 to 4 days later, regardless of class.

(*d*) *Correlations with the emission corona.*— Since the corona can be observed only at the limb of the sun, coronal correlations are necessarily stated in terms of east-limb passage (ELP) of coronal features.

ELP of regions of enhanced coronal emission in the green line (5303A.) tends to be followed by a minimum of geomagnetic activity 10 days later (CMP plus 3). This effect is strengthened if both the green and the red

uppl.
rt.II
1956

(6374 A.) lines are enhanced. This relation is based on studies during the decline of the spot cycle only; presumably it expresses again the exclusion of recurrent geomagnetic storms during CMP of active regions, with which bright coronal emissions are associated.

ELP of regions of very weak green-line emission tend to be followed by a rise in geomagnetic activity 9 days later (CMP plus 2). Most of this rise in activity is attributable to recurrent storms, which therefore appear to be associated with very weak coronal emission. Both this and the preceding relation tend to be more pronounced if the coronal regions in question are on the same side of the solar equator as is the earth.

Some regions of bright green-line emission depart from the rule stated above in that their CMP tends to precede a rise in geomagnetic activity, particularly in the form of non-recurrent sudden-commencement storms. These regions characteristically include emission in the yellow line at 5694 A., which occurs only sporadically in connection with flares.

In attempting to evaluate these correlations between solar activity and terrestrial magnetic conditions, one should bear in mind that our understanding of the interrelations among solar phenomena is far from complete. Consequently, what appear to be a diverse lot of parameters probably will be reduced and simplified in terms of more fundamental relationships, and some apparently contradictory tendencies will be resolved as new criteria of solar activity are developed.

Sup
Part
19

3.3. *Persistence*

Just as 27-day recurrence is the most reliable long-term forecasting aid, so persistence is the most reliable basis for the short-term forecast. Persistence is a very valuable principle for all types of forecasting. Basically, the probability is excellent that conditions tomorrow will be very much like they are today. Unfortunately, persistence must not be depended upon too much, for the value of forecasting lies mainly in the prediction of those occasions when the persistence tendency fails. So long as conditions remain stable, persistence is a satisfactory aid; but when conditions change abruptly — when today is entirely different from yesterday — then persistence is of no help at all. In practice, therefore, the forecaster must be cautious in his use of the persistence principle, relying upon it only when there is absolutely no specific reason to expect a change in conditions.

3.4. *Current conditions*

To predict short-term changes in radio propagation conditions, the forecaster brings to bear a final forecasting principle, the analysis of current geomagnetic, ionospheric, and radio quality indices.

The three components of the earth's magnetic field are readily measured at any location with a device called a magnetograph. Normally, the field will vary only slightly from a defined base line. When the field becomes disturbed, each recorded trace begins to drift to one side or the other of the base line. The amount of movement in a 3-hour period is measured in gammas and reduced to a standard index K. If the departure from the base line has been rapid at the beginning of the disturbance, the phenomenon is called a sudden

commencement. This type of disturbance is closely related to the passage of active sunspot regions.

The heights and reflecting characteristics of the various layers in the ionosphere can be measured by means of a recorder called an ionosonde. A signal that sweeps continuously in frequency from 1 to 25 Mc is transmitted vertically, and the echoes that are reflected back down to the receiver give the

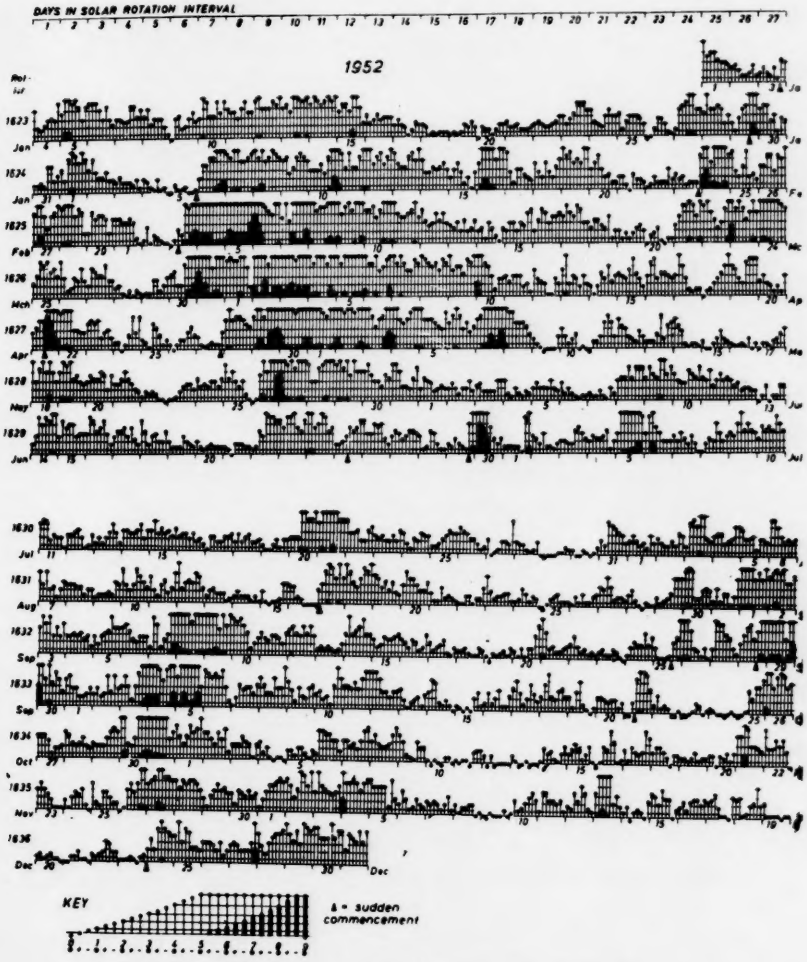

Fig. 2. Planetary magnetic three-hour-range indices, Kp, 1952

virtual height and critical frequency for each ionospheric layer. The characteristics of these layers, the *E*, *F*1 and *F*2, normally vary throughout the day, but in a fairly consistent manner. It is possible to determine roughly the maximum usable frequency (MUF) and lowest usable frequency (LUF) for a radio path from the readings of an ionosonde located near the midpoint of the

Suppl.
art.II
1956

path. When the ionosphere becomes disturbed, as during an ionospheric storm, the usable frequency range between the MUF and the LUF is reduced: under extreme conditions it may be completely wiped out. Another ionospheric anomaly, not directly related to the ionospheric storm, is the sudden ionospheric disturbance (SID). This condition is concurrent with the appearance of a strong flare on the sun and affects the entire sunlit hemisphere of the earth. Intense ultraviolet radiation from the flare is believed to intensify the ionospheric *D*-layer (below the *E* and *F*-layers) and short wave

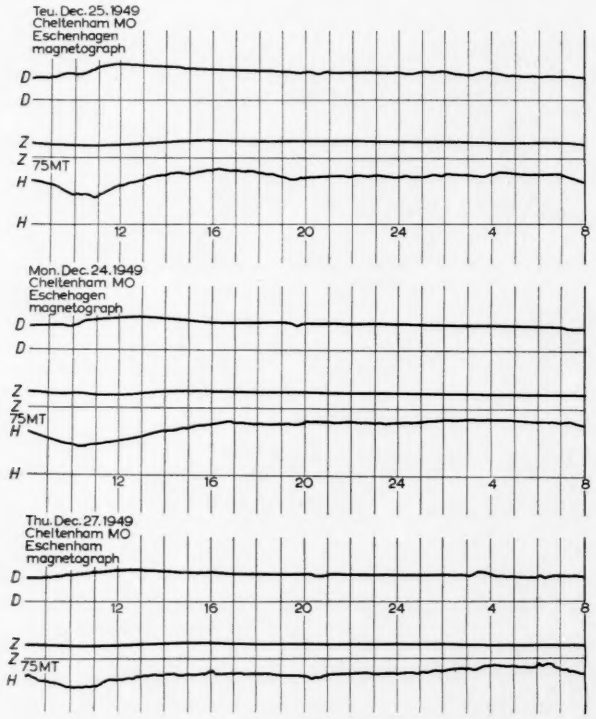

Fig. 6

signals are strongly absorbed. The resulting fadeout may persist from a few minutes to several hours, depending upon the duration of the initiating flare and the occurrence of a succession of flares.

The third component of current conditions to be considered in forecasting is the current performance of radio circuits. Unlike the phenomena we have already mentioned, radio quality is not measured. It is estimated qualitatively and this lack of an objective quality index introduces difficulties. When the Weather Bureau predicts snow, it is no problem to determine the basic accuracy of the forecast. It is very difficult, however, to determine the accuracy of an estimate of radio quality, for no truly objective technique exists for determining the quality of radio propagation. The type of transmission (voice,

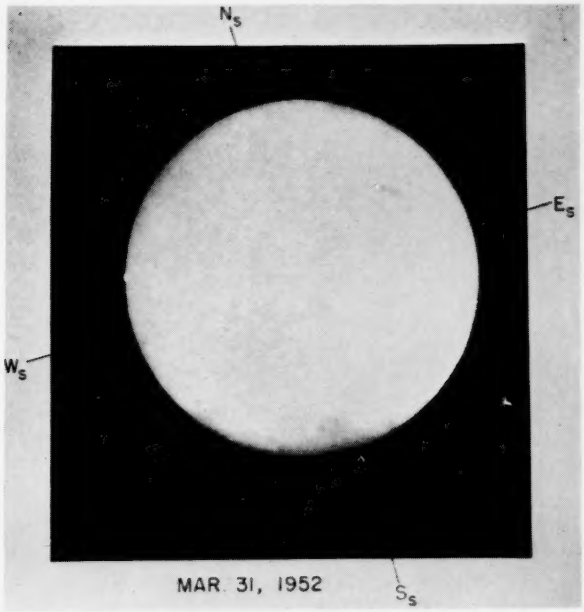

Fig. 3

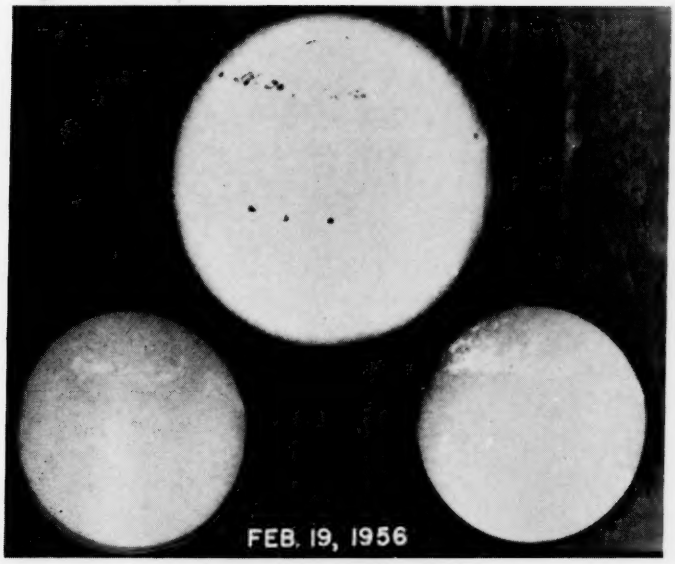

Fig. 4

Suppl.
art.II
1956

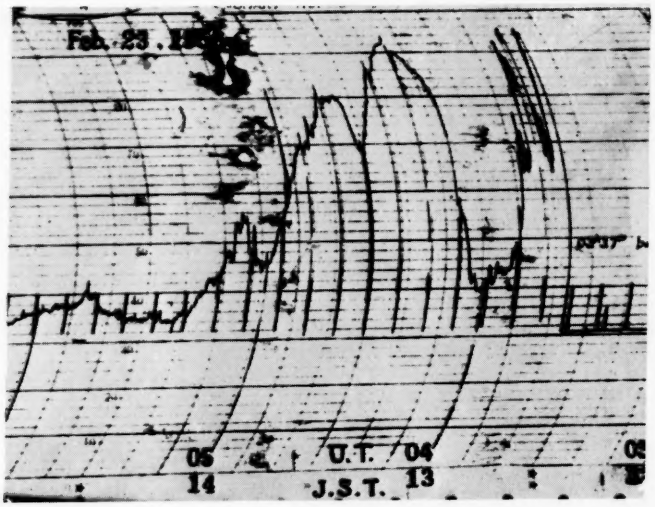

Fig. 5

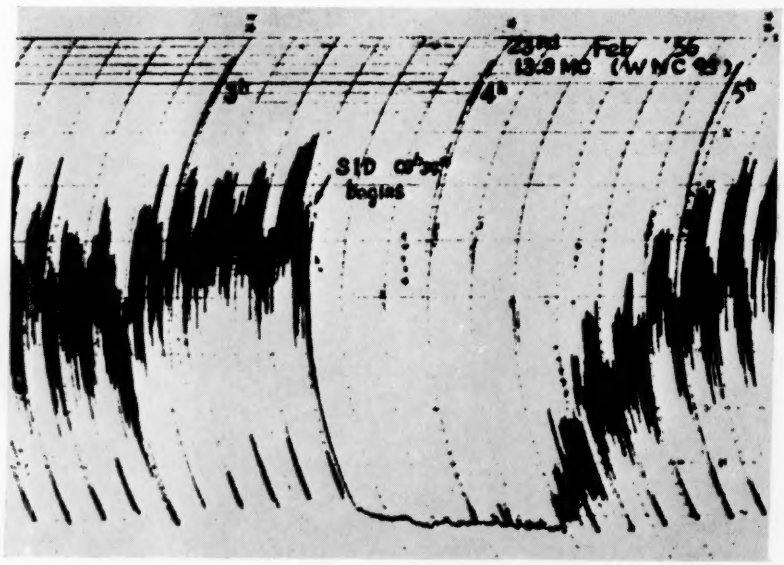

Fig. 8

CW, teletype, MUX, SSB), the transmitter power, the amount of interference (both man-made and natural), the frequency utilized, and even the experience and ability of the operator — all of these are significant factors that must be taken into account in determining the quality of radio reception.

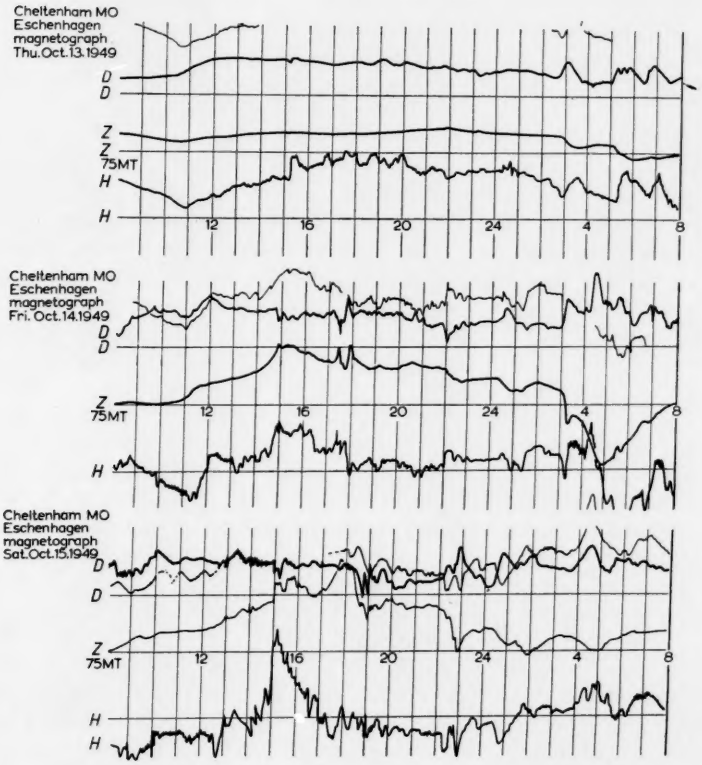

Fig. 7

Further, it is quite unsatisfactory to continue to forecast radio quality with no knowledge of the accuracy of past predictions. An index of quality is needed, and certain assumptions must be made for the sake of establishing it. The CRPL *F*-Series defines a radio quality index as a measure of the efficiency of a medium-powered radio circuit operated under ideal conditions in all respects, except for the variable effect of the ionosphere on the propagation of the signal. In practice, a normal distribution of radio quality values is assumed, with mean and standard deviation depending upon the path, time of day, and season. Outside reports of quality can then be converted to the CRPL radio quality scale by relating them to the assumed distribution. The properly weighted converted average of all values reported then becomes the quality figure.

4. Operating Procedures During Ionospheric Disturbances

Interference with communications by ionospheric disturbances can be minimized by certain operating precautions. When an SID occurs, there are two things that may be done and one that should not be done. Since the fadeout accompanying the SID is caused by absorption in the ionosphere, the lower frequencies are affected first and most severely. It is practical, therefore, to change to a higher transmission frequency, because the high frequencies will be the last to fade out and the first to recover. If the SID takes out the higher frequencies also, the only alternative is to wait until the fadeout ends. The SID will probably be over in a matter of minutes, or at most several hours. The operator should resist the temptation to become involved in a detailed check of equipment.

The ionospheric storm affects transmissions in a more complex manner than does the SID. Absorption increases, but the maximum usable frequency at the same time *decreases*. It is, therefore, advantageous to reduce frequency and increase power in an attempt to get a readable signal through the absorption. The effects of an ionospheric storm are most pronounced in the auroral zone, so that relaying messages away from that zone will improve the chances for their reception. These disturbances, however, spread toward the equator as the severity of the storm increases. Under extreme conditions, even transmissions via the "southern route" will be affected.

In the long run, the effects of an ionospheric disturbance can be best minimized by supplying the forecasting centers promptly with the solar ionospheric, and geogmagnetic data that they need to make reliable forecasts. Message centers will then be warned in time to make traffic adjustments and be ready for the disturbance when it begins.

5. Special Responsibilities of the Fort Belvoir Center in the IGY Program

The CRPL Radio Warning Service, Box 178, Fort Belvoir, Virginia, U.S.A., has been designated as the world warning agency for the International Geophysical Year program. In this capacity, it will have the final responsibility for issuing notifications of Alerts and Special World Intervals (SWI). An SWI will be declared on 8 hours notice whenever the prediction data indicate that a major solar-terrestrial disturbance is to be expected. An Alert will warn of a probable SWI several days in advance. Notifications of Alerts and SWI will be transmitted over the networks of the World Meteorological Organization. These transmissions will be supplemented by regular broadcasts from WWV and probably other regular broadcast stations. Messages of pertinent solar and geophysical data will be made available to scientists cooperating in the IGY endeavor.

In announcing Alerts and designating SWI, the CRPL center will invite the participation of all other radio or geomagnetic forecasting centers. The regular predictions and special recommendations from all centers will be taken into account in making decisions on designations.

Supp
Part.
195

DISCUSSION

Discussion on Friday, July 6th, on: *Prognostic Techniques of the Ionosphere with special reference to Arctic Regions.*

SCOTT: I should first of all say that I think Dr. Meek is much too modest in ascribing his prediction service to me because quite a number of the essential factors incorporated in the prediction service was actually worked out by Dr. Meek. I also would like to make the point that no-one should underestimate the amount of work that goes into a prediction system of this sort. It is true that we eliminate having to repeat the work involved in making charts in successive months. We do it once and for all, at least up to a point. But it does mean that a great deal of work has to be done initially. We have to produce charts for each of the 24 hours for each month, and this for each of the 12 months, and for zero sunspot number and another sunspot number (100 is what we use). We have to make similar charts for checking purposes at intermediate sunspot numbers. We have to make certain that all these charts are self-consistent one with the other diurnally and also consistent month by month. This involves a tremendous amount of smoothing and comparison, which is just plain work. I just want to point out that there is a tremendous amount of initial work.

Another point I would like to make is that the predictions we make are essentially for points rather than for the average zones. We make predictions for every 5° of latitude, and depending on the latitude, for different separations of longitude. This allows us to include any peculiarities, eccentricities due to the auroral zone not being concentric around the geographical pole. And finally, I would like to make the point that while we claim that this is a prediction service once and for all, of course this has to be taken with a grain of salt and all these linear empirical relationships have to be continually checked and revised as more data becomes available.

One other point I should make is with reference to the oblique incidence. We are now going ahead with installing automatic oblique incidence sweep recorders that will allow us to measure directly what occurs from point to point between our ionospheric stations. These will, it is planned, be installed at all our ionospheric stations.

LIED: I would like just to ask Mr. Meek — when you draw up the straight lines, do you then base that on median values of the critical frequencies or — you said the predictions were made for the quiet conditions. But are you happy if you are using median values that they do represent quiet conditions?

MEEK: This is the most logical way of working it out. We have to take account of the fact that in the polar regions there are many more disturbed days and I will not say that we use the medians indiscriminately. We not only look

at the data from a very subjective point of view, we have also found it necessary to eliminate data from some stations in order to get a consistent picture. But we do use the medians as a basis for predictions.

LIED: I have another question and that is the difference observed in the linear relationship when the sunspot number is increasing and decreasing. Have I understood it correctly that you base it on the universal connection between them and you do not discriminate between increasing and decreasing sunspot number? I know that in the question of the *E*-layer, for example, the British attitude is to discriminate between increasing and decreasing, and I would just like to hear your opinion on that.

MEEK: It is not necessary in the *F*-region at least, because there are other variations which are much greater. It is not necessary to distinguish between the two and the difference between the two is not consistent in different stations.

SCOTT: I would like to mention that we would like to add these finer points. But after all, what we are after is a simple prediction service that works for average conditions in these regions. Actual checks against the oblique incidence records do indicate that the prediction service we have is a little more accurate for our regions than the world-wide prediction service.

MAUNDER: I think that in England quite a number of us who are interested in the subject of practical prediction, have never been satisfied of the real utility of the linear empirical relationship to the extent of feeling that it was worth while putting in the enormous amount of work required to exploit it. It is true that you get finally, by doing so, a simple system of obtaining a current monthly prediction, but only at the expense of the work done beforehand. With regard to accuracy, I cannot say that I have ever tried any extensive, continued checks on the linear empirical relationship. But on the occasions when I have done so, I have never been impressed by the plot of monthly median values against the running average sunspot numbers centred on the same month. Certainly the plot for the running average ionospheric value and the running average sunspot number is very good, but that of course is not what we want. The element of error which comes in due to the scatter of the points from the "best fitting" straight line may contribute largely to the total prediction error. On the other hand, it is difficult to state a value of total predictional error which cannot be tolerated for practical purposes. For military or commercial purposes use may be made of a prediction even if it is quite largely wrong, providing that it is handed out to the user with reservations, since he will probably supplement it by his own operating experience, regarding the prediction as a guide. From that point of view, one can tolerate quite a lot of error.

There remain, of course, the other errors which occur inevitably in this system even if one admits the linear empirical relationship. I was hoping to find that some new element had been injected into this prediction over the polar region. It is one of the wide-open spaces of the world, surrounded by a ring of stations. It seems to me that in respect of interpolation over the polar region we probably have not improved matters very much. We have still much the same difficulty in getting a set of charts successively coherent in time. This problem does not apply of course only to the polar regions; it is the

problem we have of constructing charts for the whole world. One has simultaneous sets of some 70 values each and one is faced with the task of drawing charts which satisfy two conditions, namely, that they must read back to the original 70 values one started with at each given time and that any cross-section curve obtained from them must be reasonably smooth. I suppose one could put any artistically inclined person down before the values and within half an hour he would produce a tolerable chart for a given time of day. There would be a possible infinity of such charts, but he would produce one which satisfied the conditions. Now that actually is not good enough in the present case because we must have coherence in time, both daily time and seasonal time, and the difficulty here seems to be that if the work is performed by different people, they have different subjective ways of shaping the curves, and even if one person continues the work for years, he varies from chart to chart. I feel that one of the ways of getting over this difficulty in the future might be to produce some sort of set of interpolation factors for each point of the world. One might put whatever subjective elements were required into the selection of the controlling stations and once that had been done, the remainder of the work could be performed by machines, except for the final drawing. The series of such charts would contain the subjective elements in exactly the same way and therefore would be relatively comparable. They would not be necessarily the right set of charts, but, given a plausible initial hypothesis, very possibly they would be as good as any other set of charts. When the thing had been put on machines, you would probably get a chart produced extremely quickly. Then you would stand a chance of perceiving the progress of abnormalities, ionospheric storms, by a departure from typical pattern, as this departure itself could be expected to be reasonably free from subjective error.

Now, to come back to the paper that we heard this morning, the only other inquiry I would make is with reference to oblique incidence MUF and the use of the conversion nomogram which has been referred to. I believe it is similar to the CRPL nomogram, but how in fact has it been altered, may I ask, Mr. Chairman?

SCOTT: It is essentially the same. Constructionally it is different, but essentially it is the same. The data involved are the same.

MAUNDER: I know the nomogram in that case and this has always bothered me and I would like to refer to it here. I feel that quite apart from the basic prediction of the *F*-layer itself, we are also very weak on the conversion of the vertical incidence data, (even if it is observed) to oblique results, and I have been particularly puzzled about this CRPL conversion nomogram — in the old days very much more puzzled until I knew where it came from. Quite a lot of work was done in the UK by Appleton and Beynon and a set of MUF factor curves in terms of height of layers was produced. It did not turn out to be the simple mathematical problem that it appeared to be, mainly on account of the curvature of the earth, but finally a very comprehensive set of curves was worked out which we still use in the UK. But the CRPL nomogram has also been widely used on account of its simplicity. It merely needs a straight edge between two vertical scales and the answer is read off in the middle. Thus I was very interested in the earlier days to find out whether we could

uppl.
rt.II
1956

do the same thing for the Appleton-Beynon factors. I found we could, but the straight lines in the centre were not straight — they were curves — and also came down below the horizontal axis so that the nomogram became a practical impossibility. But in the course of doing that, I had to find out what the CRPL nomogram was, and of course it turned out that it came from the master MUF factor curve which was produced by Newbern Smith, the values being defined by the ratio of MUF for the distance concerned to the MUF for 2000 miles — not the critical frequency. This curve was obtained, empirically I believe, from the observed vertical incidence records by scaling. All Newbern Smith did was essentially to take the master MUF curve and expand it into a series of curves by a linear interpretation which made the nomogram work. In other words, the thing was probably done backwards. Now in order to make a comparison, I redrew the CRPL nomogram in the form of curves I was used to, and compared them and Appleton and Beynon's curves. I found that the shape was entirely different. Now it seems to me very puzzling that after Appleton and Beynon (and many other people) did so much work to try to get these MUF factors right, the CRPL nomogram should give values which are usually different, sometimes by as much as 25 per cent. If we bring in errors of the order of 25 per cent, why do we start worrying about the small errors? I feel that the answer is probably in the oblique incidence experiments, and that, for the moment, there is not very much to choose between these two methods.

MEEK: May I make one comment? Mr. Maunder was mentioning the subject of working out these charts. I would just like to point out that there is an improvement that we have made. It is true our charts are subjective, but they are made once and for all and they only change when we get more ionospheric data, about every month.

MAUNDER: That is one of my real objections — that it makes the predicted data relatively inflexible because before they can be changed you have to do a lot of work again.

MEEK: Well, that may just be an advantage actually.

MAUNDER: Yes.

SCOTT: I would just like to make one correction here. Actually, if you find new data referring to some area or some town or both, you can change the chart — it is a loose-leaf system — and you can change the numbers in the system corresponding without changing the whole thing.

I would like to agree with you that the answer is oblique incidence direction measurements. I do not think much actually of bothering with making refinements to average monthly predictions. I think the amount of work involved for the gain to be obtained for practical communication purposes is absolutely marginal.

AGY: If you know exactly where the transmission curves come from and if you know exactly where the nomograms come from, you know more than most of us at CRPL and perhaps more than anybody but Dr. Smith.

MAUNDER: There is one question, Mr. Chairman, I should like to ask: do you in Canada check the circuit data against predictions or what I might call quasi-observed data for the circuit? The point is, supposing one goes back

to last June, do you compare the circuit behaviour with the circuit predictions for last June or do you try to work out a chart based on observed values for the month and obtain your values for the circuit control points from that chart?

SCOTT: I am not altogether sure that I understand what you are asking, but what we do is, with our oblique incidence equipment that is operating continuously, to measure the MUF as seen on the record and check them against what you would obtain from the prediction.

MAUNDER: Well that is exactly what I hoped you would do. In other words you are doing your checking in two ways, you are checking the accuracy of the basic ionospheric prediction and the application of that thing?

SCOTT: Yes.

MAUNDER: I feel that often one tries to check on the accuracy of the predictions by just trying to estimate the over-all prediction error, whereas in actual fact the over-all prediction error is the error involved in the basic prediction of the ionosphere followed by the error involved in the application. You may quite often, obviously, get a small over-all prediction error when the two sets of errors are in opposite directions. For some years it has seemed that the over-all prediction error remained within certain limits which have demonstrated the practical usefulness of prediction without indicating the sources of error. It seems to me that the time has now arrived when such analysis should always be a procedure of two stages, the first where the basic ionospheric prediction is checked against what it professes to represent, the observed ionosphere, the second being a check on the radio wave propagation hypothesis assumed in the MUF prediction. The latter can only be done by employing observed or quasi-observed values, instead of predicted ones, at the control points required by the hypothesis.

uppl.
rt.II
1956

Sup
Part
19

SECTION III

Suppl.
art.II
1956

Supp
Part.
195

THE SPECTRUM OF THE ELECTRON DENSITY FLUCTUATIONS IN THE IONOSPHERE

ROGER M. GALLET
National Bureau of Standards, Boulder, Colorado

uppl.
rt.II
1956

SUMMARY OF THE COMMUNICATION

(1) In a recent publication[1] a discussion was given of the mechanisms responsible for the electronic density fluctuations in a turbulent ionospheric layer. It was shown that fluctuations arise from the vertical *transport* of air-blobs: (*a*) in the presence of a non-adiabatic temperature gradient which results in inhomogeneities of temperature and consequent density fluctuations, and (*b*) in the presence of vertical gradients of the mean electronic density.

However, in the applications to the problems of radio-scattering, phase-fluctuations, and angular deviations, a detailed knowledge of the "spectrum" of these fluctuations is required. The spectrum is the mean square value of the fluctuation of density as a function of the size of the turbulent eddy. A quite detailed and satisfactory theory of the spectrum based upon the mechanisms mentioned above has been obtained during this last year. The general relationships between the unidimensional and the spatial spectrum, the physical factors limiting the amplitude at the largest dimensions and producing the cut-off at the smallest dimensions, are discussed. Some of the causes of the turbulence, such as the shear-stresses due to the gradients of horizontal winds, are briefly discussed.

There have been attempts to obtain the density fluctuation spectrum from the spectrum of the *kinetic energy* of the turbulent eddies in an homogeneous atmosphere, using the Kolmogoroff expression (Ref. 1, Eq. 34) for this spectrum. It has been shown[1] that the fluctuations of density are practically independent of the turbulent kinetic energy, and that the use of this spectrum is unjustified.

(2) A detailed analysis will be published elsewhere, but the essential results can be condensed as follows.

The general expression for the spectrum of the fluctuations of a scalar quantity Q, such as density or temperature, in the above mentioned conditions is:

$$G_1(K_1) = \frac{2^3\pi^2}{3} (\text{grad } Q)^2 \frac{1}{K_0^3} \frac{1}{[1+(K_1/K_0)^2]^{3/2}} \times \frac{1}{[1+(K_1/K_s)^4]^{4/3}} \quad \ldots . (1)$$

$G_1(K_1)$ is the square of the amplitude of the wave of wave number K_1 in the Fourier analysis of the fluctuations measured along a specific axis labeled 1. This is the unidimensional spectrum. The wavelength of the Fourier analysis is Λ, variable from infinity to zero.

$K_0 = 2\pi/\Lambda_0$ is the wave number of the large fluctuations having the greatest amplitude. $K_1 = 2\pi/\Lambda$ is the variable wave number along the axis 1. $K_s = 2\pi/\Lambda_s$ is the wave number of the fluctuations marking the transition from the large ones in dynamic equilibrium to the very small ones, which are strongly damped by molecular effects of thermal conductivity, diffusion and viscosity. Λ_s is thus one or two orders of magnitude larger than the molecular mean free path, and measures the limit in the description of the gas on a fine scale as a continuous fluid.

The last factor expresses a cut-off of the principal spectrum given by the preceding term, when we consider fluctuations of very small dimensions. This factor was obtained from the analysis of HEISENBERG and CHANDRASEKHAR.[2]

Λ_0 was expressed in reference (1), Eq. (41), as

$$\Lambda_0 = \text{coeff.} \times \frac{\epsilon^{1/2}}{(\mathrm{d}V/\mathrm{d}h)^{3/2}} \qquad \ldots.(2)$$

where ϵ is the dissipation energy (per unit of volume, of time and of density) of the turbulent motions, and $\mathrm{d}V/\mathrm{d}h$ is the gradient of the wind velocity relative to the height. The numerical coefficient is of the order of unity. In absence of a measurement of ϵ, Λ_0 has to be obtained through direct observations (meteor trails deformations; interpretations of diffraction patterns in the reflection on the ionosphere, or direct turbulence recordings in the troposphere).

If we assume isotropy of the turbulence, then the unidimensional spectrum $G_1(K_1)$ is independent of the direction of the axis 1, and the three dimensional spectrum $G(K)$ is simply related to it by

$$G(K) = -2K\frac{\partial G_1(K)}{\partial K} \qquad \ldots.(3)$$

In $G(K)$, $K = 2\pi/\Lambda$ is the wave-number of all the waves of the spatial Fourier analysis in all directions such as

$$K^2 = K_1^2 + K_2^2 + K_3^2 \qquad \ldots.(4)$$

This relation furnishes for an isotropic turbulence

$$G(K) = 2^4\pi^2 \,(\text{grad } Q)^2 \frac{1}{K_0^3} \frac{(K/K_0)^2}{[1+(K^2/K_0^2)]^{5/2}} \frac{1}{[1+(K/K_s)^4]^{4/3}} \qquad \ldots.(5)$$

The spectra (1) and (5) give the mean square fluctuation by integration:

$$\overline{\Delta_1^2} = \int_0^\infty G_1(K_1)\mathrm{d}K_1 \quad \text{and} \quad \overline{\Delta^2} = \int_0^\infty G(K)\mathrm{d}K \qquad \ldots.(6)$$

for the fluctuations measured respectively along one axis, or in a volume. Thus

$$\overline{\Delta_1^2} = \frac{2^3\pi^2}{3}\frac{1}{K_0^2}(\text{grad } Q)^2 \qquad \ldots.(7)$$

and

$$\overline{\Delta^2} = 2\overline{\Delta_1^2} \qquad \ldots.(8)$$

The significance of (7) is viewed better by writing

$$(\overline{\Delta_1^2})^{1/2} = \sqrt{\tfrac{2}{3}}\Lambda_0 \text{ grad } Q \qquad \ldots.(9)$$

A more precise physical insight in to these results is obtained by considering the mean square gradient between two points in the fluctuation field, separated by the distance $1/K_1 = \Lambda/2\pi$. The mean square fluctuation of Q between these two points is

$$\overline{[\Delta_1(K)]^2} = \int_K^\infty G_1(K_1)\mathrm{d}K_1 \qquad \ldots.(10)$$

Hence the mean square gradient between two points $\Lambda/2\pi$ apart is

$$K_1^2 \int_{K1}^\infty G_1(K_1)\mathrm{d}K_1 \qquad \ldots.(11)$$

For $K_0 < K_1 \ll K_s$, the spectrum $G_1(K_1)$ is essentially equivalent to

$$(2^3\pi^2/3)\ (\text{grad}\ Q)^2 \,.\, K^{-3},$$

thus the mean square gradient from the expression (11) is;

$$\frac{2^2\pi^2}{3}\ (\text{grad}\ Q)^2 \qquad \ldots.(12)$$

which is independent of the distance between the two points. But when the two points are as close or closer than Λ_s, the mean square gradient becomes equal to

$$\frac{2^3\pi^2}{25}\ (\text{grad}\ Q)^2\, K^{-16/3} \qquad \ldots.(13)$$

This shows that the fluctuating gradients of temperature and of density, set up by the aerodynamical motions of the turbulence field acting on a large-scale smooth gradient in the atmosphere, are destroyed rapidly by molecular effects of thermal conductivity, diffusion and viscosity for distances d comparable with the molecular mean free path, proportionally to $d^{8/3}$. For large distances compared to the mean free path, the fluctuating gradients are constant, independent of the distance between the two points of the measurement. Naturally, for very large distances compared to Λ_0, the fluctuating gradients are smoothed out and diminish towards zero, as shown by (11), like d^{-1}.

Because there is a great deal of confusion in the publications about the spectra of temperature and density fluctuations, which are very often assumed to be the same as the Kolmogoroff spectrum, let us contrast the spectrum developed here with Kolmogoroff's one. In the main part the spectrum here discussed is varying in K^{-3}, while the spectrum of Kolmogoroff which describes the energy contained in the *velocity* fluctuations is in $K^{-5/3}$. The gradients of velocities have a completely different behavior, as well as many other consequences.

(3) The scalar quantity Q has to be specified for each physical fluctuation sought.

For the *temperature* variations of air the important factor is the potential temperature, because the fluctuations are essentially produced by the vertical transport of the air parcels by turbulence. Thus in (1) and (5)

$$(\text{grad}\ Q)^2 = \left(\frac{\mathrm{dT}}{\mathrm{d}h} + \Gamma\right)^2 \qquad \ldots(14)$$

Γ is the absolute value of the adiabatic gradient for dry air

$$\Gamma = \left(\frac{\mathrm{dT}}{\mathrm{d}h}\right)_{\text{adia}} = \frac{Mg}{k}\frac{\gamma-1}{\gamma} = 0{\cdot}990 \times 10^{-4} \text{ deg. cm}^{-1}$$

or approximately 1° for 100 m. (See reference (1), Eq. (25).)

For the *density* fluctuations of the dry air resulting from this effect, because the pressure fluctuations are negligible,

$$\Delta\rho = -\frac{\rho}{\mathrm{T}}\Delta\mathrm{T} \qquad \ldots.(15)$$

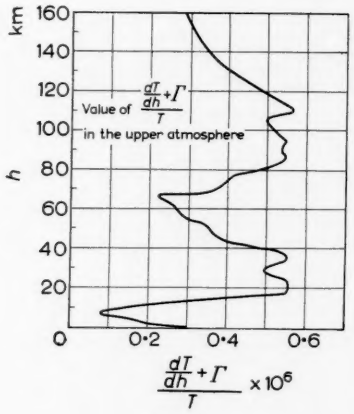

Fig. 1.

Thus, in the spectrum expressions (1) and (5)

$$(\text{grad } Q)^2 = \rho^2\left[\frac{(\mathrm{dT}/\mathrm{d}h)+\Gamma}{\mathrm{T}}\right]^2 = \left(\frac{\rho}{H}\right)^2\left(\frac{\mathrm{d}H}{\mathrm{d}h}+\frac{\gamma-1}{\gamma}\right)^2; \qquad \frac{\gamma-1}{\gamma} = 0{\cdot}285 \qquad \ldots.(16)$$

where $H = kT/Mg$ is the scale height of the atmosphere. (See reference (1), Eq. (26).)

These expressions will apply to the dry air, and particularly in the stratosphere and the medium atmosphere.

For the *density fluctuations* of a minor constituent, entrained by the turbulence of the air, the situation is slightly different. The following considerations apply to the troposphere for the water vapor, to the ozone in the medium atmosphere, and to the electronic density in the ionosphere. For the sake of definiteness let us take the electronic density. If the turbulence were acting on the electronic density alone, the vertical transports will give

$$(\text{grad } Q)^2 = (\mathrm{d}N_e/\mathrm{d}h)^2$$

But the parcel of air containing the electrons is compressed or dilated in this vertical transport according to (16) and thus this effect is added to the preceding. When N_e increases with the height the two effects reinforce each other, but when N_e decreases the two effects tend to cancel. Also even if

dN_e/dh is zero (maximum or minimum of electronic density) there is still electronic density fluctuations following the air ones. Thus, the complete expression becomes

$$(\text{grad } Q)^2 = \left[\frac{dN_e}{dh} + N_e\frac{(dT/dh)+T}{T}\right]^2 \left[\frac{dN_e}{dh} + \frac{N_e}{H}\frac{dH}{dh} + \frac{\gamma-1}{\gamma}\right]^2 \quad \ldots.(17)$$

It is interesting to note that dN_e/dh for a layer resulting from photoionization (Chapman theory, applying quite well to the E-region) is of the order of $N_{max}/2H$. In the E region dH/dh varies from 0·1 to 0·2, and $(\gamma-1)/\gamma = 0{\cdot}285$. Thus, the two terms in the brackets are of the same order of magnitude, but vary in a complementary fashion N_e being maximum when $dN_e/dh = 0$.

Further considerations along these lines are important for the study of the state of the ionosphere. For example, in regard to the factors producing anisotropy it may be shown that the vertical transport will generally give a smaller Λ_0 along the vertical than in the horizontal plane, at least at levels below that at which the magnetic field becomes the controlling factor (when $\omega_H > \nu$). Hence, in the low ionosphere the parcels of air are flattened vertically, although at higher levels they become elongated along the magnetic field. The expressions for the spectrum, naturally become more complicated.

(4) The most important application of these results is, perhaps, to the problems of scattering of electromagnetic waves. The following general relationship between the scattering coefficient $6(\theta X)$ and the density spectrum was obtained one year ago by the author.

$$\sigma(\theta,X) = -\frac{\overline{(\Delta\epsilon/\epsilon)^2}}{\overline{\Delta_1^2}}\frac{\sin^2 X}{8}\frac{k^3}{2\sin\theta/2}\frac{\partial G_1(a)}{\partial a} \quad \ldots.(18)$$

The quantity a has to be substituted for K_1 in the spectrum G_1. ϵ is the dielectric constant, directly proportional to the density, $k = 2\pi/\lambda$ is the wave number in the medium of the incident electromagnetic wave, θ is the scattering angle, X the polarization angle between the electric vector and the direction of scattering. The unidimensional spectrum $G_1(K_1)$ has to be measured along the bisector of the angle formed by the incident beam and the scattering direction, that is to say, generally along the vertical. This fact permits the application of (18) even in presence of anisotropic turbulence.

This expression has already been found very useful in the interpretation of measurements of radio wave scattering in the troposphere made by the National Bureau of Standards.[3] It differs from the expression given by VILLARS and WEISSKOPF[4] (their Eqs. 10 and 34). However, their expression appears to be incorrect because it does not reduce to the well-known expression for isolated scattering clouds, nor to that for atomic and molecular scattering by X-rays, as does equation (18) above.

Direct application of formula (18) to the spectrum (1), specifying $(\text{grad } Q)^2$ by (16) or (17) gives the scattering coefficients for the troposphere, the stratosphere, and the ionosphere. A discussion of these results is to be published elsewhere, but the scattering coefficients are in close agreement with the best measurements for the absolute magnitude, as well as for the dependence on frequency of the incident wave and angle of scattering.

References

[1] Gallet, R. M. "Aerodynamical mechanisms producing electronic density fluctuations in turbulent ionized layers" *Proc. Inst. radio Engrs., N.Y.* Vol. 43, p. 1240, 1955

[2] Chandrasekhar, S. "On Heisenberg's elementary theory of turbulence" *Proc. roy. Soc. A.* Vol. 200, p. 20, 1949

[3] Norton, K. A. "Point to point radio relaying via the scatter mode of tropospheric propagation" *Proc. Inst. radio Engrs., N.Y.* PG-4, March 1956

[4] Villars, F. and Weisskopf, V. F. "On the scattering of radio waves by turbulent fluctuations of the atmosphere" *Proc. Inst. radio Engrs., N.Y* Vol. 43, p. 1232, 1955

Suppl.
Part.II
1956

A THEORY OF LONG-DURATION METEOR-ECHOES BASED ON ATMOSPHERIC TURBULENCE WITH EXPERIMENTAL CONFIRMATION

H. G. Booker and Robert Cohen

School of Electrical Engineering, Cornell University, Ithaca, New York

A theory of long-duration meteor-echoes is developed, based on the assumption that a meteor-trail is rendered rough by the action of the small eddies in the atmosphere. This theory leads to the conclusion that, if loss of electrons from the trail by recombination and/or attachment is neglected, the field-strength of a long-duration meteor-echo in its decay-phase should be inversely proportional to the cube of time subsequent to formation of the trail. It is shown that this law is verified experimentally in the early part of the decay but that at later times the decay becomes more rapid. This can be explained in terms of the loss of electrons from the trail, provided that the loss is due to attachment to atmospheric molecules and the attachment time has an average value of the order of seven seconds.

It is shown that the spectrum of incoherent scattering associated with turbulent mixing in a gradient of electron-density may be derived experimentally by measuring the frequency-dependence of long-duration meteor-echoes during their decay-phase. This measurement is carried out, and the results are related to the CRPL experiments concerning the frequency-dependence of long-distance VHF scatter-transmission (see Fig. 13).

It is deduced that the contribution of meteoric ionization to the background-signal of scatter-transmission arises mainly from the incoherent scattering associated with mixing of this ionization by atmospheric turbulence. According to our analysis, McKinley's data concerning the contribution of meteor-trails to scatter-transmission leads to the same conclusion.

1. Introduction

Trails left by meteors during their passage through the upper atmosphere provide one of the most effective means available for studying atmospheric turbulence in the lower ionisphere. During their passage through the atmosphere, meteors shed particles that result in a trail that is both luminous and ionized. While there is some disturbance in the motion and temperature of the atmosphere in the immediate wake of the meteor, this quickly disappears, leaving the trail to disperse under substantially normal atmospheric conditions. Studies of atmospheric turbulence in the lower ionosphere based on observations of meteor-trails have been made by Liller and Whipple[1] using photographic methods, and by Greenhow[2] and others[3, 4] using radio methods. There is little doubt that the observations of Liller and Whipple refer to the distortion produced in the trail by large eddies present in the

atmosphere. The question of the size of the eddies involved in the radio observations is, however, in dispute. It seems to have been implicitly assumed by most authors that it is the largest eddies that are involved in the irregularly fluctuating signal associated with long-duration meteor-echoes. So far as the fading rate is concerned this is almost certainly true. However, BOOKER[5] has shown that the intensity of long-duration meteor-echoes is in most cases likely to be controlled by the effect on the trail of the smallest eddies in the atmosphere. Before the gross distortion of the trail by the largest eddies makes possible multiple perpendiculars onto the trail from a radar, the smallest eddies have usually rendered the trail "rough" for VHF radars. After the small eddies have made the trail rough, there is no longer any special interest attaching to perpendiculars onto the trail because an incoherent scattering theory must then be applied. It is the object of this paper to develop a rough trail theory of long-duration meteor-echoes, and to test the theory experimentally.

In a companion paper by BOOKER,[5] certain aspects of the theory of turbulence were applied to the ionosphere, and in particular to the levels at which meteor-trails are formed. For a height of 90 km the following orders of magnitude were deduced for some of the important parameters involved: For the turbulence-power per unit mass of atmosphere (which is the rate at which turbulence-energy is supplied per unit mass to the large eddies and removed by viscosity from the small eddies):

$$w = 25 \text{ W/kg} \quad \ldots.(1)$$

For the time-constant of the large eddies:

$$t_1 = 50 \text{ sec} \quad \ldots.(2)$$

For the turbulence-velocity of the large eddies:

$$v_1 = 35 \text{ m/sec} \quad \ldots.(3)$$

For the scale of the large eddies:

$$L_1 = 1{\cdot}6 \text{ km} \quad \ldots.(4)$$

For the time-constant of the small eddies:

$$t_2 = 0{\cdot}4 \text{ sec} \quad \ldots.(5)$$

For the turbulence-velocity of the small eddies:

$$v_2 = 3 \text{ m/sec} \quad \ldots.(6)$$

For the scale of the small eddies:

$$L_2 = 1{\cdot}3 \text{ m} \quad \ldots.(7)$$

These results led to the conclusion that, for wavelengths less than

$$4\pi L_2 = 16 \text{ m} \quad \ldots.(8)$$

and for time in excess of (5) subsequent to the fall of the meteor, the trail must be considered rough, and the echoes from it calculated on an incoherent scattering theory. This was regarded as ruling out the theory of KAISER and CLOSS[6] as a theory of long-duration meteor-echoes, and requiring the development of an incoherent scattering theory to replace it. It is the object of this paper to develop such a theory on the assumption that multiple scattering may be neglected, and to compare the results with appropriate observations of long-duration meteor-echoes.

For the coefficient of molecular diffusion at 90 km we have

$$D = 4 \text{ m}^2/\text{sec} \quad \ldots.(9)$$

approximately. It has been shown by BOOKER[5] that this is the appropriate coefficient of diffusion for a meteor trail only up to the time (5). After time (2), on the other hand, the rate of dispersal of the trail is controlled by the standard coefficient of eddy-diffusion;

$$v_1 L_1 = 6 \times 10^4 \text{ m}^2/\text{sec} \quad \ldots.(10)$$

from (3) and (4). For $t_2 < t < t_1$, the rate of dispersal of a meteor-trail is controlled by the coefficient of eddy-diffusion for the largest eddies that have so far caused major distortion of the trail. BOOKER[5] has shown that in this interval the appropriate coefficient of diffusion is wt^2, where w is the turbulence-power per unit mass. The coefficient of meteoric diffusion is therefore

$$\left.\begin{array}{ll} D, & 0<t<t_2 \\ wt^2, & t^2<t<t_1 \\ v_1 L_1, & t>t_1 \end{array}\right\} \quad \ldots.(11)$$

approximately. The variation of the coefficient of meteoric diffusion with time t subsequent to formation of the trail is plotted in *Fig. 1* using the numerical values quoted above.

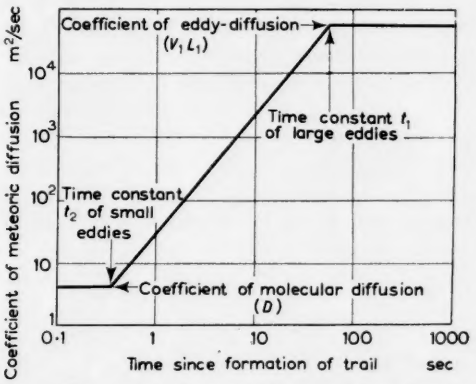

Fig. 1. The coefficient of meteoric diffusion as a function of time subsequent to formation of the trail

The extreme importance of eddy-diffusion in the rate of dispersal of a meteor-trail is obvious from *Fig. 1*. Indeed it might well be wondered how echoes can persist for any appreciable time after eddy-diffusion begins to control dispersal of the trail. The reason is as follows. It is quite true that the process of eddy-diffusion results in individual irregularities of electron-density rapidly decreasing in intensity. But the very process of eddy-diffusion creates additional irregularities of electron-density at a rapid rate. Moreover, the portion of the trail that contributes to the echo is no longer restricted by Fresnel zone considerations after incoherent scattering has been established. Thus, after the time (5), we have a situation in which the number of relevant irregularities of electron-density is rapidly increasing, while the importance of an individual irregularity is rapidly decreasing. We shall show that the

combination of these two effects for a meteor-trail leads to an incoherent echo for which the overall intensity decreases only slowly with time at times sufficiently large compared with (5). It is believed that this is the true explanation of long-duration meteor-echoes.

Since, in accordance with *Fig. 1*, the coefficient of meteoric diffusion varies with time, some consideration has to be given to solution of the equation of diffusion under these circumstances. This is done in Sec. 2. The basis for relating turbulence to the mean gradient of electron-density is described in Sec. 3, and in Sec. 4 the theory of back-scattering from a rough meteor-trail is developed on the assumption that multiple scattering is unimportant. This leads to a simple formula for the decay of a long-duration meteor-echo, and this formula is tested against our own experimental observations in Sec. 5 and those of McKinley in Sec. 6. Previous estimates of the line-density of intense meteor-trails are vitiated by neglect of the effect of atmospheric turbulence in the theory of Kaiser and Closs.[6] While the theory presented in Sec. 4 is not adequate to determine with precision the line-densities of intense meteor-trails, nevertheless, the orders of magnitude are not in doubt and are discussed in Sec. 7. Having obtained satisfactory agreement between the observations and the rough-trail theory, attention is turned in Sec. 8 to the frequency dependence of long-duration meteor-echoes in the decay-phase. This function is the spectrum-function required to describe all aspects of radio scattering in the lower *E*-region by irregularities in electro-density arising from the existence of atmospheric turbulence in a mean gradient of electron-density. Observational results derived in this way from meteor-echoes are combined with those of Bailey, Bateman, and Kirby[15] for long-distance VHF scatter-transmission to give an experimental spectrum for radio scattering extending over nearly a decade of frequency. The spectrum-function turns out to be roughly of the type required to fit in with the Kolmogoroff-Heisenberg theory[7, 8] of turbulence with a scale of small eddies having roughly the value (7). The bearing of these results on the explanation of long-distance scatter-transmission is discussed in Sec. 9.

2. The Effect of Eddy-Diffusion on the Dispersal of Meteor-Trails

To describe the dispersal of a meteor-trail, we are required to solve the equation of diffusion under conditions when the coefficient of diffusion varies with time in accordance with (11). We assume that the trail is initially straight, and that there are Q electrons per unit length. For the time being we neglect the effects of recombination and attachment, but we shall return to this point in Sec. 4.

For $0<t<t_2$ we have a constant coefficient of diffusion, D. In these circumstances a standard solution of the equation of diffusion gives, for the dependence of electron-density N on radial distance r at a time t

$$N=\frac{Q}{\pi r_t^2}\exp\left(-\frac{r^2}{r_t^2}\right) \qquad \ldots.(12)$$

where

$$r_t^2=4Dt \qquad \ldots.(13)$$

This formulation assumes that the radius of the trail at $t=0$ is zero. If we

require to consider a finite initial radius r_0 of the trail and can assume that the initial distribution of N with r is Gaussian, then (13) is replaced by

$$r_t^2 = 4Dt + r_0^2 \qquad \ldots.(14)$$

For $t_2 < t < t_1$, the appropriate coefficient of diffusion varies with time in accordance with (11), and the equation of diffusion is

$$\nabla^2 N = \frac{1}{wt^2}\frac{\mathrm{d}N}{\mathrm{d}t} \qquad \ldots.(15)$$

This may be rewritten as

$$\nabla^2 N = \frac{1}{w/3}\frac{\mathrm{d}N}{\mathrm{d}(t^3)} \qquad \ldots.(16)$$

This equation is of the same form as that for a constant coefficient of diffusion $w/3$, with time t replaced by t^3. The appropriate solution, from (14), is (12) with

$$r_t^2 = 4(w/3)(t^3 - t_2^3) + r_2^2 \qquad \ldots.(17)$$

where r_2 is the value of r_t at $t = t_2$.

For $t > t_1$, we return to an equation of diffusion with a constant coefficient of diffusion $v_1 L_1$. The distribution of N with r and t is therefore (12), with

$$r_t^2 = 4(v_1 L_1)(t - t_1) + r_1^2 \qquad \ldots.(18)$$

where r_1 is the value of r_t at $t = t_1$.

We see, therefore, that the distribution of electron-density N with radial distance r is always described by (12), and that the variation of r_t with time is given by

$$r_t^2 = \begin{cases} 4Dt, & 0 < t < t_2 \qquad \ldots.(19) \\ \frac{4}{3}w(t^3 - t_2^3) + r_2^2, & t_2 < t < t_1 \qquad \ldots.(20) \\ 4(v_1 L_1)(t - t_1) + r_1^2, & t > t_1 \qquad \ldots.(21) \end{cases}$$

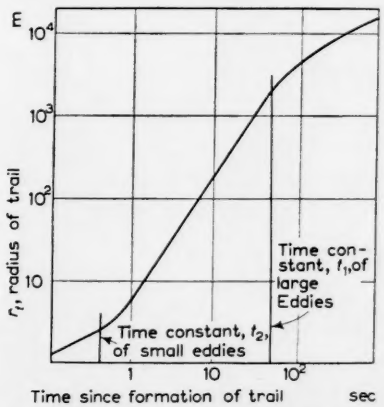

Fig. 2. The radius of a meteoric trail as a function of time subsequent to formation of the trail

provided that we take the initial radius of the trail to be zero. The variation of the "radius" r_t of the trail with the time t since its formation is plotted in *Fig. 2*, using the numerical values quoted in Sec. 1. If eddy-diffusion had been neglected, the rectilinear behavior in *Fig. 2* for $t < t_2$ would have continued

indefinitely. It is clear that neglect of eddy-diffusion for $t > t_2$ would lead to conclusions bearing little resemblance to reality.

The maximum electron-density over the cross-section of the trail occurs where r vanishes. It follows from (12) that the maximum electron-density N_m is given by

$$\frac{N_m}{Q} = \frac{1}{\pi r_t^2} \qquad \ldots.(22)$$

The ratio of the maximum electron-density over the cross-section to the line-density of the trail is therefore equal to the reciprocal of the cross-sectional "area" πr_t^2 of the trail. This is plotted in *Fig. 3*, using the numerical values quoted in Sec. 1. From this diagram may be calculated the time taken for a trail of given initial line-density to become underdense at a given radio frequency. For example, if at 30 Mc/s a trail becomes underdense 10 sec after formation, the ratio of the critical electron-density for 30 Mc/s to the line-density of the trail must be 10^{-5}. Now the critical electron-density at 30 Mc/s is $1{\cdot}1 \times 10^{13}$ electrons/meter.[3] Hence the line-density of the trail must be 10^{18} electrons/meter. An enormous initial line-density is thus required to keep a trail overdense at 30 Mc/s for as long as 10 sec. Thus the effect of eddy-diffusion is to make even strong trails underdense in the VHF band within a few seconds after formation of the trail.

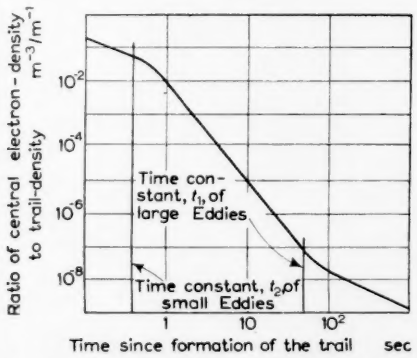

Fig. 3. The ratio of the central electron-density of a trail to the initial line-density as a function of time subsequent to formation of the trail

3. The Relation between Turbulence and Incoherent Scattering of Radio Waves by Meteor-Trails

Turbulence can cause irregularities of electron-density in an ionized medium in three ways:

(i) Through the pressure-fluctuations associated with turbulence. This mechanism would work even if there were no mean gradients of electron-density or temperature.[9]

(ii)* Through the randomization of a mean gradient in electron-density.[10]

(iii)* Through the randomization of a mean gradient in temperature.[11]

* For application to ionospheric layers these statements must be interpreted in the "potential" sense understood in meteorology, but this point is unimportant for meteor-trails.

There is little doubt that, for meteor-trails, mechanism (ii) is the predominant one.

Incoherent scattering of radio waves in a medium containing irregularities is described by means of a scattering cross-section σ per unit volume. The quantity σ is a function of the frequency f and the angle θ through which scattering takes place, but if multiple scattering is neglected, these two parameters only occur in the combination

$$f \sin \frac{\theta}{2} \qquad \ldots.(23)$$

σ also depends on the scale (4) of the large eddies and the scale (7) of the small eddies. Moreover σ is proportional to the mean square deviation of electron-density from the mean, and, in the case of mechanism (ii), this implies proportionality to the square of the mean gradient* of electron-density:

$$| \operatorname{grad} \mathcal{N} |^2 \qquad \ldots.(24)$$

We therefore assume that

$$\sigma = | \operatorname{grad} \mathcal{N} |^2 S\left(f \sin \frac{\theta}{2}\right) \qquad \ldots.(25)$$

where S is a spectrum-function which also contains as parameters the scales L_1 and L_2 of the large and small eddies. It must be remembered, however, that (25) does not include the effect of multiple scattering.

In applying formula (25) to calculation of incoherent scattering by a rough meteor-trail, it will not be necessary for us to assume a special form for the spectrum-function S. We shall in fact develop a method whereby radio measurements of long-duration meteor-echoes may be used to determine this spectrum experimentally over an interesting range of the variable.

Application of the function (25) to a meteor-trail implies that turbulence has caused the development of a volume containing electron-irregularities and that something approaching a statistically steady state has been reached. For the irregularities associated with the small eddies a statistically steady state is approached after time t_2 given by (5). As we consider irregularities in electron-density of progressively larger sizes, longer times must elapse before a statistically steady state is approached. For the irregularities associated with the largest eddies a statistically steady state will only be approached after time t_1 given by (2). Now for back-scattering at wavelengths less than (8) we are primarily concerned with the electronic irregularities associated with the small eddies. Hence we may apply the formula (25) soon after the time (5), and this is adequate for a theory of long-duration meteor-echoes.

For a meteor-trail the relevant gradient of $\mathcal{N}$ in (25) is the radial value $\mathrm{d}\mathcal{N}/\mathrm{d}r$. The incoherent echoing area per unit volume of a meteor-trail at times sufficiently large compared with t_2 is therefore

$$\sigma_B = (\mathrm{d}\mathcal{N}/\mathrm{d}r)^2 S(f) \qquad \ldots.(26)$$

provided that multiple scattering may be neglected.

Neglect of multiple scattering in calculating the echo from a meteor-trail is by no means a trivial assumption. The assumption implies that a wave incident upon the trail is, to a first approximation, undisturbed by the presence

* For application to ionospheric layers these statements must be interpreted in the "potential" sense understood in meteorology, but this point is unimportant for meteor-trails.

of the trail, but this is only true after the trail has become underdense. Applicability of (26) requires not only that the time subsequent to formation of the trail be greater than t_2 but also that the trail has become underdense. A theory of back-scattering from a rough meteor-trail derived from (26) will, in short, describe the echo during its decay-phase.

KAISER and CLOSS[6] have contemplated the possibility that a meteor-trail giving a long-duration echo might remain overdense for most of the life-time of the echo. These authors neglected, however, the tremendous effect of eddy-diffusion after time t_2 (see *Fig. 3*). In our experiments long-duration meteor-echoes entered upon their decay-phase after only a few seconds, and during much of their life-time they were in a phase of slow decay. The problem of explaining the existence of long-duration meteor-echoes is thus basically one of accounting for the slowness of the decay. Our assumption will be that, in the decay-phase, formula (26) is applicable at wavelengths less than (8).

4. Calculation of Incoherent Echoing from a Rough Meteor-Trail Neglecting Multiple Scattering

The back-scattering coefficient (26) per unit volume has to be integrated through the volume of the trail. Let us first carry out this integration over a normal cross-section of the trail, thereby obtaining the echoing area for incoherent back-scattering measured per unit length of the trail. This is

$$\Sigma_B = \int_0^\infty \sigma_B 2\pi r \, \mathrm{d}r, \qquad \ldots.(27)$$

$$= S(f) \int_0^\infty (\mathrm{d}N/\mathrm{d}r)^2 2\pi r \, \mathrm{d}r \quad \text{from (26)}$$

$$= S(f) \frac{8Q^2}{r_t^8} \int_0^\infty r^3 \exp\left(-\frac{2r^2}{r_t^2}\right) \mathrm{d}r \quad \text{from (12)}$$

$$= S(f) \frac{Q^2}{r_t^4} \qquad \ldots.(28)$$

on carrying out the integrations.

To obtain the complete echoing area of the rough trail, (28) has to be integrated along the length of the trail, possibly taking into account the finite pulse-length of a radar. In general this should be done allowing not only for the variation of Q along the trail but also for the variation with height of the parameters involved in r_t and $S(f)$, particularly w and L_2. We shall assume, however, that these quantities may be evaluated at a mean height which we shall take as 90 km. It is then merely necessary to multiply (28) by the length of the trail, or by that part of the length which falls within the pulse of a radar. Having calculated the echoing area of the rough trail in this way, we use it in the radar equation in the usual way.

In (28), $S(f)$ is independent of time. If we neglect recombination and attachment for the moment, Q is also independent of time. Hence (28) shows that, during the decay-phase of a long-duration meteor-echo, the power received is inversely proportional to the fourth power of the radius of the trail, plotted in *Fig. 2*. The received field strength is, therefore, inversely proportional to the square of the radius of the trail, or in other words proportional to (22). *Fig. 3* may therefore be reinterpreted as giving, for t sufficiently

greater than t_2, the received field strength on an arbitrary scale as a function of time subsequent to formation of the trail. We may use (20) and (21) to express analytically the time-variation of the field strength of a long-duration meteor-echo during its decay-phase. The field strength is proportional to $1/r_t^2$ from (28), and from (20) and (21) this factor is given by

$$= \frac{1}{r_t^2} \begin{cases} \dfrac{1}{\frac{4}{3}w(t^3 - t_2^3) + r_2^2}, & t_2 < t < t_1 \quad \ldots.(29) \\ \dfrac{1}{4(v_1 L_1)(t - t_1) + r_1^2}, & t > t_1 \quad \ldots.(30) \end{cases}$$

A meteor-echo is not a long-duration echo unless it lasts longer than the time constant t_2 of the smallest eddies. On the other hand, comparatively few meteor-echoes last longer than the time-constant t_1 of the largest eddies. Hence the formula that is normally required to describe the variation of field strength with time during the decay-phase of a long-duration meteor-echo is (29). Since this formula is required for values of t large compared with t_2, it may be written approximately

$$\frac{1}{r_t^2} = \frac{1}{\frac{4}{3}wt^3}, \quad t_2 \ll t < t_1 \quad \ldots.(31)$$

It follows from (28) and (31) that the time variation in the field strength of a long-duration meteor-echo is

$$E(t) \propto \frac{Q}{t^3}, \quad t_2 \ll t < t_1 \quad \ldots.(32)$$

If the total number Q of the electrons in the trail per unit length does not decrease, the field strength of a long-duration meteor-echo in its decay-phase should be inversely proportional to the cube of time subsequent to formation of the trail. It should be easy to ascertain experimentally whether or not this is true.

For sufficiently long-duration meteor-echoes it is likely that electrons are removed from the trail either by recombination or by attachment and that as a result Q in (28) and (32) decreases with time. If Q_0 is the initial line-density of the trail, and Q is the line-density at time t, then for recombination with a recombination-coefficient α we have

$$Q = \frac{Q_0}{1 + (t/t_R)} \quad \ldots.(33)$$

where t_R is the recombination-time given by

$$t_R = Q_0 \alpha \quad \ldots.(34)$$

The same formula would apply to electron-attachment in the case of attachment to the atoms or molecules produced by break-up of the meteor. In the case, however, of attachment to atmospheric molecules we have

$$Q = Q_0 \exp\left(-\frac{t}{t_A}\right) \quad \ldots.(35)$$

where t_A is the attachment-time. Either (33) or (35) must be substituted into (28) and (32) in order to allow for loss of electrons from the trail.

It should be noted that the time t_R given by (34) depends on the initial line-density in the trail and consequently varies considerably from meteor to

meteor. The time t_A involved in (35) on the other hand is independent of the line-density in the trail, although it does depend somewhat on altitude.

In performing experiments to check equation (32), it might be expected that the effect of electron-loss would become noticeable for echoes of sufficiently long-duration. It might then be possible to distinguish between the mechanisms described by (33) and (35), and also to measure either t_R or t_A.

Let us now suppose that experiments with long-duration meteor-echoes have been performed to check the time-dependence given in equation (28), and that the check is satisfactory. Then it further follows from (28) that the frequency-dependence of long-duration meteor-echoes during their decay-phase is a direct measure of the spectrum-function S involved in (25). To evaluate the spectrum-function applicable whenever irregularities of electron-density are caused by the action of turbulence in a mean gradient of ionization at the meteoric level, therefore, we merely have to measure the frequency-dependence of long-duration meteor-echoes during their decay-phase.

5. Experimental Investigation of the Decay of Long-Duration Meteor-Echoes

With a view to checking the time-dependence involved in equation (32) a program of continuous wave observations of meteor-trails was begun. The transmitter consisted of a Wilcox 99A arranged so as to be capable of radiating continuously on frequencies of 17·31, 30·38, and 49·78 Mc/s. The detector-outputs of the receivers were connected to a dual-channel Sanborn recorder having a time-constant of about 0·01 second. The deflection of the stylus of the recorder varied in a substantially linear manner with the voltage appearing at the terminals of the receiving antennas.

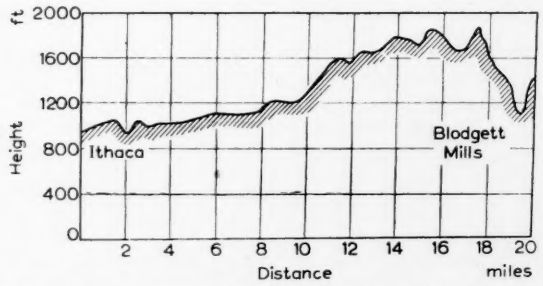

Fig. 4. Profile of terrain between transmitting and receiving sites allowing for standard atmospheric refraction

The receiving site was at the Ionosphere Laboratory, Ithaca, New York, and the transmitting site was at Blodgett Mills, New York. The distance between the two sites is 31 km and the intervening terrain profile is as shown in *Fig. 4*. Half wave antennas were used for each frequency, both for transmission and reception. The dipoles at each site were erected on a common mast at 0·35 above the ground and were oriented along the great circle path joining the sites. The arrangement resulted in complete suppression of the direct signal between transmitter and receiver on all three frequencies.

Separation of the transmitting and receiving sites by 31 km causes departure from the condition of exact back-scattering to an extent that depends on the location of the meteor-trail. At worst this involved a correction of 1·2 per cent in the parameter (23). It has therefore been assumed that the observations may be compared with theoretical formulas appropriate strictly to back-scattering.

Observations were made almost exclusively between 0000 and 0700 local time. Data were gathered both during known meteor showers and when the meteors were presumably of sporadic origin only. More than fifty long-duration meteor-echoes were recorded on pairs among the available frequencies. An example of a pair of observations on 17·31 and 30·38 Mc/s is shown in *Fig. 5*: there is a little mechanical limiting of the lower frequency echo at its extreme peaks in this case. Another example, employing 30·38 and 49·78 Mc/s, is shown in *Fig. 7*.

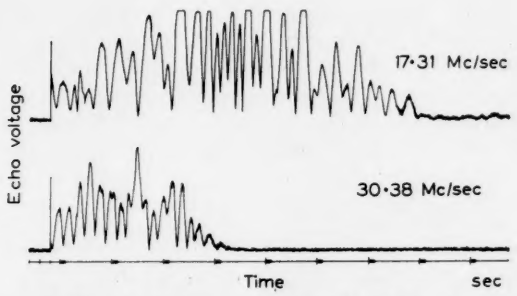

Fig. 5. Example of records of long-duration meteor-echoes observed simultaneously on 17·31 and 30·38 Mc/s

Meteor-echoes of the following varieties were observed:

(i) Echoes which rise fairly suddenly and which decay more or less exponentially to noise-level within a few tenths of a second.

(ii) Echoes which rise fairly suddenly, which develop irregular fading after a few tenths of a second, and which last from one to ten seconds and occasionally longer. The echoes shown in *Figs. 5* and *7* are examples of this type.

(iii) Echoes which do not have a sudden start and which always develop irregular fading. These echoes gradually rise out of the noise, attain a maximum response after a second or two, and then decay like echoes of type (ii).

There are also a few echoes that do not fit into the above categories and that we do not understand.

Analysis of the data is based on the following interpretation of the three categories of echoes described above:

(i) The first type of echo arises from specular reflection from a trail which quickly becomes underdense and to which the theories of LOVELL and CLEGG[12] and of HERLOFSON[13] may be applied.

(ii) Echoes other than those of the first type involve trails which remain overdense for an appreciable fraction of a second and even for several seconds. Echoes of this second type involve, for the first few tenths of a second, a phenomenon of specular reflection described by the theory of KAISER and

CLOSS.[6] After a few tenths of a second, however, atmospheric turbulence mixes the trail and use must be made of an incoherent scattering theory such as that developed in Sec. 4. When echoes of this type begin to decay, they should do so in accordance with formula (32).

(iii) Echoes of the third type are supposed to be identical with those of the second type except that the "echo point" on the initial trail lies outside the section of trail that is strongly ionized. Consequently there is no observable specular reflection, but incoherent scattering develops as the trail is mixed by atmospheric turbulence.

Echoes of the first variety are of no especial interest here except insofar as they can help to check the relative calibration of the equipment on the three frequencies. Echoes of the third type are inconvenient for our analysis because the time of formation of the trail, and therefore the zero time in (32), is not recorded. Our analysis has therefore been confined to echoes of the second type.

To compare echoes of the kind shown in *Figs. 5* and *7* with a relationship of the form (32), it is necessary to remove the irregular fading by a smoothing process so as to arrive at the mean amplitude. To do this each record was divided into intervals of length τ, overlapping $\frac{1}{2}\tau$, and planimeter integration was used to find the area under the curve for each interval. The interval τ was taken to be 0·4 or 0·8 sec, depending upon the fading rates involved and the length of the event being studied. A moving average was then formed from the sequence of areal values generated in this way as follows:

(*a*) For the third interval and all successive intervals, a running mean extending over five successive values was used.
(*b*) For the second interval, a running mean over three successive values was used.
(*c*) For the first interval no further averaging was done.

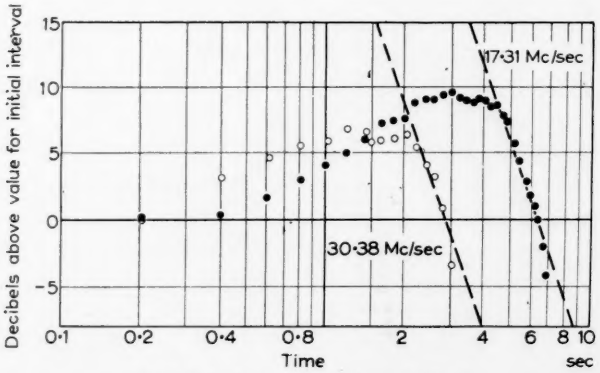

Fig. 6. Analysis of records shown in Fig. 5

The smoothed amplitudes derived in this way from the echoes shown in *Figs. 5* and *7* are plotted, at positions as measured by the center times of the integration-interval, in *Figs. 6* and *8* respectively.

In *Figs. 6* and *8*, smoothed echo-voltage is shown relative to that for the first interval, so that all curves start from zero on the decibel scale. Both signal amplitude and time are plotted on logarithmic scales, so that the t^{-3} relation involved in formula (32) corresponds to the slope indicated in *Figs. 6* and *8* by the dashed lines. If recombination, represented by (33), and attachment, represented by (35), are neglected, the decay of the echoes in *Figs. 6* and *8* should be parallel to the dashed lines.

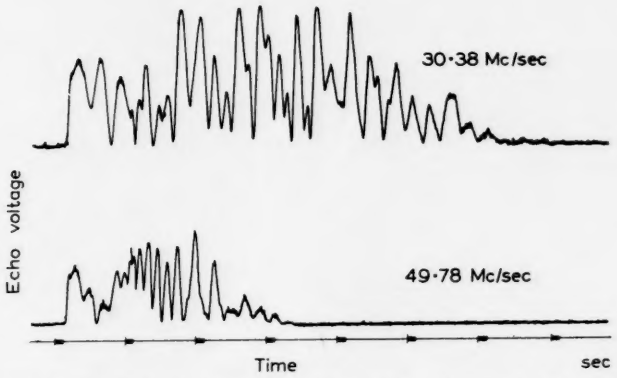

Fig. 7. Example of records of long-duration meteor-echoes observed simultaneously on 30·38 and 49·78 Mc/s

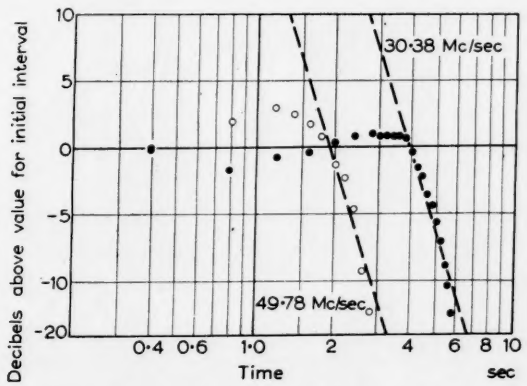

Fig. 8. Analysis of records shown in Fig. 7

Of eighty curves analyzed in the manner described, about half show the degree of agreement with the t^{-3} law illustrated in *Figs. 6* and *8*. This agreement is reasonably good, but there is an indication of some systematic departure from the simple t^{-3} behavior. Roughly another quarter of the curves analyzed show no significant departure from the t^{-3} law. The remainder indicate a t^{-3} behavior but involve departures in the form of kinks or knees that might be associated with the superposition of small meteor-echoes upon the event being studied.

The conclusion is drawn that, when a long-duration meteor-echo begins to decay, it does so in accordance with the t^{-3} law, but that as time increases there is indication that the echo falls somewhat below the value corresponding to this simple law. To demonstrate such a departure from the t^{-3} law, instrumentation would be required with a larger dynamic range than was applied here.

6. Comparison with McKinley's Observations of Long-Duration Meteor-Echoes

While many investigators in the radio meteoric field have presumably had access to observations of the kind presented in the previous section, it does not seem possible to find in the literature an amplitude-time analysis of these observations such as we have carried out. It has been pointed out by Eshleman,[14] however, that some data presented by McKinley[4] are relevant to

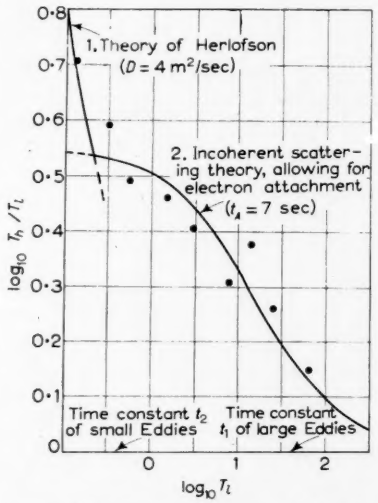

Fig. 9. A theoretical interpretation of experimental data of McKinley[12]

the decay rate of long-duration meteor-echoes, and in particular to the question of a possible departure from the t^{-3} law indicated in *Figs. 6* and *8*.

McKinley did not obtain, in the experiments referred to, the details of the decay of any long-duration meteor-echo. He did, however, measure the total duration of meteor-echoes simultaneously on two radar equipments whose frequencies were nearly identical and which had been measured to have a difference in sensitivity of 33 decibels. McKinley did not present results for individual meteor-echoes, but averaged the results for a number of events to obtain the experimental points reproduced in *Fig. 9*. In this diagram is plotted the logarithm to the base ten of the ratio of the echo duration, T_h, on the high power equipment, to the echo duration, T_l, on the low power equipment, as a function of log T_l. Curve 2 of *Fig. 9* is not, however, the empirical one given in McKinley's paper but is based on the theory presented in this paper.

It can readily be shown that, if the decay of an echo follows any power law, whether t^{-3} or not, the theoretical curve to be drawn in *Fig. 9* for comparison with the experimental points is a horizontal straight line. There is a clear discrepancy therefore between the experimental results shown in *Fig. 9* and any decay formula involving only a power law. For the t^{-3} law and for radars whose sensitivities differ by 33 decibels, the horizontal line to be drawn in *Fig. 9* intersects the vertical scale at 0·54. It will be observed that, if we disregarded temporarily the points in *Fig. 9* corresponding to

(*a*) short-duration meteor-echoes (shorter than 0·4 sec), and
(*b*) the extremely long-duration meteor-echoes (longer than 5 sec on the low power equipment),

then the average value of the ordinates for the remaining points is about 0·54. But for durations longer than 5 sec on the low power equipment the ordinates are well below 0·54. If this statement is converted into a form suitable for comparison with results such as those presented in *Figs. 6* and *8* we obtain the following: For echoes whose durations are of the order of a few seconds, the decay in echo amplitude is given roughly by t^{-n}, where n is around 3: but for longer durations the decay is faster. In other words, McKinley's observations prove the reality of the tendency indicated in *Figs. 6* and *8* for the echo-intensity to fall below the t^{-3} law as t increases.

That there should be a departure from the t^{-3} law with increasing values of t follows from the theory presented in Sec. 4, if account is taken of the loss of electrons to the trail because of recombination and/or attachment. Moreover, McKinley's observations are adequate to decide which of these mechanisms is more important and to estimate the time-constant involved.

Let us consider first the recombination formula (33). This would apply if electrons disappeared as a result of their capture or recapture by atoms or molecules of meteoric origin. When $t \ll t_R$ in (33) the effect of recombination is negligible. When $t \gg t_R$ the recombination formula merely changes the t^{-3} law to a t^{-4} law. After time t_1 this would become a t^{-2} law in accordance with (30). Thus the theoretical curve to be drawn in *Fig. 9* would consist of several horizontal sections and could not be a good fit to the observational points. Moreover, allowance has to be made for the fact that the recombination time $_R$ given by (34) would vary considerably from trail to trail. Thus, with the recombination formula (33), one would expect the experimental points in *Fig. 9* to occupy a roughly horizontal band with a mean of about 0·54. This is clearly not the case, and we conclude that the observed departure from the t^{-3} law cannot be explained in terms of capture or recapture of electrons by meteoric atoms or molecules.

Let us now consider disappearance of electrons from the trail by attachment to atmospheric molecules. On this basis the decay in the echo amplitude should, in accordance with (32) and (35), be given by

$$E(t) \propto t^{-3} \exp\left(-\frac{t}{t_A}\right) \qquad \ldots.(36)$$

where t_A is the time of attachment. In general, (36) should be replaced by the product of (29/30) and (35). The decay law (36) leads to a theoretical curve

in *Fig. 9* which fits the data quite well if a suitable choice is made for the time of attachment. Curve 2 of *Fig. 9* is one for which

$$t_A = 7 \text{ sec} \qquad \ldots.(37)$$

Curve 1 represents the short-duration echoes based on the theory of HERLOFSON.[13] The appropriate curve to be compared with McKinley's points is, therefore, the composite continuous curve, suitably rounded at the junction. It is clear that the agreement between this theoretical curve and the observations is good.

We conclude that the decay of long-duration meteor-echoes is satisfactorily described by the rough-trail theory developed in Sec. 4, that electrons disappear from the trail by attachment to atmospheric molecules, and that the time of attachment has an average value of the order of seven seconds. The time of attachment may well vary from a few seconds to a few tens of seconds depending on the meteoric altitude under consideration.

7. ESTIMATION OF THE LINE-DENSITY OF INTENSE METEOR-TRAILS

In principle it should be possible from equation (28) to estimate the line-density Q of a meteor-trail that gives a long-duration meteor-echo. However, it is not yet possible to be sufficiently confident concerning the properties of the function $S(f)$ to make this a practicable method of determining Q at the present time. An alternative method for estimating Q roughly is the following:

Figs. 5–8 illustrate the fact that a long-duration meteor-echo normally enters upon its t^{-3} decay an appreciable time after it develops irregular fading. Let t_c be an estimate of the time at which the t^{-3} decay commences. Then t_c is usually greater than the time t_2 at which irregular fading sets in. For $t<t_2$ the theory of KAISER and CLOSS[6] applies. For $t>t_c$ the theory of Sec. 4 applies. For $t_2<t<t_c$ however no satisfactory theory is at present available. It is our assumption that during this interval the central part of the trail is still overdense, so that an incident wave cannot pass through the trail undisturbed, even to a first approximation. In the interval $t_2<t<t_c$, what is required is a theory of irregular scattering that takes into account the effect o multiple scattering. On this picture the time t_c is roughly that at which the central part of the trail ceases to be overdense. We can therefore estimate the central electron-density of the trail at time t_c and then use *Fig. 3* to deduce Q.

The critical electron-density N_c at which the meteor-trail becomes underdense depends on the frequency f of the radio wave in accordance with the formula

$$N_c = 1{\cdot}24 \times 10^{10} f^2 \qquad \ldots.(38)$$

where N_c is measured in electrons/meter^3 and f in megacycles/second. From the fact that N_c increases with frequency, we should expect that t_c would decrease with frequency. No exception to this rule has occurred in our observations. This feature of long-duration meteor-echoes may be seen in *Figs. 6* and *8*.

Quantitively, however, the ratio of the two values of t_c observed for a particular event on either of the pairs of frequencies involved in *Figs. 6* and *8* is some thirty per cent different on the average from what it should be on the simple ideas outlined in this section. This is demonstrated in *Fig. 10* where values of Q deduced by this method on one frequency are plotted against

values deduced on another frequency for an event simultaneously observed on both frequencies. The value for the higher frequency is plotted as ordinate and that for the lower frequency as abscissa, using logarithmic scales. Ideally the points should all lie on the line drawn. It is clear that estimates of Q are somewhat less for the higher frequency than for the lower frequency. The reason for this is not known, but it is doubtless associated with the lack of a theory incorporating multiple scattering.

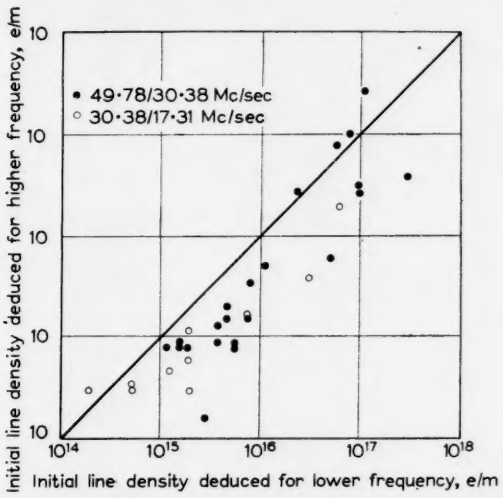
• 49·78/30·38 Mc/sec
○ 30·38/17·31 Mc/sec
Initial line density deduced for higher frequency, e/m
Initial line density deduced for lower frequency, e/m
10
10
10

It was for this purpose that all the observations that we have made of long-duration meteor-echoes have been recorded simultaneously on two frequencies as shown in *Figs. 5* and *7*. But to use this data to deduce the spectrum-function $S(f)$, certain difficulties have to be overcome.

It will be noticed in *Figs. 5* and *7* that the echo recorded on the lower frequency does not usually enter its decay-phase until the echo recorded on the higher frequency has disappeared into the noise. This situation would be improved by using equipment with a bigger dynamic range. With our equipment this difficulty was overcome as follows: Straight lines corresponding to a t^{-3} law were fitted to the data as shown in *Figs. 6* and *8*. The amplitude ratio on the two frequencies in the decay-phase was then read by comparing the levels of these straight lines at any arbitrary time common to both.

To derive the spectrum-function $S(f)$ it is in principle necessary to calibrate the equipment on the various frequencies in use and to verify that the calibration is maintained. It was decided to circumvent this procedure by the following device: The frequency variation of short-duration meteor-echoes has been investigated both theoretically and experimentally by LOVELL and CLEGG.[12] A further experimental investigation has been made by GREENHOW.[2] By assuming the validity of this work, it is possible to use the relative intensities of short-duration meteor-echoes on the various frequencies as a means of relative calibration of the equipment at the several frequencies. Furthermore, it has been shown by KAISER and CLOSS[6] that if, during the first few tenths of a second, specular reflection is obtained from a trail giving a long-duration meteor-echo, this specular reflection depends upon frequency

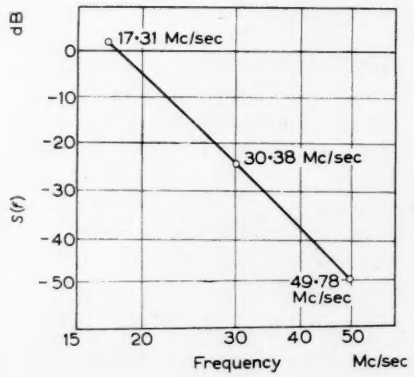

Fig. 11. The spectrum-function for incoherent scattering deduced from long-duration meteor-echoes

in the same way as for short-duration meteor-echoes. The assumption we have made, therefore, is that the magnitude of the initial rise in records such as those reproduced in *Figs. 5* and *7* varies with frequency in accordance with the specular reflection theories of LOVELL and CLEGG[12] and of KAISER and CLOSS.[6] With this assumption one may then deduce the frequency response in the decay-phase of long-duration meteor-echoes from the dashed lines fitted to the observations shown in *Figs. 6* and *8*, as discussed above. By operating in

this way all that is required of the equipment is that its performance should not vary during the course of an individual long-duration meteor-echo.

By analyzing our observations in the way just described, using the three frequencies available, we arrive at the results shown in *Fig. 11*. The spectrum function is plotted with ordinates in decibels using an arbitrary zero. Frequency is plotted as abscissa on a logarithmic scale. For each long-duration meteor-echo simultaneously recorded on 17·31 and 30·38 Mc/s, a figure was derived for the decibel difference in the echoing area of the trail during its decay-phase. The average of these is the decibel difference plotted in *Fig. 11*

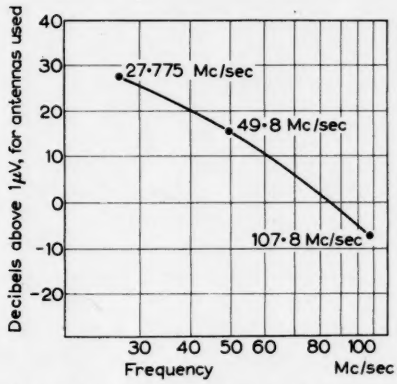

Fig. 12. The frequency variation deduced from long-distance scatter-transmission between Cedar Rapids, Iowa, and Sterling, Virginia, for constant aperture antennas

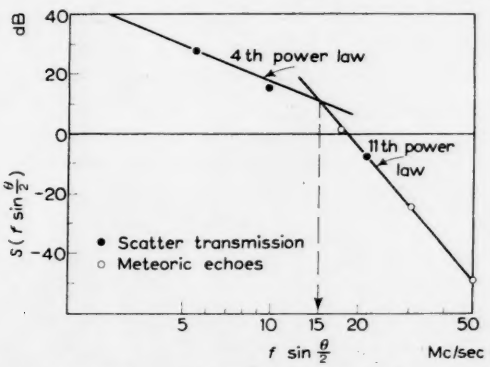

Fig. 13. The spectrum-function for incoherent scattering deduced by combining the observations derived from long-duration meteor-echoes with those derived from long-distance scatter-transmission

for those frequencies. A similar procedure was followed for the frequencies 30·38 and 49·78 Mc/s. The nearly linear variation in *Fig. 11* corresponds approximately to an f^{-11} variation of scattered power with frequency.

It is interesting to compare the frequency response plotted in *Fig. 10* with that obtained for VHF ionospheric scatter-transmission. The results of BAILEY, BATEMAN, and KIRBY[15] are reproduced in *Fig. 12*. A straight line variation between the points in *Fig. 12* corresponding to 27·775 and 49·80

Mc/s would correspond to an $f^{-4.7}$ variation of power with frequency. A straight line variation between the points corresponding to 49·80 and 10·78 Mc/s would correspond to an $f^{-6.9}$ variation of power with frequency.

The two types of observations depicted in *Figs. 11* and *12* are brought together in a single diagram in *Fig. 13* with the aid of the parameter (23). It is assumed that the same basic scattering formula (25) applies in both phenomena. It is further assumed that any parameters involved in (25) have the same value in both phenomena. This applies particularly to the value of the scale L_2 of the small eddies. These assumptions are reasonable because the same ionospheric level is involved in both phenomena. *Fig. 13* was prepared by plotting scattered power as a function of $f \sin \frac{1}{2}\theta$, in accordance with (25), allowing for the fact that $\sin \frac{1}{2}\theta$ is approximately unity in the meteor observations and approximately one-fifth in the long-distance transmission measurements. The absolute levels of the two sets of points were adjusted to make them fit together, because the information available regarding absolute values was insufficient to justify a more elaborate procedure. The vertical scale in *Fig. 13* should, therefore, be regarded as having an arbitrary reference (although this has been placed at the same level as that in *Fig. 12*). *Fig. 13* may be regarded as indicating the variation in the spectrum-function S in equation (25) over almost a decade of the variable $f \sin \frac{1}{2}\theta$, extending from about 5·5 to 50 Mc/s.

From the theory of turbulence developed by KOLMOGOROFF[7] and HEISENBERG,[8] some information is available concerning the form of the spectrum-function involved in (25) and plotted in *Fig. 13*. The information relates to frequencies such that $f \sin \frac{1}{2}\theta$ exceeds the frequency corresponding to the wavelength

$$4\pi L_1 \qquad \ldots.(39)$$

where L_1 is the scale of the large eddies. According to BOOKER[5] the value of (39) at 90 km is about 20 kilometers. Whatever the exact value of (39) may be at the ionospheric levels under discussion, there is no doubt that the frequencies considered in *Fig. 13* are high compared with the frequency corresponding to the wavelength (39). In these circumstances the Kolmogoroff-Heisenberg theory predicts a spectrum-function of the form

$$(f \sin \tfrac{1}{2}\theta)^{-m} \qquad \ldots.(40)$$

at frequencies such that $f \sin \frac{1}{2}\theta$ is appreciably less than the frequency corresponding to the wavelength

$$4\pi L_2 \qquad \ldots.(41)$$

where L_2 is the scale of the small eddies. At frequencies such that $f \sin \frac{1}{2}\theta$ is appreciably larger than the frequency corresponding to the wavelength (41), the spectrum-function should follow an inverse power law

$$(f \sin \tfrac{1}{2}\theta)^{-n} \qquad \ldots.(42)$$

where n is greater than m.

The precise values of m and n in (40) and (42) are still under discussion. According to BATCHELOR[16] and SILVERMAN[17]

$$m = 11/3 \qquad \ldots.(43)$$

but according to VILLARS and WEISSKOPF[10]

$$m = 5 \qquad \ldots.(44)$$

According to BATCHELOR[16] and SILVERMAN[17] it would follow from HEISENBERG[8] that

$$n = 9 \qquad \ldots.(45)$$

but according to WHEELON[18]

$$n = 13. \qquad \ldots.(46)$$

We regard the observations plotted in *Fig. 13* as describing the transition from an mth power law on the low frequency side to an nth power law on the high frequency side, with the values of m and n being of the order of magnitude required to fit the Kolmogoroff-Heisenberg theory of turbulence. On this basis a value for the scale L_2 of the small eddies at the meteoric level may be deduced from *Fig. 13* using the fact that the transition between the power laws occurs near the wavelength (41). In *Fig. 13* a line has been drawn corresponding to $m = 4$ and one corresponding to $n = 11$ so as to fit the data in an appropriate manner. These two lines intersect at a frequency of about 15 Mc/s, corresponding to a wavelength of 20 meters. Equating this to (41), we deduce that

$$L_2 = 1{\cdot}6 \text{ meters} \qquad \ldots.(47)$$

approximately, and this applies to a height of the order of 90 km. This value is to be compared with the value (7) deduced for the meteoric level by BOOKER[5] using another argument based on different observational data.

9. APPLICATION TO VHF SCATTER-TRANSMISSION

For some years there has been discussion of the role of meteors in long-distance VHF scatter-transmission. The results presented in this paper have a bearing on this question. Discussion of this phenomenon has often implied a choice between reflection from meteor-trails and scattering associated with atmospheric turbulence. What has been demonstrated in this paper, however, is that an important part of the phenomenon of radio returns from meteor-trails has itself to be interpreted in terms of incoherent scattering due to atmospheric turbulence. Moreover it turns out that it is precisely the turbulence features of meteor-echoes that are most likely to be important in long-distance VHF scatter-communication. Thus the background-signal involved in the transmission-phenomenon is likely to result from incoherent scattering associated with atmospheric turbulence whether or not meteors are the primary cause of ionization at this altitude.

It is desirable to state more precisely the nature of the controversy that has been in progress concerning the cause of ionospheric scatter-communication.

(i) The explanation of BAILEY *et alia*[19] was that the phenomenon was caused by incoherent scattering resulting from the influence of atmospheric turbulence upon ionization at the relevant level in the ionosphere. The cause of the ionization might be ultra-violet light, meteors, auroral particles, or indeed any ionizing agency whatsoever. The nature of the diurnal variation that they observed led them to suggest, however, a combination of a solar origin and meteoric origin for the ionization. Subsequent observations indicated also the importance of auroral ionization.[15]

(ii) The explanation originally suggested by ESHLEMAN and MANNING[20] was that atmospheric turbulence was not involved, and that the phenomenon could be explained entirely by specular reflection from rectilinear meteor-trails.

It should be stated that the authors who originally supported explanation (ii) have subsequently taken the view that other factors, presumably those involved in explanation (i), may be important. It is of course true that the signal received in ionospheric scatter-transmission possesses, in addition to an irregularly fading background-signal, randomly spaced spikes with which are associated Doppler whistles. There never has been any doubt that these spikes are accounted for by explanation (ii). It is the view of the present authors that explanation (ii) is important only in connection with the spikes, and that explanation (i) is required to account for the background-signal.

It should be emphasized that meteoric ionization is involved both in explanation (i) and in explanation (ii). So far as meteoric ionization is concerned, the question is whether the contribution of meteor-trails to the background-signal is the specular reflection produced while the trails are essentially straight, or the incoherent scattering produced after the trails have been mixed by atmospheric turbulence. It might be supposed that specular reflection from straight meteor-trails would be particularly important in scatter-transmission because the length of trails is large compared with the wavelength. However, although this greatly enhances the influence of appropriately located straight trails, it restricts to a compensating extent the number of trails that are important for specular reflection. For incoherent scattering from trails that have been mixed by atmospheric turbulence there is no corresponding restriction on the number of trails to be counted. Thus, even on a qualitative basis, incoherent scattering from a large number of irregular trails that have been mixed by atmospheric turbulence is not likely to be less important than specular reflection from a smaller number of appropriately located straight trails.

Important information concerning whether the meteor contribution to the background-signal in scatter-transmission is caused by specular reflection from straight trails or by incoherent reflection from meteoric ionization that has been mixed by atmospheric turbulence is contained in the analysis of McKinley.[21] He set out to use observations concerning back-scattering from meteor-trails to calculate the contribution of meteors in long-distance scatter-transmission at 50 Mc/s between Cedar Rapids, Iowa, and Sterling, Virginia. Now frequency f and scattering-angle θ enter into the computations through the combination (23), and $\sin \frac{1}{2}\theta$ for the path studied was about one-fifth. It follows that the relevant radar for meteors should be taken on a frequency of the order of one-fifth of 50 Mc/s, or about 10 Mc/s. McKinley did not have data available at this frequency but presented data for the VHF band, from which a useful extrapolation to 10 Mc/s can be made. He concluded that the meteoric contribution to ionospheric scatter-communication is of the right order of magnitude to explain the signals received. It is important, however, to notice from what type of meteor-echoes the contribution arises. Data deduced from McKinley's Table VIII are presented in the following table:

Frequency (Mc/sec)	*Time during which meteor-echoes are obtained (sec/hr)*	*Critical duration t_c used by McKinley (seconds)*	*Per cent of time accounted for by echoes of duration $>t_c$*
106	8·4	0·4	67
56	118	1·0	8
33	550	3·0	73

The table shows that most of the time during which meteoric radar echoes are obtained is accounted for by echoes whose duration is so long that they must be irregularly fading echoes associated with atmospheric turbulence. Moreover it follows from (5) and the observations of GREENHOW[2] that this table should be corrected to use a uniform value of 0·4 sec in the third column at all three frequencies. This would increase somewhat the percentage in the last column at 56 Mc/s, and substantially increase the percentage at 33 Mc/s. After making these corrections, the data should then be extrapolated to 10 Mc/s to obtain the radar conditions corresponding approximately to long-distance transmission at 50 Mc/s with a scattering-angle θ for which $\sin \frac{1}{2}\theta = \frac{1}{5}$. If one uses McKinley's data in this way he cannot escape the conclusion that it is the contribution of the irregularly fading long-duration meteor-echoes that permitted McKinley to account for the continuous background-signal in scatter-communication by means of meteors. Thus the conclusions that can now be drawn from McKinley's data are:

(*a*) The order of magnitude of the signal received in ionospheric scatter-transmission can be accounted for by meteoric ionization, although this may not be the only important source of ionization.

(*b*) The contribution from those meteor-echoes that indicate specular reflection is too small to permit an explanation of the background-signal by the theory of ESHLEMAN and MANNING.[20]

(*c*) The contribution from those meteor-echoes that exhibit irregular fading predominates, indicating that any influence of meteoric ionization on the background-signal of scatter-transmission arises through the effect of atmospheric turbulence on the ionization.

The current status of our understanding of the cause of ionospheric scatter-transmission appears to be as follows: In middle latitudes, at night, this phenomenon arises mainly from the effect of atmospheric turbulence on ionization of meteoric origin. During the daytime, however, ionization of meteoric origin is subordinate to ionization of solar origin. In high latitudes, ionization of meteoric origin is frequently overshadowed even at night by ionization presumed to be associated with incoming charged particles. In all cases, however, the background-signal is sustained by the effect upon the ionization of atmospheric turbulence.

REFERENCES

[1] LILLER and WHIPPLE. *Rocket Exploration of the Upper Atmosphere*, p. 112, Pergamon Press, London, 1954

[2] GREENHOW. *Proc. Phys. Soc. B.* Vol. 65, p. 169, 1952

[3] MANNING, VILLARD, and PETERSON. *J. geophys. Res.* Vol. 57, p. 387, 1952

[4] MCKINLEY. *Canad. J. Phys.* Vol. 31, p. 758, 1953

[5] BOOKER. *J. geophys. Res.* Vol. 61, p. 673, 1956 and p. 52 of this volume

[6] KAISER and CLOSS. *Phil. Mag.* Vol. 43, p. 1, 1952

[7] KOLMOGOROFF. *C.R. Acad. Sci. U.R.S.S.* Vol. 30, p. 301; Vol. 32, p. 16, 1941

[8] HEISENBERG. *Z. Phys.* Vol. 124, p. 628, 1948

[9] VILLARS and WEISSKOPF. *Phys. Rev.* Vol. 94, p. 232, 1954

[10] VILLARS and WEISSKOPF. *Proc. Inst. radio Engrs., N.Y.* Vol. 45, p. 1232, 1955

[11] GALLET. *Proc. Inst. radio Engrs., N.Y.* Vol. 43, p. 1240, 1955

[12] LOVELL and CLEGG. *Proc. Phys. Soc. B.* Vol. 60, p. 491, 1948
[13] HERLOFSON. *Rep. Progr. Phys.* Vol. 11, p. 444, 1948
[14] ESHLEMAN. Discussion at URSI Spring meeting, Washington, D.C., 2 May 1956
[15] BAILEY, BATEMAN, KIRBY. *Proc. Inst. radio Engrs., N.Y.* 43, p. 1181, 1955
[16] BATCHELOR. *Cornell Univ. School of EE Research Report* EE–262. 1955
[17] SILVERMAN. Paper presented at URSI Spring meeting, Washington, D.C., 3 May 1956, to be published
[18] WHEELON. Paper presented at URSI Spring meeting, Washington, D.C., 1 May 1956
[19] BAILEY, BATEMAN, BERKNER, BOOKER, MONTGOMERY, PURCELL, SALISBURY, and WEISNER. *Phys. Rev.* Vol. 86, p. 141, 1952
[20] ESHLEMAN and MANNING. *Proc. Inst. radio Engrs., N.Y.* Vol. 42, p. 530, 1954
[21] MCKINLEY. *Canad. J. Phys.* Vol. 32, p. 450, 1954

Supp
Part.
195

SOME IMPLICATIONS OF SLANT-E_S

E. K. SMITH AND R. W. KNECHT
Boulder Laboratories, National Bureau of Standards, Boulder, Colorado

THE phenomenon of slant-E_s has been noted as an interesting anomaly on ionosonde records for many years. It seems to occur in two different forms; one in the arctic and the other near the magnetic equator. As this is an arctic symposium, attention is focussed on the arctic type. Three examples of arctic slant-E_s are seen in the ionograms of *Fig. 1*. All of these are from College, Alaska, and represent different stages of the same event on 27 February, 1955. The first and last record in this group are two hours apart. The slant-E_s trace in the top example of *Fig. 1* is by definition that part which commences at a virtual height of 120 km and a frequency of 4·8 Mc and then traverses the record diagonally with a slight upward curvature to 400 km. While quite faint and scattered in appearance in the first ionogram, the trace becomes quite heavy in the second record. In the third record only the upper piece of the trace remains, but it is seen to extend up to about 540 km. The dense trace in this record which rises very gradually from 105 km at 2 Mc to 140 km at 8 Mc with a gentle slant is not what is meant by slant-E_s in this paper. It may be classed as auroral E_s following the work of KNECHT[1].

For the sake of comparison, the second type, the low latitude slant-E_s, is shown in *Fig. 2*. The top ionogram shows a rare case of slant-E_s at Maui, Hawaii, and the lower one, the much more common phenomenon, as seen at Huancayo, Peru, near the magnetic equator. Low latitude slant-E_s traces are. fainter and shorter (rising normally to equivalent heights of 250 and 300 km as contrasted to 400 to 500 km for the arctic cases). They also appear to have their lower termini in the regular E-layer near fxE (critical frequency of the extraordinary wave) whereas in the arctic slant-E_s is typically that seen in the top two ionograms of *Fig. 1* where the slant trace appears to emanate from a well-defined sporadic-E trace at a frequency just below fE_s (critical frequency of sporadic-E).

The seasonal distribution of slant-E_s in Alaska is seen in *Fig. 3*. The data for this figure were taken from the unpublished work of V. AGY and D. BRYAN It is actually only valid to compare months for which non-zero values of per cent of time are shown. The zero values represent months which were not analyzed and this could mean either no slant-E_s, very little slant-E_s, or perhaps, even that the records for that month were not available. Despite this, the following conclusions may be drawn: There is more slant-E_s seen at College than at Pt. Barrow or Anchorage, the equinoxes are preferred over solstices and the winter over the summer months, and finally there was more slant-E_s observed during the first few months of 1952 than for the corresponding period in 1951.

A more detailed analysis of slant-E_s for a short period in 1955 for College, Alaska, has been made by MATSUSHITA[2] at CRPL. He investigated the correlation noticed by K. L. Bowles (SMITH[3]); namely that slant-E_s appears

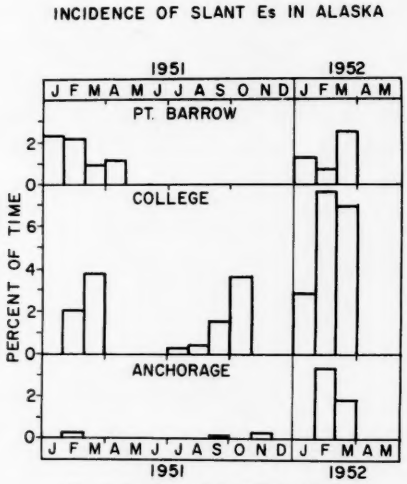

Fig. 3. Incidence of slant-E_s in Alaska

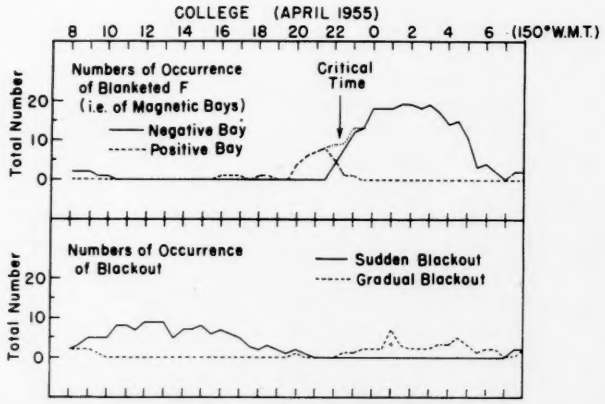
COLLEGE (APRIL 1955)
8 10 12 14 16 18 20 22 0 2 4 6 (150°W.M.T.)
Numbers of Occurrence of Blanketed F (i.e. of Magnetic Bays)
Negative Bay
Positive Bay
Critical Time
Total Number
Numbers of Occurrence of Blackout
Sudden Blackout
Gradual Blackout

Fig. 4. Number of occurrences of blanketed F and number of occurrences of blackout (courtesy of S. Matsushita)

associated with bay disturbances. Shown in *Fig. 4* is Matsushita's analysis of the occurrence frequency of bay disturbances at College. It is seen in *Fig. 4* that bays are a night-time phenomenon (positive bays occur before 2300 hrs, negative bays after this) at College. All substantial bays during this period showed slant-E_s according to Matsushita, but the converse was not quite true; there was a magnetic storm during the period (a non-bay disturbance) which had slant-E_s associated with it.

Suppl.
art.II
1956

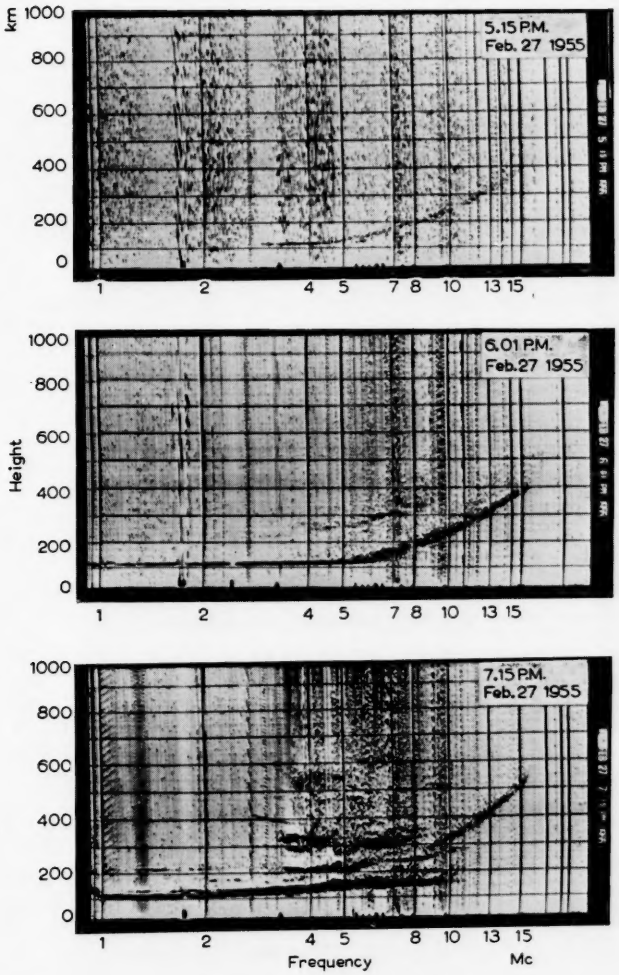

Fig. 1. Slant-E_s at College, Alaska

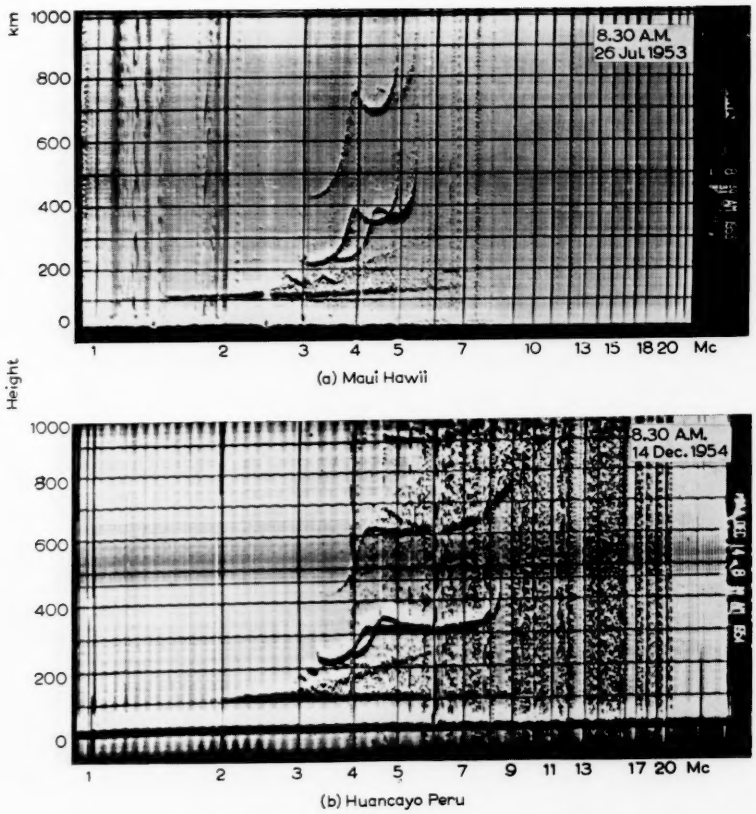

Fig. 2. Non-auroral slant-E_s

Sup
Part
19

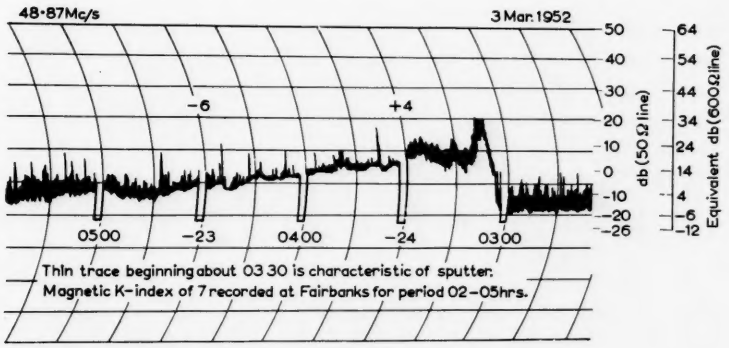

(*a*)

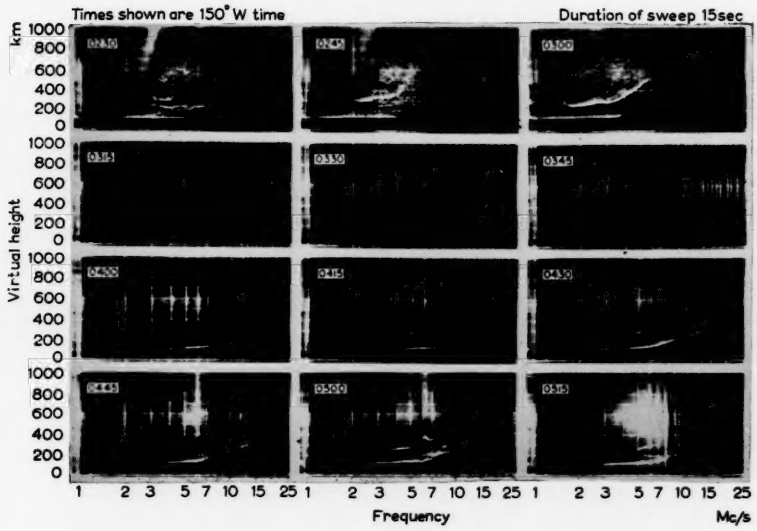

(*b*)

Fig. 5. h'F records — Fairbanks (College) Alaska — 3 March 1952 (top); Signal intensity record, Anchorage — Barrow Path, 3 March 1952 (bottom) (courtesy of Bailey, Bateman, and Kirby[4])

Sup
Part
19

It has further been noticed that slant-E_s is associated with sputter propagation over ionosphere forward-scatter paths (BAILEY, BATEMAN, and KIRBY[4]). This "sputter" is associated with a multipath condition where in addition to the regular CW signal there is another component arriving somewhat later than the first and modulated in the manner of the auroral reflected signals described FORSYTH[5], by BOWLES[6], DYCE[7] and others. When this signal exceeds the amplitude of the regular component, it creates a characteristic "thin trace" on paper tape recorders where the system time constant is of the order of seconds. An example of this is seen in *Fig. 5*, where the association of auroral sputter with slant-E_s is illustrated.

Pulse measurements have been made on the forward-scatter circuits

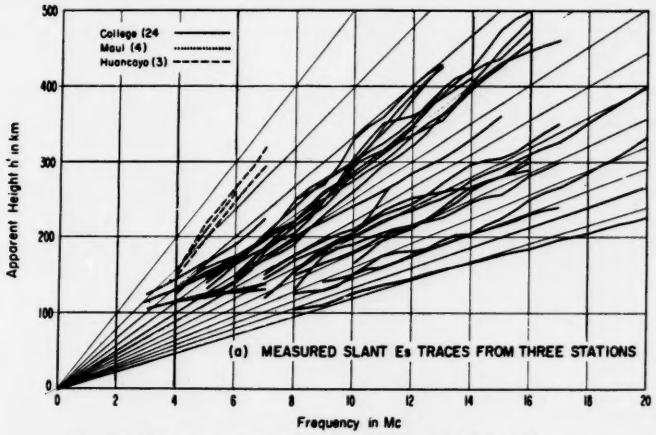

Fig. 6. Linear representation of measured and computed slant-E_s curves

during conditions of "sputter" and have been reported in the BAILEY, BATEMAN, and KIRBY[4] paper. Delays of the order of 1 millisecond were typical for the Anchorage to Barrow path and were somewhat longer on 24 than on 49 Mc.

An interesting feature of slant-E_s discovered by AGY in 1951 (private communication), is demonstrated by plotting the slant-E_s trace on a linear instead of the semi-logarithmic scale of the ionogram. The slant trace then appears as a straight line radiating from the origin as seen by the example in *Fig. 6*. Considering the plane earth situation for the moment, a possible explanation for this observation is as follows:

Let h'_0 = virtual height of reflection from an ionized layer for vertical incidence at a frequency f_0

h' = virtual slant range for an oblique reflection at h'_0

θ = angle of incidence associated with h' in Martyn's theorem for a frequency f.

Then $$h' = h'_0 \sec\theta \qquad \ldots.(1)$$

and by the "secant law" $$\sec\theta = \frac{f}{f_0} \qquad \ldots.(2)$$

therefore $$h' = \frac{h'_0}{f_0} f \qquad \ldots.(3)$$

if f_0 increases towards the critical frequency of the layer, then, ignoring magneto-ionic splitting, f approaches the maximum usable frequency and equation (3) defines the envelope of rays which may be reflected from the layer in question. Equation (3) also defines a direct proportionality between an apparent height (h') and frequency (f) which would fit the observations of *Fig. 6.*

We are interested, therefore, in a mechanism which returns a signal from some part, or all, of an annular ring in the reflecting layer at a radius from the transmitter equal to the skip distance. A first reaction is that any mechanism chosen is apt to fill in the area above and to the left of the slant trace as seen on a ionogram. This objection may be surmounted by specifying that the reflecting layer have sufficient thickness to give a degree of "focussing" at the skip distance. The caustic focussing invoked here is very similar to that made use of by DIEMINGER[8] to explain the ground-scatter trace which looks very much like slant-E_s. *Fig. 7* illustrates this case. The height and frequency

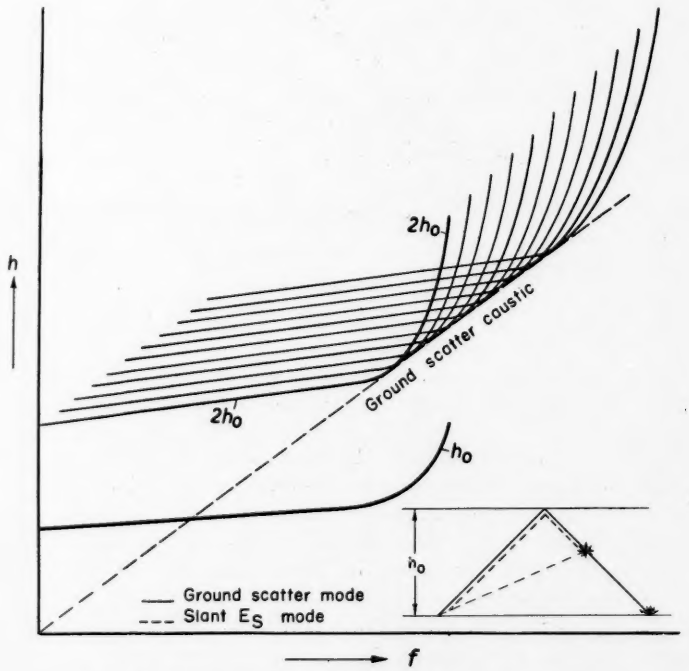

Fig. 7. Application of caustic focussing to slant-E_s through analogy to Dieminger's ground scatter case

scales are both linear. Each curve of the family which starts with that marked $2h_o$ represents a particular value of θ, the equivalent angle of incidence on the ionosphere, and the family is derived from the $2h_o$ curve by proportional vertical and horizontal expansion as indicated from equation (3). On an ionogram only the intensified signal falling along the ground-scatter caustic

appears, the rest of each trace is presumed to be lost in noise. The small chart inserted in the lower right hand corner of *Fig. 7* illustrates the similarity of one of the slant-E_s modes to the ground-scatter situation covered by Dieminger.

Four of the possible slant-E_s modes are illustrated in *Fig. 8*. It is very difficult to properly credit the originators of the following explanations of these modes as they have mostly been passed around by word of mouth. The "direct back-scatter" case of *Fig. 8* (*a*) assumes that the specular-reflection

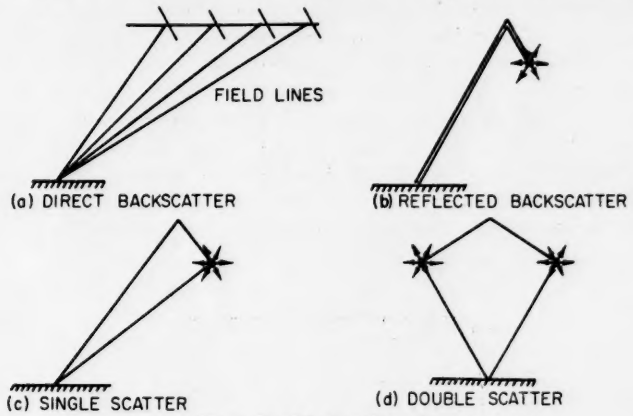

Fig. 8. Possible slant-E_s modes

condition (ray back-scattered at normal incidence to field-aligned blobs) is most nearly met at the higher frequencies but becomes increasingly less severe with lower frequencies thus allowing shorter path lengths. Although qualitatively giving results in the right direction, this does not make use of relation (3), nor is there any reason for the resultant trace to be well defined.*

The mechanisms favored in this paper are given in *Fig. 8* (*b*) and (*c*). "Reflected back-scatter" in (*b*) requires the returning ray to follow the same path traversed by the outgoing ray after undergoing direct back-scatter. Each direction suffers one reflection from the sporadic-*E* or regular-*E* layer so that the focussing action takes place twice. The "single-scatter" mechanism in (*c*) is quite similar to the "reflected back-scatter" one except that the ray traverses a triangular circuit and undergoes one scattering process (at an angle which will vary from 0° to almost 180°) and one reflection. The "double-scatter" mechanism in (*d*) is of interest chiefly because it completes the family of basic possibilities. It is not very palatable from a practical standpoint due to the two scattering processes involved. It does result in a slant curve which is much shallower than the ones associated with the slant-E_s modes of *Fig. 8* (*b*) and (*c*) and which can be made to fit the very mild slant (lower of the two traces) in the ionogram for Maui in *Fig. 2*.

It is very difficult to decide which of the two preferred modes ("reflected back-scatter" or single-scatter) is dominant in any given situation. The attack here is to consider two sets of extreme conditions, first that the scattering

* A modification of the direct back-scatter case which shows more promise has recently been suggested by A. G. McNish (private communication to V. Agy, September 1956) McNish suggests that the specular condition is retained at all frequencies and in order to attain this the ray is deviated inside the sporadic-*E* layer by amounts which depend on frequency.

process is isotropic and second that it is "specular" (as from infinitely long cylinders) from field-aligned inhomogeneities.

If the scattering is isotropic, it is not difficult to make a rough comparison of the expected fields from the two mechanisms (*Fig. 8* (*b*) and (*c*)) as follows. As computed by ECKERSLEY[9] and PETERSON[10], the signal intensification by "angle" focussing at the skip distance rises to infinity for a parabolic model of an ionospheric layer. AGY[11] has recently reported on some measurements of $F2$ propagated signals showing the enhancement at the skip distance obtained with the NBS sweep-frequency oblique-incidence equipment over a 2370 km path. The measurements are shown in *Fig. 9*. The abscissa scale is the ratio of the observing frequency to the MUF at the time of observation. A measure of the observed intensification can be obtained by comparing the signal level on the 50 per cent curve at $f/\text{MUF} = 0{\cdot}98$ to that of $f/\text{MUF} = 100$. It is seen that 20 db represents the order of magnitude of intensification observed for the $F2$-layer. This figure is, of course, not necessarily applicable to the regular-E or an E_s-layer, but it will be used here for lack of anything better.

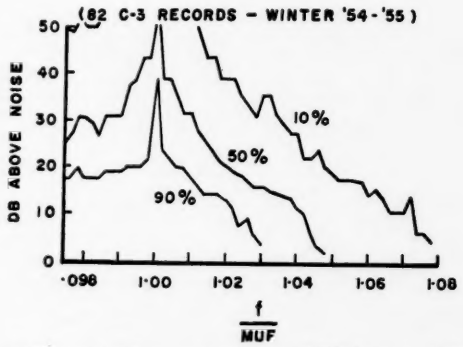

Fig. 9. Field strength at frequencies near 2370-MUF (courtesy of V. Agy)

For this comparison we need not consider the absolute level of signal returned by the scattering process but only the level relative to that which would be returned by direct back-scatter. It is necessary therefore, only to concern ourselves with that part of the expression for the scattering cross section $\sigma(\theta)$ which affects angular dependence. From BAILEY *et al.*[12] we have:

$$\sigma(\theta) \sim \left[1 + \left(\frac{4\pi l}{\lambda}\right)^2 \sin^2 \frac{\theta}{2}\right]^{-2} \qquad \ldots.(4)$$

where θ = scattering angle
l = scale of fine structure
λ = wavelength of the radio wave.

It is apparent from (4) that as long as $(\sin \frac{1}{2}\theta)$. $4\pi l/\lambda \gg 1$ the angular dependence is only a function of θ and will not be affected by l and λ. This fact is illustrated in *Fig. 10* where the angular dependence is shown for three different frequencies and a scale size $l = 100$ m. Only as one approaches the

forward-scatter situation ($\theta = 0°$) do the curves separate. To gain 20 db relative to back-scatter ($\theta = 180°$), it is seen from *Fig. 10* that it is necessary to approach within 40° of the forward-scatter case. For isotropic scattering we therefore expect slant-E_s to be attributable to the "single-scatter" mechanism for the first 10 km or so, and after that for the "reflected" back-scatter mechanism to take over.

The result is very different if it is assumed that the scattering takes place from long trails of electrons laid down by incoming charged particles and oriented along the lines of the earth's magnetic field. In this case the determining criterion is how close the scattering process comes to the "specular" case. The specular case will be defined here to occur when the bisector of the

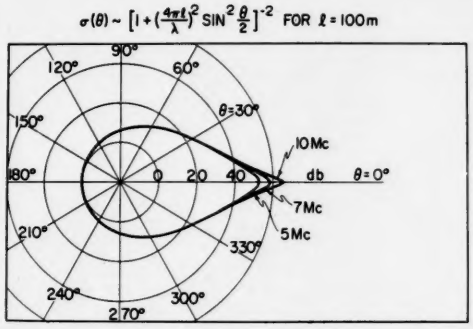

Fig. 10. Scattered power referred to back-scatter — Isotropic case

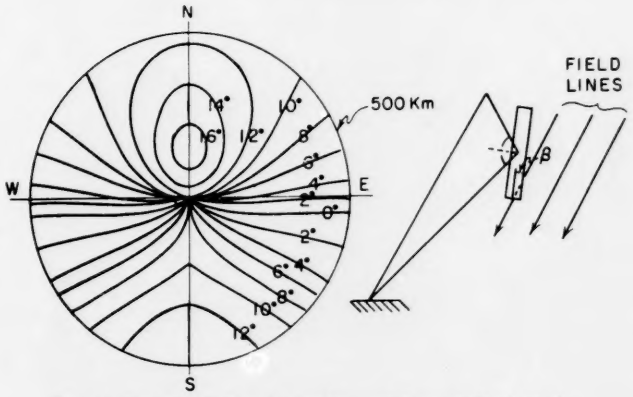

Fig. 11. Deviation β from the specular condition — College, Alaska (single-scatter case)

scattering angle is perpendicular to the scattering filament. One may then consider the angle of deviation β of the bisector of the scattering angle from the perpendicular. An angle of $\beta = 0°$ indicates that the specular condition is met. *Fig. 11* shows the variation of β for the "single-scatter" case at College, Alaska. The plan view on the right of the figure illustrates the variation of β out to a distance of 500 km from College. Smoothed values of surface dip were used to determine the lines of the earth's magnetic field. The contours were

computed for a reflecting height of 110 km and a scattering height of 90 km but β is relatively insensitive to the heights used. It is apparent from *Fig. 11* that a sector about 45° wide exists somewhat south of due east and west on either side of the station for which the deviation β is less than 5°.

The corresponding diagram of β for the reflected back-scatter case is given in *Fig. 12*. In this instance it is only after attaining a ground distance of 360 km to the south that β becomes less than 5° for an ionosonde located at College. It seems unlikely, therefore, that the reflected back-scatter mode will be important except at long ranges under the assumption of field aligned and highly aspect-sensitive scatterers.

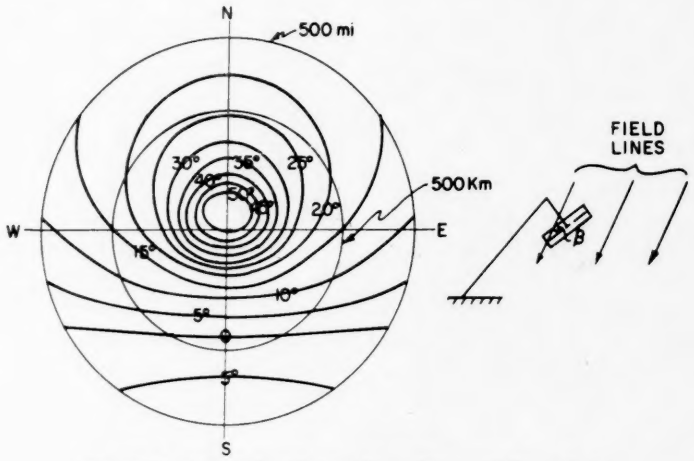

Fig. 12. Deviation β from the specular condition — College, Alaska (reflected back-scatter case)

It may be of interest at this point to mention that the same analysis of these two modes at the magnetic equator indicates that the reflected back-scatter mode is strongly preferred to the single-scatter mode if aspect sensitivity is assumed and blobs are considered oriented horizontally in a north-south direction. However, the width of the effective angle of acceptance at the ionosonde decreases rapidly with increasing distance for this mode. This offers a possible explanation of why the equatorial slant-E_s is systematically of shorter range than its arctic counterpart.

One important feature about these speculations is that it is possible to test them. There has been a scatter-sounder operating at 12 Mc at College. If operated simultaneously with the ionosonde during a period of slant-E_s, it should be possible to isolate the slant-E_s trace on the scatter-sounder and determine the direction from which it is coming. The following conclusions would then be indicated:

1. If the signal comes from all azimuths equally the scattering process is isotropic, the scattering level is below the E_s-layer and the mode is first "single-scatter" and then "reflected back-scatter."

2. If the echoes are from the north, the mechanism is "direct back-scatter" or, more probably, the McNish extension (refracted back-scatter) and

the scattering level is probably above the E_s-layer and from field aligned electron filaments.

3. If the echoes are from the east and west the single-scatter mechanism is indicated, reflections are from below the E_s-layer and electron filaments accomplish the scattering.

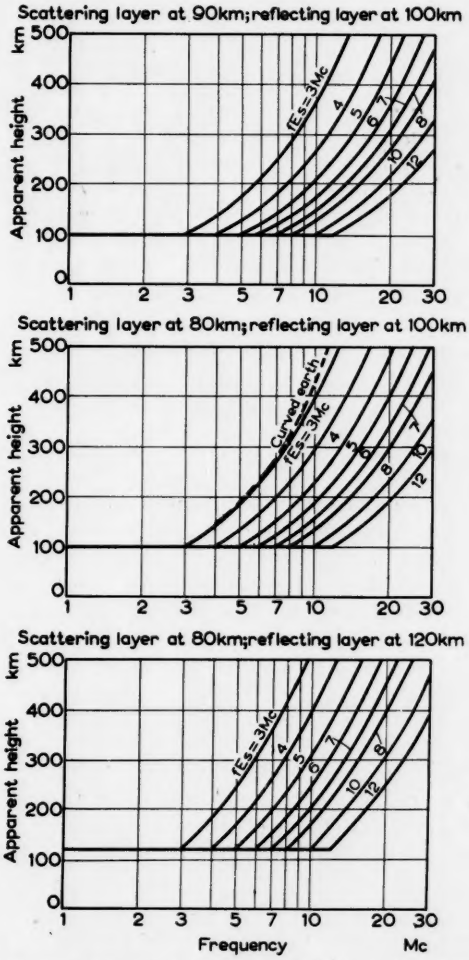

Fig. 13. Families of theoretical slant-E_s curves assuming a single scattering mechanism and plane earth

4. Echoes from the south would be expected only at long range and would carry the same implications as (3) and indicate direct back-scatter to be active.

If it were possible to determine which mechanism were operative by use of a scatter-sounder or similar equipment, further information could also be derived. *Fig. 13* illustrates families of theoretical "single-scatter" curves for different combinations of reflecting and scattering heights. These can be

plotted in such a way as to overlay directly on ionograms of slant-E_s. Through successive trials it is possible to arrive at an estimate of the scattering height although the determination is not a very sensitive one. *Fig. 14* illustrates the

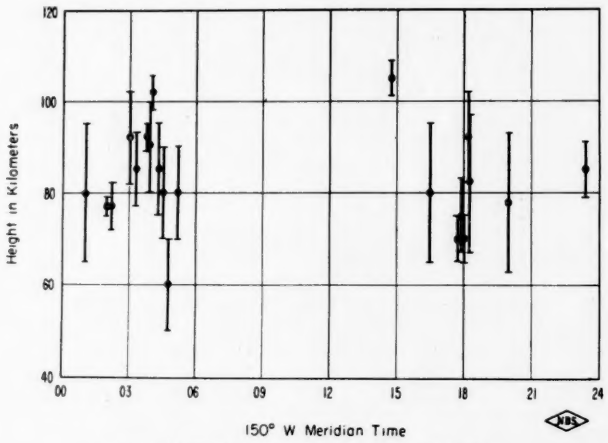

Fig. 14. Scattering layer heights deduced from slant-E_s
Single-scatter mode assumed College, Alaska: April and December, 1954

sort of height information which is forthcoming from the assumption that the single-scatter mechanism is active throughout (SMITH[3]). Twenty-one cases of slant-E_s are involved in *Fig. 14* and the diurnal variation they reflect is quite typical from College. The height ranges shown are subjective estimates of goodness-of-fit. The scattering levels should not be taken literally as it is evident from the discussion above that the situation is most probably considerably more complicated than that assumed here.

REFERENCES

[1] KNECHT, R. W. *J. geophys. Res.* Vol. 60, March 1956
[2] MATSUSHITA, S. *URSI Spring Meeting*, Washington, D.C. 1956
[3] SMITH, E. K. *Ph.D. Thesis*, Cornell University, 1956
[4] BAILEY, BATEMAN and KIRBY. *Proc. Inst. radio Engrs., N.Y.* Vol. 43, p. 1181, 1955
[5] FORSYTH, P. A. *J. geophys. Res.* Vol. 58, p. 53, 1933
[6] BOWLES, K. L. *Ph.D. Thesis*, Cornell University, 1955
[7] DYCE, R. B. *Ph.D. Thesis*, Cornell University, 1955
[8] DIEMINGER, W. *Proc. Phys. Soc.* B Vol. 64, p. 142, 1951
[9] ECKERSLEY, T. L. *J. Instn. Elect. Engrs.* Vol. 71, p. 405, 1932
[10] PETERSON, A. M. *Conf. Ionos. Res., Penn. State*, F, 1949
[11] AGY, V. L. *URSI Spring Meeting*, Washington, D.C., 1955
[12] BAILEY, BATEMAN, BERKNER. *et al. Phys. Rev.* Vol. 86, p. 141, 1952

RESULTS OF SCATTER MEASUREMENTS AT 36 MC/S OVER A 1200 KM PATH

TOR HAGFORS

Norwegian Defence Research Establishment

Suppl.
art.II
1956

1. INTRODUCTION

IN 1952 the first results were published of test transmissions utilizing the scattering effect of irregularities in the ionosphere.[1] It at once became apparent that the particular properties of the signal might make it useful for communication purposes in Arctic Regions. Work on ionospheric scatter propagation was taken up by the Norwegian Defence Research Establishment nearly two years ago. The work was aiming at increasing the understanding of the physical mechanisms involved in long distance ionospheric scatter propagation. Some of the results of this investigation are described in this paper.

2. EXPERIMENTAL SET-UP

The transmitter used is essentially a crystal controlled 36 Mc/s, 5 kW power amplifier feeding into a rhombic aerial of leg length 80 m designed to give maximum radiation at an elevation of 6 deg. in the direction of the receiver. At the receiving end an ordinary commercial receiver with a preamplifier was used for measuring the voltage across antenna terminals. This voltage was recorded on pen-recorders, a large time constant being involved in most cases to ease the calculation of median signal level. Both rhombic and yagi receiving aerials of gain 22 db and 13 db respectively were used. The transmitter was situated in the South of Norway and the receiver in the North, the distance between the two being 1130 km.

3. RESULTS

3.1. *Diurnal signal variation*

Hourly median signal voltage across antenna terminals was plotted against time of day in a scatter diagram. These diagrams were drawn for each month of observation. Monthly median of field strength could then be extracted, and the variation of this median with time of day was found. *Fig. 1* shows four of these monthly plots.

In all cases there is seen to be a more or less pronounced maximum at midday. For all months there is also a minimum in the early evening. During the summer months there appears to be another maximum in the early morning, and diurnal variation is rather pronounced, the ratio between maximum and minimum median power being about 10. During the winter months variation in field strength over the day is much smaller. Transmission loss relative to free space is of the order of 80 to 95 dB.

This diurnal variation, which has been observed to be of similar nature at other geographical locations[2, 3] suggests at least two causes of the signal received, the component giving rise to strong signals at midday probably being due to direct solar influence on ionization, and the other component possibly being due to ionization by the numerous meteors impinging on the earth's atmosphere.

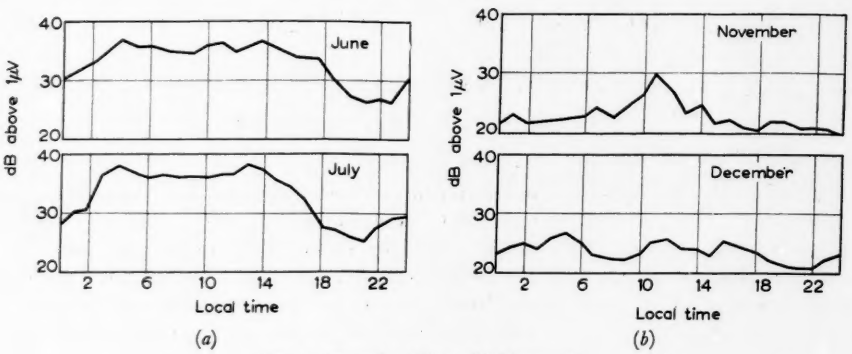

Fig. 1. Diurnal variation of field strength

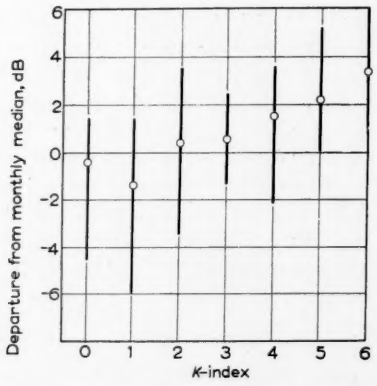

Fig. 2. Relation between K-index and field strength

From our limited number of measurements it does not appear possible to determine the relative strength of the two signal components, and besides the aerial system in use strongly favours a scatter signal as compared with a meteor signal.[4]

3.2. *Relation between field strength and ionospheric and magnetic data*

Detection of correlation between ionospheric data and field strength is rendered difficult owing to the fact that ionospheric recordings are taken regularly only in places very far removed from the area believed to be responsible for the signal.

Magnetic disturbances, as measured by K-index, are not of the same localized character as ionospheric conditions. In fact, it has been possible to relate field strength and K-index as observed in Tromsö. Field strength is increasing with K-index, i.e. the signal increases during magnetic disturbances. This is shown in *Fig. 2*, which is a plot of departures of field strength from normal plotted against K-index.

Similarly, comparing field strengths measured during ionospheric disturbances as indicated on *h'f* recordings with normal field strengths shows that under such conditions the signal is enhanced by about 4 db.

3.3. *Angular dependence of scattering cross section*

In scatter theory it has become standard practice to define a scattering cross section per unit of volume and per unit of solid angle[5] in such a way that:

$$dP_r \sim \frac{1}{r_1^2 r_2^2} \cdot \sigma \cdot dV \qquad \ldots.(3.1)$$

where dP_r is power received from element of volume dV which is at a distance r_1 from the transmitter and a distance r_2 from the receiver. It is generally accepted that σ is a function of $K = (1/\lambda) \sin(\Theta/2)$ where λ is wavelength and Θ scattering angle. Very often it is assumed that σ can be written as a power function in K, such that

$$\sigma \sim K^{-n} \qquad \ldots.(3.2)$$

where n has been given all different values between 4 and 11.

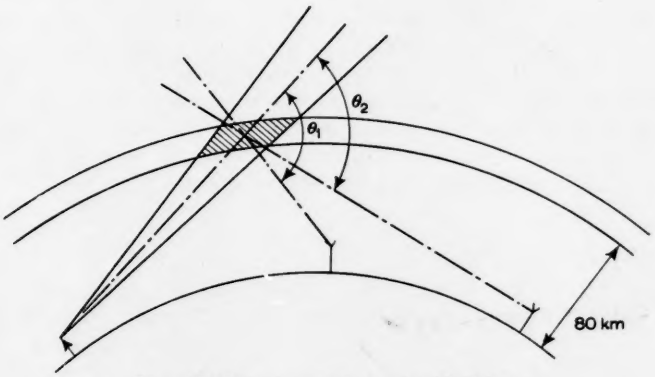

Fig. 3. Variation in scattering angle with distance

For the field strength measurements performed the transmitting aerial was fixed giving maximum radiation at 6° elevation. With the narrow beam angle of the transmitting aerial, and the wide lobe of the receiving aerial, the scattering volume can be assumed fixed by the transmitting lobe, and by the height of the scattering area. This is shown in *Fig. 3*. From *Fig. 3* and equation 3.1 it is obvious that the only variables influencing the received power are r_2, the distance between scattering volume and receiver, and θ, the scattering

angle. *Fig. 4* shows how the received power increases with distance, as can be expected if the angular dependence is rather strong.

From distance dependence measurements and the above remarks, an expression for the angular dependence of σ can obviously be estimated. On assuming that the turbulent area responsible for the scatter signal is at a height of 80 km estimation of scattering cross section gives a value of the exponent n of equation 3.2 of about 10, which is higher than expected according to most theories.

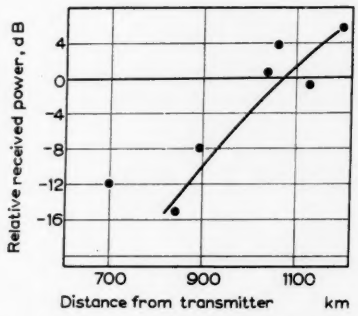

Fig. 4. Relation between field strength and distance

3.4. *Frequency dependence of transmission loss*

In order to determine frequency dependence of transmission loss, the frequency was changed several times between 36 and 46·8 Mc/s within a week. The observed change in transmission loss was found to be nearly 4 db.

From this result the frequency dependence of scattering cross section was found. If a power law is assumed for σ, as indicated above, the value of n deduced is only 3·25 which is in disagreement with the value of n found previously. Similar discrepancies have also been met with by others. [2, 3]

A really satisfactory explanation has not yet been given.

3.5. *Signal fine structure*

The fading characteristics of the normal signal resemble those of noise passed through a narrow bandpass filter. This is particularly true for relatively strong signals and when meteor activity is low. Speed of fading corresponds to 2–3 cycles per second, or to put it more precisely, the autocorrelation function of signal amplitude falls to 50 per cent after about 0·3 of a second.

Occasionally the signal amplitude shows an abrupt increase followed by a more gradual decay, which is often, but not always exponential in form. The duration of these echoes is mostly of the order of a few tenths of a second, and their frequency of occurrence ranges from a few per hour to something like 20 to 30 per minute. These signals are typical of echoes received by reflection from meteoric trails. In many cases echoes of this nature are preceded by whistles which are always of a descending pitch. Whistles, on the other hand, are not always accompanied by very pronounced echoes.

Supp
Part.
195

Examples of a normal signal, and a signal with frequent meteoric echoes are shown in *Fig. 5*. Field strength is a linear function of deflection.

Observation of signal fine structure on aerials of different gain has shown that speed of fading is faster with low gain than with high gain antennas. This indicates that significant signal components can be received from areas normally not illuminated when highly directional aerials are in use. The

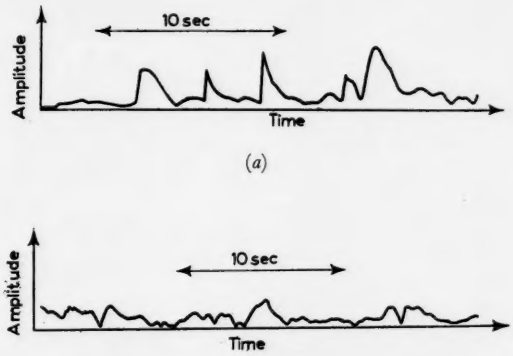

Fig. 5. Examples of signal fine structure

difference in speed of fading is obviously due to the fact that the phase difference produced by a certain displacement of an irregularity is larger the farther it is from the midpoint of the path. Obviously the space diversity distances measured will be a function of aerial gain to a large extent. When examining the diversity properties of the mechanism itself rather low gain aerials should therefore be used.

4. Conclusion

A large number of questions concerning ionospheric scatter are still not satisfactorily answered. More detailed correlation between ionospheric condition at the control point and the scatter signal transmission loss should be obtained. A thorough examination of the angular law of scattering should be undertaken to throw some light on the nature of the turbulent spectrum in the lower ionosphere.

References

[1] Bailey, D. K. *et al. Phys. Rev.* Vol. 86, pp. 141–145, 1952

[2] Bailey, D. K. *et al. Proc. Inst. radio Engrs. N.Y.* Vol. 43, pp. 1181–1230, 1955

[3] Bray, W. J., Saxton, J. A., White, R. W., and Luscombe, G. W. *Proc. Inst. Elect. Engrs. B.* Vol. 103, pp. 236–260, 1956

[4] Eshleman, V. R. and Manning, L. A. *Proc. Inst. radio Engrs.* Vol. 42, pp. 530–536, 1954

[5] Booker, H. G. and Gordon, W. E. *Proc. Inst. radio Engrs., N.Y.* Vol. 38, pp. 401–412, 1950

DISCUSSION

Discussion on Friday, 6 July in connection with the papers read on: *Absorption*

LIED: We have today had mention from quite a number of speakers of the big solar flare on 23 Feburary. I think it was mentioned in the lecture by Mr. Knecht and then by Mr. Little and then now in our last lecture. It just occurs to me that the over-all pattern of what happened that morning about 0330 universal time is not quite clear because, as far as I have seen, for example from the Alaska record, the heavy absorption started together with the flare. Was that wrong?

MOORE: I believe there was a delay of the order of 40 minutes. From 0335 to about 0410 there was very little indication of absorption and then it began to increase fairly linearly for several hours. The first absorption was at the Tooley station beginning five minutes to four universal time.

LIED: So then the picture starts getting a bit more clear. The flare occurred at Kjeller at about 0440 LT, about 0340 UT, and as far as I can see then, the heavy absorption in Alaska and Tooley started somewhat after the flare. But Dr. Weekes' results, as far as I can see, published in *Journal of Atmospheric and Terrestial Physics* in the last issue, show that the effect on Rugby was rather instantaneous.

WEEKES: Simultaneous with the cosmic rays, not with the flare. The flare was going at 0335 anyway.

LIED: We were measuring absorption both here and in Tromsö by the technique I have described to you earlier, and the effect on the integrated absorption was not noticeable whatsoever before about 6 o'clock in the morning, and similar results were obtained on the $P'f$-recorders. We had $h'f$ records both here and in Tromsö for a few hours after the flare — we take only records once every whole hour so I cannot say it exactly — but the absorption measurements were being done continuously and they did not show here any catastrophic event really. The absorption here at Kjeller was quite normal up to 6 o'clock, it then started increasing, while the normal diurnal absorption starts increasing approximately 2 hours later. We were able to follow the heavy absorption the whole day through, the form of the whole thing was rather normal, just starting earlier and lasting longer, the magnitude of the D-figure being of the order of four times the normal value. I would like to ask if anybody can see the integrated picture of this. I suppose it must be the point that we are in the shadow and that we perhaps altogether missed the first catastrophic event.

WEEKES: I might add a little to this story. I think the event was complex. On the long waves things started to happen at 0345, when the height of reflection decreased, reached a minimum about 0410 then increased a bit as if

it were recovering. Round about 0600 it decreased again more or less as it would have done on a normal day, though starting rather earlier. On slightly higher frequencies again there was a catastrophic effect at 0345. There is a very interesting result, which I gather will be published in the *Journal of Atmospheric and Terrestrial Physics* which was observed in New Zealand by Crombie and his collaborators using GBR (16 kc/s). They are observing in the same way as Dr. Pierce in America. They compare the phase of GBR throughout the day with the phase of a stable local oscillator. The changes of phase will appear as changes of apparent frequency (which is the way in which they talk of it). The drift of the two oscillators gives a linear phase shift, or a constant frequency difference which may be removed fairly easily and one is left with the change of phase of the signal from GBR. The New Zealand work is expressed in apparent frequency changes, which are differentials of the phase changes.

For a normal S.I.D. the apparent frequency shows a large but relatively short positive change followed by a smaller negative change of longer duration — the areas under these two parts of the frequency time curve are equal so that this corresponds to a drop of phase height followed by an equal increase. On the event of 23 February, the frequency showed a positive change at about 0330 just as in a normal S.I.D., the frequency change showed a decrease to a minimum, still positive, and showed a further increase at about 0345. Thus it looked like a normal flare effect up to about 0345 but instead of recovering there was an additional decrease in phase height coincident with the cosmic ray increase; later the frequency decreased to its normal value.

uppl.
rt.II
1956

ROACH: Can you put one more time in that?

WEEKES: These comments are from memory. Now I would say that the minimum frequency occurred at about 0334 and the frequency reached normal at about 0415.

The other thing that one observed on GBR on the Cambridge steep incidence instruments was that at about sunrise time curious things happened. But the midday value of the height of refraction was something like 5 km lower than usual, and at 300 km from GBR I think it was even more than 5 km lower. Now even remembering that the GBR 16 Kc/s waves require very little extra ionization, and putting in this amount of ionization between 70 km and 65, it is going to have a pretty big effect on the absorption. I think that is where the extra absorptions come from. The early start of the extra absorption can easily be associated with the GBR decrease originally.

KNECHT: There is one thing that has not been mentioned yet and that is the magnetic effect. At the Canadian stations of Resolute Bay and Baker Lake it seemed to be at about 0405 that this disturbance started. However, below Baker Lake, for instance at College, Alaska, there seemed to be no effect at that time so there may be an associated magnetic effect at above say 73–74° N geomagnetic. However, there was no large storm at the time.

HARANG: I may have mentioned that we had some scintillation work going on just on these days and on the day when the disturbance occurred there were less scintillations than the day before or the day after that.

LITTLE: One point in the same connection. A very striking feature of the absorption records at College was the fact that the absorption, though con-

siderable, reaching about 8 db at vertical incidence on 30 Mc/s, did not vary rapidly. A typical disturbed day shows many variations in absorption, but the day following the flare, at College we only had one smoothly varying curve of absorption reaching a peak round about local noon.

FINDLAY: Just a very brief general point. This was a most interesting event, particularly because a cosmic ray burst produced effects as well. Is anybody collecting it? Is there anywhere where all the people who have got observations are sending them to, so that one body can attempt to produce an overall picture of it? It would be very interesting to have if it can be done in the end.

WEEKES: We have been endeavouring to get information from anybody who likes to send it to us, and some people have done so.

Sup
Part
19

Suppl.
art.II
1956

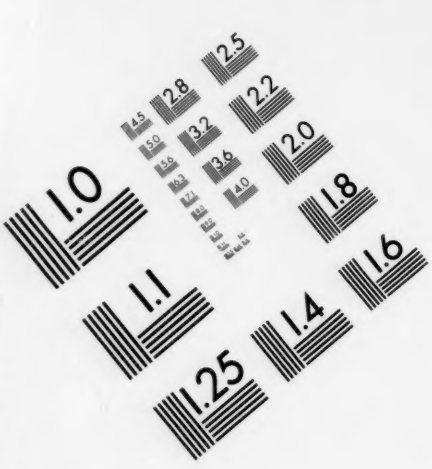

NATIONAL MICROGRAPHICS ASSOCIATION

MS303-1980

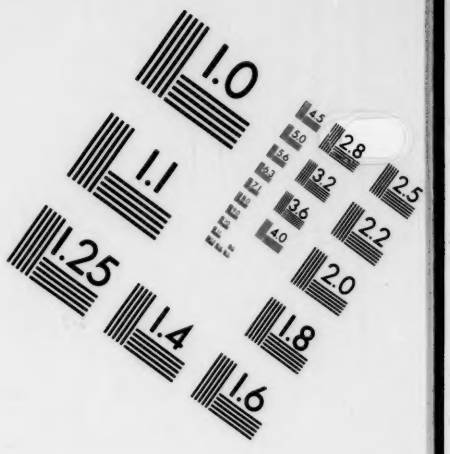

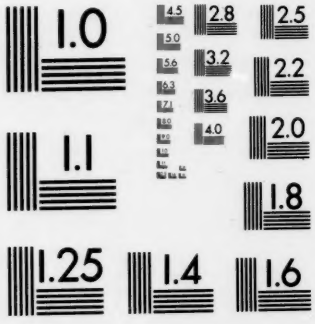

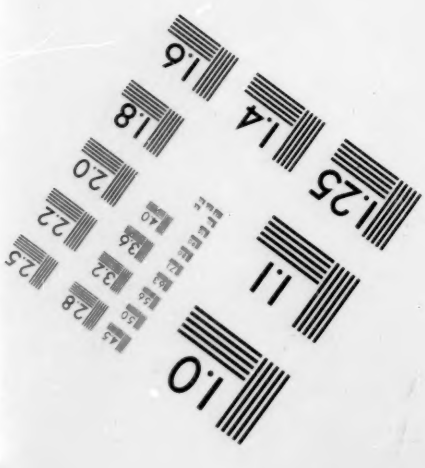

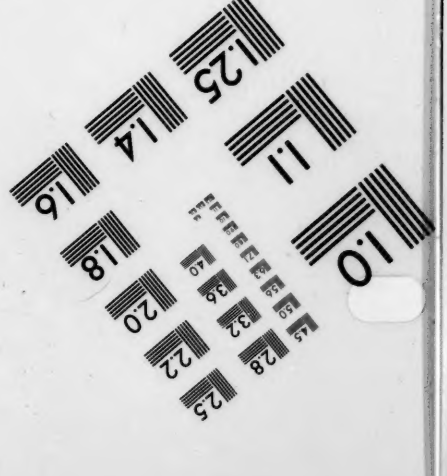

PERGAMON PRESS INC.

MICROFORMS INTERNATIONAL
MARKETING CORPORATION
FAIRVIEW PARK, ELMSFORD, NEW YORK 10523

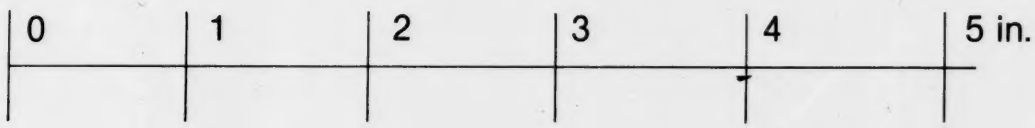

PRODUCED AT

**MIMC MICROFORMS LABORATORY
ELMSFORD, NEW YORK**